Development of Reference ELISA Assays For Urinary Oestrone-3 α-Glucuronide and Pregnanediol-3 α-Glucuronide Using Timed Urine Specimens

A thesis presented in partial fulfilment of the requirements for the degree of
Master of Science
in
Biochemistry

at Massey University, Palmerston North, New Zealand

JANETTE ELIZABETH BINNIE

1999

Abstract

Enzyme-linked immunosorbent assays (ELISA) have been developed which measure oestrone glucuronide (E1-3G) and pregnanediol glucuronide (PdG) in timed, diluted urine samples. Measurement of these urinary metabolites allows information to be collected, non-invasively, on the hormonal interplay between the ovaries and the hypothalamic-pituitary axis, which determines or helps to make predictions about the potentially infertile and fertile phases of the human menstrual cycle.

Immunoglobulin Class G (IgG) antibodies raised in sheep against the analyte of interest (E1-3G and PdG) were adsorbed onto polystyrene microtitre wells. The enzyme conjugate tracer was horseradish peroxidase (HRP), and was prepared by conjugation with either E1-3G or PdG using the active ester coupling procedure. A direct competitive immunoassay configuration in which both analyte and tracer were added to the wells simultaneously allowed a direct competition between them for the immobilised antibody sites. A chromogenic detection system involving o-phenylenediamine (OPD) was used for the measurement of the amount of bound tracer (HRP conjugate) which could be related to the amount of analyte in a urine sample.

The sensitivity of the E1-3G assay was 3.4 nmoles/ 24 h, and for the PdG the sensitivity was 0.5 µmoles/ 24 h. Both assays were reliable, and were successfully validated against World Health Organisation (WHO) assays performed on the same urine samples in a multicentre study of the Ovarian Monitor (project #90905).

The E1-3G and PdG reference assays developed in the present study are acceptable for use in the laboratory and can be used to validate new non-instrumental colour tests, or other home fertility kit assays currently being developed.

Acknowledgements

My thanks particularly to my supervisor Associate Professor Leonard Blackwell for his enthusiastic encouragement and guidance during this work.

I am grateful to my Biochemistry colleagues Bryce Cummock and Delwyn Cooke for their assistance during the first few months of this research. Thanks also to Dr Yinqiu Wu and Dr Mark Smales for their discussions with me concerning the organic chemistry components of my work. I very much appreciate the thoughtful and conscientious way in which Dr Simon Brown fulfilled his role as my second supervisor.

Thanks to Dr Keith Henderson of AgResearch for his invaluable help with setting up the ELISA, and for his clear and uncomplicated telephone conversations during the various trouble shooting expeditions with ELISA.

To my partner John for his wit, passion for cooking, and good nature which ensured that home was a tranquil haven in which to study, thank you.

Table of Contents

List of Tables

Abbreviations

Aromatase	Oestrogen synthetase
A_{278}	Absorbance at 278 nm
A_{280}	Absorbance at 280 nm
A_{404}	Absorbance at 404 nm
A_{490}	Absorbance at 490 nm
B/B_0	Absorbance value of the steroid standard divided by the absorbance value of the zero standard
CAb	Capture antibody
CV	Coefficient of Variance
DCC	Dicyclohexylcarbodiimide
DMF	Dimethylformamide
`E'	Mean absorbance reading for the steroid glucuronide standard
`E_0'	Mean absorbance reading of the zero standard
ED_{50}	At the midpoint of a normalised standard curve
ED_{20}	At a point 20% from the bottom of a normalised standard curve
EIA	Enzyme Immunoassay
ELISA	Enyme Linked Immunosorbent Assay
E1-3G	Oestrone-3 α-Glucuronide
E1-3G-HRP	Oestrone-3 α-Glucuronide-Horseradish Peroxidase Conjugate
Fab	Antigen-binding fragment of antibody
Fc	Constant fragment of antibody
FSH	Follicle Stimulating Hormone
HEWL	Hen Egg White Lysozyme
HRP	Horseradish Peroxidase
IgG	Immunoglobulin Class G
LH	Luteinising Hormone
NC	Nitrocellulose paper
NHS	N-hydroxysuccinimide
NSB	Non specific binding
OPD	O-phenylenediamine
PBS	Phosphate buffered saline

Pd	Pregnanediol
PdG	Pregnanediol-3 α-Glucuronide
PdG-HRP	Pregnanediol-3 α-Glucuronide-Horseradish Peroxidase Conjugate
RZ	reinheitzahl
RIA	Radioimmunoassay
SD	Standard Deviation
SEM	Standard Error of the Mean
SPI	Solid Phase Immunoassay
Tween(20)	Polyoxyethylene (20)-sorbitan monolaurate
ΔT	Change in Transmission
T_0	Transmission at time zero
T_{20}	Transmission time of 20 minutes
WHO	World Health Organisation

Chapter One: General Introduction

1.1 Oestrone-3 α-glucuronide (E1-3G) and Pregnanediol-3 α-glucuronide (PdG): Their Relationship to Ovarian Function

It has been well established that a complex communication system exists between the hypothalamic-pituitary axis and the ovaries and is necessary for the process of ovulation to occur (Pohl & Knobil, 1982; Mahesh, 1985; Ireland, 1987; Ganong, 1991; Adashi, 1994). Because ovulation occurs approximately every 28 days, the secretory patterns of the ovarian steroid hormones oestradiol and progesterone, and the pituitary glycoprotein hormones (called gonadotrophin hormones) follicle stimulating hormone (FSH) and luteinizing hormone (LH) are usually studied as a menstrual cycle group (see figure 1.1) and compared from month to month. Further, the excretion patterns of the urinary metabolites of oestradiol and progesterone can give useful information about ovarian function. The Ovarian Monitor (Brown *et al.*, 1989) is a device which measures the key menstrual cycle markers, oestrone glucuronide (E1-3G) and pregnanediol glucuronide (PdG) in urine, to detect fertility status.

1.1.1 Regulation and Control of Ovarian Function

Ovarian steroid hormones secreted in response to gonadotropic stimulation (Leung & Armstrong, 1980) are important components of feedback mechanisms that regulate gonadotrophin secretion via actions upon the hypothalamic-pituitary system (Karsch, 1987), particularly with regard to the feedback regulation of LH (Brown, 1978). Further, FSH and LH regulate ovarian oestradiol secretion by actions at biochemically distinct sites (Armstrong *et al.*, 1979); LH stimulates the synthesis of androgens, which are then converted to oestrogens via an aromatase enzyme system under the specific stimulation of FSH.

Ovarian oestradiol production is associated with the pre-ovulatory growth of the follicle, whereas, after ovulation, progesterone production is associated with the establishment of the corpus luteum; respectively known as the "follicular phase" and "luteal phase" of the menstrual cycle (see figure 1.1). Cycle lengths can vary among women, but last on average 28 to 30 days, although very few women have absolutely regular cycles (Bonnar, 1994). It is the follicular phase that is usually responsible for the variable length of the menstrual cycle, and which needs to be clearly defined for improved fertility prediction. At the beginning of the menstrual cycle the FSH level increases slowly (figure 1.1) until

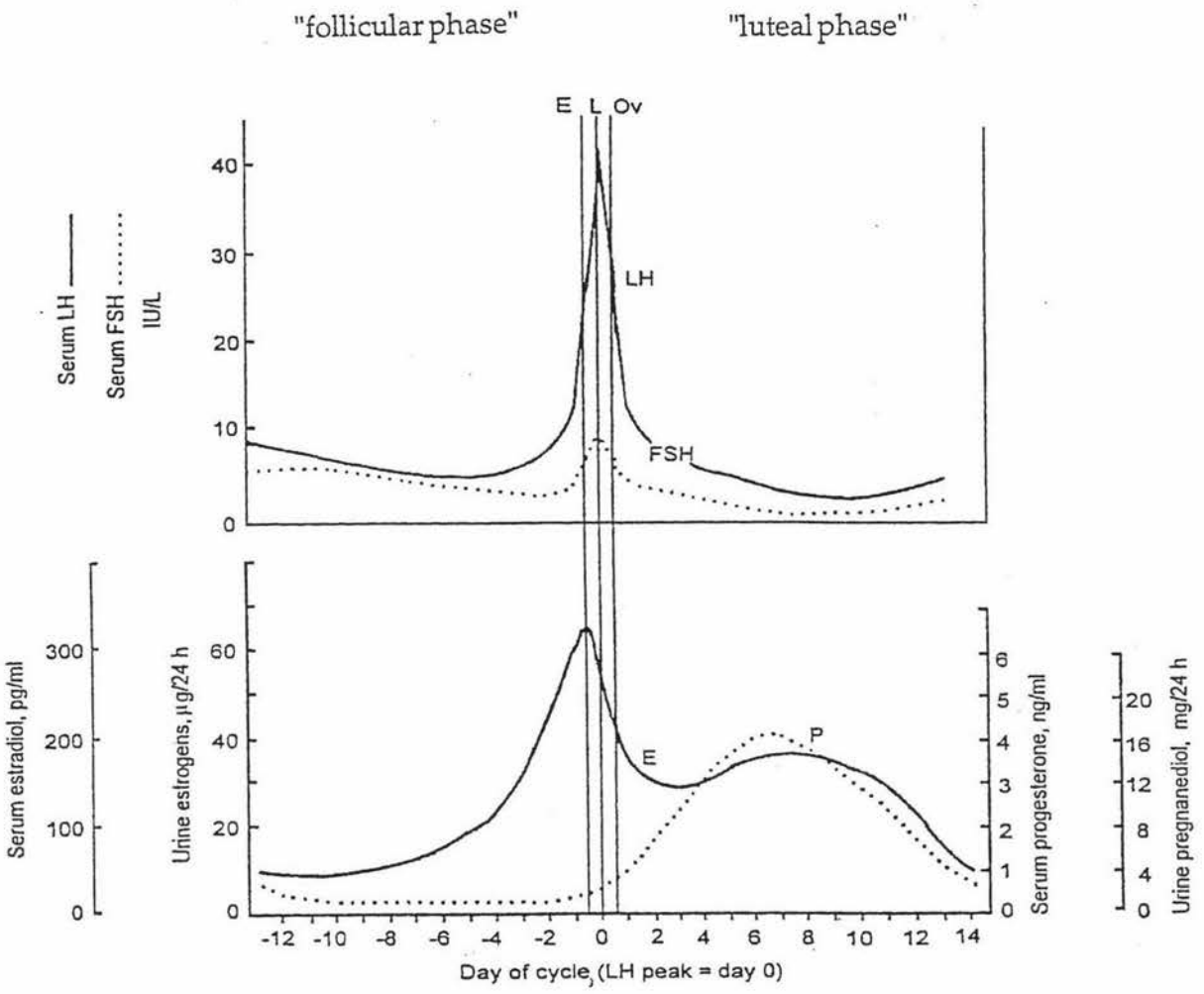

Figure 1.1: Levels of serum luteinizing hormone (LH), follicle stimulating hormone (FSH) and oestradiol (E), and urinary pregnanediol (P) throughout a typical menstrual cycle. The vertical lines show the oestrogen peak (E), the luteinizing hormone peak (L) and ovulation (Ov).

The Follicular phase begins after menstruation with the establishment of baseline oestradiol secretion levels (shown from about cycle day -12) and lasts until an ovarian follicle ruptures and an oocyte is released. This process, known as ovulation, is the central event of the menstrual cycle and forms the basis of the regular pattern of events which occurs every month.

The Luteal phase begins after ovulation with the establishment of the progesterone secreting corpus luteum (formed from the remnants of the ruptured follicle) and lasts until regression of the corpus luteum causes progesterone secretion to fall resulting in menstruation (about day 14).

[Brown *et al.*, 1987]

the threshold level of the most sensitive follicles is exceeded (Brown *et al.*, 1978; Zeleznik & Kubik, 1986), and a cohort of follicles is recruited. The FSH stimulates the granulosa cells of the follicles to divide and hence the follicle increases in size. By mechanisms still not completely understood (Brown *et al.*, 1978) one of the cohort becomes dominant, all other follicles in the cohort undergoing atresia (the atrophy of the follicle). The dominant follicle undergoes a conversion from an androgen environment to an oestrogenic environment due to acquisition of the aromatase system. Thus, the presence of the dominant follicle is signalled to the hypothalamic-pituitary axis by increasing levels of oestradiol above a previous baseline (figure 1.1). A negative feedback mechanism then suppresses FSH excretion and the levels fall so that no more follicles are recruited.

An investigation carried out by Zeleznik and Kubik (1986) to determine experimentally the relationship between plasma gonadotrophin concentrations and ovarian follicular development, gave good supporting evidence of the role that plasma gonadotrophins are presumed to play in the control of folliculogenesis. In that study eight adult macaque monkeys were treated with an antagonist to gonadotrophin releasing hormone which is a hypothalamic decapeptide hormone that initiates the release of (FSH) and (LH) from the anterior pituitary gland. This suppressed the natural levels of FSH and LH to baseline values. Human FSH and LH were then administered by pulsatile infusion to mimic physiological conditions as much as possible (one three minute pulse an hour). The amount of LH delivered remained constant and resulted in a plasma concentration of 9-12 mIU/ml. Because LH was kept at a constant level it is difficult to assess its influence on the resulting folliculogenesis. No elevation of serum oestradiol or antral follicle growth was detected in the four control animals with a constant infusion dosage of plasma FSH maintained at 7.5-10 mIU/ml for 13 days. By contrast in the four experimental animals the amount of FSH per pulse was increased until the serum oestradiol concentrations began to rise above baseline. The amount of FSH in the experimental animals was doubled on day 5 resulting in plasma FSH concentrations of 11-15 mIU/ml, but oestradiol plasma concentrations remained at 25-50 pg/ml (baseline values). On day 8 the FSH infusion dosage was again doubled and oestradiol concentrations responded by rising above baseline values for the first time, as plasma FSH concentrations elevated to 15-20 mIU/ml. As soon as the oestradiol rise was detected the pulse dosage of FSH was reduced by 12.5%/day for the final 5 days. Despite the reduction in FSH dosage oestradiol levels continued to rise exponentially as in the normal cycle, even at concentrations (8-10 mIU/ml) which had been unable to initiate oestradiol production

earlier. On the basis of these experiments, Zeleznik and Kubik (1986) concluded that threshold plasma FSH concentrations in the range of 15-20 mIU/ml were associated with the initiation of oestradiol production. These concentrations agree well with levels seen during the early follicular phase of the macaque menstrual cycle and histological sections showed large antral follicles in the experimental animals which were lacking in the controls.

This research supports the hypothesis first suggested by J.B. Brown in 1978 (Brown *et al.*, 1978; Brown, 1978), that an FSH threshold plasma concentration level is necessary to initiate oestradiol production by the follicle, but that once this threshold has been reached oestradiol production becomes independent of FSH concentration (Hillier & De Zwart, 1981) as endocrine and receptor changes occur (Ireland, 1987), which are not completely understood, to allow the dominant follicle(s) to continue to produce oestrogen. Consequently, subthreshold levels of FSH are unable to stimulate follicle growth and atresia of the follicles occurs no matter how long the FSH supply is continued.

Evidence that the high circulating levels of oestradiol which occur during follicular growth induces the rapid pre-ovulatory FSH decline and the atresia of subthreshold follicles (refer section 1.1.2.1), is provided by further experiments of Zeleznik *et al.* (1981) and Dierschke *et al.* (1985). Following the administration of exogenous oestradiol during the early follicular phase, FSH levels dropped and the follicular phase lengthened. To investigate the effect of continuous exposure of the ovaries to elevated gonadotrophin hormones, Zeleznik *et al.* (1985) neutralised oestradiol by adding an anti-oestradiol antibody during the mid to late follicular phase. Secondary follicles were shown to be maturing in the experimental animals and not in the controls, suggesting that the determinant of follicular selection is the duration of the ovaries' exposure to elevated gonadotrophins. The maturing or dominant follicle, by producing high amounts of oestradiol, reduces gonadotrophin levels and thereby prevents continuation of secondary follicular growth. In a model of follicular growth and development, Ireland (1987) suggests, within the framework of recruitment, selection and dominance of follicles, that a number of spontaneously growing preantral follicles become responsive and dependent upon gonadotrophins, especially FSH, for their continued growth and differentiation, but that most of these follicles undergo atresia during folliculogenesis by the release of inhibitory factors from the dominant follicle, namely, oestradiol and to a lesser extent oestrone.

It has been well established that gonadotrophin release is suppressed by high oestrogen levels (Ganong, 1991). A plasma threshold of oestradiol of approximately 600 pmol/L lasting for about 50 hours positively feeds back to the brain to trigger a surge in LH (Burger, 1989), which leads to the final maturation of the follicle and ovulation. The variation in time taken to reach this threshold is now recognised as the main cause of cycle length variability among women. The first identifiable rise in oestradiol above the early follicular phase baseline which signifies the entry of a follicle into the rapid growth phase can vary from 10 to 3 days (mean 5.5 days) before the LH peak (Blackwell & Brown, 1992).

1.1.2 Steroidogenesis

Falck (1959) was the first to conclude that the production of oestradiol is dependent on an interplay between the two main cell types in the follicle of the rat. Armstrong *et al.*, (1979) formulated the working hypothesis that follicular estrogen biosynthesis occurs through the co-operation of two separate cell types, with the theca interna cells (under LH stimulation) producing the C-19 androgens (testosterone and androstenedione). These are then transported to the granulosa cells, where they are converted (under FSH stimulation) to C-18 oestrogens (oestradiol 17-β being the ovarian oestrogen), and the hypothesis became known as the "two-cell, two-gonadotrophin" theory (refer to figure 1.2; Leung & Armstrong, 1980).

A key event in the life cycle of a follicle is the expression of the aromatase enzyme in the granulosa cells which enables the androgens to be converted to oestrogens. It is now clear that a single P_{450} enzyme with a single active site is responsible for catalyzing the conversion of androstenedione to oestrone and of testosterone to oestradiol (Hall, 1998). Details of the mechanism of this reaction are of great importance because of the physiological significance of oestrogens, and the roles of these steroids in various pathological states, including cancer. The search for a mechanism-based inhibitor to control aromatase activity is at present extremely intense (Hall, 1998).

The steroidogenic pathway is initiated when low density lipoprotein (LDL) is brought into the cell via the LDL receptor system, and cholesterol is released (Hadley, 1966; Adashi, 1994); refer figure 1.3(a). Steroid hormones contain a maximum of 21 carbons whereas cholesterol contains 27 (Stryer, 1989), hence significant chemical change is required (figure 1.3b). This is brought about by a controlled sequence of enzyme

catalysed steps (figure 1.3b). Cholesterol is converted into pregnenolone by activation of the mitochondrial side chain cleavage enzyme system a (cytochrome P_{450}), where the C-20 and C-22 atoms of cholesterol are hydroxylated and then the bond between them is cleaved

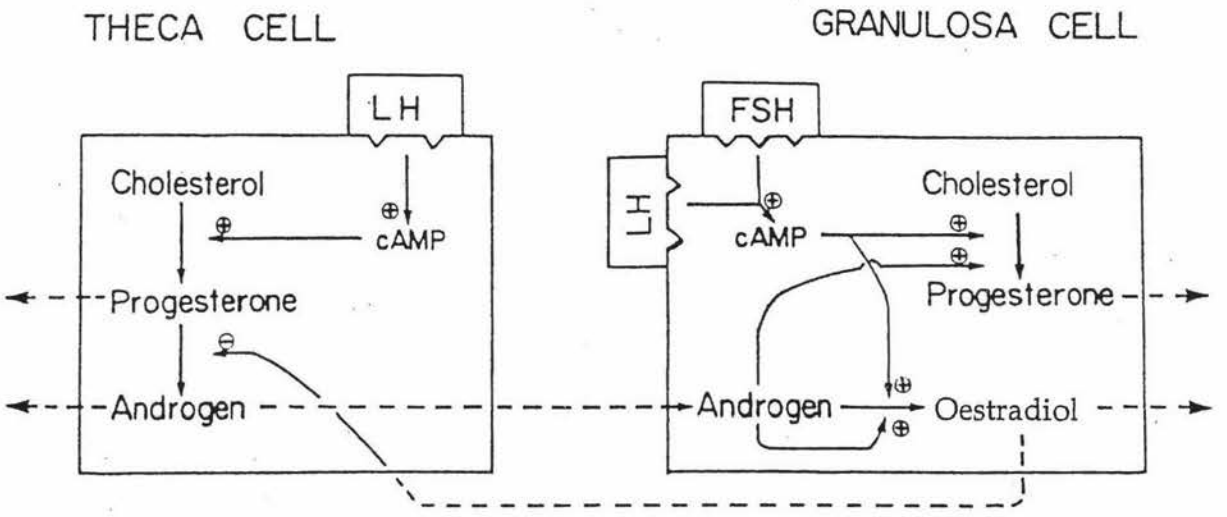

Figure 1.2: Control of steroidogenesis in the ovarian follicle; cell-cell interactions. Solid lines represent simplified steroidogenic pathways and intra-ovarian actions of various hormones, (+ stimulation, - inhibition). Dotted lines represent inter-cellular flow of steroids. [Leung & Armstrong, 1980]

Progesterone is synthesized from pregnenolone by a two step process (figure 1.3b) in which C-3 is oxidised from a hydroxyl to a ketone group by a dehydrogenase and the Δ 5 double bond is isomerised to a Δ 4 double bond. Androgen biosynthesis is dependent upon the CYP17 gene which is expressed within the ovaries, predominantly, if not exclusively by the thecal cells (and mature granulosa) and is regulated by LH which activates a cyclic AMP/Protein Kinase-A signalling pathway (Hillier *et al.*, 1994a). The expression of the CYP17 gene results in a cytochrome P_{450} enzyme called 17-α-hydroxylase and the activity of this hydroxylase is vital for steroidogenesis because without C-17 hydroxylation androgens could be neither synthesized nor metabolised to produce oestradiol (Hall, 1986; Hall, 1998), and folliculogenesis would cease. Cleavage of the side chain following C-17 hydroxylation forms the 17 keto group androgen, androstene-3,17-dione (figure 1.3b). Testosterone, another androgen (androgens always have 19 carbon atoms) is formed from androstenedione by reduction of the keto group at C-17 to give an hydroxyl group (figure 1.3b). Both androgens (androstenedione and testosterone) diffuse from the thecal cells (figure 1.2) and some diffuses into the cells surrounding the ovum, called granulosa cells.

Oestrogen biosynthesis is dependent upon the CYP19 gene which is expressed exclusively in granulosa cells and encodes another cytochrome P_{450} enzyme called oestrogen synthetase (the more popular name "aromatase" will be used here) which converts androgens to oestrogens (figure 1.3a). Granulosa cells are the only cells in the female body known to express FSH receptors (Whitelaw *et al.*, 1992). Binding of FSH to these receptors activates another cyclic AMP/Protein Kinase A mediated intracellular signalling pathway (Hsueh *et al.*, 1984), which is responsible for the induction of numerous genes crucial to mature granulosa cell follicular function. CYP19, which codes for aromatase is one of these genes (Hillier *et al.*, 1994a). The presence of androgen also promotes aromatase synthesis in the granulosa cells via an androgen receptor mediated mechanism (Hillier & De Zwart, 1981). The oestrogens are synthesized from androgens by the loss of a methyl group at C-19 and the formation of an aromatic ring by aromatase (figure 1.3a and figure 1.3b).

Oestrone retains the C-17 ketone group, whereas oestradiol having two hydroxyl groups, the C-3 being phenolic rather than alcoholic, is many times more bioactive than oestrone. Paradoxically, while granulosa cells are able to synthesize the aromatase enzyme system, they are unable to synthesize androstenedione because they do not express the CPY17

gene which encodes for 17-α-hydroxylase. While CPY17 mRNA is increased by the presence of LH, it appears that in unstimulated cells CYP17 is completely repressed, presumably because of the pressure of a negative transcription factor or the absence of a positive factor (Hall, 1998). Clearly, oestrogen production is dependent on the concerted action of both thecal and granulosa cells (Hillier *et al.*, 1994b), the "two-cell type" theory (figure 1.2). The production of the ovarian steroid hormones oestradiol and progesterone, while regulated by gonadotrophin hormones, are also involved in complex feedback loops to the hypothalamus and pituitary where they are involved in gonadotrophin hormone release.

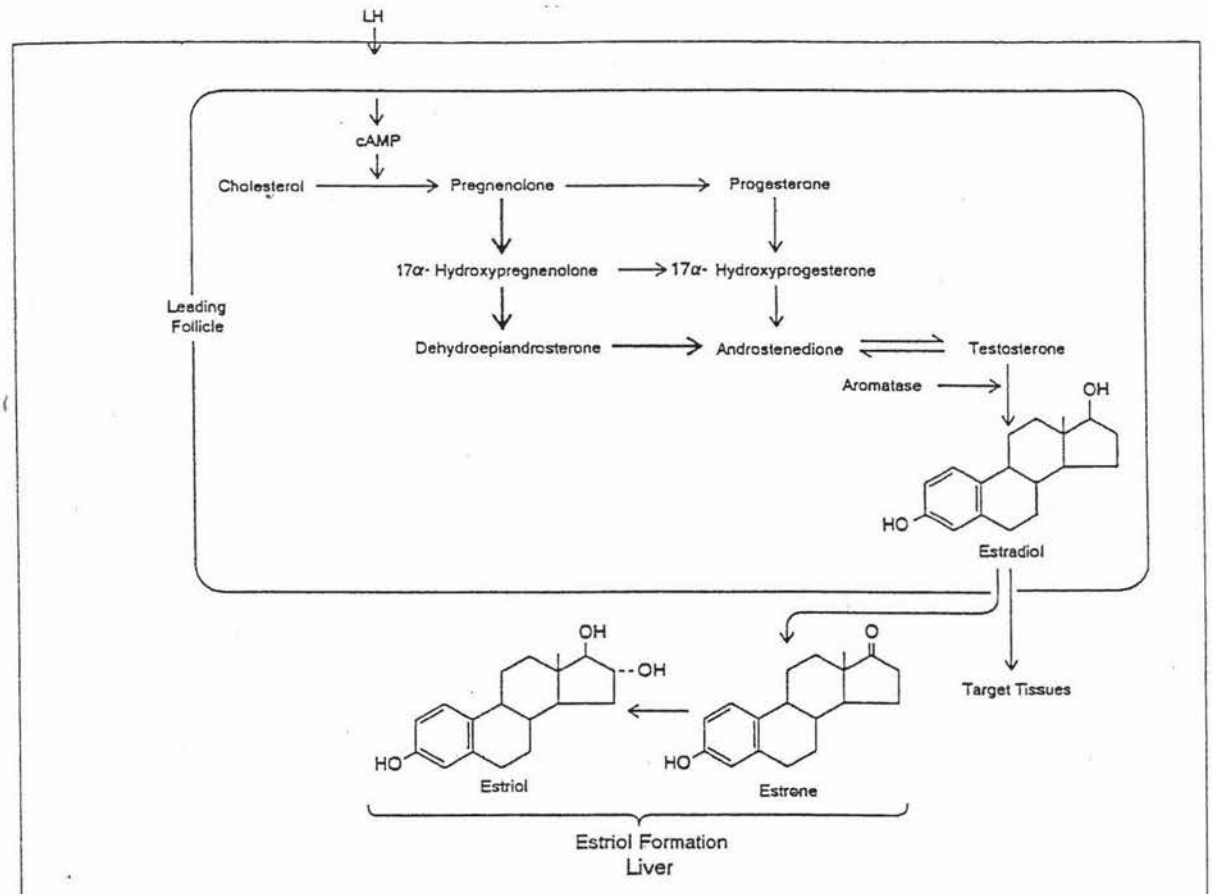

Figure 1.3(a): Biosynthesis and metabolism of oestradiol. [Hadley, 1966]

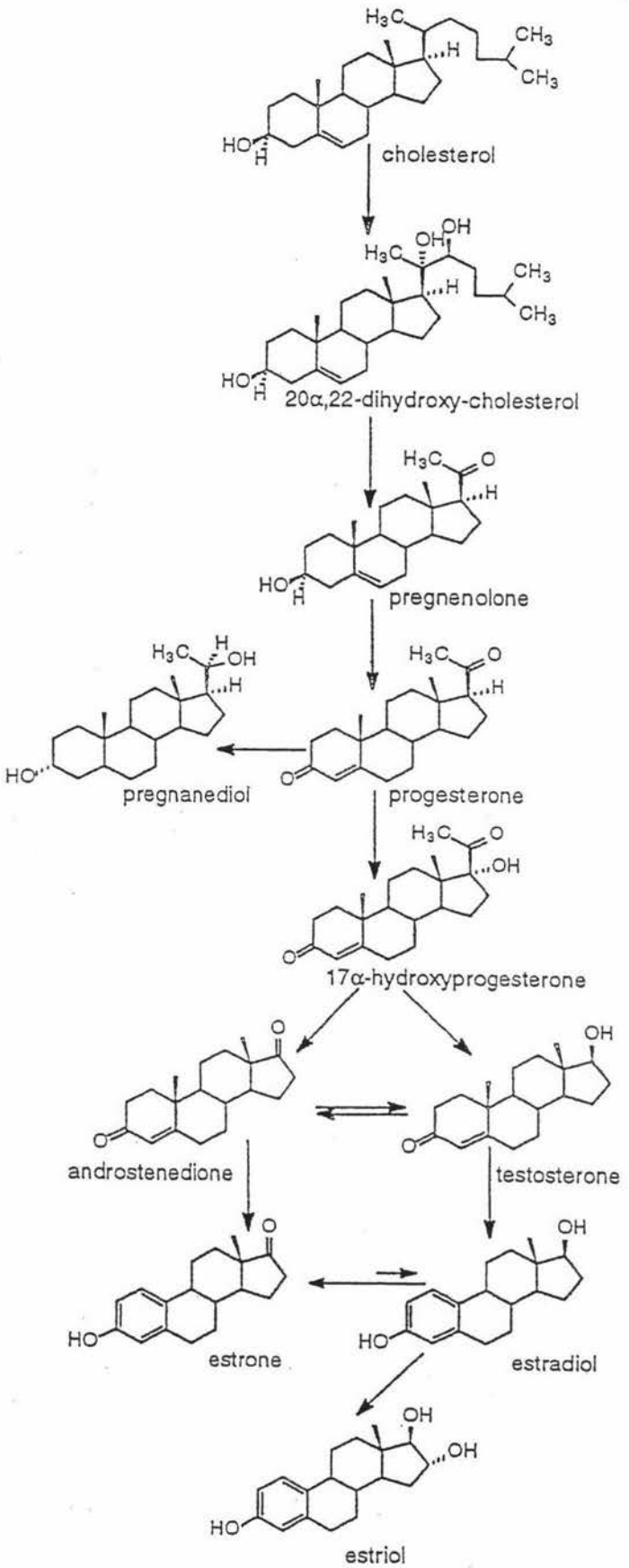

Figure 1.3(b): Biosynthesis of Oestrogens and Progesterone

1.1.2.1 Follicle Dominance

Accumulating evidence suggests that local intra-ovarian paracrine signalling mechanisms sustain the exponential increase in oestradiol production by the dominant follicle. Once it has entered its rapid growth phase androgen receptors are found in the granulosa cells of the dominant follicle and androgens have been shown to increase the FSH sensitivity of granulosa cells *in vitro*. Experimental evidence (Hillier, 1991; Findlay, 1993) shows that a protein called inhibin enhances LH-stimulated thecal androstenedione synthesis dose-dependently *in vitro*. Hillier (1991) suggests that a development related ability in granulosa cells to emit paracrine signal(s) which feedback locally to enhance thecal androgen synthesis is likely to involve inhibin. Locally produced androgens are also vitally important to follicle dominance. Knowledge of how each pre-ovulatory follicle escapes atresia is dependent upon understanding the FSH initiated onset of oestradiol synthesis. Elucidation of the molecular mechanisms and hormonal regulation of the suicide program in ovarian follicular cells should help in the design of new therapeutic modalities for the treatment of ovarian disorders characterized by excessive cell degeneration and infertility, such as premature ovarian failure and polycystic ovary syndrome (Kaipaia & Hsueh, 1997).

1.1.2.2 *The Potentially Fertile Phase*

After the key event (LH induction of the aromatase gene CYP19), when the dominant follicle starts to grow, a rise in ovarian oestradiol as a result of aromatization can be expected and this is a marker for the beginning of the potentially fertile phase. Once a follicle enters its rapid growth phase there are only two alternatives: it can proceed on to ovulation or undergo atresia. The dominant follicle grows to produce over 90% of circulating oestrogens in the body, rising about 4-fold per day during the four to five days leading up to ovulation (Hillier *et al.*, 1994a; Baird & Fraser, 1974). The pre-ovulatory exponential oestrogen increase associated with follicular growth (figure 1.1) generally begins 5-7 days before ovulation, but women vary in the time which a follicle takes to mature and grow (Czekala *et al.*, 1986). Although the pattern of total oestrogen excretion is constant for each woman, the actual amounts found in the urine of different women vary over a considerable range (Brown, 1955). Therefore, because the follicular phase is of variable length, the pre-ovulatory oestradiol surge is difficult to predict accurately. The oestradiol peak is usually taken as the mid-cycle marker, and ovulation follows approximately 36 h afterwards (Brown *et al.*, 1989). Thus any rise in total oestrogen excretion above a preceding baseline is an important marker to detect because it signals

follicular growth, and the beginning of potential fertility.

It is well established that the human ovum is viable for fertilization for a relatively short time after erupting from its follicle (Austin, 1975). The survival time of the ovum is short, being 12-24 hours or less (Wilcox *et al.*, 1995). Although fertilization can only occur after the release of the ovum from the follicle, evidence from epidemiological research indicates that the fertilizing life of sperm is about five days, and less commonly eight days. Austin (1975) reported that the chances of conception were less than 5% 5 days before ovulation, reaching a maximum the day before ovulation and falling below 5% 10 h after ovulation. According to the World Health Organisation (1983) the mean survival time is 3-4 days. The survival of the sperm depends in part on the presence and quality of the cervical mucus and elegant studies by Professor Odeblad in Sweden (1994) have shown how the sperm may survive in cervical crypts for long periods of time in the presence of the so-called fertile mucus. Brown *et al.* (1989) reported several pregnancies resulting from 5-day sperm survivals as determined by hormone assays, and perhaps one resulting from a six day sperm survival, and therefore, more accurate objective methods for timing ovulation are required for further studies.

The luteal phase, which follows ovulation, lasts on average 14 days (Berkow, 1987), a range of between 11 to 17 days (Brown *et al.*, 1979) being normal. The rise in the level of progesterone as the corpus luteum is established indicates the end of the potentially fertile period. Various markers for the begining and the end of the fertile period have been considered, and are discussed below.

1.1.3 Fertility Markers

Good fertility markers need to accurately reflect ovarian activity, to be rapidly available for measurement, to be present in high concentrations, and show a large difference between baseline and peak levels.

1.1.3.1 *Self-Observed Indicators*

While patterns of cervical mucus (probably types of glycosaminoglycans, formerly called mucopolysaccharides) and temperature both are often good markers of the fertile period (Billings *et al.*, 1972), the numerous reasons for mucus variations such as sexual intercourse, sexual arousal, infection and other physiological phenomena, and for temperature variations, such as fever, time of day, physical exertion, excitement/anxiety

or alcohol means allowance needs to be made for these factors when using these methods. Consequently, the potentially fertile time on average is defined as lasting 17 days, for example using the Billings ovulation method (Billings *et al.*, 1972; Brown *et al.*, 1989). For this reason there has been continuing interest in the use of hormone measurements and other techniques as additional markers for the definition of the fertile period.

1.1.3.2 *Urinary Steroids*

Because steroids are more concentrated in urine than in blood they are more easily detected, and the urinary patterns of steroid excretion are well documented (Klopper *et al.*, 1955). The relatively non-invasive nature of urine sampling is of considerable importance from a practical point of view (Blackwell & Brown, 1992; Lasley *et al.*, 1994). Serum assays have the advantage that they measure the levels of circulating analyte at the time of sampling, whereas urine samples often have the disadvantage that they can only be used to measure a metabolite of the analyte, and then only after its excretion (i.e. the appearance of an analyte or its metabolite in the urine is determined by the compounds metabolic clearance rate). Because ovarian hormone production often increases and decreases very rapidly (Baird & Fraser, 1974) interpretation of serum hormonal levels is difficult to assess and therefore the measurement of the rate of excretion of urinary compounds is a better alternative. Furthermore, urinary excretion rates are more closely related to ovarian secretion rates of oestradiol and progesterone, and integrate the pulsatile secretion of these hormones (Kulin *et al.*, 1975). To correct for variation in urine production, specimens are diluted, for example to 150 ml/h for use in the Ovarian Monitor, (refer section 1.1.5) and timed over a minimum collection period of three hours (Brown *et al.*, 1989), yielding a more accurate measure of real changes in ovarian hormonal excretion rates. Any temporary variations in serum levels are automatically averaged out if the associated urine specimens are "timed", and the collection period is long enough to minimize the influence of short-term biological variations (Csako, 1996). Urinary free steroid hormones (as hydrolysis products) often occur in the presence of high concentrations of related metabolites (glucuronides and sulphates) and can interfere with the analytical assay, due to antigenic cross-reactivity (Csako, 1996). However, this effect may be largely overcome by using fresh urine. Deviations from normal excretion patterns may represent altered liver and renal metabolism as well as changes in the production of the steroid (Whitley *et al.*, 1996). Antibodies need to be raised against the urinary form of the steroid (Luke *et al.*, 1988), because the molecule is immunochemically altered from that present in blood. A non-invasive determination of the chemical flow of information

between the ovaries and the hypothalamic-pituitary axis, by the measurement of the excretion rates of time-diluted urinary metabolites allows predictions to be made about potentially infertile and fertile phases of the menstrual cycle.

Urinary steroid concentrations have traditionally been adjusted using creatinine on the assumption that the excretion rate is constant, however recent research (Zacur *et al.*, 1997) has found that mean baseline urinary creatinine declined with increasing age in non-smokers and was not affected by race or baseline weight. For example, an excellent correlation between PdG and serum progesterone existed except when PdG concentrations were adjusted using creatinine measurements in older individuals (Zacur *et al.*, 1997), and therefore creatinine adjustment was unacceptable for the present study.

1.1.4 Choice of Steroid Markers

1.1.4.1 *Choice of Oestrogen as a Marker for the Beginning of the Potentially Fertile Phase:*

The principle oestrogen secreted by the ovaries during the follicular phase is 17-β-oestradiol, but this is extensively metabolised on entering the peripheral circulation. Although the main circulating oestrogen in the plasma of the human female is oestrone sulphate, the three oestrogens produced in significant quantities in the human female are β-oestradiol, oestrone and oestriol (Baird & Fraser, 1974). Oestriol is a very weak oxidative product derived from oestradiol and oestrone and formed mainly in the liver (Hadley, 1996). As oestradiol is derived almost exclusively from the ovaries, its measurement is often considered sufficient to evaluate ovarian function. Further, amounts are large enough to be measured by assay, for example the production of oestradiol is approximately 100 to 300 µg/day, and oestrone is approximately 100 to 200 µg/day in normal non pregnant women (Whitley *et al.*, 1996).

The ovary is not the only source of oestrogens; oestrone is also produced at an approximately constant rate throughout the cycle by peripheral aromatization of androgens, mainly derived from the adrenals, as well as low levels from the ovaries. In contrast to ovarian production peripheral aromatisation of adrenal androstenedione to oestrone is much greater than the aromatisation of adrenal testosterone to oestradiol (Baird *et al.*, 1969; Baird & Fraser, 1974), thus the major circulating oestogen in plasma is oestrone sulphate. Adrenal androgen aromatization is the source of the more or less constant oestrogen baseline observed in the early follicular phase (Brown *et al.*, 1989) and

hidden (the iceberg effect). The first detection of oestrogen increase above baseline therefore is taken as the beginning of the pre-ovulatory potentially fertile phase.

1.1.4.2 *Oestrogen Metabolism*

In the ovary, the equilibrium position is such that 17 β-oestradiol is the major aromatisation product and is the major oestrogen of biological importance (Hall, 1985; Hall, 1998). Once the 17 β-oestradiol leaves the ovary, the equilibrium shifts in favour of the formation of oestrone and as a result the metabolite oestrone sulphate is the major circulating steroid in ovulating women (Baird & Fraser, 1974). Oestradiol is metabolised to the less bioactive oestrone by oxidation of the 17α-OH group by transhydrogenases within the liver (Hadley, 1996), the major site of metabolic transformations of oestrogens. Oestrone may then become α-hydroxylated at the 16 position before 17 keto reduction to form oestriol, the least bioactive of the oestrogens (figure 1.3a); by hepatic conversion within the peripheral circulation (Ganong, 1991; Whitley *et al.*, 1996). This is an important control feature of steroid metabolism as the rapid removal of potent oestrogens is necessary to ensure the rapid response of the body to changes in the level of oestrogen production in the ovaries (Baird & Fraser, 1974).

Oestradiol 2-hydroxylase in brain tissue converts oestrogens to catecholeoestrogens by hydroxylation at the C-2 position of the aromatic A ring. Higher concentrations of these compounds are found in the pituitary and hypothalamic regions of the brain, compared to native oestrogens, where they are likely to play a physiological role in feedback regulatory mechanisms (McEwen, 1976).

Oestrogens and their metabolites are excreted primarily as water soluble glucuronides, sulphates and mixed glucuronides and sulphates synthesized in the liver. The principle conjugates are the C-3 glucuronates of oestrone (oestrone-3-glucuronide or E1-3G) and of 2-hydroxyoestrone (2-hydroxyoestrone glucuronide or 2-OH-E1-3G) and oestrone sulphate esterified at C-3. Sulphonation at C-17, as well as formation of the 3,17-disulphate of oestradiol also occurs in urine.

Although there is a large range of values about the mean for the daily rate of urinary excretion for each of the three main urinary oestrogens as measured individually by the split oestrogen method (the separate measurement of oestrone, oestradiol and oestriol), the ratios between the various oestrogens do tend to be relatively constant throughout the

menstrual cycle for a given woman (Brown, 1955). Five urinary steroid metabolites (Table 1.1) were originally assessed during the development of an homogeneous immunoassay using lysozyme, incorporated in what is now known as the Ovarian Monitor.

Table 1.1: The Oestrogens and their Major Urinary Metabolites

Steroid	Steroid Conjugate	Abbreviation
Oestrone (E1)	Oestrone-3-glucuronide	E1-3G
	2-Hydroxyoestrone-glucuronide	2-OH-E1-3G
Oestradiol (E2)	Oestradiol-17 β-3-glucuronide	E2-17 β-3G
Oestriol (E3)	Oestriol-16-glucuronide	E3-16G
	Oestriol-3-glucuronide	E3-3G

Oestradiol glucuronide (E2-17 β-3G) is present in the urine at low concentrations, and is not a major urinary metabolite of oestradiol (Musey *et al.*, 1972), even though it is the first metabolite to be excreted (Hobrick & Nilsen, 1974), and has a steep rise from baseline values (Stanczyk *et al.*, 1980). Oestriol glucuronides (E3-3G and E3-16G), although excreted in large amounts, have limitations as a fertility marker because excretion is delayed by approximately 12 hours due to a complex enterohepatic circulation involving bilary excretion and reabsorption (Brown, 1955). Simultaneous studies in five major centres world-wide have focused on a choice of either oestrone-3-glucuronide, oestriol-3-glucuronide or oestriol 16-α-glucuronide as possible oestrogen metabolites to act as markers for the beginning of fertility (Adlercreutz *et al.*, 1982). Oestrone-3-glucuronide (referred to as E1-3G) correlates better than either oestradiol glucuronide or oestriol glucuronide with circulating levels of oestradiol, (Baird & Fraser, 1974; Baird *et al.* 1969), due to the conversion of oestradiol to oestrone in the liver and was finally selected as an oestrogen marker for the first oestrogen rise (Adlercreutz *et al.*, 1982). Next to oestradiol glucuronide, E1-3G has the highest ratio of peak to baseline prior to ovulation, it is found in the urine at five times the concentration of E2-17 β-3G and is usually excreted rapidly. The major disadvantage of measuring E1-3G is its possible lack of suitability for all women, as not all women excrete oestrone as a major urinary metabolite. In some women most of the oestradiol and oestrone is metabolised to oestriol conjugates (Conway, 1986) and for this minority of women it would be better to assay for oestriol conjugates or the sum of the two.

1.1.4.3 *Excretion Profile of E1-3G*

The total urinary oestrogens (the sum of oestrone, oestradiol and oestriol) can be measured by the chemical method of Brown *et al.* (1968), a highly specific (Kober-Ittrich) and accurate procedure. There is a close correlation between the rate of urinary total oestrogen excretion measured by this procedure and the rate of serum oestradiol excretion (refer figure 1.1), and since there is also a close correlation between circulating levels of oestradiol and E1-3G, this method constitutes a reference assay against which E1-3G levels obtained using immunoassay techniques were validated. During the follicular phase the baseline oestrogen excretion is almost always under 20 µg/24 h (Brown *et al.*, 1989) for the total oestrogen assay of Brown *et al.* (1968), equivalent to 100 nmoles/24 h for E1-3G using the Ovarian Monitor (figure 1.4). From a database of 140 ovulatory cycles Brown *et al.* (1989) reported that baseline urinary oestrogen levels differed considerably between women (4-20 µg/24 h), and the length of time between the first identifiable rise in oestrogen excretion above this baseline and the pre-ovulatory oestrogen peak position varied from 10 to 3 days. A method capable of distinguishing between 19 and 23 µg/24 hrs was therefore recognised as being required for identifying the follicular phase oestrogen rise approximately four days before the pre-ovulatory peak (-4) and 5-6 days before ovulation. This defines the order of sensitivity (4 µg/24 h), and precision of an assay required for the earliest identification of the urinary oestrogen rise. It is essential that noise contributed by the assay is minimal so that the rise can be distinguished as early as possible and to define the day of maximum fertility (i.e. day of ovulation) for the sub-fertile couple. Ovulation occurs approximately 36 hrs after the total oestrogen peak (Blackwell *et al.*, 1992), or 24 hrs after the serum LH peak. The total oestrogen peak was approximately 100 µg/24 h (Brown *et al.*, 1989), equivalent to a rate of E1-3G excretion of 213 nmoles/24 h, analysed from 61 ovulatory menstrual cycles from 40 fertile women aged 20-40.

Blackwell & Brown (1992) applied Trigg's tracking signal procedure (Trigg, 1964) to a database of 142 cycles to determine the first statistically significant increase as a marker for the beginning of the potentially fertile phase. In the menstrual cycle successive oestrogen observations are serially dependent (or correlated) once a follicle enters its rapid growth phase. Thus, from this point onward oestrogen values can be predicted with a variable degree of accuracy. This serial dependence forms the basis of a statistical approach to chronological data known as time-series or trend analysis (Chatfield, 1984). One method of trend analysis (Brown, 1962) has been modified (Trigg, 1964) and

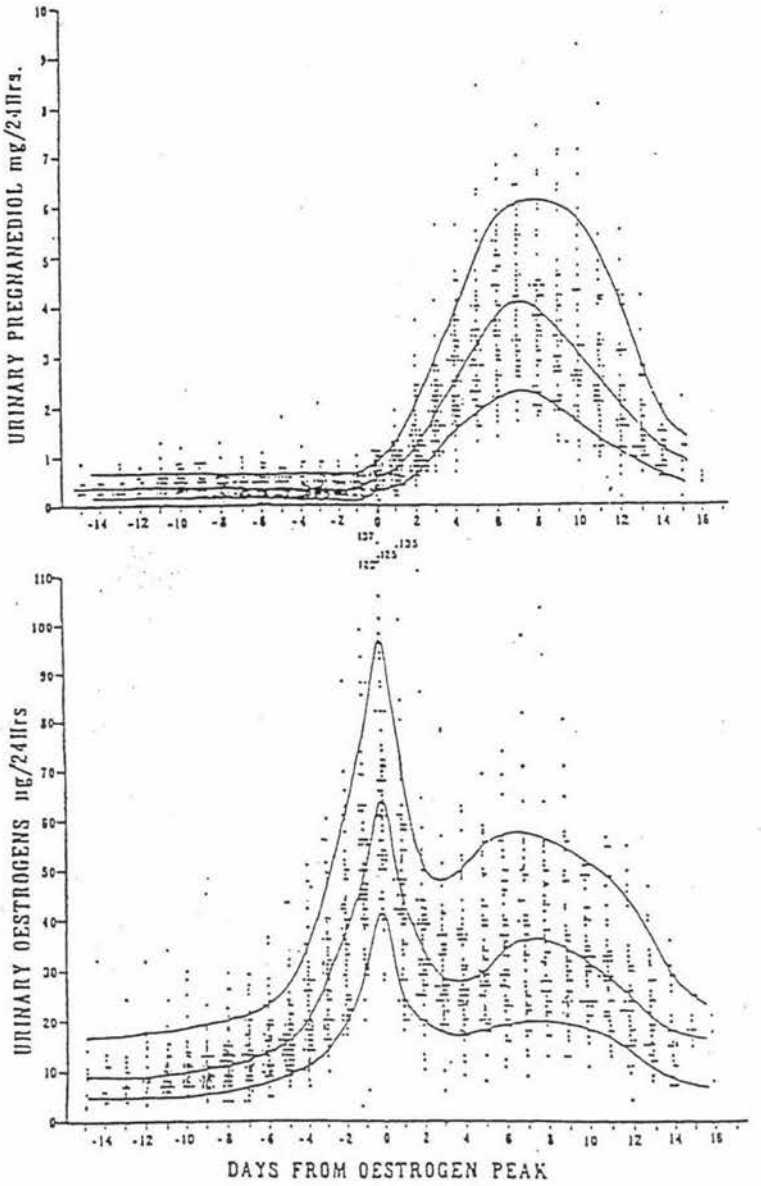

Figure 1.4: Daily urinary oestrogen and pregnanediol values throughout 61 ovulatory cycles from 40 women aged 20-40 years. The 10th, 50th and 90th percentile lines are shown. Days are numbered from the day of the pre-ovulatory oestrogen peak (day zero). [Brown *et al.*, 1989]

optimized (Cembrowski *et al.*, 1975) for the detection of long-term systematic changes in a mean value. Only non-random changes in the data will result in the steadily increasing or decreasing smoothed forecast errors (SFE) indicative of significant increases or decreases in the mean. The statistical measurement of the significance of these changes from the mean is based on the ratio known as Trigg's tracking signal (Trigg, 1964). Trigg's tracking signal is the normalised smoothed forecast error and was calculated by dividing the smoothed forecast error by the mean absolute deviation to determine the first total oestrogen rise (Blackwell & Brown, 1992).

Results showed total urinary oestrogen baselines varied from 3 to 28 µg/24 h, with the majority of the 142 individual cycles being between 3-16 µg/24 h, and 10% between 16-28 µg/24 h, while only 4% (6) had a baseline over 20 µg/24 h. For the majority of the women after 20/µg 24 h was reached the total oestrogen values increased progressively without interruption to the peak value and then decreased rapidly. The peak values ranged from 40 µg/24 hr to 100 µg/24 h with a mean of 60 µg/24 h total oestrogen. The values obtained were approximately 68% of the true value for the sum of oestriol, oestrone and oestradiol with a coefficient of variation of 8% (n=100).

1.1.4.4 *Marker for the End of Fertility: Choice of Progesterone*

Predictions about the end of the potentially fertile phase taken from the oestrogen peak are not reliable evidence of ovulation because several peaks may be observed before ovulation occurs (Brown *et al.*, 1988). Further, ultrasound measurements have shown the relationship between the urinary LH peak and the process of ovulation to be variable (Blackwell *et al.*, 1998). For example, Bischof *et al.* (1991) reported the urinary LH peak preceded ovulation by from 9 to 51 h (n=35), while in a small but significant number of women Adekunle *et al.* (1988) reported 33% of LH peaks occurred after ovulation. Clearly, as for the oestrogen peak, the urinary LH peak can not be accurately used to make predictions about the end of the potentially fertile phase. Progesterone was chosen as a more reliable end of fertility marker than either the oestrogen peak or the luteinizing hormone peak, because although, as has been well documented, the pre-ovulatory oestrogen peak occurs approximately 36 hours prior to ovulation, and the luteinizing hormone surge generally occurs 17 hours prior to rupture, there are unacceptable levels of variability within the system. The biosynthetic pathway for the formation of progesterone from cholesterol is via pregnenolone, and progesterone is an intermediate in androgen synthesis. The beginning of the luteal phase following ovulation is

accompanied by a rapid rise in progesterone production, which is associated with the luteinization of the follicle (Blackwell *et al.*, 1998; Hoff *et al.*, 1983). A surge in blood progesterone concentrations can be used to indicate the phase of absolute infertility in the fertile cycle, which lasts until the time of the next menstruation (Brown *et al.*, 1991). While circulating progesterone levels increase essentially in a biphasic fashion, Hoff *et al.* (1983) showed there were multiphasic increments prior to ovulation. A first phase just prior to ovulation shows an increase of circulating progesterone that parallels the rising oestradiol levels, with a doubling time of 57.6 hours. The second phase begins with a sudden increase in progesterone, with a new doubling time of 12.2 hours, beginning 12 hours before and lasting until 12 hours after the onset of the LH surge. A third phase, a plateau, occurs between 14 and 34 hours after the onset of the LH surge, and then is followed by a final phase, consisting of another rapid rise with a doubling time of 11.7 hours which continues for about 7 days (Hoff *et al.*, 1983). The initial phase of progesterone production, being parallel to the rate of oestradiol production, may reflect the acquisition of LH receptors by the granulosa cells of the leading follicle.

1.1.4.5 *Excretion Profile of PdG*

As pregnanediol-3 α-glucuronide (PdG) is the major urinary metabolite of progesterone a marked post-ovulatory rise in urinary PdG following the second-phase increase in serum steroid levels should provide a strong marker for the end of fertility. PdG is excreted in large amounts and correlates well with circulating progesterone levels, (Adlercreutz *et al.*, 1982; Munro *et al.*, 1991). Although PdG is also derived in low levels from pregnenolone from the adrenal gland (Adlercreutz *et al.*, 1982), excretion from this source is at a constant level, around 2 to 4 μmoles/24 h throughout the follicular phase, and effectively constitutes the PdG baseline. Surprisingly, identification of the end of the fertile phase has proved difficult. Early morning urine samples analysed from a number of centres (Adlercreutz *et al.*, 1982) gave a significant percentage of contradictory data, where the end of the fertile phase occurred before ovulation, using PdG as an end of fertility marker. Preliminary experiments for detecting the first significant rise in urinary PdG as a marker of infertility were also performed by Blackwell *et al.* (1998), using a time-series analysis of a database of pregnanediol (Pd) data obtained from time diluted urine samples representing 113 cycles and contributed by 83 women of proven fertility. The pregnanediol determinations were performed by the method of Barrett and Brown (1970), which involved acid hydrolysis of the sample, extraction of the neutral fraction and then measurement of the Pd by gas liquid chromatography (GLC). Only small amounts of free

Pd are ever excreted in the urine, and so the measured amount of Pd should accurately reflect the rate of PdG excretion which is the source of the Pd analysed by this method after hydrolysis. The time-series results though were unsuccessful: Of all the cycles for which a pregnanediol baseline period was available (N=170), at a 95% confidence level, 33% of the cycles showed a significant pregnanediol rise before or on the day of the total oestrogen peak, while the remaining 67% showed a significant rise following the total oestrogen peak day. Remembering that the oestrogen peak usually occurs one day (36 h) before ovulation, and that the lifespan of the ovum is often only 12 to 24 hours, the fertile period does not end until the second day following the oestrogen peak. Even at a confidence level of 99%, 22% of the cycles still gave false negatives of fertility, showing a significant rise in pregnanediol excretion on or before the day of the pre-ovulatory peak which is clearly unacceptable as an end of fertility marker.

As an alternative to marking the end of the fertile period by the determination of the first significant rise in pregnanediol excretion, further studies by Blackwell *et al.* (1998) focused on obtaining a threshold value for pregnanediol from the database as a reliable marker. Because the mean concentration of pregnanediol in the pre-ovulatory rise was 0.71 ± 0.25 mg/24 h, the minimum value which could serve as a threshold value was taken as 1.2 mg/24 h (mean + 2 standard deviations). Three threshold pregnanediol values (1.2, 1.4 and 1.6 mg/24 h) were next chosen, and all cycles from the database for which both the known oestrogen peak day and sufficient pregnanediol data were available (N=181) were analysed with these. At the lowest level (1.2 mg/24 h), 1.6% of the urine samples gave false positives, and were reached on or before the day of ovulation. Threshold values of 1.4 and 1.6 mg/24 h gave no false positive results, but the 1.6 mg/24 h threshold was deemed unsuitable, as this was not reached in some cycles until days +6, +7 or +8 relative to the presumed day of ovulation or the peak day. The threshold value of 1.4 mg/24 h was therefore chosen. Further support for this value came from the fact that once this level was reached, no cycle in the database showed evidence of subsequent ovulation until after the next bleed (as indicated by the hormonal patterns and the length of the luteal phase). The Pd value of 1.4 mg/24 h is directly equivalent to a PdG value of 6.3 µmoles/24 h when measured by the Ovarian Monitor based on the 24 hour urine volume, the relative molar masses and the percentage of recovery (cleavage) of the Pd assay procedure. This "cut-off" value of 6.3 µmoles of PdG per 24 hours applied to all women provided correction was made for urine volume (Brown *et al.*, 1989; Munro *et al.*, 1991). Thus this level constitutes a "threshold" at and above which pregnancy can not occur and

a threshold value of 6.3 µmoles/24 h of PdG was chosen as a marker for the end of the fertile cycle (Blackwell *et al.*, 1998). This value accommodated the pre-ovulatory rise (avoids the errors or false positive results associated with the first significant rise from the PdG baseline), as well as variable follicle growth times (the variable length of the pre-ovulatory oestrogen surge) and baseline levels. The days when the PdG value reached 6.3 µmoles/24 h were clustered between two days after the pre-ovulatory oestrogen peak (day +2) and day +5 (Brown *et al.*, 1989). Day +2 may appear to be too close to ovulation for safety. The fact that no pregnancies in use of this threshold (Blackwell *et al.*, 1998) occurred indicates that the PdG rise is probably more closely related to the time of ovulation at this critical time than is the E1-3G peak, and supports the view that the fertilizable life-span of the ovum after ovulation is very short. Mean Pd levels at mid luteal phase were 6-7 mg/24 hrs (Brown *et al.*, 1989), over 61 cycles from 40 fertile women (figure 1.4). Thus post-ovulatory changes are identified very clearly and unambiguously. The PdG excretion profile shows baseline levels during the follicular phase, followed by the biphasic PdG rise, (i.e. the small pre-ovulatory rise, and the PdG rise as the corpus luteum is established).

1.1.4.6 *Sensitivities Required for E1-3G and PdG Assays*

Brown *et al.* (1988) showed that a home assay must be able to measure E1-3G at levels of 25-50 nmoles/24 h equivalent to a total oestrogen value of 7 -14 µg/24 h and PdG at levels of 3 µmoles/24 h equivalent to a PdG value of 0.7 mg/24 h to be useful. Brown *et al.* (1998) later argued that a home assay required a sensitivity for E1-3G of 15 nmoles/24 h, and for PdG of 3 µmoles 24 h, with a coefficient of variation of less than 10%. Furthermore the PdG assay must be maximized to measure the threshold value of 6.3 µmoles/24 h (Blackwell *et al.*, 1998), with absolute reliability. Although the theoretical potentially fertile period is approximately seven days, current hormonal assays which are applicable for all women require an assay with improved sensitivity to better define the potentially fertile days.

1.1.5 The Ovarian Monitor

The Ovarian Monitor is a device to measure E1-3G and PdG hormonal levels at home (figure 1.5). This homogeneous lysozyme immunoassay has been developed over many years (Brown *et al.*, 1988; Brown *et al.*, 1989) and was originally calibrated against the chemical reference methods used by the Melbourne group. The working range of the PdG standard curve using the Ovarian Monitor also provides an indication of the PdG rise

which occurs before the PdG threshold value of 6.3 µmoles/24 h is reached, marking the end of the fertile period (Blackwell *et al.*, 1998). Furthermore, the Ovarian Monitor has been set to be at its greatest sensitivity over the range of 2 to 9 µmoles/24 h, which is the range of greatest information (near the PdG threshold of 6.3 µmol/24 h) in the present application (Blackwell *et al.*, 1998).

These lysozyme immunoassays are being used routinely in the laboratories of two hospitals in Melbourne for the management of infertile women. The E1-3G lysozyme immunoassay has been used since April 1987 for monitoring oestrogen responses during hyperstimulation in a large *in vitro* fertilization (IVF) programme requiring up to 60 assays per day, 7 days a week. Unlike the GLC method (refer section 1.1.4.5), the Ovarian Monitor assay for PdG has a small urine bias which becomes noticeable at the lowest levels of PdG (Brown *et al.*, 1988), therefore data require larger changes from baseline levels before a statistically significant rise is registered than with the Pd data.

The Ovarian Monitor assay is based on the direct homogeneous enzyme immunoassay procedure first reported by Rubenstein *et al.* (1972) in which lysozyme was conjugated to carboxymethylmorphine by a mixed anhydride coupling reaction. The lysozyme activity was then determined by changes in light transmission of a suspension of the bacterial substrate *Micrococcus lysodeikticus*. Rubenstein's research showed that the addition of morphine antibodies inhibited the enzyme activity of a lysozyme conjugate with carboxymethylmorphine up to 98%. Furthermore, the more free morphine added to the assay system the less inhibited the enzymatic activity became, thus inhibition was inversely proportional to the amount of free morphine in the system. As a consequence this system could be used to measure the concentration of morphine by a simple lytic assay measurement.

Hen egg white lysozyme (HEWL), conjugated to the appropriate steroid glucuronide (E1-3G or PdG) is used for the lysozyme Ovarian Monitor assay. Three dimensional models of lysozyme-EIG conjugates with bound anti-progesterone antibody (Smales, 1997) indicate that the large bacterial substrate (*Micrococcus lysodeikticus*) cannot approach and/or bind productively into the active site of the enzyme. Because the enzyme in the immune complex is sterically inhibited (and hence not active) a simple measurement of the lytic activity gives a direct measure of the hormone concentration without resorting to any time consuming separation steps.

The apparatus for the Ovarian Monitor, consists of a small photometer to measure and display solution turbidity, and a specially designed capped cuvette. Since the assay is homogeneous all of the constitutents of the assay can be freeze dried into a single assay tube (enzyme conjugates, antibodies and bacteria). The various freeze dried reagents of the assay are attached at optimal positions relative to each other within the assay tube, to maximize the efficiency of the three separate individual assay reactions which are carried out sequentially within the same tube (figure 1.5) (Brown *et al.*, 1988).

The assay begins by placing 50 µl of time-diluted urine into the cuvette. Antiserum containing an antibody specific for the hormone to be measured and coated on the bottom of the tube, either E1-3G or PdG, dissolves in the mixture of urine and buffer salts. Five minutes incubation time allows the free steroid glucuronide in the urine to bind with the antibody (the binding of steroid to antibody is effectively irreversible on the time scale of the assay, from an equilibrium point of view).

In the second step, distilled water (220-300 µl) is added to dissolve the steroid glucuronide lysozyme conjugate freeze dried in sucrose on the wall of the assay cuvette. Horizontal shaking followed by ten minutes incubation allows free antibody remaining from the first step to bind to the steroid glucuronide part of the conjugate thereby sterically inhibiting the active site of the lysozyme component. The amount of antibody available to bind to the conjugate complex will be inversely proportional to the amount of antibody neutralised by free steroid glucuronide during the first step.

Finally, in the third step, *Micrococcus lysodeikticus*, a bacterial substrate for HEWL, is suspended by quickly shaking the assay tube. The assay tube is then placed into the pre-heated (40°C) cell of the Ovarian Monitor. Because HEWL cleaves cell wall polysaccharides, the mechanical strength of the cell is reduced and the cell bursts under its internal osmotic pressure. As bacterial cells are lysed by the free lysozyme conjugate a clearing of the turbid bacterial suspension enables a measurement to be made of the change in the transmission of light through the sample by the Ovarian Monitor. The amount of lytic activity depends on the amount of conjugate which has been sterically inhibited by the appropriate antibodies. A first light transmission value is recorded and the tube is left incubating at 40°C until the second transmission value is recorded and the difference between the transmission values (ΔT) with respect to time (a choice of 5 minutes for PdG or 20 minutes for E1-3G is programmed by a switch) is a direct measure

of urinary levels of the corresponding steroid glucuronide. The PdG incubation time is shorter because excretion rates are about 100 times higher than those for E1-3G. The change in transmission values with respect to time are plotted against known concentrations of either E1-3G or PdG to produce a standard curve.

Since the standard curves of the freeze dried tubes are so reproducible, there is no need to run one with each assay (Cook, 1993). This means that it is possible to do a one-off assay for either E1-3G or PdG whenever it is required, and the hormonal result can be calculated by reference to the standard curve provided for the batch of tubes rapidly and with a high degree of accuracy. A typical cycle is illustrated in figure 1.6 as defined by the Ovarian Monitor. The data (Blackwell, unpublished results) produced by a woman in a study conducted by the World Health Organisation of the Ovarian Monitor (figure 1.6), shows the first definite rise in the rate of E1-3G excretion at day 11, with the peak value occurring on day 15. Ovulation is presumed to occur on average 36 hours after this peak day (Brown *et al.*, 1989). Day 19 shows the first PdG rise equal or above the 6.3 μmoles/24 h threshold, and marks the first day of infertility. Therefore the data provides for 6 days warning of an 8-day fertile period. A working range of about 100 to 800 nmoles/24 h for E1-3G is sensitive enough to provide sufficient warning of an oestrogen rise, and to allow measurement of the oestrogen peak without extra dilution of the urine samples. The working range of the PdG standard curve also provides indication of the PdG rise before reaching the threshold value of 6.3 μmoles/24 h, marking the end of the fertile period (Blackwell *et al.*, 1998).

1.1.5.1 *The Limitations of the Ovarian Monitor*

While the Ovarian Monitor provides clear and useful results for people who wish to monitor fertility, there is a perception that the assay is difficult to learn and the results hard to interpret. Clearly, a more user-friendly assay would be desirable. Although there is no doubt that both the E1-3G and PdG assays are completely suitable for application in the majority of patients being treated for infertility (Brown *et al.*, 1989), infertility clinics involved in IVF and embryo transfer programs also require more sensitive and rapid assays. There is a research group at Massey University involved in developing new methods to replace the present lysozyme immunoassay, and their research is aimed at producing a colour test, which is expected to be much faster and simpler than the Ovarian Monitor in use. One of the main obstacles to achieve the new colour test strip has been the limitations of the human eye. It can not discriminate between the small increases in

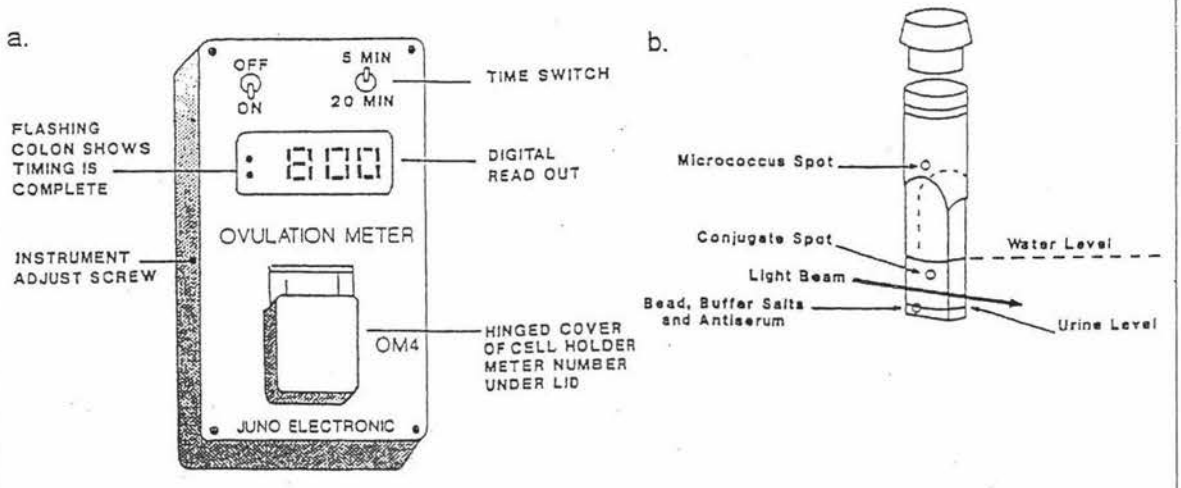

Figure 1.5: Illustration of the Ovarian Monitor, a., which measures the transmission of light passing through a sample-containing Immunotube, b.

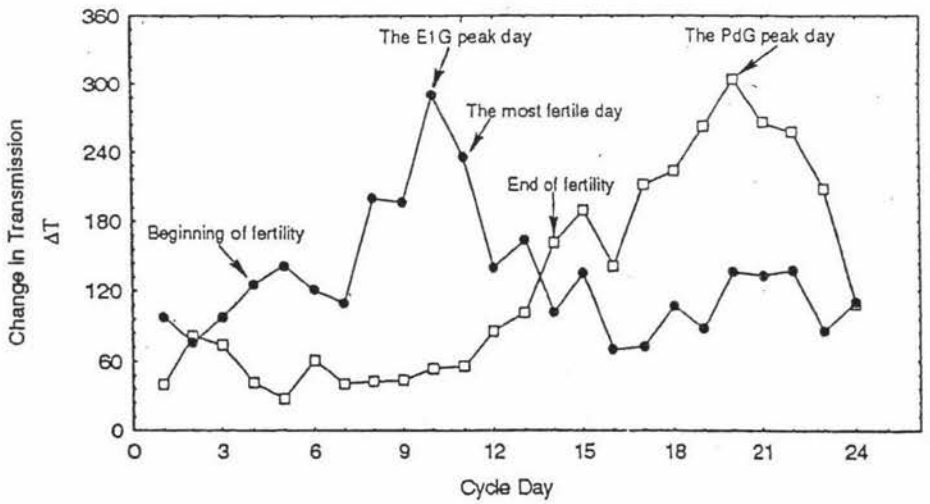

Figure 1.6: Normal menstrual cycle obtained by a woman at home using the Ovarian Monitor.

colour intensity that occur as fertility begins (about 20% increase per day). Hence, a search for new highly active enzyme systems, instead of using lysozyme, for the preparation of enzyme-steroid glucuronide conjugates for use in home assays for fertility has been the main goal (Wu, 1996). There is therefore a need for reference assays for E1-3G and PdG to calibrate any new colour test for the markers of fertility. Although the best reference methods were the chemical procedures used by J.B. Brown in Melbourne, as discussed earlier (in sections 1.1.4.2 and 1.1.4.3), these are no longer available to us. Because the Ovarian Monitor was designed for home use, it has the added disadvantage of being less practical for large scale sampling in a laboratory. The requirements of new reference assays are: to be more sensitive than the Ovarian Monitor, as precise, and with an equivalent or wider dynamic range, and also to be validated against known reference assays such as the World Health Organisation reference assays. In order to be of value the new reference assays must be as accurate as the Ovarian Monitor. The new reference assays need to be convenient and require little expensive equipment. Immunoassay techniques were therefore reviewed for possible use as reference assays in the laboratory to replace the total oestrogen method (Brown *et al.*, 1968) and gas liquid chromatography procedures for pregnanediol (Barrett & Brown, 1970).

1.2 Review of Immunoassay Techniques

Immunoassays are defined as tests which exploit the reaction between an antibody and an antigen *in vitro* (Kemeny, 1991). For example radioimmunoassay (RIA) as an analytical technique was first introduced by Yalow and Berson (1959) and electrophoretic immunoprecipitation in agar was pioneered by Ekins (1960), both being applied, with exceptional success, to the determination of hormones in biological fluids. Immunoprecipitation techniques have a limited sensitivity since extensive aggregation of the immune complex must occur before a precipitate is observed. The two broad approaches to the conduct of immunoassay are: those which rely on the competition between antigen labelled with a molecule which can be readily observed (for example a radioisotope or an enzyme) and unlabelled antigen for a limited number of antibody binding sites; and those in which the antibody is available in excess and for which there is no competition for binding sites, (Holme & Peck 1993). Both competitive and non-competitive immunoassays require the measurement of immunocomplexes in the presence of free antibodies and/or antigens. In heterogeneous immunoassays (competitive and non-competitive) this is accomplished by first separating the immune complex from the free immunoreactants. In homogeneous immunoassays, a modulation

of the signal occurs as a result of the immunoreaction, hence the immunecomplex formation can be monitored directly without prior separation of the bound and free tracer (Christopoulos & Diamandis, 1996). Immunochemical assays which require a separation of the free from the bound label are termed heterogeneous; those that do not are called homogeneous (Kricka *et al.*, 1996). `Indirect' refers to configurations where one antibody species is specific for another antibody species.

1.2.1 Enzyme-Linked Immunosorbent Assay (ELISA)

The observation that proteins are spontaneously adsorbed to hydrophobic surfaces (Catt & Tregear, 1967) led to the development of contemporary solid phase immunoassays, although adsorption of protein to synthetic surfaces such as polystyrene latex and glass had been studied earlier (Bull, 1956). The use of enzymes as an alternative to radioisotopes potentially reduces the tedious procedures for the separation of the bound and free reactants and eliminates the risk of radiation. The term enzyme-linked immunosorbent assay (ELISA) was coined by Engvall and Perlmann (1971) for a non-competitive enzyme immunoassay (EIA) configuration, whereas EIA historically denotes a competitive assay. Voller *et al.* (1974) were the first to adapt ELISA to the microtitre plate format which is a very powerful technique utilizing both antibodies and enzymes. The ELISA technique is regarded as more convenient in both its protocol and instrumentation than is RIA. The enzyme conjugate complex is safer to handle and has a longer shelf life than its radioactive counterpart, and deleterious effects on the assay components because of radioactive disintegrations are avoided, along with disposal problems.

There are several variants of the ELISA technique employing both competitive and non-competitive systems (Holme & Peck 1993; Kemeny, 1991), but the technique is best used in combination with two monoclonal antibody types, in the so called "two-site" or "sandwich" ELISA configuration. Because the two site non-competitive immunoassays involve two antibodies, they offer better specificity (Christopoulis & Diamandis, 1991) and higher sensitivity (Jackson & Ekins, 1986) than the competitive assay. Antigens must contain at least two antigenic sites (Crowthers, 1995) capable of binding to antibody, which may be a problem where lower-molecular weight antigens, of limited antigenic potential are being used, or where antigenic sites are concentrated on one surface. Some difficulties can be encountered using the same monoclonal antibody in sandwich assays, since the capture step may bind to the only epitope expressed on a small antigen

(Crowthers, 1995). The two-site configuration (sandwich) is probably better used for large or protein molecules, rather than for small antigens such as steroids, unless anti-idiotypic antibodies (Barnard & Kohen, 1990) are used.

A modification of the direct labelled antigen ELISA is a well established method to measure progesterone (Crowthers, 1995) using competitive conditions. Antigen is labelled with enzyme and captured with antibodies adsorbed to the solid-phase usually after crude fractionation (IgG fraction). Competitive assays involve simultaneous addition of two competitors for a limited number of antibody binding sites. Sample analyte competes with enzyme labelled analyte and the degree of inhibition of binding of the labelled antigen with the solid phase is measured. The signal from the enzyme tracer is inversely related to the analyte concentration. This direct competitive heterogeneous immunoassay used to estimate hormone concentration is analogous to many radioimmunoassay methods (Crowthers, 1995) and offers comparable sensitivity and precision (Henderson *et al.*, 1995; Maggio, 1980).

Alkaline phosphatase was found by Henderson *et al.* (1995) to be less sensitive than horseradish peroxidase (HRP) as an enzyme label in both the antigen coated competitive enzyme immunoassay and the antibody coated competitive enzyme immunoassay, which may in part be due to the higher detection limit of alkaline phosphatase relative to HRP (Porstmann & Kiessig, 1992). When protein (bovine serum albumin) conjugated to E1-3G was adsorbed to polystyrene in the "antigen coated ELISA", HRP conjugated to monoclonal anti-E1-3G antibody (raised in mice) was used as the enzyme label. When monoclonal anti-E1-3G antibody was adsorbed to polystyrene in the "antibody coated ELISA", HRP conjugated to E1-3G was used as the enzyme label. The sensitivity of both E1-3G standard curves, when antibody was coupled to HRP (3.6 ± 0.3 pg/well) was used, and when E1-3G coupled to HRP (3.6 ± 0.3 pg/well) was used were the same. In contrast the E1-3G standard curve was less sensitive when antibody coupled to alkaline phosphatase (9.4 ± 0.3 pg/well) was used and when E1-3G coupled to alkaline phosphatase (12 ± 2 pg/well) was used than when HRP was used as the enzyme label (Henderson *et al.*, 1995). Steric hinderance may be a factor in the reduced sensitivity of the E1-3G ELISA when alkaline phosphase conjugates are used in the assays. A disadvantage of using the antigen coated ELISA would be the inconvenience and expense of having to perform two coupling procedures: to couple the enzyme label to antibody, and also to couple a steroid to a protein such as bovine serum albumin which adsorbs to

plastic. Conversely, the antibody coated ELISA requires the preparation of a single E1-3G-HRP conjugation product and can be used with polyclonal antibodies (Crowthers, 1995).

Measurement of E1-3G concentrations using early morning urine (EMU) samples (from the first void on waking) from six women with natural, regular menstrual cycles by means of the coated-antigen competitive ELISA (Henderson *et al.*, 1995) produced values (E1-3G peak concentration of 100 ng/ml) and profiles similar to those reported previously by others using RIA (Munro *et al.*, 1991), ELISA (Shah & Josh, 1982) and time-resolved fluoroimmunoassay (Kesner *et al.* 1994), by means of the coated-antibody format. Furthermore, the pre-ovulatory urinary LH surge was consistently associated with pre-ovulatory elevated E1-3G concentrations (100 ng/ml).

1.2.2 Properties of Horseradish Peroxidase for use as an Enzyme Detection System

The enzyme detection system chosen utilizes the properties of horseradish peroxidase (HRP) isoenzyme C. A chromogenic substrate for HRP, o-phenylenediamine (OPD), acts as a hydrogen donor to form a coloured product on oxidation, as shown by the following simplified formula: $H_2O_2 + AH_2(OPD) \rightarrow 2\,H_20 + A$(coloured product). The appearance of the oxidized donor is measured spectrophotometrically using a micro-plate reader.

HRP is useful for analytical applications because of its high forward catalytic rates (rapid kinetics) and highly sensitive reactions with a variety of substrates, over a pH range of 4-8 (Ryan *et al.* 1994). Care needs to be given to maintenance of the optimum pH at 5-7 (Ngo, 1991), and to the quality and molarity of hydrogen peroxidase used. HRP is stable for long periods of time at room temperature over the pH range 5-10 (Dunford, 1991). The pH range can be extended to 4-11 for shorter intervals. Experiments can be conducted at 40°C, at ionic strengths up to 0.4 M, and temperatures as high as 80°C are possible for short time intervals. The immunochemical consequences of steric hindrance in ELISA favours the use of HRP because of its small size (Koertge & Butler, 1985). However, interference of endogenous peroxidases and phosphatases in some specimens can be a disadvantage. Although HRP has relative molecular stability, isoenzyme C is not as stable in soluble form as alkaline phosphatase for example, and is inactivated slowly at 4°C in the presence of the phosphate ion ($P0_4^{2-}$). Glycerol prevents protein aggregation and proteolysis, and Tween may also be used to delay inactivation (Porstmann *et al.*, 1981b).

HRP contains six lysine residues (Ugarova *et al.*, 1978) which can be targeted using the cross-linking reagents dicyclohexylcarbodiimide (DCC) and N-hydroxysuccinimide (NHS) for conjugation procedures such as the active ester method (Anderson *et al.*, 1964; Tijssen, 1985; Porstmann *et al.*, 1987). However, in direct competitive ELISA's bridging groups between steroid and enzyme also participate in the interaction of the antigen with the antibody (Paek *et al.*, 1993), and such interference is magnified considerably when the bridging group includes the lysine residue of the protein (Bachas & Meyerhoff, 1986) or in the case of RIA, hemisuccinate derivates. Bridging group recognition problems can be overcome by using different bridging groups/linkers (Bachas & Meyerhoff, 1986), and are also often noted in classical RIA procedures. When using a direct competitive ELISA the properties of the conjugate (of the enzyme and the analyte synthesized) substantially affect the quality of the analytical method (Paek *et al.*, 1993). It is well established that the number of analyte molecules reacting with the enzyme cannot be easily controlled.

HRP was considered an appropriate enzyme research tool to use in this present study involving ELISA procedures. The urinary metabolites oestrone glucuronide (E1-3G) and pregnanediol glucuronide (PdG) are key markers of fertility. Their chemical structures are shown in figure 1.7. The carboxyl group on the glucuronide sugar allows attachment to a protein by an amide linkage, which is useful for the conjugation of enzyme to the steroid glucuronide.

Oestrone-3 α-Glucuronide

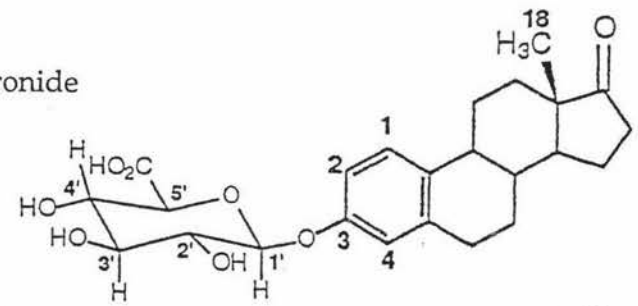

Pregnanediol-3 α-Glucuronide

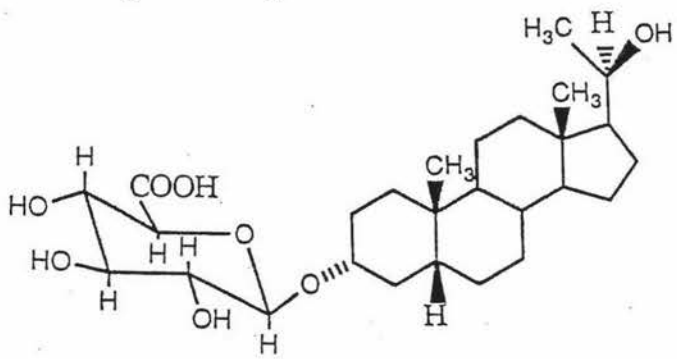

Figure 1.7: The chemical structure of Oestrone-3 α-Glucuronide and Pregnanediol-3 α-Glucuronide.

However, in the assay of HRP, the enzyme is progressively inhibited by its hydrolysis products so over long periods substrate reactions are not linear. The substrate hydrogen peroxide is unstable (especially in response to light) and the other substrates used auto-oxidise. Possibly the best substrate available is o-phenylenediamine (OPD), although it is mutagenic, (Tijssen, 1985).

1.2.3 Immunoglobulins (Antibodies)

Immunoglobulin class G (IgG) is one of the most prevalent immunochemical reagents in use today. Currently the other immunoglobulin classes, IgA, IgM, IgD and IgE, do not play an important role in immunochemical analysis (Kricka *et al.*, 1996). IgG is a glycoprotein (molecular weight [MW] 160,000) composed of two duplex chains with each set being made up of a heavy (γ) and a light (λ) chain joined by disulphide bonds (figure 1.8). The variable amino acid sequence at the amino terminal end of each chain determines the antigenic specificity of the particular antibody. Each unique amino acid sequence is a product of a single plasma cell line or clone, and each plasma cell line produces antibodies with a single specificity. A complex antigen, therefore, is capable of eliciting a multiplicity of antibodies with different specificities that are derived from different cell lines. Antibodies derived in this manner are termed *polyclonal* and exhibit diverse specificities in their reactivity with the immunogen (Roitt, 1988). An *immunogen* induces the formation of antibody, while antigen is capable of reacting with an antibody without necessarily inducing antibody formation. A *hapten* is a chemically defined determinant that, when conjugated to an immunogenic carrier stimulates the synthesis of antibody specific to the hapten. Haptens such as E1-3G and PdG are capable of binding antibody but cannot by themselves stimulate an immune response. In contrast to a heterogeneous mixture of antibodies produced by many cell clones in response to immunization, *monoclonal* antibodies are the product of a single clone or plasma cell (Roitt, 1988).

The strength of energy of interaction between the antibody and antigen is described by two terms: *Affinity* refers to the thermodynamic quantity defining the energy of interaction of a single antibody binding site (each IgG contains two binding sites) and its corresponding epitope on the antigen; *Avidity* refers to the overall strength of binding of antibody and antigen and includes the sum of the binding affinities of all the individual binding sites on the antibody (Kricka *et al.*, 1996).

Polyclonal antibodies are often used to determine the potential of a new immunoassay, before monoclonal antibodies are used, due to the time and expense involved in producing and preparing the latter (Campbell, 1996). A polyclonal antiserum is frequently used in immunoassays for its "specificity bonus" effect against low molecular-weight antigens (Tijssen, 1985). The spectrum of affinities of the various antibodies generated in a polyclonal antiserum may be quite different and each may have various degrees of cross-reactivity with antigens, other than the analyte of interest. Because the cross reacting antigens are different for the various antibodies, the effect of each species of cross reacting antigen is diluted relative to the analyte of interest.

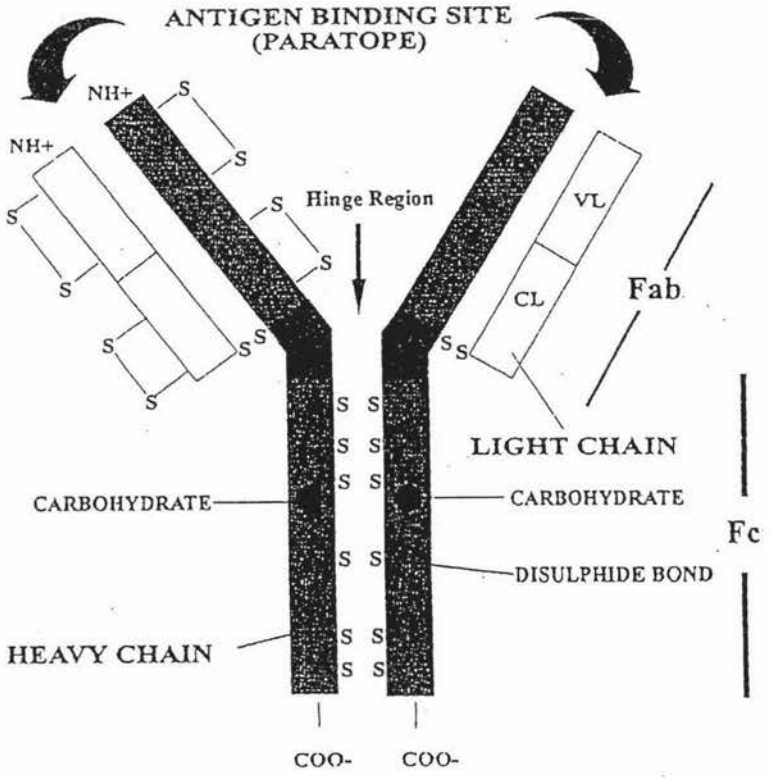

Figure 1.8: Structural elements of an immunoglobulin class G (IgG) antibody molecule. The antigen binding sites (paratopes) are formed by the variable amino acid sequences at the amino terminal of each chain of the IgG light and heavy chains. [Crowthers, 1995]

Furthermore, monoclonal antibodies lack the additivity of binding affinity conferred by two different antibodies creating a higher affinity bond than any one alone. This is known as the bonus effect. Therefore, for small molecules in particular, the primary advantages of moving to monoclonal reagents are that they are standard (Campbell, 1996) and provide ongoing replicates.

1.2.4 Properties of Passive Adsorption and Desorption of Proteins from Plastic

1.2.4.1 *Passive Adsorption of Proteins to Plastic*

The characteristics of passive adsorption at alkaline pH (pH 9.6) on polystyrene, follows typical saturation principles. Saturation with IgG antibodies corresponds to the addition of about 1000 ng/ 200 µl in a microtitre well (Cantarero *et al.*, 1980; Sorensen & Brodbeck, 1986). Although the sides of the microtitre wells exposed to antibody decreases by half when 100 µl instead of 200 µl is added to microtitre wells, the area of the base does not change (figure 1.9). Saturation levels of between 50 and 500 ng/well have been found valid for a variety of proteins when added as 50 µl volumes (Salonen & Vaheri, 1979; Crowthers, 1995). Adsorption geometry in Nunc-Immuno Products is based on the estimate that the surface can adsorb 400 ng protein per cm^2, and for the optimal set-up of solid phase immunoassays it is often essential to know the dimensional relationship between the vessels involved and the volumes of liquid, (NUNC catalogue 97/98).

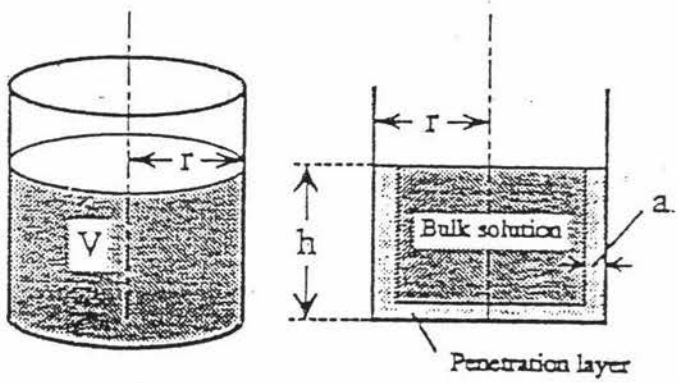

Figure 1.9: Geometry of a microwell (a, is the thickness of the penetration layer; r, is the inner radius of the microwell; h, is the height of liquid in the microwell; and V, is the volume of liquid in the microwell).

Adsorption of the antibody at alkaline pH was initially described by Engvall and Perlmann (1971) and has been retained in current ELISA technology. A region in which the proportion of adsorbed IgG (or protein in question) remains constant irrespective of the protein concentration, is called a "linear binding region" (Cantarero *et al.*, 1980). The linear binding regions are only observed at alkaline pH (Cantarero *et al.*, 1980), indicating that binding is independent of concentration (Butler *et al.*, 1992). Avidity differences of proteins for plastic appear to be correlated with molecular mass, (Cantarero *et al.*, 1980; Joshi *et al.*, 1992) where bovine IgG-1 at 158 kDa shows higher binding levels than bovine IgG-2a at 152 kDa, while even higher binding is shown for bovine IgM at 1000 kDa. Irradiated forms of plastic do exhibit less difference (Butler, 1996), as hydrophilic bonds are introduced. Conformational changes occur as proteins unfold and permit internal hydrophobic side chains to form strong hydrophobic bonds with the solid phase.

These are very stable if adsorption occurs within the linear binding region (Cantarero *et al.*, 1980), but protein adsorbed above the linear binding region generally appears less stable. Studies by various investigators (Butler *et al*, 1991; Butler *et al.*, 1992) generally reach the same conclusions about the stability and integrity of proteins passively adsorbed to polystyrene; adsorbed proteins may suffer the loss or alteration of antigenic epitopes; loss of enzymatic activity; generation of new epitopes; demonstrable physicochemical changes, and therefore general loss of capture antibody (CAb) activity-affinity. That more than 90% of monoclonal and 75% of polyclonal antibodies are denatured by passive adsorption was quantitatively demonstrated by Butler *et al.* (1993). However, even if only 6% of high affinity antibodies adsorbed on microtitre wells survive in a functional state, it is sufficient to provide an ELISA with (the more linear region of the standard curve is known as the *working range* of the standard curve), a working range of 2-200 ng/ml (Butler, 1996), which is adequate for most applications and typical of assays reported in the literature.

Physical adsorption of polyclonal immunoglobulin, class G antibody (IgG) was considered more practical and satisfactory for this present study than alternative immobilization procedures, such as via the G protein (protein G binds selectively to the Fc region of immunoglobulins and leaves the paratope free for complex formation with antigens) or chemical binding via the Fc segment to polylysine coated wells. Schramm and Paek (1992) reported that chemically bound antibody bound both iodinated and conjugated progesterone with approximately the same affinity, and found there was not

much difference for passively adsorbed antibody for the smaller antigen (iodinated progesterone). In contrast, the binding constant for the conjugate (progesterone-HRP) was found to be lower (Schramm & Paek, 1992) for passively adsorbed compared to chemically bound antibody. Iodinated progesterone may not have behaved in the same way as uniodinated progesterone in the assay and therefore needs to be weighed up against the easier option of using the immobilization of antibody by passive adsorption. In fact the lower affinity constant of the labelled antigen (e.g. E1-3G-HRP or PdG-HRP) may substantially increase the sensitivity of the competitive ELISA (Bachas & Meyerhoff, 1986) on the assumption that the more easily the labelled tracer is displaced the less native antigen is required. The sensitivity of competitive immunoassays depends on the affinity constants between the antigens (labelled and unlabelled) and the antibody (Jackson & Ekins, 1986).

1.2.4.2 *Desorption of Proteins from Plastic*

Owing to the noncovalent nature of the (polystyrene) plastic-protein interactions, desorption (also called leaching) may take place during the various stages of the assay (Crowthers, 1995). During a 16 h incubation period in the presence of nonionic detergent (tween) and blocking proteins (gelatine) desorption can be as much as 15%. In the absence of exchangeable protein (blocking protein such as gelatine) desorption is < 10%, and without detergent only 1-2% of adsorbed protein is released (Butler *et al.*, 1992; Butler, 1996). Immobilising antibody to microtitre wells covalently using the sodium periodate method (Sanderson & Wilson, 1971) for example, where poly-L-lysine coated wells create stable imide bonds with the antibody, would prevent such desorption. Higher concentrations of protein encourage desorption from solid phases (Butler, 1996), while using less than monolayer-forming concentrations of antibody may increase non-specific binding. However, differences in the properties of the polystyrene used may result in some variation in the amount of desorption of the passively adsorbed proteins occurring by up to 20-30% (Lehtonen & Vijanen, 1980; Engvall & Perlmann, 1971) for the earlier ELISA assays. Loosely bound proteins can be removed by thorough washing immediately after coating (Tijssen, 1985). There is little or no information on the stability of macromolecules adsorbed at neutral and acid pH, nor is there much information on the effects in relation to mechanisms involved in adsorption on surfaces other than polystyrene. However, if conditions are standardized, then this does not affect the validity of the majority of assays.

1.2.4.3 *Polystyrene vs. Blotting Membranes*

Various blotting membranes, such as nitrocellulose paper, show a much higher capacity for adsorption per planar surface area than do plastics. The membranous absorptive surface is 100-1000 times greater than plastic (Butler, 1993), presumably owing to their immense internal surfaces. Also the porous nature of membranes allows "flow-through" technology to be employed in immunoassay, which also reduces the diffusion-dependent phase of the solid-phase immunoassay. Much more protein binds to nitrocellulose, so that enough native protein may survive to allow denaturation to be overlooked. Further more, there is evidence that hydrophilic as well as hydrophobic forces are involved in the adsorption on immunoblotting membranes, which suggests that conformational alteration may not be as severe as it is on polystyrene (Butler, 1996). Although adsorption of IgG on polystyrene microtitre wells from various manufacturers at alkaline pH differs only subtly (Butler *et al.*, 1991), there is a greater heterogeneity among membranes and proteins (Brown *et al.*, 1991). Desorption and background problems hinder nitrocellulose use in quantitive assays, whereas polystyrene exhibits a low background in most assays, the binding is reproducible and the assay is readily adapted to automation. The much larger surface area and membraneous matrices of solid-phases like nitrocellulose is probably never covered with anything approaching a monolayer, consequently blocking protein solutions are typically used during every incubation step after receptor immobilisation, whereas on polystyrene, protein blockers and even nonionic detergents can be omitted after receptor immobilisation. Polystyrene microtitre wells were therefore considered appropriate for this present study since they are practical for large scale laboratory experiments where there is a need to process many samples at the one time, rapidly and efficiently.

1.2.4.4 *Blocking Agents*

Protein solutions and nonionic detergents are the most popular blocking agents. Tween appears to be the most popular, and is unusual in having the capacity for preventing both non-specific adsorption to polystyrene and non-specific protein-protein interactions during subsequent steps in an immunoassay conducted on polystyrene, (Butler, 1996). These non-specific interactions are known as "non-specific binding" (NSB) effects and reduce the sensitivity of immunoassays. Higher sensitivity can in part be associated with a greater signal-to-noise ratio which is enhanced if NSB effects are low. There are differences of opinion regarding both the need and mechanism of action of blocking agents. It is generally a question of trial and error (Kemeny, 1991) and is dependent on

the particular ELISA components. For example, there is some evidence that bovine serum albumin binds oestrogens (Podesta *et al.*, 1997), and is therefore clearly unacceptable for the development of the E1-3G and PdG assays in the present study. Protein blocking agents typically are serum albumin, casein, gelatin, new born calf serum, or dilute skim milk. They are often added after immobilization of the solid-phase receptor and are believed to "fill-in" stretches of the solid phase not occupied by immobilised receptor, thereby reducing NSB by blocking excess reactive sites on the solid-phase. Skim milk and casein based blockers appear most effective on both polystyrene and nitrocellulose surfaces (Christopoulis & Diamandis, 1996), and were shown to inhibit NSB by over 90% (Vogt *et al.*, 1987). This is believed to be due to the predominance of low molecular weight casein and other small proteins or peptides in skim milk, which theoretically would have a greater opportunity to fill in the small areas between the larger immobilised receptor molecules, but evidence of a mechanism is lacking. While fish skin gelatine is comparable to skim milk and casein in reported reduction of background or non-specific binding in ELISA (Vogt *et al.*, 1987), it has the added advantage of not solidifying (even at high concentrations under refrigeration) and is an excellent NSB blocker for nitrocellulose. Bovine gelatine (Henderson *et al.*, 1995; Schramm & Paek, 1992) will be used in this present study together with Tween (20), rather than Tween (80), triton or SDS detergents.

1.2.5 Immunochemical Interactions at Fluid Solid-Phase Interfaces

As discussed, immobilized reactants, whether antibody or antigen, may not be conformationally displayed in the same manner as in solution, as is well established for passively adsorbed proteins on polystyrene (Butler 1992; Butler *et al*, 1993; Cantarero, 1980). While solid-phase immunoassays (SPI) obey general Mass Law principles their reaction kinetics differ from kinetic interactions occurring in solution, for example: While diffusion in the bulk solution is three dimensional, once the interface in which soluble and immobilised reactants interact on the surface of the solid phase (reaction volume) has been reached diffusion becomes two dimensional (figure 1.10) consisting of only lateral and rotational diffusion, leading up to the formation of the encounter complex and subsequent antigen-antibody binding (Paek & Schramm, 1991). Diffusion or mass transfer is needed to move reactants into this interfacial volume (Butler, 1996). Solid phase antigen-antibody reactions are confined to the fluid-solid phase interface, probably to within the attraction distance of the strongest primary bond, a distance which is < 100 angstroms and probably closer to 10 angstroms. Such "microenvironments" (Schramm & Paek, 1991) create a theoretical volume which needs to be penetrated for solid-phase

antibody-antigen reactions, and this reaction volume is therefore also known as the "penetration layer" (figure 1.10). Interfacial reaction kinetics have been shown (Franz & Stegemann, 1991) to display a pronounced diffusion dependence when conducted in polystyrene microtitre wells (Butler, 1994).

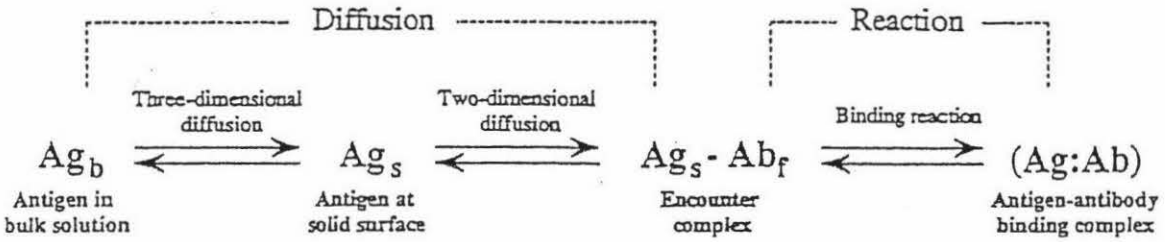

Figure 1.10: Diffusion and reaction processes leading to the formation of the antigen-antibody complex. The two dimensional diffusion consists of lateral and rotational diffusion. The three diffusion processes result in the formation of the encounter complex which is the pre-condition for the formation of the antigen-antibody complex. [Paek & Schramm, 1991]

The time required for equilibrium to be reached in SPI is therefore greater than for solution phase interactions (except microparticles), and increases in proportion to the ratio of the volume occupied by the liquid to that occupied by the interfacial receptor. However, by reducing the ratio of the solution-phase volume to the volume of the reactant interface, the diffusion dependence of the SPI can be reduced. This can also be reduced by vortex agitation, by forcing the reactive solution into a small volume using an inert plunger, by using porous matrix with a large surface such as nitrocellulose, and by using microparticles as the solid phase. Sadana and Madugula (1993) found that the sensitivity of immunoassays was enhanced with higher antigen concentrations near the surface. When not limited by diffusion, it is also found that the intrinsic forward and reverse reaction rates are lower for surface reactions compared to reactions in solution. Dissociation rates for interfacial reactions may be two orders of magnitude lower than those occurring in solution. Adsorbed antibodies appear to cluster (Butler, 1992; Davies *et al.*, 1994; Nygren, 1988), and the increased avidity is due to reduced dissociation of

multivalent complexes (Metzger, 1992; Sadana & Madugula, 1993). In other words, the more valencies holding the antigen (cross linking after initial binding of antibody to antigen) the less likely it is to be lost when the complex dissociates at any one binding site (Roitt, 1988), resulting in exponentially reduced chances of dissociation compared to the chances of dissociation in the absence of cross-links and in solution. The phenomenon of "hysteresis" whereby the energy of antibody-antigen dissociation is higher than the energy of association, indicates the gradual formation of additional antibody-antigen bonds of lesser specificity (van Oss *et al.*, 1979; Absolom & van Oss, 1986), and may also account for the observed synergistic behaviour of such interactions using monoclonal antibodies (Ehrlich *et al.*, 1983). A very high solid-phase reactant concentration, especially as might occur in clusters (Schramm & Paek, 1992), and resulting from a confined interfacial reaction volume, could facilitate more rapid reassociation of dissociated analyte than would occur in fluid-phase systems. This might account for the higher antigen affinity of antibodies when tested in SPI versus in solution (Lehtonen, 1981). Antigen-antibody reactions at solid-liquid interfaces can often be considered as practically irreversible and limited by mass transport or steric interactions (Nygren *et al.*, 1987; Stenberg & Nygren, 1988), and therefore longer incubation times maybe needed for equilibrium to be reached using SPI, such as ELISA.

1.3 Aims of the Present Study

Because the reference assays used to develop the Ovarian Monitor are no longer available there is a need to develop new reference standards for use in the laboratory and to validate new non-instrumental colour tests currently being developed for use in the field.

The aim of the study was therefore to develop competitive ELISA assays optimized to measure oestrone-3 α-glucuronide (E1-3G) and pregnanediol-3 α-glucuronide (PdG) in timed and diluted urine using polyclonal antibodies.

This study is presented in three sections:

i. development of the E1-3G ELISA
ii. development of the PdG ELISA
iii. comparative and clinical studies using both ELISA assays

Chapter Two: Development of an ELISA Assay for Oestrone-3 α-Glucuronide (E1-3G) in Timed Urine Samples

2.1 Introduction

The main aim of this chapter is to develop an Enzyme-Linked Immumosorbent Assay (ELISA) optimized to measure oestrone glucuronide (E1-3G) in timed urine specimens to serve as a reference method to replace the now defunct total urinary estrogen method of Brown *et al.*, (1968). In this procedure after acid hydrolysis and extraction of the phenolic fraction, spectrophotofluorometry using the highly specific Kober-Ittrich reaction measured the major urinary metabolites of oestradiol (oestrone glucuronide, oestriol-3-glucuronide, and oestriol-16-glucuronide). There is a close correlation between the rate of urinary total oestrogen excretion measured by this procedure and the rate of serum oestradiol excretion (Renowden, 1975). A direct competitive ELISA was used in this study in combination with the immobilized antibody format as discussed in section 1.2.1. Briefly (figure 2.1), antibody is immobilised by adsorption to a polystyrene matrix followed by the simultaneous addition of analyte (E1-3G) and horseradish peroxidase coupled to E1-3G as the tracer (E1-3G-HRP conjugate). After the removal of any unbound antigen (E1-3G and E1-3G-HRP) the signal produced by the enzyme (HRP) is measured and is inversely related to the E1-3G concentration in the test sample.

The dynamic, (functional) or working range of a direct competitive immunoassay is determined by the number of functional antibodies adsorbed to the microtitre plate (Butler, 1993). However, the sensitivity of the assay is compromised as antibody concentration increases (Ekins, 1983) because more analyte (E1-3G) is required to give a signal above baseline. While the analyte must be the substance in limiting amounts in a direct competitive assay to allow conjugate to bind and a signal to be obtained, more binding sites may be available to the smaller analyte (E1-3G) than to the tracer (E1-3G-HRP conjugate) at high antibody concentrations. For example, antibody immobilised to planar surfaces has been shown to take up about 10 fold more of the small antigen progesterone before the tracer (HRP-progesterone) begins to be prevented from binding to the sites accessible to the larger antigen (Schramm & Paek 1992).

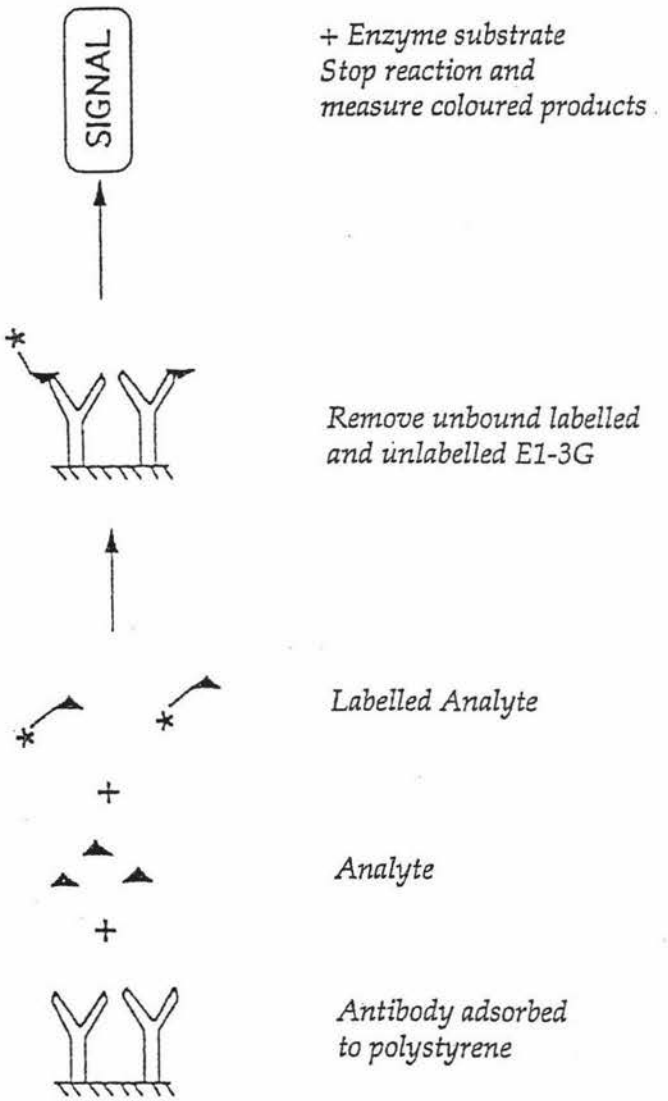

Figure 2.1: Configuration for the Direct Competitive Immunoassay using immobilised antibody. Analyte (E1-3G) from the sample competes with labelled analyte (E1-3G-HRP) for a limited number of antibody binding sites.

Also, it appears that iodinated progesterone has access to antibody binding sites which are inaccessible to the bulky HRP conjugated to progesterone. Consequently the conjugate will not be prevented from binding until a large amount of analyte has already bound to the immobilised antibody, resulting in low sensitivity (resolution) compared to the higher sensitivity expected with a lower immobilized antibody concentration where both the analyte and tracer theoretically have more equal access to binding sites.

In contrast, it has been reported (Lindmo *et al.*, 1990; Butler, 1996) that the lower the antibody concentration the more an assay can be compromised by increased non-specific binding, and perhaps antibody instability if the antibody concentration is below the (Cantarero *et al.*, 1980) linear binding region (refer section 1.2.4.1). The addition of a blocking agent after antibody adsorption, generally has been shown to reduce the percentage of any potential non-specific binding sites, and thus prevent other enzymes (or other substances) for example from adsorbing to the polystyrene surface between the already adsorbed antibodies. Serum albumin, caseine and gelatine all have been reported to reduce the background or non-specific binding in ELISA (Vogt *et al.*, 1987). The need to reduce the available binding sites in this assay (E1-3G ELISA) is an important factor because of the disparity in size between the analyte and conjugate, (Schramm & Paek, 1992) which can influence the sensitivity of competitive assays as discussed above. Therefore, optimization of the E1-3G immunoassay with respect to the minimum amount of functional antibody which, after forming an immunocomplex, gave a reading of about 1.0 absorbance units at a wavelength of 490 nm, was carried out. By convention this is achieved by determining the dilution of antiserum which will bind 50% of the tracer in the absence of analyte (Holme & Peck, 1993).

Another important determinant of ELISA performance is the concentration of tracer used. The competitive dynamics between the conjugated and unconjugated E1-3G determines the sensitivity of the standard curve, as follows. For example, excess conjugated E1-3G-HRP tracer may prevent E1-3G binding resulting in artificially low E1-3G levels being measured (Butler, 1994), and sensitivity is lost when there is insufficient conjugated E1-3G-HRP present in the assay to distinguish between very small changes of E1-3G concentration (Kemeny, 1991). The standard curve for E1-3G is required to measure E1-3G levels which range from the individual's E1-3G baseline to the E1-3G peak values which occur just prior to ovulation. The constant production of oestrone originating from the adrenals is likely to be the main contributor to baseline levels of E1-3G during the

early follicular phase (refer section 1.1.4.3; figure 1.4) of the menstrual cycle. This adrenal activity gives rise to a baseline level of about 3 µg/24 h total urinary oestrogens (Blackwell & Brown, 1992), which is equivalent to E1-3G levels of approximately 10 nmoles/24 h. Brown *et al.*, (1988) initially suggested that a sensitivity for E1-3G levels of 25-50 nmoles/24 h (equivalent to a total oestrogen value of 7-14 µg/24 h) was required, and later (Brown *et al.*, 1989) argued that a suitable home assay required an E1-3G sensitivity of 15 nmoles/24 h equivalent to a total oestrogen value of approximately 4 µg/24 h. E1-3G peak levels of over 400 nmoles/24 h (Brown *et al.*, 1989) have been recorded using the Ovarian Monitor for a woman receiving gonadotropin therapy for the induction of ovulation. Using early morning urine specimens (20 µl) and antigen coated (6-ketoestrone conjugated to bovine serum albumin) competitive ELISA assays, Henderson *et al.*, (1995) reported E1-3G levels (averaged over 6 women) of 100 ng/ml equivalent to an E1-3G excretion rate of 768 nmoles/24 h. The lowest mean (N=6) E1-3G level was 20 ng/ ml which is equivalent to about 153 nmoles/24 h. Not surprisingly these mean E1-3G levels (Henderson *et al.*, 1995) are higher than those expected in this study where timed and diluted urines are used, as for the Ovarian Monitor assay. The working range of the Ovarian Monitor is about 100 to 800 nmoles/24 h for E1-3G (Cummock, 1998) which is sensitive enough to provide sufficient warning of an oestrogen rise and to allow measurement of the oestrogen peak. This is the range to be measured by the E1-3G ELISA assay to be developed in this thesis.

During the evaluation of an assay the reliability, sensitivity and validity also require assessment. The reliability of an immunoassay is determined by the variability of a number of replicate measurements. The sensitivity of an assay on the other hand is determined by the smallest amount of analyte which can be discriminated from the zero standard (refer section 2.3.5). A valid assay therefore will need to be reliable, and to have the sensitivity to detect very small amounts of steroid glucuronide, that is; to be able to discriminate between them. An assay may have high sensitivity but if at such small amounts of analyte the results are highly variable it will lack reliability/ precision. For use as a reference method the assay must also be be valid; that is it must measure the analyte specifically and give the correct or accurate amount. An assay may be precisely wrong if it is not valid as well. Antibodies can be raised to have an affinity for mainly one substance. This property of antibodies which is referred to as specificity is used in immunoassays to ensure that they are valid, for example to make the ELISA in the present study "a valid immunoassay for E1-3G".

To characterize the specificity of the E1-3G immunoassay, procedures are undertaken to establish whether other urinary steroids are binding to the E1-3G antibody and whether such cross-reactivity is considered significant enough to compromise the accuracy of the imunoassay. The validation of an immunoassay is ensured if it can be compared with an existing reference assay. This is an essential step in the validation of a new assay and involves a comparison of the values obtained in the test assay with the values obtained from the reference assay for the same samples. In this way matrix effects and any biases in the results can be recognised. Examination of non-specific binding is also required to determine whether, or to what extent, other substances in the urine sample other than steroids interfere with the E1-3G immunoassay by non-specific binding (NSB) Non-specific binding is defined as a low affinity, unsaturable binding of the ligand to the solid phase (Christopoulos & Diamandis, 1996). Any such NSB found in the presence of urine compared to a lack of such NSB in the absence of urine is called "the urine effect". The matrix effect may also show itself by non-parallelism between the urine spiked E1-3G standard curve (refer section 2.3.5.4) and the unspiked E1-3G standard curve. This generally gives higher values than the true values, particularly for low levels of the analyte. The unknown E1-3G concentration is calculated (refer section 2.2.6.8) from the E1-3G standard curve on the assumption that both the E1-3G standard and the urine sample are subjected to exactly the same treatment.

In summary, the aims for the chapter are: To develop an ELISA assay to measure E1-3G levels accurately in timed menstrual cycle urines; for the E1-3G ELISA to have a similar working range (<100 to 800 nmol/24 h) and sensitivity (<15 nmol/24 h) to the E1-3G levels measured by the Ovarian Monitor.

2.2 Materials and Methods

2.2.1 Equipment

A Hewlett Packard 8452A diode array spectrophotometer was used to measure absorbance values. Sephadex G-25 (fine, packed in a 1.5 x 30 cm column) chromatography was used for the purification of E1-3G-HRP conjugate. The new generation varian spectrophotometre (Cary 1E/Cary 3E UV-Vis) was used to measure HRP enzyme activity, using the commercial enzyme kinetic software. A Diaflow ultra-filtration system was used to concentrate HRP-conjugate solutions. The Diaflow apparatus was attached to a cylinder containing nitrogen (stored in the cold room) which forces the liquid through a semi permeable membrane. Low pressure liquid chromatography for purification of

protein conjugates was performed on an Econo System from Biorad Laboratories (Richmond, CA 94804, USA). A CM Sepharose cation exchanger was packed in a 1.5 x 30 cm column (CL-6B Sigma). Pellets of molecular sieves, type 4A (BDH, product 54 005 4) were added to DMF to ensure that it was dry. A dessicator was used to store the equipment and reagents required for the conjugation of HRP to E1-3G for 48 hours prior to the active ester procedure being carried out. Centrifugations were carried out using an RC2-B Sorvall/Dupont SS-34 rotor angle (rpm 5,000), at 34°C. Macrosep centrifugal concentrators with a 10,000 Dalton cut-off membrane from Filtron Technology Corp (Northborough, MA 01532, USA) were used for the final ultrafiltration and concentration of HRP conjugate samples, (membranes were stored in 20% ethanol). Antibodies were precipitated in Eppendorf tubes and separated using a small benchtop centrifuge. An alumimium heating block was used for incubating samples when lytic assays were carried out using the Ovarian Monitor. The home Ovarian Monitor equipment including meter and E1-3G immunotubes were provided by Professor Jim Brown, University of Melbourne, Australia. ELISA microtitre plates (Maxisorp C12 with 96 fixed wells) and the Nunc Catalogue (1997/98) were obtained from Nalge Nunc International (Kamstrup, Roskilde, Denmark). Plates were stored in a dry cupboard bagged in lots of five, and remained wrapped until use. Maxisorp immunoproducts have a polystyrene surface with a high affinity to molecules with mixed hydrophilic/hydrophobic domains such as proteins. Nunc 15 ml screw cap centrifuge tubes were used for most dilutions where larger volumes of enzyme or antibody solutions were required. An 8 channel single-beam microplate absorption photometer (Anthos Labtec Instruments Ges.m.b.H., Jakob Haringerstrasse 8, A-5022 Salzburg) was used to measure absorbances at 490 nm to obtain the ELISA results. A multipipetter and four troughs was used to perform ELISA washing procedures and to dispense some of the reagents. A heated magnetic stirrer was used to dissolve gelatine when required for ELISA buffers, and used unheated for other buffer procedures.

2.2.2 Reagents

Micrococcus lysodeikticus was supplied by Sigma Chemical Co. (St. Louis, MO, USA), and was used as the substrate for lysozyme. o-Phenylenediamine powder (Merck-Schuchardt) was used as the substrate for horseradish peroxidase. Testosterone, pregnanediol, androstenedione, progesterone and oestriol were all used in cross-reactivity studies and all were obtained from Mann Research, (N.Y.). Oestrone was from Sigma Chemicals Co. (St. Louis, MO, USA). Oestrone sulphate was supplied by Dr Keith Henderson of

AgResearch, Wallaceville. Oestrone glucuronide (E1-3G) was synthesized by Dr Y. Wu of the Institute of Fundamental Sciences, Massey University (MW = 446.5). N,N'-dicyclohexylcarbodiimide (DCC) was from Sigma, (product no. D3128), (MW = 206.3), and N-hydroxysuccinimide (NHS) was also from Sigma, (product no. H-7377), (MW = 115.1) as was horseradish peroxidase (HRP) isoenzyme C., (product 814 393), (MW = 40,000), approximately 70% pure. The liquid solvent dimethylformamide (DMF) from BDH, (Analar, product 10322) was used. Gelatine powder from BDH, (Poole, product 44045). All reagents were of analytical grade or better. Water was milli-Q grade.

2.2.3 Buffers

HEPES

A 0.15 M N'-2-hydroxyethylpiperazine-N'-ethanesulphonic acid (HEPES) buffer was prepared using 35.72 grams Hepes in one litre of milli-Q water, adjusted to (physiological) pH 7 using NaOH.

Tris-maleate buffer

Stock tris-maleate buffer (1.0 M) was prepared by mixing maleic acid (7.25 g), tris (19.80 g), NaCl (12.75 g), Tween 80 (20 ml of a 1/100 dilution in Milli-Q water) and HCl (2.8 ml of concentrated acid) in a total volume of 375 ml. The pH was adjusted to 7 with HCl as required.

ELISA Buffers

Coating Buffer (Carbonate - Bicarbonate)

Coating buffer was prepared with 31.59 g carbonate ($Na_2 CO_3$ and 2.93 g bicarbonate $NaHCO_3$ made up to 1 litre with Milli-Q water, adjusted to pH 9.6 and stored at 4°C.

0.5% Gelatine Blocking Buffer

Blocking buffer was prepared by the addition of a 0.5% solution of gelatine to the coating buffer, and heated gently to aid dissolution and then stored at 4°C or room temperature.

Substrate Buffer (Citrate-Phosphate Buffer)

To make up the citrate-phosphate buffer, 24.3 mls of 0.01 M citric acid (2.1 g citric acid in 100 mls milli-Q water) and 25.7 mls 0.2 M phosphate buffer (2.84 g Na_2HPO_4 anhydrous) in 100 ml milli-Q water were made up to 100 mls with 30 mls milli-Q water, adjusted to pH 5 and stored at 4°C for up to one week.

Washing Buffer (0.01 M phosphate buffer + Tween 20)

Washing buffer was prepared with 0.2 g KH_2PO_4, 2.9 g $Na_2HPO_4.12H_2O$, 8 g NaCl and 0.5 ml Tween 20 made up to 1 litre with milli-Q water, adjusted to pH 7.4 and stored at 4°C or room temperature.

0.1% Gelatine Assay Buffer

Gelatine assay buffer (0.1%) was prepared by making up washing buffer with 0.1% gelatine. Once the buffer had cooled down a 0.01% thiomersal solution was added, the mixture being adjusted to pH 7.4 and stored at 4°C.

Substrate-Chromogen Solution for HRP

To prepare the substrate solution, 40 mg o-phenylenediamine powder (OPD) was added to 100 mls of citrate-phosphate buffer (approximately 30 minutes before use) then 40 µl of 30% hydrogen peroxide H_2O_2 was added immediately before use. Because OPD is light sensitive upon the addition of H_2O_2, the container was wrapped in tinfoil to avoid a light catalysed reaction.

Stopping Solution

The stopping solution of 2.5 M sulphuric acid H_2SO_4 was prepared in Milli-Q water and stored at room temperature.

2.2.4 E1-3G Standards

E1-3G standards were made up from a stock solution which contained 500,000 nmoles/24 h (the stock solution was made up in 10 mM tris-maleate buffer pH 7.4; refer to section 2.2.3), and then diluted to 1,000, 500, 250, 150, 100, 70, 50, 30, 20, 12.5, 10, 3.4 and 1.137 nmoles /24 h with assay buffer (refer section 2.2.3). No other stabilizer or preservative was used and the standards were stored frozen in aliquots of approximately 500 µl.

The molar E1-3G concentration is multiplied by 3.6 to convert the E1-3G concentration to nmoles per 24 hours. This is based on the the fact that the menstrual cycle urines for the Ovarian Monitor use are all diluted to the equivalent of 150 ml of urine per hour of collection. Hence the expected total daily average urine production is 3.6 litres.

2.2.5 Urine Samples (WHO)

Timed and diluted (refer section 2.2.4) menstrual cycle urine samples (from study #90905), were collected as part of a World Health Organisation (WHO) study of the Ovarian Monitor. The urine samples were preserved in boric acid and stored frozen in small tubes with rubber stoppers. Cycle days 13 and 15 from menstrual cycle 6 from subject 021R, and cycle days 15 and 19 from subject 014X were used as quality control samples to monitor the performance of the E1-3G assay (used in reliability studies; refer section 2.3.5.2).

2.2.6 Methodology

2.2.6.1 Conjugation of E1-3G to Horseradish Peroxidase

The Active Ester Method

The active ester procedure (Anderson *et al.*, 1964; Rajkowski & Cittanova, 1981; Tijssen, 1985; Smales *et al.*, 1994) was carried out in two steps (figure 2.2). The first was to generate the active ester derivative of the carboxyl-containing steroid hapten (the hapten was E1-3G), and the second step was for the reaction of the activated hapten with the protein (horseradish peroxidase) in which one of the seven lysine residues of the protein react with the active ester functional group to form stable amide linkages between the protein and the steroid glucuronide.

Although dicyclohexylcarbodimmide (DCC) is a good leaving group (figure 2.3), the E1-3G-DCC complex is insoluble in water and hence, will react only very slowly with horseradish peroxidase (HRP) in aqueous solution. Thus, a substitution of the DCC, was made before the conjugation of E1-3G to HRP. This was achieved by the addition of the compound N-hydroxysuccinimide (NHS) which displaces dicyclohexylurea (DCU) and forms an active E1-3G-NHS ester. Since DCC is insoluble in water, any unreacted DCC does not react with the protein to generate cross linking between protein molecules as is the case with protein conjugates utilizing water soluble carbodiimides.

Because it is important to have the same molar ratio between the reagents, the amount of each substance (in mg) required to give a concentration of 5.3 µM was prepared in dry dimethylformamide (not less than 50 µl) resulting in solutions of 2.5 mg/50 µl oestrone glucuronide (E1-3G) (5.3 µM); 1.1 mg/50 µl dicyclohexylcarbodiimide (5.3 µM); and 0.6 mg/50 µl N-hydroxysuccinimide (5.3 µM). It was easier to weigh 2-5 mgs of each reagent and then adjust the volume of DMF to give a required concentration (5.3 µM).

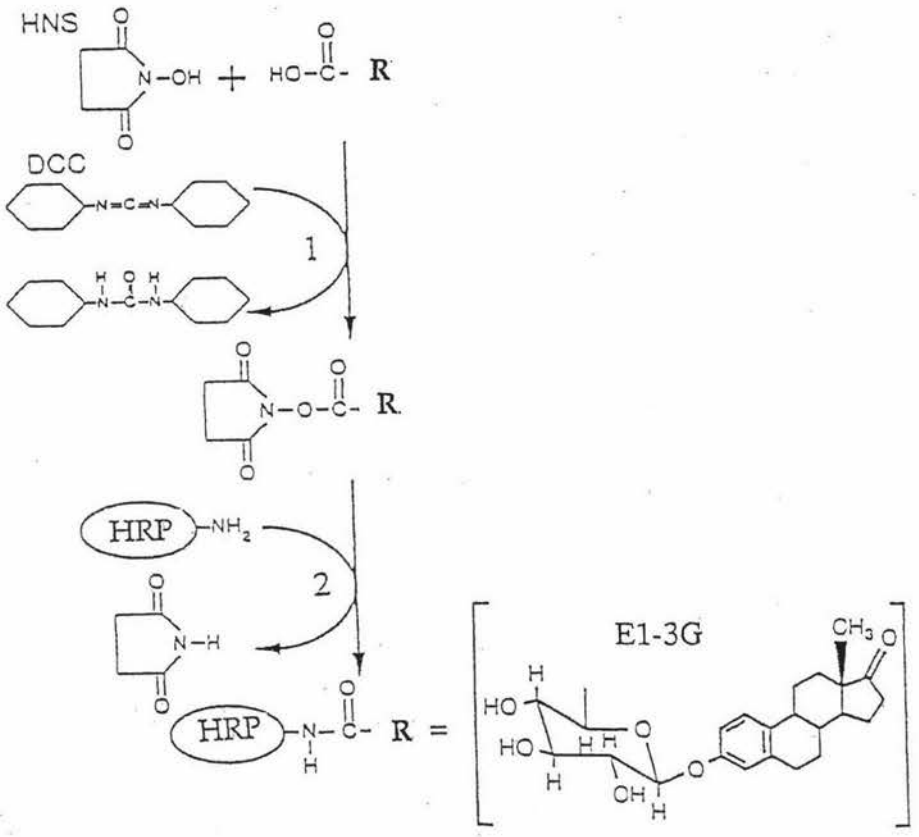

Figure 2.2.: The Active Ester Method, for the conjugation of steroid hapten (E1-3G) to an enzyme (HRP) or other protein. This procedure is carried out in two steps (1 & 2), the first to generate the active ester derivative of the carboxyl containing hapten, and the second for the reaction of the activated hapten with the protein.

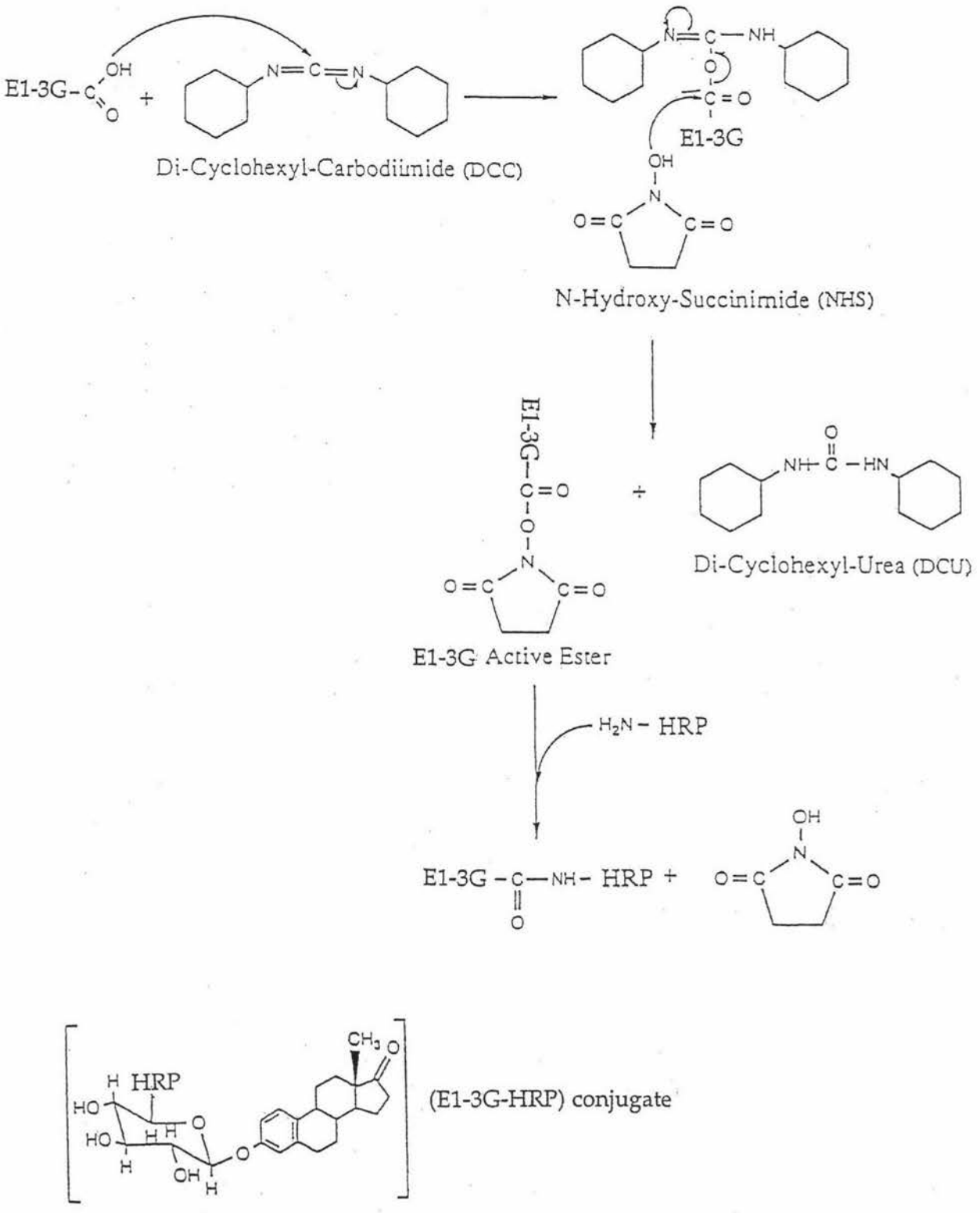

Figure 2.3: The synthesis of Oestrone Glucuronide by the Active Ester Method

To a reaction vial was added 50 µl of the E1-3G solution followed by 50 µl of the carbodiimide and then 50 µl of the N-hydroxysuccinimide solutions. The reagents were mixed and let stand for 90 minutes at room temperature (~20°C).

Horseradish peroxidase (5 mg) was dissolved in 500 µl of 0.13 M $NaHCO_3$, pH 7 and stirred gently at room temperature. The mixture of E1-3G, carbodiimide (DCC) and N-hydroxysuccinimide (NHS) was added to the HRP solution in 3 x 50 µl aliquots and the solution turned cloudy almost immediately. Stirring was continued slowly for 2.5 h at room temperature and the pH was maintained at 7. Finally, the mixture was dialysed overnight at 4°C against distilled water and passed through a Sephadex G-25 column using HEPES 0.15 M at pH 7 as the eluant. Fractions (1 ml) were collected and pooled, the horseradish peroxidase conjugate fractions being clearly distinguished by their orange/brown colour. The oestrone glucuronide-horseradish peroxidase (E1-3G-HRP) conjugate was stored at 4°C. Thiomersal was added to give a final concentration of 0.01% (e.g. 50 µl/ml of a 2 mg/ml solution was added) and then frozen in aliquots of 500 µl.

For purification of the E1-3G-HRP conjugate Sephadex G25 (~10 g) was weighed out and allowed to swell overnight in ~75 ml saline. The column (1.5 x 30 cm) was poured and washed with ~50 ml saline (0.13 M adqueous $NaHCO_3$ 1.09 g/100 ml water, adjusted to pH 7 with 0.1 M HCL) and the conjugate loaded after dialysis. Fractions (1 ml) were collected and the absorbance read at 280 nm. The protein fractions were pooled and their absorbance re-read at 280 nm the protein yield being calculated on the basis that 10 mg/ml of HRP has an absorbance of 6.67 (Henderson personal communication).

2.2.6.2 *Protocol for Horseradish Peroxidase Activity Assay*

A new generation varian spectrophotometer with temperature control and software for enzyme kinetics was used (refer section 2.2.1). The assay protocol was as follows; citrate buffer pH 5.3 (0.1 M) was pre-incubated at 40°C in a water bath. An aliquot of 1.9 ml was transferred into a 2 ml plastic cuvette and left to come to temperature (37°C) equilibrium. A solution of o-dianisidine (20 µl of a 10 mg/ml solution in methanol), was freshly sonicated on the same day for 5-10 minutes. The HRP conjugate (20 µl) was diluted appropriately and was added and mixed by inversion with parafilm. The machine was blanked by addition of 20 µl of the reaction mixture at 460 nm and the assay begun by addition of 20 µl of a 1/100 diln. of 30% commercial stock hydrogen peroxide in water. The cuvette was mixed by inversion with parafilm immediately and the assay run for 60

seconds. The assay was performed in duplicate with a total reaction volume of 1960 µl.

2.2.6.3 *Production of Oestrone-3 α-Glucuronide Antisera*

Antibodies were raised against E1-3G by Dr Keith Henderson, AgResearch, Wallaceville Animal Research Centre, Upper Hutt, New-Zealand, by innoculating sheep with synthetic thyroglobulin-estrone glucuronide conjugates, as prepared by Smales (1997). A large carrier protein is necessary because haptens such as E1-3G are too small to elicit a response alone (refer section 1.2.3). After three to six months good antisera were obtained.

2.2.6.4 *Preparation of Antibody*

Ammonium Sulphate Precipitation

Serum from sheep 243 (bleed 4), containing E1-3G-specific polyclonal antibodies was purified by ammonium sulphate precipitation (Harlow, 1988). A saturated ammonium sulphate solution (1.5 ml, 4.1 M) was added slowly to the serum (3 ml) with stirring. After leaving overnight at 4 °C, the antiserum was pelleted by centrifugation (6000 rpm, 30 min), and the supernatant was discarded. The pellet was then washed by resuspension in a 2.05 M saturated solution of ammonium sulphate, followed by a second centrifugation, and the supernatant was removed again. Resuspension of the pellet and dialysis against milli-Q water to remove the lipoproteins was followed by a second dialysis against phosphate buffered saline (PBS), before storage in tris-maleate buffer (refer section 2.2.3).

2.2.6.5 *Ovarian Monitor Protocol (refer section 1.1.5)*

2.2.6.6 *Inhibition Assays Using the Ovarian Monitor*

The concentration of anti-estrone glucuronide antiserum binding sites was estimated by titration with oestrone glucuronide (E1-3G) conjugated to hen egg white lysozyme (HEWL) using the Ovarian Monitor (refer section 1.1.5). Theoretically, each antibody molecule is able to bind two molecules of hapten (E1-3G), and thus inhibit two molecules of the conjugate. The end point of such a titration is defined as being the point where addition of further antibody to the assay has no further effect on the lysis rate of the conjugate. These inhibition assays were performed by measuring the rates at varying amounts of antibody and a constant known concentration of HEWL-E1-3G conjugate as described below.

An homogenised suspension of *micrococcus lysodeikticus* (15 mg) in 2 ml of 75 mM tris-maleate buffer pH 7 (refer section 2.2.3) sonicated to obtain a uniform suspension was first prepared. E1-3G-lysozyme (10 µl) was added to each of a set of assay cuvettes at an appropriate dilution. Following the addition of different (increasing) volumes of antisera, each assay tube was made up to 350 µl with appropriate amounts of 40 mM tris-maleate buffer (pH 7) and pre-equilibrated for 5 minutes at 37°C on an aluminium heating block (refer section 2.2.1). To each tube a 10 µl aliquot of the *micrococcus lysodeikticus* solution was then added. The tubes were vortexed, and then the initial transmission (T_0) was measured for each tube by the Ovarian Monitor. Each tube was incubated at 37°C for twenty minutes, after which the final transmission values (T_{20}) were determined. The differences between the initial and final values $\Delta T = (T_{20}-T_0)$ over 20 minutes were calculated as a measure of lytic activity of each assay tube.

2.2.6.7 Enzyme-linked Immunosorbent Assay (ELISA) Protocol

(refer section 2.2.3 for information about buffers)

Day 1: Anti-E1-3G antibody was diluted (refer section 2.3.3) in fresh coating buffer and then an aliquot (100 µl) was added to each well of the microtitre plate. The plate was covered with tinfoil and held at 4°C overnight. The blocking buffer (section 2.2.3) was prepared for use on day 2.

Day 2: All of the liquid in the wells was shaken from the plate with excess liquid being knocked from the wells by banging the inverted plate onto paper towels on the bench. Blocking agent (250 µl) was added to each well and the plate covered and left for 0.5 to 1 hour at room temperature after which the liquid was removed as before. The plate was then washed (3X) by adding washing buffer (250 µl) to each well and allowing the plate to stand for 3 minutes, followed by the removal of the washing buffer as above. Care was taken to prevent the wells drying at each stage. Assay buffer (50 µl) was then added to each well followed by an aliquot (150 µl) of the incubation mixture. The incubation mixture was prepared (in an Eppendorf tube) by adding labelled (E1-3G-HRP) and unlabelled (E1-3G standard or urine sample) antigen, diluted as required in assay buffer. The main variation to this protocol in this thesis will involve differences in the incubation mixture in the Eppendorf tubes. Assay buffer (150 µl) was added to those wells required for assay blanks. The plate was covered and incubated at 4°C for 2-3 hours or 16 hours (overnight).

Day 3 (or second half of Day 2): The liquid was removed from the plate as described above and the plate washed (3X) as above. Substrate solution (100 µl) was added to each well

and left at 37°C for approximately 20 minutes. Stopping solution (50 µl) was added and the absorbances were read (490 nm) on the microplate reader (refer section 2.2.1).

To mimimize operater error, uniformity of operation is important; it must be systematic and planned. The same plates were processed in the same order for each operation. This was particularly important when dispensing the substrate and stopping agent, as the enzyme in all wells had to be exposed to the substrate for the same length of time. Standardization of ELISA plate colour differences: early reports of ELISA assays using microtitre plates often mentioned well-to-well variation in assays (Voller *et al.*, 1979; Burt *et al.*, 1979), the so-called "edge effects". These are manifested by greater colour development in the outer wells, caused by differences in temperature (Kemeny, 1991), as these wells generally run slightly hotter. However this effect can be largely overcome by keeping the plates separated rather than stacked, and using a rotator during incubation, (Avrameas *et al.*, 1991; Crowthers, 1995; Kemeny, 1991). This was an important observation, because even and efficient binding is needed for a reproducible and sensitive assay. Some variation may be due to the "batch effect" (a batch is defined as specimens processed at the same time, Whitley *et al.*, 1996) when experiments are performed at different times.

2.2.6.8 Calculation of E1-3G Levels from the Standard Curve

Absorbance values from the microplate reader printout were keyed into a commercial computer graphics package called PRISM. E1-3G standard concentrations (nmoles/24 h) on the X axis were transformed to log values. A non-linear regression analysis using a non-linear fit was then performed to fit the E1-3G standard curve, and unknown X values were returned by the programme from all the unpaired Y values. The X values read from the E1-3G standard curve were then transformed from log back to anti-log values. These data represented the E1-3G concentration values (in nmoles/24 h), and a menstrual cycle graph was created by plotting these on the Y axis with the appropriate cycle day opposite on the X axis (see figure 2.25). This means, therefore, that any departure of the urine sample volume from that used in the E1-3G standard dilution in the incubation mixture, requires a dilution factor to be used to adjust the E1-3G concentration in the urine sample from the E1-3G standard curve (see section 2.3.5.4, urine blank effect).

2.3 Results and Discussion

2.3.1 Coupling of Horseradish Peroxidase to E1-3G

Conjugation of horseradish peroxidase with E1-3G by the active ester coupling procedure was carried out (refer section 2.2.6.1), following the method developed by Keith Henderson (personal communication) (refer section 2.2.6.1). The active ester method was used to attach the oestrone glucuronide to horseradish peroxidase because glucuronides have a carboxyl group (see figure 1.7 section 1.2.2.) which can be activated through the use of DCC and NHS to form an N-hydroxy succinimide ester. Such an activated carboxyl group can then react with amino groups on lysine residues of HRP to form a stable E1-3G-HRP conjugate (refer figure 2.3).

Three solutions, E1-3G, DCC and NHS, were made up using the appropriate volume of DMF as the solvent (refer section 2.2.6.1). All relevant chemicals and equipment (pipette tips, containers etc.) remained in a dessicator overnight to ensure they were dry for the conjugation procedure. The E1-3G solution (50 µl) was added to a reaction vial followed by DCC (50 µl) then NHS (50 µl) and the vial was secured with a screw top. The solutions were mixed gently by shaking and left for 90 minutes at room temperature. Since the insoluble by-product dicyclohexylurea had not formed in the reaction vial a centrifugation step was not carried out. Elution profiles (figure 2.4) were generated after the gel filtration procedure, from the absorbance values 278, 280 and 404 nm, as a further aid to fraction selection and also to assess the purity of the HRP conjugate. The absorbance peaks were not symmetrical giving a tail on the lower molecular weight side.

Haemin and apoprotein, which make up the HRP enzyme, absorb light at different wavelengths. The haemin cofactor when bound to the apo-protein absorbs maximally at 404 nm wavelength and the apoprotein (and haemin end absorption) absorbs at 280 nm wavelength. This property of HRP has allowed a ratio between the two to be used to determine the purity of the enzyme, known as the reinheitzahl or `RZ Value' (Dunford, 1991), a German purity index. The RZ value is determined by dividing the A_{404} value by the A_{280} value where the highest purity value for native HRP has been established as about 3; that is an RZ Value of 3.

Since it appeared from the RZ value that some haemin had dissociated from HRP after the initial conjugation and gel filtration step (figure 2.4), the conjugate solution was passed through a CM sepharose cation exchanger, using sodium acetate as the eluant in a step

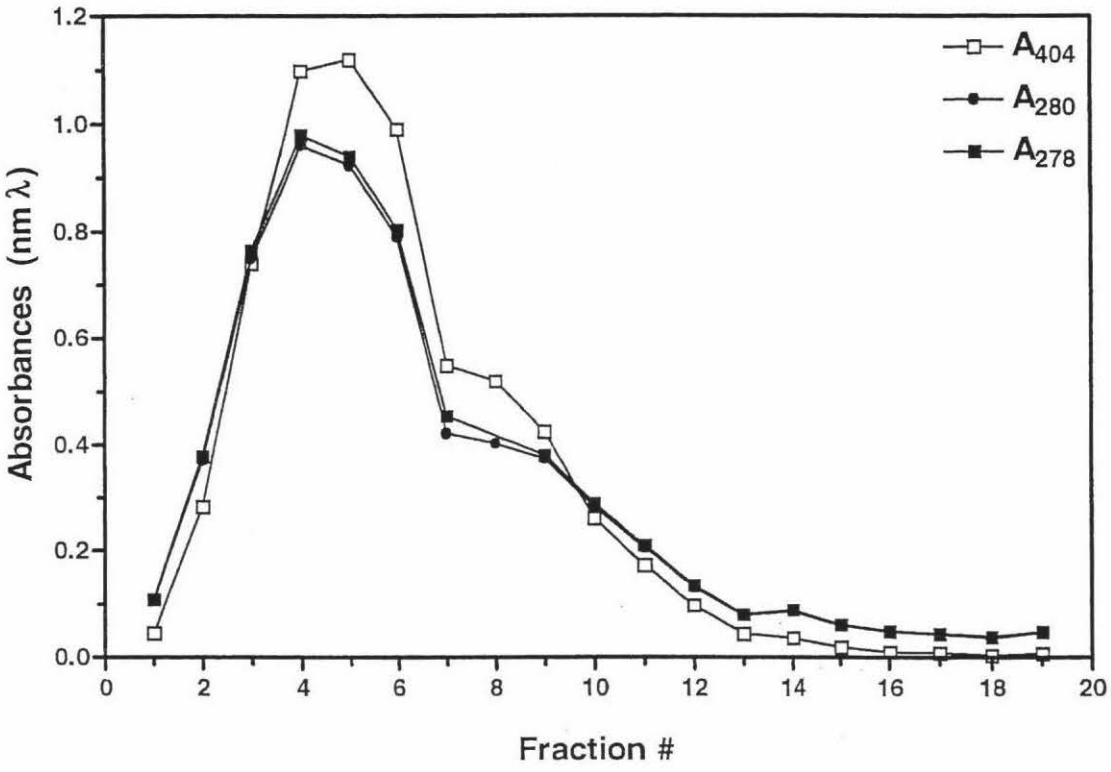

Figure 2.4: The E1-3G-HRP elution profile (for 1 ml fractions) generated following G-25 gel column chromatography.
(RZ A_{404} / A_{280} = 1.2)

gradient on the Econo System (refer section 2.2.1) to separate the resulting aproprotein from the HRP. Sodium acetate (5 mM) buffers were made up to pH 4.4 using HCl and the column equilibrated. The pH and electrical conductivity (measured in S cm^{-1} i.e. specific conductance) were measured throughout the procedure to ensure that the ionic concentration and pH remained constant. To buffer A 50 mM of NaCl was added and to buffer B 500 mM of NaCl was added. The step gradient was programmed for 90 minutes at a chart speed of 150 mm h^{-1}, a flow rate of 2.90 mls min^{-1} and absorbance units full scale (AUFs) 0-0.1 range. During the first 30 minutes only Buffer A was used, at 31 minutes 10% of Buffer B was used together with Buffer A, and from 61 minutes 100% Buffer B was used. As buffers A and B mixed the salt concentration increased and HRP was expected to elute during the second half hour followed by the apoprotein which binds more tightly under these conditions during the last half hour of the programme. Over the first hour (figure 2.5) the absorbance at 278 and 404 nm remained close to zero and there was no HRP enzyme activity detectable (refer section 2.2.6.2). Although the A_{278} and A_{404} peaks occurred virtually simultaneously during the last half hour (figure 2.5) they were both low and the concentration of HRP conjugate for fraction 77 (see figure 2.5) calculated from the absorbance at 404 nm (0.062) being only 575 nM. The specific activity was 320 ΔAU min^{-1} mg^{-1}, with an RZ value of 0.87. RZ values were variable particularly on the right side of the slope and the yield of product was insufficient for the requirements of assay development. In an attempt to increase the HRP conjugate yield a haemin reconstitution procedure (Wu, 1996) was carried out to reassociate the haemin with any apoprotein conjugate in solution and hence to restore the enzymatic activity of HRP. Then after gel filtration using DEAE-cellulose (DE-52, packed in pasteur pipettes) to remove excess haemin from solution (DiNello & Dolphin, 1981), a salt gradient was programmed for 90 minutes on the Econo System (10% Buffer B was used 0-31 mins, and 100% Buffer B for 32-90 mins) resulting in a more rapid salt increase rather than the initial step gradient. However, there was no increase in the yield of active E1-3G-HRP conjugate. The coupling reaction of horseradish peroxidase with E1-3G was repeated and examination of the next elution profile (figure 2.6) generated after the gel filtration column, clearly showed that the RZ value was 2.3 being approximately 76% of the original stock HRP. At all stages the absorbance values were read at 278 nm, 280 nm and 404 nm on the HP 8452A spectrophotometor using a quartz cuvette (refer section 2.2.1.). These results were comparable with those of Henderson (personal communication) who recovered around 70% of the HRP protein concentration following the G-25 chromatography step on the basis of the A_{280}. Although, a protein concentration based on the A_{280}, as for the coomassie

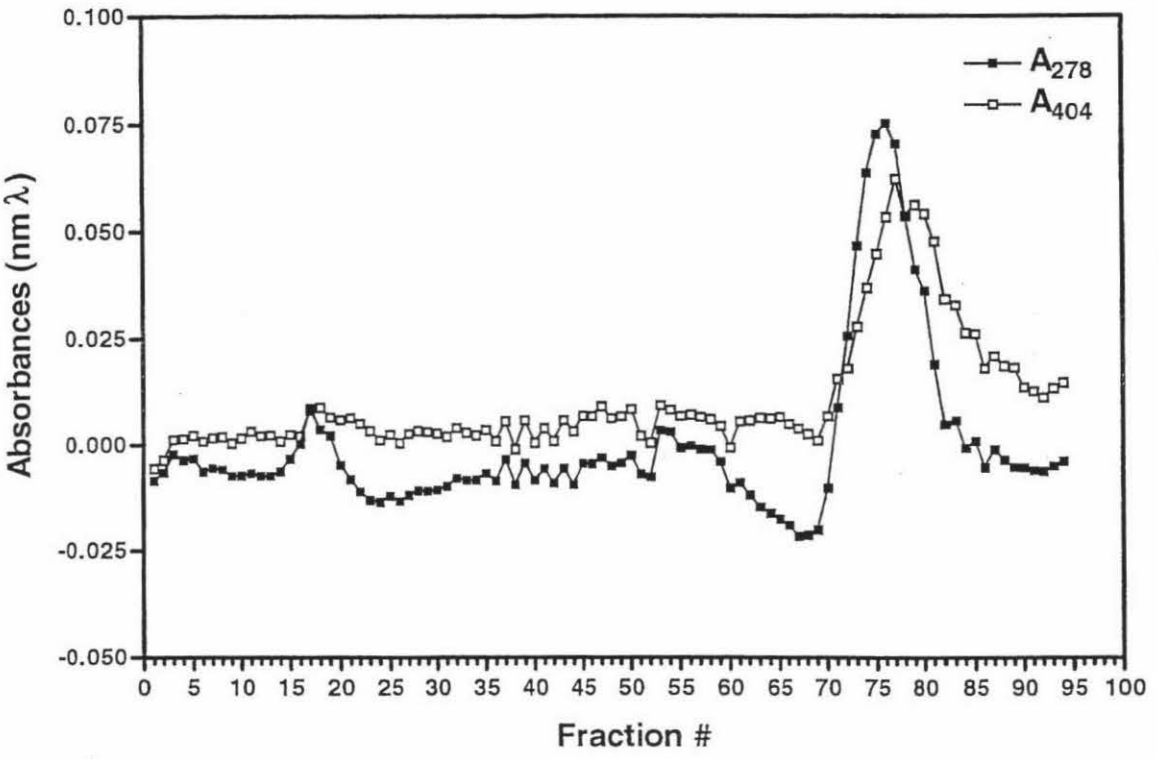

Figure 2.5: The E1-3G-HRP elution profile following a step gradient programme using an Econo system attached to a CM sepharose cation exchange column. (RZ value < 1.0)

method will of course include any apoprotein which may still be present in the conjugate mixture.

One main peak followed by two smaller peaks on the elution profile (figure 2.6) showed that the A_{404} and A_{278} overlapped completely indicating a single compound. Hence fractions (1-8) from the main peak were pooled and further purification procedures were not considered necessary after the resulting 16 mls were concentrated to 3.5 mls by utilizing a Diaflow System (refer Section 2.2.1). An increased concentration of HRP has been reported (Ryan *et al.*, 1994) to stabilize and preserve the integrity of HRP enzymatic activity. Although some loss of HRP may occur during the concentration procedure on the Diaflow system there was no evidence of HRP activity in the eluant and the RZ Value remained near 2, at 1.98. To further stabilize the conjugate 0.01% of thiomersal was added after the concentration procedures (50 µl/ml of a 2 mg/ml solution), and the conjugate was stored frozen in 0.50 ml aliquots. While the RZ value may have increased marginally due to smaller proteins being lost during the concentration procedure, the conjugate had a RZ value (2.3) higher than that of earlier conjugations which demonstrates there is purity variation between conjugates even though the same conjugating and purifying procedures are used.

Specific activities were calculated from the slopes of plots of A_{460} versus time using a Carey spectrophotometer (refer section 2.2.1 and 2.2.6.2) and from the horseradish peroxidase concentration determined from the absorbance value at 404 nm and an extinction coefficient of 107,700 (A_{404}/107,700). Therefore, the concentration of the E1-3G-HRP conjugate used in the assay development was 8.26 µM. The specific activity of the conjugate was about 45% of the native HRP control, and represents a physical loss of HRP and/or damage to the structural integrity of the enzyme during the purification and conjugation procedures. Commercial HRP samples usually include a percentage of salt and therefore are generally not pure when purchased and since the salt should easily be removed by dialysis calculations of initial HRP specific activities are probably affected by the presence of the salt.

The lower RZ values for the conjugate indicates that apoprotein is present (which of course does not absorb at 404 nm) and thus it may consist of a mixture of free and E1-3G conjugated apoproteins. As apoprotein conjugated to E1-3G will specifically bind to immunoassay antibody binding sites, and without the production of a detectable signal

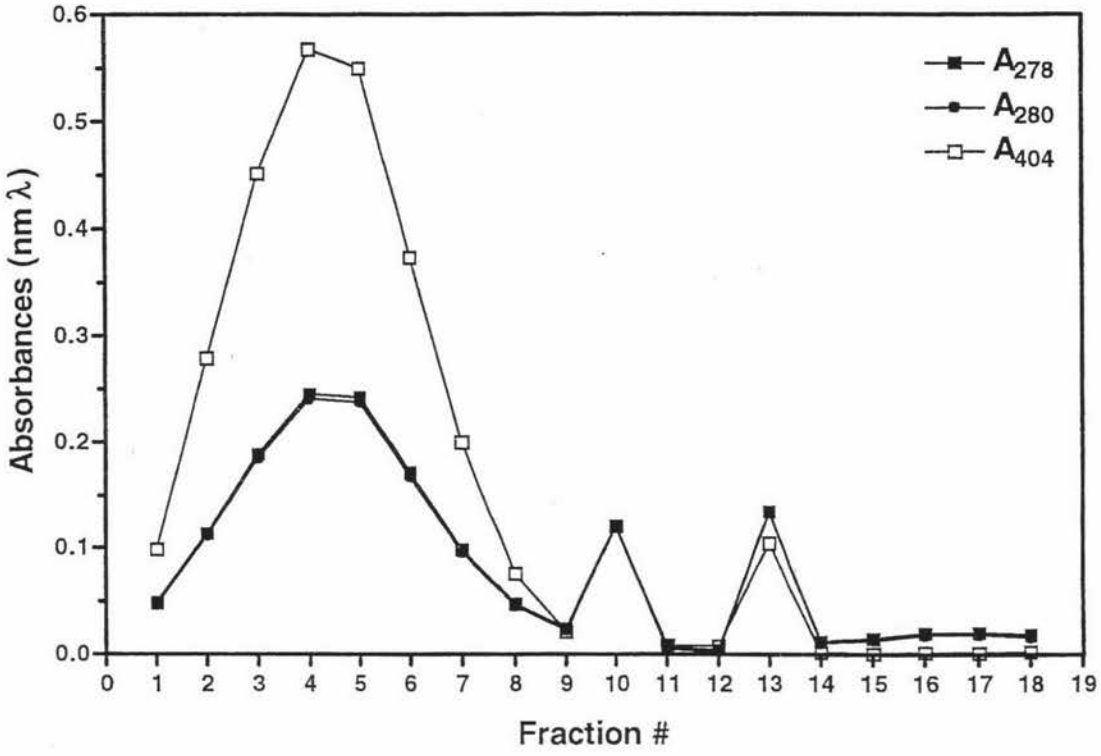

Figure 2.6: Elution profile of E1-3G-HRP (from repeat conjugation) after gel (G-25) filtration column chromatography. (RZ A_{404}/A_{280} = 2.0)

since enzymatic activity depends on the presence of haem, the sensitivity of the assay may be jeopardized. Thus, this material has the potential to interfere with the dynamics of the assay if it changes from conjugate preparation to conjugate preparation. Because the ratio of conjugated to unconjugated HRP may vary even though the same conjugation procedure is used, the standardisation of the proportion of apoprotein present may be difficult; ideally the ratio between the E1-3G HRP conjugate and the E1-3G apoprotein conjugate should be consistent from assay to assay.

A problem with the presence of unconjugated HRP in the conjugation sample is the potential for non-specific binding (NSB), where a signal is produced even when no steroid is attached to the protein and this can reduce the sensitivity of the immunoassay by increasing the noise to signal ratio, as discussed in the introduction of this chapter. Although, excess unconjugated HRP is mostly expected to be removed during a heterogeneous immunoassay (such as ELISA) by the washing procedures, NSB could occur at the enzyme incubation stage which is prior to washing.

2.3.1.1 The Difficulty of Knowing How Much Conjugate is Present in the Samples

Calculation of the correct HRP concentration and specific activity gave no indication of whether the HRP molecules were conjugated to E1-3G or remained unconjugated, or indeed of the amount of E1-3G coupled to each enzyme, given that HRP has six lysine residues (Ugarova *et al.*, 1978) for potential E1-3G coupling. While the ratio of the conjugate to the unconjugated HRP concentration remains unknown, the conjugate concentration is unable to be determined accurately , making it difficult for the assay to be replicated exactly by other researchers.

Smales *et al.* (1994) purified E1-3G-lysozyme conjugates by separating the conjugated lysozyme from unconjugated lysozyme using ion-exchange column chromatography and hydrophobic interaction chromatography in 7 M urea. This separation appears to be unique for lysozyme conjugates and when EIG-HRP conjugates are dissolved in 7 M urea the haeme dissociates. Also, for the HRP conjugates, in the absence of 7 M urea there are no visible chromatographic differences (Blackwell personal communication). To avoid the denaturing effects of urea, Smales *et al.* (1998) purified small amounts of lysozyme-estrone glucuronide conjugates using acid-polyacrylamide gel electrophoresis (PAGE) and separated six E1-3G lysozyme conjugate species (the active ester method was used to couple E1-3G to lysozyme). However due to time constraints the purification of E1-3G-

HRP conjugate using acid PAGE was not carried out in this present work.

Schramm and Paek, (1992) purified an HRP-progesterone conjugate (HRP-P) by first using exclusion chromatography on Bio-Gel P-30, and finally on an immunoaffinity column where anti-progesterone IgG antibody was immobilized on cyanogen bromide (CNBr)-activated sepharose 4B gel. They claim that the enzymatic activity of the conjugate was preserved without loss for over one year in phosphate buffer (10 mM) stabilized with $NaIO_4$ (1 mM) and gelatine (0.1%). They isolated three P-HRP conjugate species, on the basis of their different affinity constants with the antibody (the first peak contained unconjugated HRP). Two of the conjugate fractions were shown to contain a single progesterone ligand bound to HRP, and a third fraction contained two progesterone ligands attached to HRP. The P-HRP conjugates were characterised by binding to immobilized monoclonal antibody in microtitre wells using Scatchard analysis (Scatchard, 1949). A comparison was made of the binding constants from the affinity chromatography and from the Scatchard analysis which demonstrated that the divalent conjugate bound to the immobilized antibody in microtitre wells by a single attachment since the binding constant obtained with antibody immobilized on gel (three dimensional compared to two dimensional planar surfaces) was twice as high as that measured with antibody in the microwells. This means theoretically, that more conjugate can bind to antibody, since each conjugate occupies only one of the available antibody binding sites (although the greater bulk of the conjugate may be the limiting factor). There is, therefore, potential for a greater variation in the range of the signal from the (enzymatic amplification) conjugate, and hence the potential for ELISA assays with a greater working ranges. Such a one to one ratio, of conjugate to antibody binding sites, also provides the potential for an intrinsically more sensitive ELISA assay.

The different binding constants of the different species of conjugate may be a result of the different charge distributions surrounding the analyte molecules conjugated to the enzyme, and therefore to the different ionic interactions between the analyte and the binding site of the antibody. Further, the attached analyte may protrude from the protein periphery with a variable distance (figure 2.7) according to the positions of the different conjugation site and therefore provide varying bridge lengths between the two conjugated molecules. Steric hindrance of the divalent conjugate would prevent the simultaneous binding of both ligands at the same time. Not only may the divalent conjugate have reduced flexibility to bind antibody on a microtitre well, but the steroid binding sites on

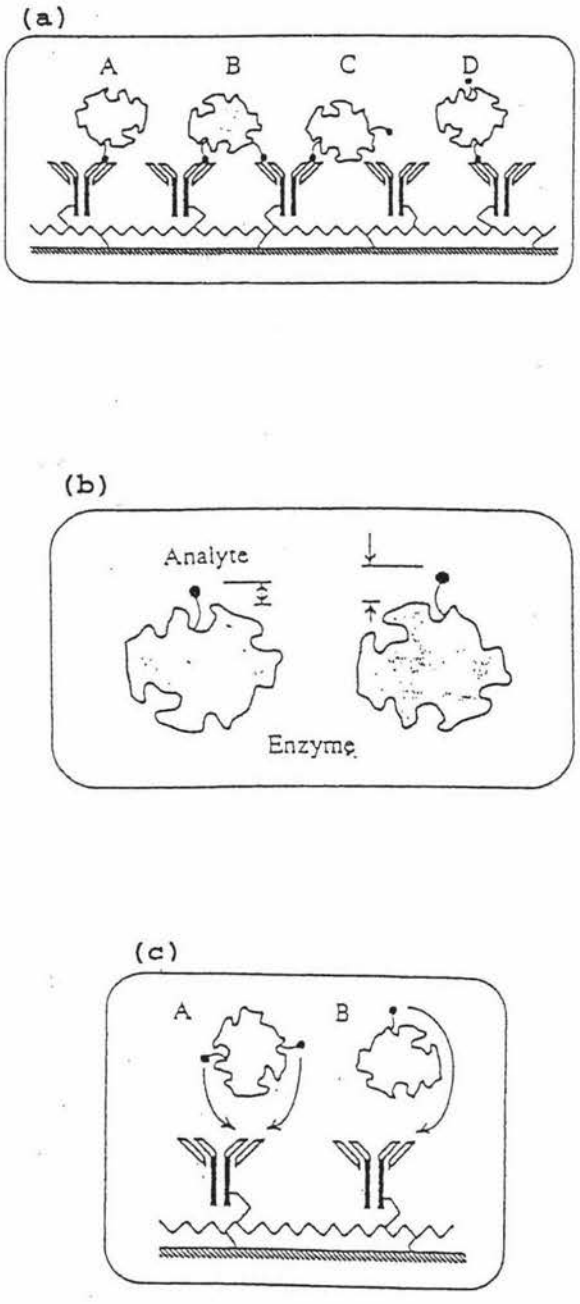

Figure 2.7: (a) Different hypothetical binding patterns of E1-3G-HRP conjugate to immobilized antibody with one ligand, and the conjugate with multiple ligands at different positions. (b) The conjugate with two ligands bound to two antibody binding sites. (c) Protrusion of small conjugated analyte molecules (such as E1-3G) at variable distances from the periphery of an enzyme molecule (such as HRP). [Paek *et al.*, 1993]

HRP may be distal to each other, making it impossible for them both to bind without denaturing the enzyme (figure 2.7). However, in the context of the present ELISA development it is the assumption that only one HRP conjugate seems to bind to antibody that is relevant, rather than the nature of the differences between the conjugate species.

Although there are six available conjugation sites on HRP to bind glucuronides via stable amide linkages only two seem to be available for chemical conjugation under mild reaction conditions (Francois *et al.*, 1972: Nakane & Kawaoi 1974). Such mild conditions include both the active ester method and the method used by Paek *et al.*, (1993) (Bragg & Hou, 1975), where progesterone-N-(4-aminopentyl)-4-pregnen-11-α-ol-3,20-dione succinyl amide (P-CAD) was chemically reacted with HRP via disuccinimidyl suberate (DSS) as a cross-linking reagent dissolved in anhydrous dimethyl sulfoxide (DMSO). It seems therefore reasonable to assume that conjugation of HRP to E1-3G via the active ester method may also contain three conjugate species each with different binding affinities for immobilized E1-3G-antibody. The remaining four amino groups can react only under strong acylating conditions with anhydrides (Ugarova *et al.*, 1978) and dithioesters where the protein is likely to become partially denatured. It may be that lysines are involved in haem stabilization and/or glycosylation sites are near some lysines, and thus further E1-3G couplings are prevented using mild conjugation conditions. It was not considered part of this thesis to prepare immunoaffinity resins and attempts to separate the individual conjugate fractions. The crude conjugate preparation was used without further purification.

2.3.2 Purification and Estimation of E1-3G-Antibody

It is generally recognised that purification of crude antiserum gives better control over ELISA assays since many interfering proteins are removed. The Ovarian Monitor (refer section 1.1.5) was used for lysozyme conjugate inhibition studies (refer section 2.2.6.6) to estimate the concentration of the E1-3G antibody in solution before and after an ammonium sulphate precipitation (refer section 2.2.6.4) purification procedure (Harlow, 1988) was carried out.

The results of the lysozyme inhibition assays are shown in figure 2.8 where the varying volumes (µl) of antibody are plotted against the percentage inhibition of the lysozyme conjugate. The lysozyme-E1-3G conjugate was maximally inhibited by the crude E1-3G-antibody at an 'endpoint' volume of 5 µl before the antibodies were purified and at an

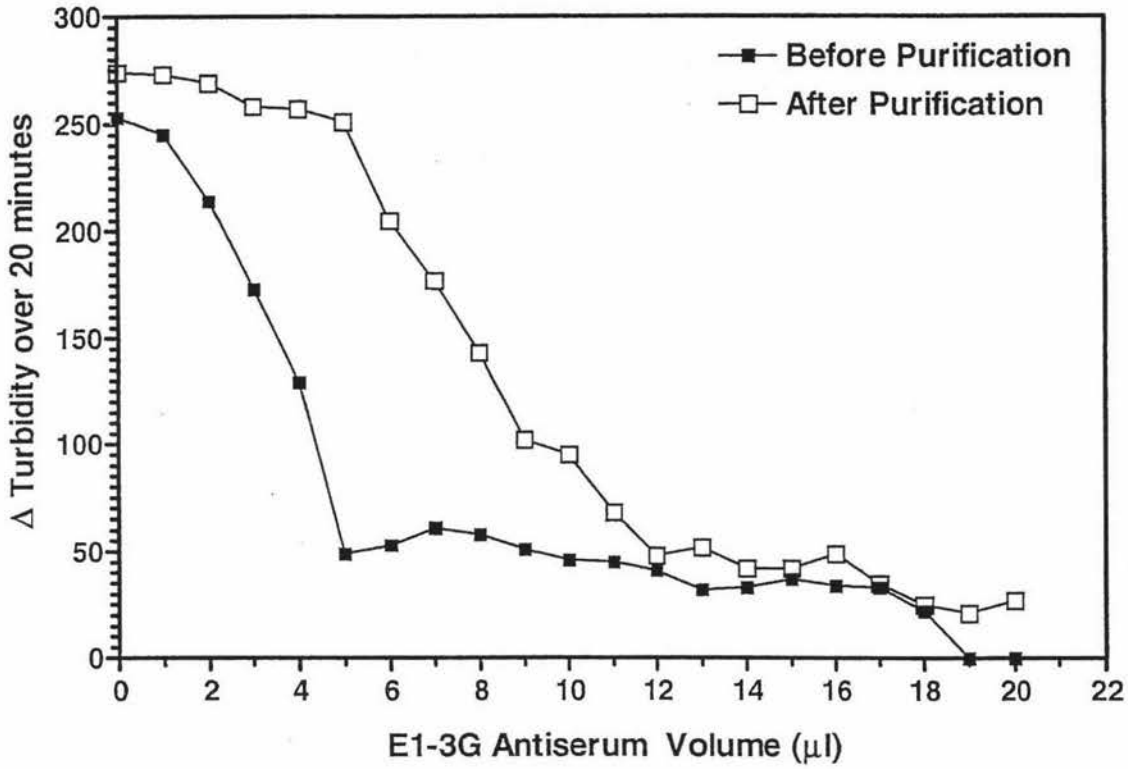

Figure 2.8: Inhibition assays using the Ovarian Monitor (section 2.2.6.6) to assess E1-3G antibody concentration before and after the ammonium sulphate precipitation procedure: An endpoint volume of 12 µl of E1-3G antiserum (1/50 dilution) was required to inhibit the E1-3G lysozyme (10 µl, 1/800 dilution).

'end-point' volume of 12 µl of a sample of a 1/50 dilution of antiserum after the antibodies were purified. Using a 1/800 dilution of the E1-3G lysozyme conjugate the concentration of the HEWL-E1-3G conjugate in the assay was calculated based on the assumption that a given 1/50 dilution of a lysozyme conjugate solution will generate an absorbance value of 0.299 at 280 nm., and the fact that a concentration of 1 g/100 mls of lysozyme has an absorbance at 280 nm of 26.4. Using the molecular weight of HEWL-E1-3G of 14,746 Da, (lysozme plus 1 E1-3G residue) the concentration of the conjugate was then calculated as 10.49 nM in the assay tube. The total concentration of the antibody-binding sites in the original serum was therefore equal to 350/12 x 10.49 nM x 50 or 15.3 µM, where the total assay volume was 350 µl. Each antibody molecule can bind two conjugate molecules thus the concentration of antibody is actually half this value or 7.65 µM. However, since we do not know the structure of the E1-3G-HRP conjugate and whether one or two HRP conjugate molecules can bind at the same time the antibody concentrations were expressed as total antibody binding site concentrations. The end-point of HEWL-E1-3G titration, before the antibodies were purified, was also used to give the total concentration of antibody binding sites in the original serum which was 350/6 x 10.49 nM x 100 or 61.2 µM. Because the antibody solution was more dilute after titration, the concentrations were adjusted so that the yield could be calculated. From the concentrations before titration (183 nmoles in 3 ml) and after titration (107 nmoles in 7 mls), the antibody yield was estimated as approximately 59% (107/183). While some antibody loss was inevitable the recovery was expected to be more than 59%. Cummock (1998) reported an antibody recovery of 90% after ammonium sulphate precipitation, and confirmed that the majority of the antibody was indeed retained in the supernatant after lipoprotein precipitation procedures where 83% of the original antibody was recovered.

2.3.3 Optimization of Assay Parameters

Optimal transmittance for minimum relative errors in spectrometric readings

The absorbance reading of spectrometric measurements using conventional spectrophotometers should be between 0.1 and 1.0 (or 1.5) absorbance units (see figure 2.9) (The Beer Lambert Law, in Swinehart, 1962). A nearly constant minimum-error occurs over the range of 20-65% T (0.7 to 0.2 Abs). Thus the percentage transmittance should fall within 10 to 80% T (1.0 to 0.1 Abs) in order to prevent large errors in spectrometric readings. Hence samples should be diluted or concentrated, and standard solutions prepared, so that the absorbance falls within the optimal range.

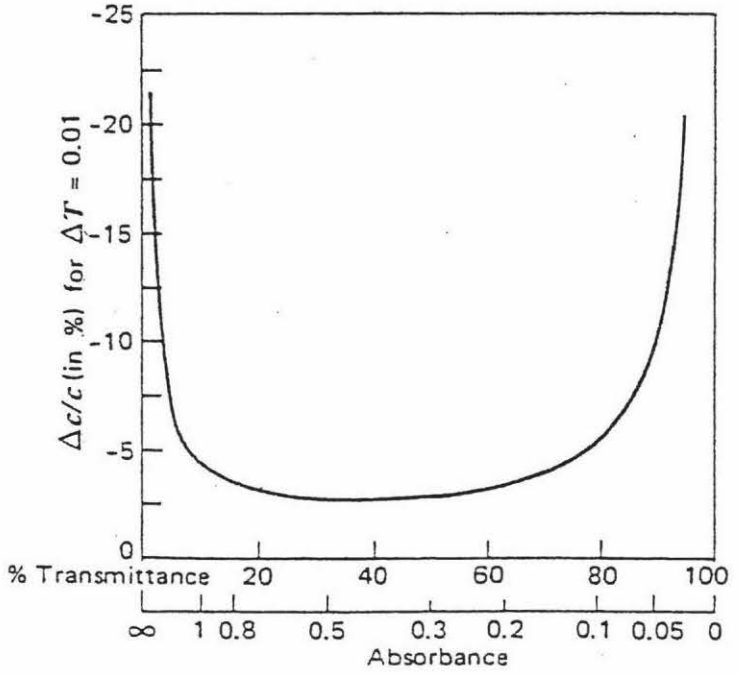

Figure 2.9: The relative concentration error as a function of transmittance for a 1 % uncertainty in percentage transmittance. [Christian, 1994]

Given the difficulty of precisely measuring either very small or very large decreases in absorbance, and given the negative correlation between the intensity of colour produced in the assay and the concentration of unconjugated steroid, the optimal reading for the zero standard was targetted as 1.0 absorbance unit at 490 nm.

The best antiserum dilutions were found to be between 1/3,000 and 1/1,000 from initial checkerboard titrations and a further set of antiserum dilutions were investigated including a dilution series for both the E1-3G-antibody and the E1-3G-HRP conjugate. These were then put into the microtitre wells using the ELISA Protocol (section 2.2.6.7) in a checkerboard fashion and left to incubate for 2 hours at 4°C. figure 2.10 (a) shows the results of the initial checkerboard titration, where each line represents a different dilution of antibody (1/30 to 1/10,000) plotted against a dilution range of the E1-3G-HRP conjugate (1/40 to 1/10,000). There was clearly a region of conjugate concentrations giving maximum colour development for each antiserum dilution between 1/3,000 and 1/10,000. The next experiment therefore tested a smaller range of antibody dilutions from 1/500 to 1/3,000, with increased conjugate dilutions up to a 1/24,000 dilution. The results showed (figure 2.10 (b) an increase in conjugate binding (as shown by the colour development) with increasing conjugate dilution with a tendency for the highest antibody concentration (1/500 dilution) to show a maximum amount of conjugate binding as the conjugate solution became more dilute. Figure 2.10 (c) shows the effects of increasing conjugate dilutions (to 1/35,000) on the colour development for a series of antiserum dilutions up to a maximum antibody dilution of 1/2,000. This suggests that a high dose hook effect is operating and since increasing conjugate dilution should lead to decreasing colour development it was necessary to increase the conjugate dilutions further. This "High Dose Hook Effect" has been reported by Paek *et al.*, (1993) to occur in the presence of high HRP concentrations. They showed that free HRP forms aggregates, and that such aggregates also contain progesterone, thus preventing the progesterone from binding to anti-progesterone antibodies. When the HRP solution containing the HRP aggregates was diluted the binding of progesterone to anti-progesterone antibodies increased; clearly demonstrating a positive correlation between dilution and binding. Alternatively, high enzyme concentrations may encourage antibodies to leach (Crowthers, 1995) from the polystyrene surface of the microwells. In agreement with these suggestions figure 2.10 (d) shows the expected results at the highest HRP conjugate dilutions (1/20,000 to 1/70,000) with a series of antibody dilutions between 1/500 and 1/3,000. A series of parallel lines were obtained and an antibody dilution of 1/2,500 and an E1-3G-HRP conjugate dilution of 1/35,000 were chosen which together produced a value of approximately 1.00 absorbance unit at A_{490}. These optimal dilutions were then used to develop the ELISA for E1-3G and the same procedure was followed after each new conjugation of E1-3G to HRP.

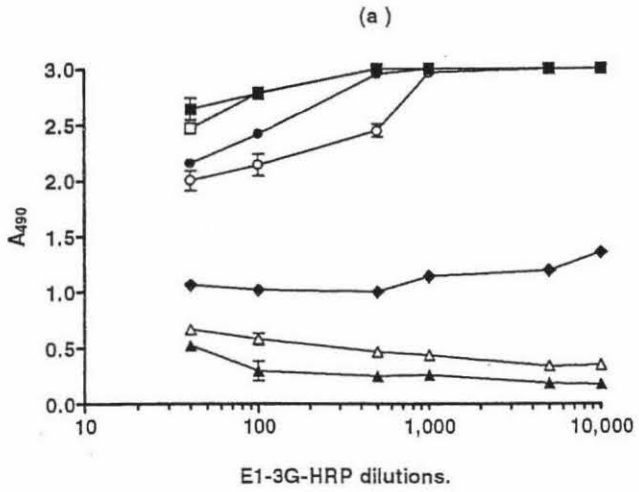

Figure 2.10 (a): The initial checkerboard titration of E1-3G antibody (dilutions; —■— 1/30 —□— 1/100 —●— 1/500 —○— 1/1,000 —◆— 1/3,000 —△— 1/6,000 —▲— 1/10,000) against E1-3G-HRP conjugate (dilutions; 1/40 to 1/10,000).

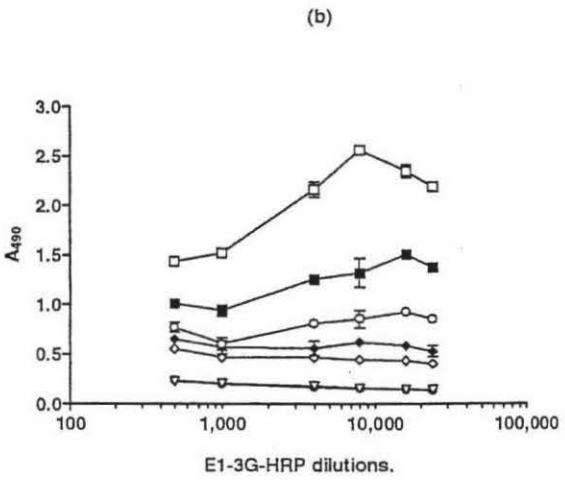

Figure 2.10 (b): Checkerboard titration of E1-3G antibody dilutions (—□— 1/500 —■— 1/1,000 —○— 1/1,400 —◆— 1/1,800 —◇— 1/2,200 —▽— 1/2,600 —●— 1/3,000), up to a 1/24,000 dilution of conjugate.

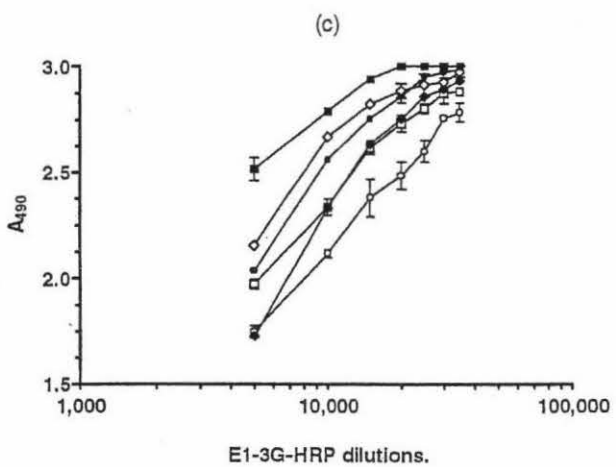

Figure 2.10 (c): Checkerboard titrations: Effects of increasing the conjugate dilutions (to 1/35,000) on the colour development for a series of antiserum dilutions (—■— 1/500, —◇— 1/750, —◆— 1/1,000, —◆— 1/1,250, —□— 1/1,500, —○— 1/2,000).

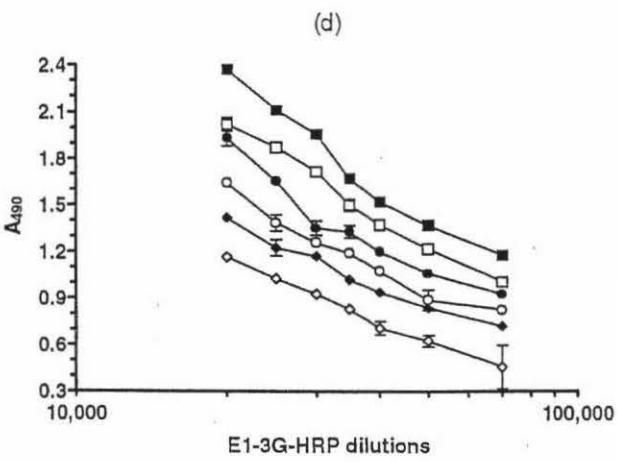

Figure 2.10 (d): Checkerboard titrations: using high HRP conjugate dilutions (1/20,000 to 1/70,000) with a series of antibody dilutions (—■— 1/500, —□— 1/1,000, —●— 1/1,500, —○— 1/2,000, —◆— 1/2,500, —◇— 1/3,000).

E1-3G-Antibody Dilutions (ng/well)

Although the amount of E1-3G is defined in this assay as a rate of excretion in "E1-3G nmoles/24 h" a comparison between the various E1-3G antibody dilutions in ng per well (as shown in Table 2.1), is useful as a comparison with other methods especially in conjunction with the amount of analyte per well.

The concentration of E1-3G antibody was 15.3 µM (refer section 2.3.2) and the amount of E1-3G-anti-serum used in the ELISA (100 µl/per well of a 1/2,500 dilution) was therefore equal to 0.612 picomoles, or 97 ng per well, using a molar mass for the antibody of 160,000.

Table 2.1: E1-3G-Antibody in ng/microwell (100 µl) for Each Dilution

diln.	1/ 500	1/ 1,000	1/ 1,250	1/ 1,500	1/ 2,000	1/ 2,500	1/ 3,000
ng/well	489	244	195	163	122	97	81

2.3.4 Generation of an E1-3G Standard Curve

The optimization of the E1-3G standard and E1-3G-HRP conjugate concentrations were required to generate a standard curve. While the optimal volume of the E1-3G-HRP (1/35,000) dilution has been determined, the optimal E1-3G-HRP volume required in the presence of E1-3G standards was investigated. Varying volumes of E1-3G standards (prepared as in section 2.2.4) were used to generate standard curves and hence to determine the optimal volume of the E1-3G standards required to add to the assay. Initially, four standard curves were generated using volumes of 10 µl, 50 µl, 100 µl and 150 µl of the E1-3G standard in a total volume of 450 µl in an Eppendorf tube. The tubes contained E1-3G-HRP conjugate (300 µl) at the optimized dilution of 1/35,000 (refer section 2.3.3) and 0.1% assay buffer (refer section 2.2.3). After vortexing, aliquots (150 µl) from the mixture in the Eppendorf tube were put into each microplate well so that duplicate or triplicate wells could be prepared for each data point, and the plates were then left overnight at 4°C to incubate. As shown (in figure 2.11) the higher volumes of the E1-3G standards (100 µl and 150 µl) saturated the majority of the available antibody binding sites at low nominal E1-3G concentrations and prevented sufficient E1-3G-HRP label binding for a standard curve to be generated. The lesser volume of E1-3G standard of 50 µl allowed more E1-3G-HRP to bind, but the smallest of the lower standard

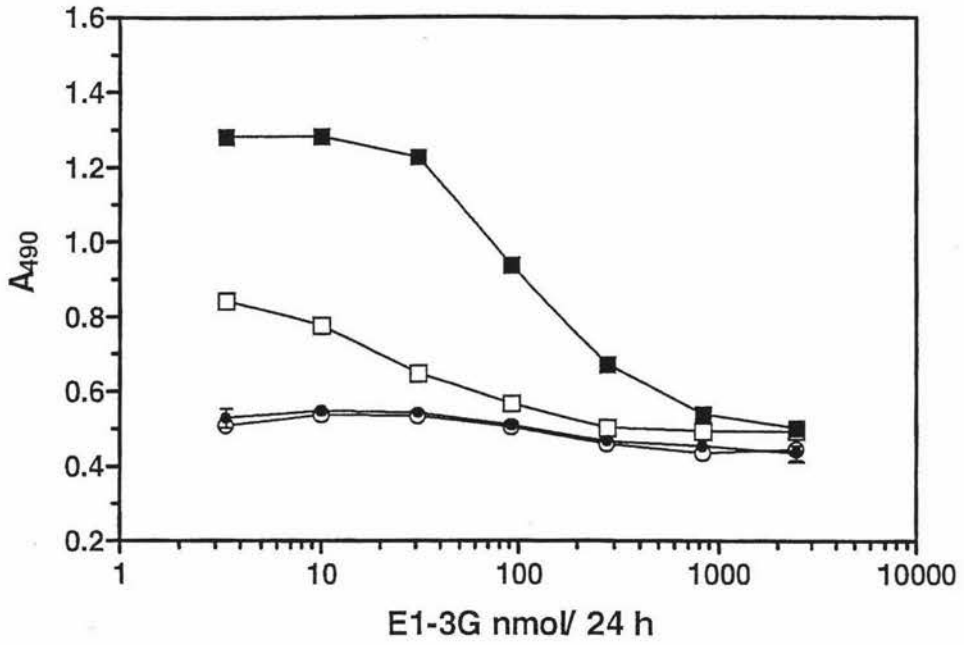

Figure 2.11: Effect of varying the volume of E1-3G standard (—■— **10 µl,** —□— **50 µl ,** —•— **100,** —○— **150 µl**) on the E1-3G standard curves.

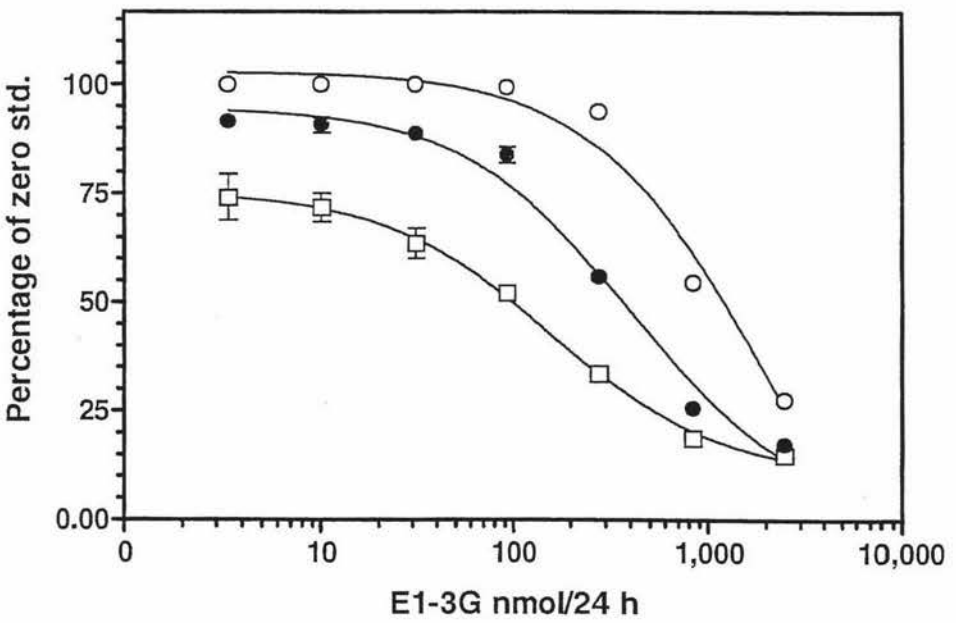

Figure 2.12: A series of standard curves generated with ○ **2 µl,** • **5 µl,** and □ **10 µl** E1-3G standards (Total volume of 450 µl; E1-3G-HRP, 300 µl; overnight; 4°C).

concentrations volume of E1-3G standard (10 µl) was the only one which generated an acceptable standard curve using the same E1-3G standards employed with the Ovarian Monitor (nmoles/24 h).

Three further standard curves were generated (see figure 2.12) with smaller volumes of the E1-3G standards (2 µl, 5 µl and 10 µl) in a total volume of 450 µl made up with E1-3G-HRP (300 µl) and assay buffer as above, and left overnight at 4°C. The lower volumes of the E1-3G Standards (2 µl and 5 µl) were insufficient to reduce the level of E1-3G-HRP binding for the three lowest E1-3G standards (3.4 nmoles/24 h, 10 nmoles/24 h and 31 nmoles/24 h) thus comprising the working range of the standard curves. The optimal E1-3G standard volume was therefore 10 µl in a total incubation volume of 450 µl with E1-3G-HRP (300 µl) and assay buffer. Lower volumes of E1-3G-HRP conjugate in the Eppendorf incubation mixture (150 µl an 200 µl) were also used to generate more sensitive standard curves. However, there was very little advantage between these curves (figure 2.13) and those generated with 300 µl of E1-3G-HRP conjugate but as the concentration points tended to cluster near the top this suggested that extra E1-3G standards were needed.

Standard curves were therefore generated from a mixture containing E1-3G-HRP (300 µl) and E1-3G standards and assay buffer as above, and incubated overnight at 4°C, but with extra E1-3G standards. The standard curve generated was excellent and the data points were spread over a wider range (figure 2.14) probably due to the overnight incubation. The extra E1-3G standards contained lower E1-3G concentrations (3.4 nmoles/24 h and 10 nmoles/24 h) and also an E1-3G standard containing a high E1-3G level (2,400 nmoles/24 h). The higher antibody dilution (1/2,500) gave a more sensitive curve than did the curve using a 1/1,500 dilution of antiserum. Since the mid-points of the curves were similar the higher dilution was regarded as the optimum for further assay development.

The choice of optimum volume of E1-3G standards to give a suitable standard curve was important to simplify the use of the assay to determine urinary E1-3G excretion rates measured in nmoles/24 h. The Ovarian Monitor standards are designed to allow the E1-3G levels to be read directly from the monitor standard curve. If the same volume of an unknown urine sample is added to the assay as is used for the standards, the assay response can be read directly from the standard curve to give the required rate of E1-3G

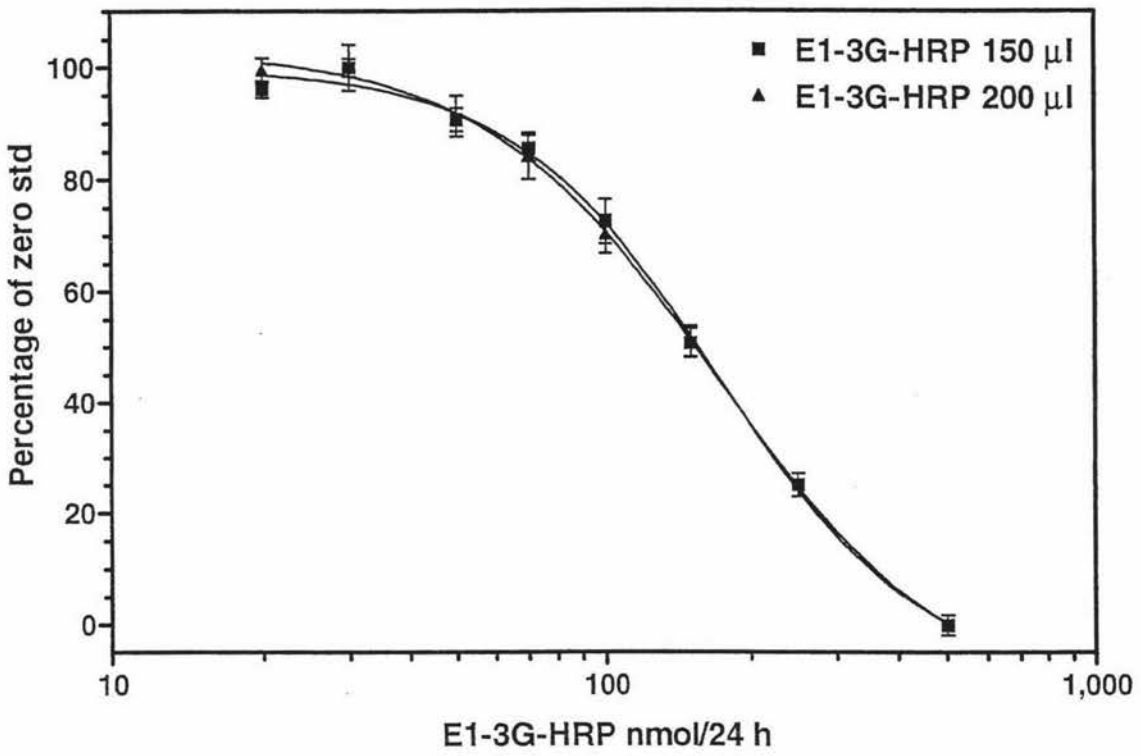

Figure 2.13: Standard curves constructed using 150 µl and 200 µl of E1-3G-HRP conjugate. (E1-3G-HRP conjugate dilution 1/35,000; E1-3G monitor standards 10 µl; E1-3G-antibody 1/2,500 dilution; 2 h incubation; 4°C)

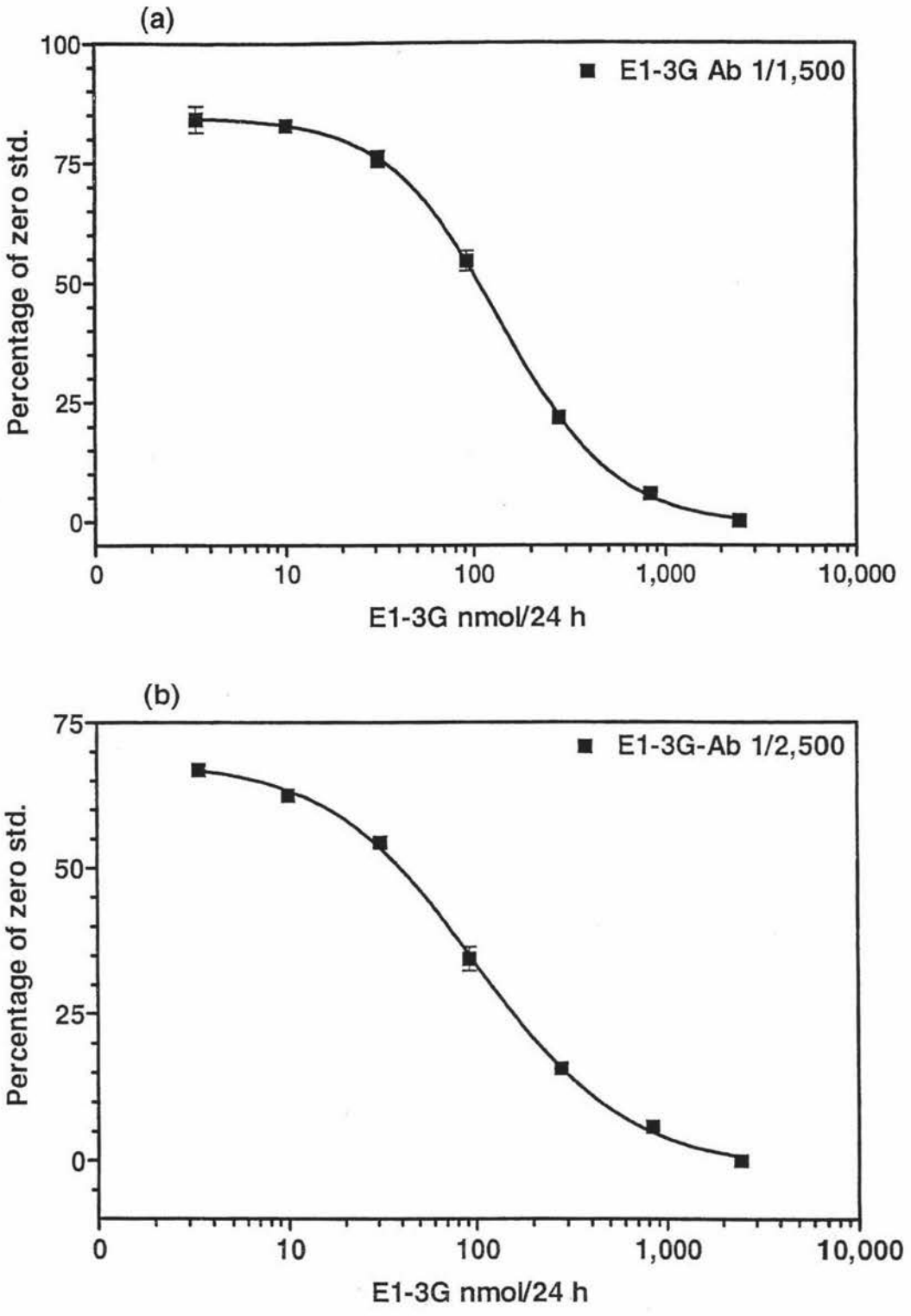

Figure 2.14: Standard curves generated using lower E1-3G standards (3.4 nmol/24 h and 10 nmol/24 h) and an E1-3G standard containing a high E1-3G level (2,400 nmol/24 h). A higher E1-3G antibody concentration (a dilution of 1/1,500) was used to construct the standard curve shown in (a) than the E1-3G antibody concentration (a dilution of 1/2,500) used to construct the standard curve shown in (b) to compare the effect of different antibody dilutions on the standard curve. (E1-3G HRP 300 µl, 1/35,000 dilution; E1-3G monitor standards 10 µl ; 16 h incubation; 4°C)

excretion. Hence, in the ELISA system if 10 µl of the timed urine sample (section 2.2.5) is added to the assay instead of the E1-3G standards, the absorbance at 490 nm can be read directly from the standard curve to give the rate of E1-3G excretion, assuming all other things are equal.

The E1-3G standard curve was optimized to measure E1-3G levels between 20-500 nmoles/24 h. As discussed in the introduction (refer section 2.1) while E1-3G baseline levels vary between individual women, the majority of E1-3G baselines are below 100 nmoles/24 h, and the data point for this amount (see figure 2.14) was on the most sensitive part of the standard curve (i.e. at the midpoint). A significant percentage of E1-3G baselines are around 15 nmoles/24 h (Brown *et al.*, 1989) and total urinary oestrogen analysis indicates some E1-3G baselines may be much lower (Blackwell & Brown, 1992). This standard curve therefore is ideal for the determination of the first E1-3G rise from baseline, but more concentrated urine samples will probably require extra dilution which raises the question of the influences of any matrix effects (refer cross reactivity in section 2.3.5.3, and the blank urine effect in section 2.3.5.4).

The assay blank (in which assay reagents only were put into microwells with immobilized E1-3G antibody) absorbance values (i.e. around 0.03) were very low and obviously showed little effect. Colour in these wells may increase if unconjugated HRP non-specifically binds to the antibody or adsorbs to plastic, however a gelatine blocking buffer (refer section 2.2.3) was used successfully in the ELISA (refer section 2.2.6.7) to control such binding/adsorption. The E1-3G standard curves were normalised using the assay blanks defined as 0%, and the zero blanks (no E1-3G standards were present) defined as 100%, to allow comparisons between different E1-3G standard curves.

2.3.4.1 E1-3G and E1-3G-HRP Amounts Per Microwell (ng/well)

Although the absolute amount of E1-3G in this immunoassay is defined in units of E1-3G nmoles/24 h, the E1-3G amount in pg/well was determined for the E1-3G-HRP conjugate and for the E1-3G standards (see Table 2.2) to enable comparisons to be made with other research. Although the E1-3G-HRP conjugate concentration was established from the peroxidase concentration of the conjugate mixture (refer section 2.3.1), and the antibody concentration was an estimation (refer section 2.3.2) the amounts (pg/well) in Table 2.2 enables trends and ratios to be compared.

Given that the stock E1-3G-HRP conjugate concentration was 8.26 µM (refer section 2.3.1) and that the optimum dilution was 1/35,000 for an optimal volume per Eppendorf of 300 µl, then the maximum concentration of the conjugate was 0.0708 picomoles in 300 µl, or 3.15 ng per Eppendorf (0.0708 picomoles X Mr 44,468.5 = 3.148 ng). Since 150 µl of this mixture was added to each microwell this corresponds to 1.049 ng of E1-3G-HRP per microwell. The amounts contributed from the E1-3G samples were calculated based on a molecular weight for E1-3G of 468.5.

The components of the E1-3G ELISA (in picograms per well) are given in Table 2.2 where it is apparent that for example the E1-3G-HRP conjugate (300 µl/Eppendorf) and E1-3G standard (100 nmoles/24 h) represent a tracer (1,049 pg/well) to analyte (43 pg/well) ratio of approximately 25 : 1 respectively, and an E1-3G antibody (97,000 pg/well) to E1-3G standard (100 nmoles/24 h) ratio of approximately 2,255 : 1. Since E1-3G-HRP conjugate is only a fraction of the total HRP present these ratios represent upper limits. The true E1-3G-HRP conjugate to E1-3G ratio is < 25 : 1. Research by Schramm & Paek (1991) reported that approximately 25 pg/well of progesterone was required to inhibit 50% of the enzyme tracer (HRP-progesterone) at incubation times over 30 minutes. In comparison, the E1-3G standard curve (figure 2.14) used in the present work required about 43 pg/well of E1-3G to inhibit 50% of the E1-3G-HRP conjugate at an incubation time of 16 h, and therefore compares well.

Henderson *et al.* (1995) generated a standard curve using affinity purified E1-3G monoclonal antibodies rather than the polyclonal E1-3G antibodies purified by ammonium sulphate precipitation method (2.2.6.4) used in the present study. The lower amount of polyclonal E1-3G antibodies (97 ng/well) used in the present study compared to E1-3G monoclonal antibodies (250 ng/well) represents a 2.5 fold difference between the two types of antibodies. The amounts of E1-3G standard compares favourably with this present study: their range 2 pg/well to 500 pg/well; this study 1.4 pg/well to 434 pg/well. Both studies used an unpurified HRP conjugate.

Table 2.2: Components of the E1-3G ELISA (Grams /Microwell)

E1-3G Standards		E1-3G-HRP	Antibody
nmoles/24 h	pg/well	pg/well	ng/well
1,000	434	1,049	97
500	216	"	"
300	130	"	"
250	108	"	"
150	65	"	"
100	43	"	"
70	30	"	"
50	22	"	"
30	13	"	"
20	9	"	"
12.5	5	"	"
10	4	"	"
5	2	"	"
3.4	1.4	"	"
1.137	0.5	"	"

2.3.5 Evaluation of the ELISA E1-3G Standard Curve

Tests were performed to evaluate the accuracy of the E1-3G standard curve, reliability, sensitivity, cross-reactivity and non-specific binding.

2.3.5.1 Sensitivity

Assay sensitivity was defined (Henderson *et al.*, 1995) as the amount of E1-3G producing a decrease in the percentage of bound E1-3G-HRP value (E/E_0) two standard deviations below that of the zero standard (refer section 2.3.4). Here `E' is defined as the mean absorbance reading for the E1-3G standard (refer section 2.2.4), which is divided by the mean absorbance reading of the zero standard `E_0'. The lowest E1-3G standard concentration used to construct the standard curve was 3.4 nmoles/24 h and therefore this E1-3G standard was tested first. Because each standard curve had the E1-3G standard (3.4 nmoles/24 h) and the zero standard (no E1-3G added) points done in duplicate or triplicate it was necessary to first find the mean of each of these absorbance values for each standard curve. The standard deviation (S.D.) for both the mean absorbance for the E1-3G standard (3.4 nmoles/24 h) and for the mean absorbance for the zero standard (no E1-3G) was calculated, and then the S.D. with the highest value was selected. The selected S.D. was then multiplied by 2 (two standard deviations) in preparation for subtraction. This 2 S.D. value was then subtracted from the mean absorbance reading for the zero standard. The mean absorbance reading for the E1-3G standard point was then divided by the mean absorbance reading of the zero standard minus two S.D., and the resulting value multiplied by 100 to determine the percentage. If a percentage was more than 100 the E1-3G standard being tested (nmoles/24 h) would fail the sensitivity test, and show the signal resulting from it in the assay was not significantly different from the zero standard. The next E1-3G standard (nmoles/24 h) would then be tested until a significant decrease was calculated and this was taken as the sensitivity.

Each individual E1-3G standard curve carried out under optimised conditions had a sensitivity of at least 3.4 nmoles/24 h (1.4 pg/well, refer section 2.3.4; Table 2.2), since the percentage calculated for the data shown in figure 2.14a was 93.2%. The intra-assay sensitivity was therefore 3.4 nmoles/24 h (1.4 pg/well). The inter assay sensitivity was also calculated as 3.4 nmoles/24 h (1.4 pg /well), since all of the individual E1-3G standard curves gave the same sensitivity results. However, if there had been variation in sensitivity between the standard curves, the assessment of the inter assay sensitivity would be performed as above using the absorbance readings from all of the PdG standard

points corresponding to the monitor standard of 3.4 nmoles/24 h from all of the E1-3G standard curves. These readings would be pooled, averaged and the standard deviation from the mean calculated (refer Table 2.3). The same method would be used to find the mean and S.D. for the pooled absorbance readings for the zero standards. The mean values and S.D. for both the E1-3G standards and the zero standards used to assess inter assay sensitivity are shown in Table 2.3.

Table 2.3: The Means (A_{490}) and Standard Deviations (S.D.) of both the E1-3G Standard (3.4 nmoles/24 h) and the Zero Standards Used to Calculate the Sensitivity of the E1-3G Standard Curves.

	Zero Standard (0 nmoles/24 h) A_{490}	E1-3G Standard (3.4 nmoles/24h) A_{490}
Mean	1.245	1.126
S.D.	0.0183	0.014
C.V.	1.47	1.24

The calculation of Intra/Inter-assay sensitivity = $E/(E_0\text{-}2SD) \times 100$.
$1.245 - (2 \times 0.0183 = 0.0366) = 1.208$; $1.126/1.208 \times 100 = 93.2$ %

Henderson *et al.*, (1995) reported their E1-3G standard curve to have a greater sensitivity of 3.6 pg/well with a tracer E1-3G-HRP concentration at 10 ng/well. This present study has an E1-3G (1.4 pg per microwell) to E1-3G-HRP (1,049 pg/ well; refer section 2.3.4.1) ratio of approximately 1 : 750 while Henderson *et al.*, (1995) reported an E1-3G to E1-3G-HRP ratio of approximately 1 : 2,800. These ratios show the present study, where polyclonal antibodies are used, had 3.7 times less tracer in contrast to the E1-3G immunoassay which used monoclonal antibodies. Antibody concentration in this present study has been assessed as (polyclonal) 97 ng/well, while 250 ng/well is reported for the assay where monoclonal antibodies were used.

The coefficient of variation (C.V.) is a relative standard deviation and expresses the standard deviation as a percentage of the mean value, and provides a value which gives an easier appreciation of the precision (Holme & Peck, 1993). Since the CV for this assay is excellent the assay is reliable at this level of sensitivity.

2.3.5.2 *Inter-Assay Reliability*

E1-3G standard curves (12) from six different ELISA microtitre plates (figure 2.15) were normalized (refer section 2.3.4) and compared.

Table 2.4: Characteristics of the E1-3G Standard Curves Using ELISA

E1-3G Standards	Mid-point ED_{50} pg/well	High-point ED_{20} pg/well
Mean ± S.D.	43 ± 2	130 ± 0.3
C.V.	4.65	0.23

At the mid-point (50%) of the normalised E1-3G standard curves the mean estimated dose (ED_{50}) of E1-3G was 43 ± 2 pg/well, equivalent to 100 nmoles/24 h. The high point, or the mean estimated dose of E1-3G at a point 20% from the bottom of the normalized standard curve (ED_{20}) was 130 ± 0.3 pg/well, equivalent to 300 nmoles/24 h. Since the coefficient of variation (CV) calculated for the ED_{50} was 4.65 and for ED_{20} was 0.23 these results gave excellent precision and therefore good inter assay reproducibility. However, because all of the ELISAs were performed on the same day a batch effect on the reproducibility cannot be excluded (refer section 2.3.6.2). These results compare favourably with those of Henderson *et al.* (1995) where an ED_{50} of 27 ± 3 (CV 11%) and an ED_{20} of 110 ± 17 (15.5%) were reported, and an intra assay CV of 6.7% and an inter assay CV of 12.4%, calculated from sample and quality control replicate values was recorded. In this present work, WHO urine samples (refer section 2.2.5) were identified early in the study as having low, medium and high E1-3G levels. These samples were selected as quality control samples to monitor the performance of the E1-3G assay. These samples were stored frozen in aliquots of 0.5 ml and assayed in replicate in all subsequent ELISA's. The assessment of E1-3G assay performance using these quality control samples gave an intra assay (E1-3G measurements were repeats on the same ELISA plate) CV of 3.8% and an inter assay (E1-3G measurements were repeats on different ELISA plates) CV of 10% which also compares well against those of Henderson *et al.*, (1995).

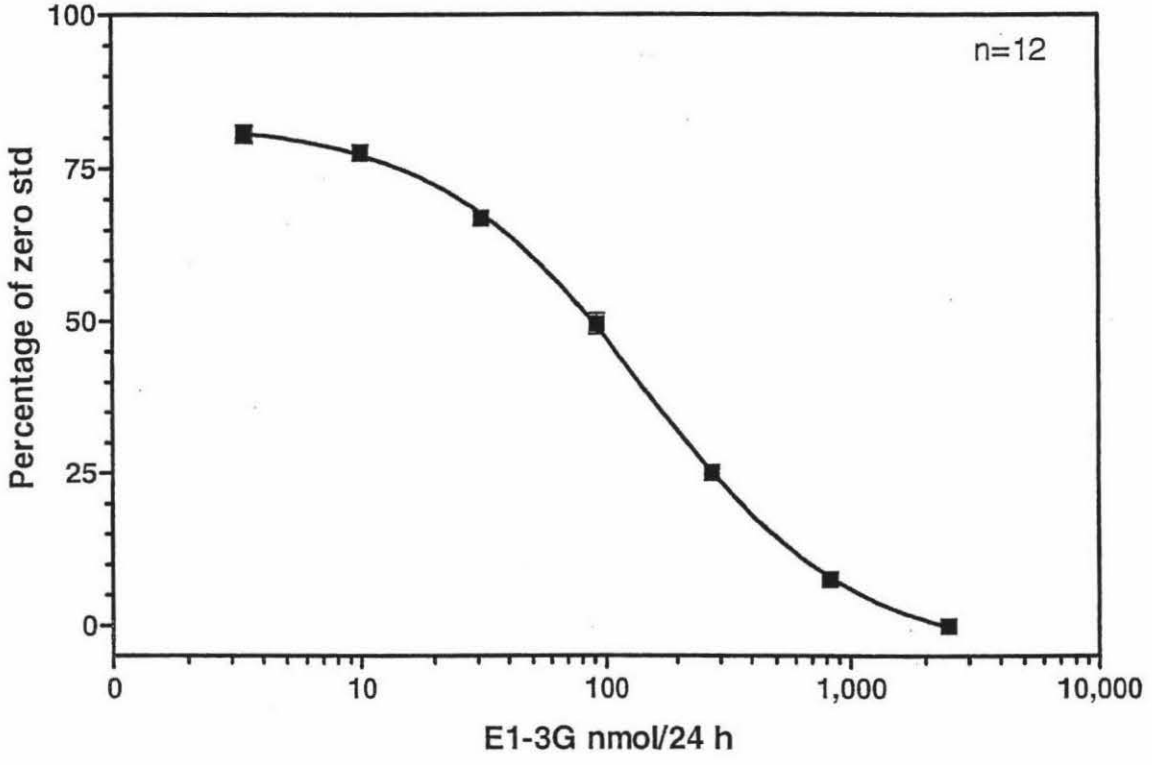

Figure 2.15: Normalised E1-3G standard curves (n=12) from six different ELISA microtitre plates. Showing the standard error from the mean (S.E.M.). (E1-3G-HRP 300 µl, 1/35,000 dilution; E1-3G monitor standards 10 µl; E1-3G-antibody 1/2,500 dilution; 16 h incubation; 4°C)

2.3.5.3 Cross-reactivity

The extent of cross-reactivity with other steroids was determined by comparing the relative amounts of E1-3G and the potentially cross-reacting steroid required to produce an absorbance value 50% that of the zero standard (refer section 2.3.4.1). Initially, a broad range of available steroids (pregnanediol, PdG, testosterone, oestradiol, progesterone, androstenedione, oestrone and oestrone sulphate) at high dose levels (1,000 times that of the largest E1-3G standard of 1,000 nmoles/24 h) were used to construct a standard curve. The highest amount of E1-3G (1,000 nmoles/24 h) was expressed as a molar concentration after division by 3.6 (1,000/3.6 = 277.78 nM) (refer section 2.2.4) to calculate the concentration of the cross-reacting steroid, and the cross reacting steroid effect was then expressed as a percentage ([E1-3G]/[cross reacting steroid] X 100). Substances which exhibited less than 0.1% inhibition of the binding of the analyte to the antibody were considered not to cross react significantly.

As shown in Table 2.5 most of the steroids tested in fact cross-reacted with E1-3G in the assay by less than 0.1% showing that the antiserum has a high degree of specificity. However, oestrone and oestrone sulphate which inhibited binding of the enzyme tracer to the antibody at these very high doses were examined in greater detail at lower doses. The higher cross reactivity of these steroids was not unexpected as they share many structural features in common with E1-3G.

Lower doses of the steroids were used to construct complete dose-response curves from which the ED_{50} values could be determined, following the same procedure as above. These further results showed (Table 2.5) that oestrone cross reacted by 1.9% (figure 2.16) and oestrone sulphate by 14.28% (figure 2.17).

The reported values of Henderson *et al.*, (1995) for their monoclonal antibodies were oestrone 7% and oestrone sulphate 18% respectively and hence these results are in close agreement with the current findings.

If the cross reacting steroid yields the same shaped dose-response in the immunoassay as the analyte, it is said to exhibit parallelism, and demonstrates that the percentage of cross reactivity with the E1-3G standard curve remains constant at all dose levels. In fact the dose response curves for oestrone (see figure 2.16) and (to a lesser extent) oestrone sulphate (see figure 2.17) were non parallel curves.

Table 2.5: Percentage Cross-Reaction of Various Steroids in the Antibody Coated ELISA for Oestrone-3 α-Glucuronide

Steroid	Percent (%) Cross-Reaction with E1-3G	
E1-3G	100	
Oestrone sulphate	14.28	
Oestrone	1.9	
Androstenedione	0.054	< 0.1
Progesterone	0.049	< 0.1
Oestradiol	0.049	< 0.1
Testosterone	0.011	< 0.1
PdG	0.009	< 0.1
Pregnanediol	nil	< 0.1

Such uneven interference, where cross reactivity is greater near the top of the standard curve (at the lower E1-3G concentration of 3.4 nmoles/24 h) than at the bottom (high E1-3G concentration of 1,000 nmoles/24 h) is more difficult to control for and standardize. This may be a particular concern because the older urines used in this study may produce oestrone by bacterial contamination with β-glucuronidases and subsequent hydrolysis of the sugar moiety of E1-3G. However, the cross reactivity of oestrone is relatively small and the effect is reduced with fresh urine samples. Also excretion in urine of unconjugated oestrogens is low relative to that of conjugated oestrogens (Wright *et al.*, 1979). E1-3G, the major oestrogen glucosiduronate excreted into urine, is excreted in amounts 2-7 times that of oestrone sulphate (Wright *et al.*, 1978), and therefore a cross reactivity with E1-3G of 20% is not considered significant for the present purposes.

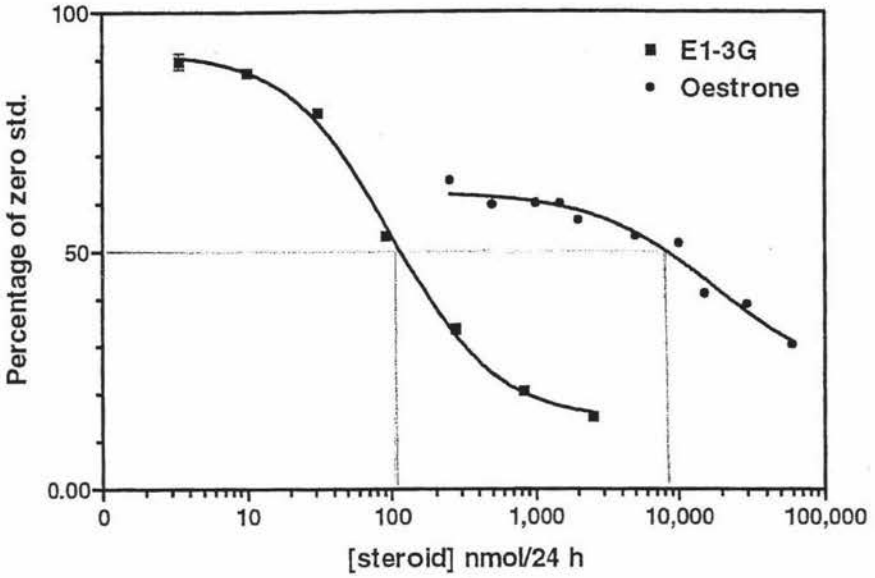

Figure 2.16: The E1-3G control standard curve, and the oestrone dose response curve used to determine the percentage of cross reacting of oestrone with E1-3G antibodies. ([0.617] / [30.86] x 100 = 1.9%) (E1-3G-HRP 300 µl, 1/35,000 dilution; E1-3G monitor standard 10 µl; Oestrone standard 10 µl; E1-3G-antibody 1/25,000 dilution; 16 h incubation; 4°C)

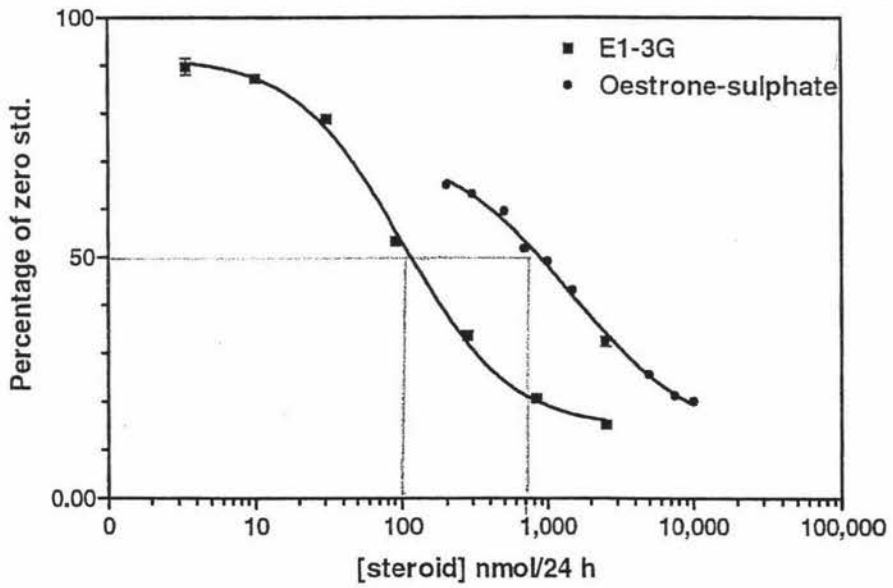

Figure 2.17: The E1-3G control standard curve and the oestrone sulphate dose response curve used to determine the percentage of cross reacting of oestrone sulphate with E1-3G antibodies. ([100] / [700] x 100 = 14.28%) (E1-3G-HRP 300 µl, 1/35,000 dilution; E1-3G monitor standard 10 µl; Oestrone sulphate standard 10 µl; E1-3G antibody 1/2,500 dilution; 16 h incubation; 4°C)

2.3.5.4 Urine Blank Effect

In an immunoassay everything in the sample other than the analyte constitutes its matrix (Grotjan & Keel, 1996; Holme & Peck, 1993). Common matrices for example include serum, plasma, urine, saliva and tissue extracts. Body fluids are complex mixtures of substances which can disrupt immunoassays in a variety of ways; by interfering with the binding of the analyte to a primary antibody, either via a competing compound (refer cross reactivity section 2.3.5.3) or in a nonspecific manner (Grotjan & Keel, 1996). To examine the "urine effect" on the assay results blank urine samples were obtained. Blank urine samples are urine samples for which there are expected to be minimal (if any) amounts of the urinary steroids being measured. Such samples were obtained from the urine of a prepubertal male (aged 5 years), and were timed and diluted to 150 ml/hour of collection (refer section 2.2.4). A series of E1-3G standard curves were generated, in the presence of varying amounts of the blank urine sample (10 µl, 20 µl and 30 µl) and hence these E1-3G standard curves were effectively urine-spiked E1-3G standard curves. These were compared with the usual unspiked E1-3G standard curves which contained no urine. The effects of adding the varying amounts of blank urine (10 µl, 20 µl and 30 µl) on the E1-3G standard curve are shown in figure 2.18 (a) together with an unspiked E1-3G standard curve control.

If the B/B_0 values for the 20 nmol/24 h E1-3G standard for the three urine spiked standard curves are read off the control (unspiked) standard curve, apparent E1-3G values of 47, 70 and 93 nmol/24 h respectively are obtained. Subtracting the actual E1-3G standard concentration of 20 nmol/24h from each of these values gave apparent E1-3G concentrations of 27, 50 and 73 nmol/24 h for the 10, 20 and 30 µl volumes of the blank urines added to the Eppendorf incubation mixtures. If these values for the E1-3G content of the blank urine are then added to the concentration of each of the standards used to construct the standard curves and the B/B_0 data replotted, the urine-spiked standard curves superimpose with the control standard curve within experimental error as shown in figure 2.18 (b). Thus, the blank urine actually contains about 25 nmol/24 h of E1-3G (or some other cross reacting material) for each 10 µl of the original urine sample diluted to 150 ml/h. There is therefore only a minimal matrix effect in this assay at these volumes of time diluted urine samples using a 2 h incubation (see figure 2.18 b). An overnight incubation (16 h) of a control (unspiked) E1-3G standard curve and a urine spiked (10 µl) E1-3G standard curve (without any correction) exhibited no matrix effect at all (figure 2.19).

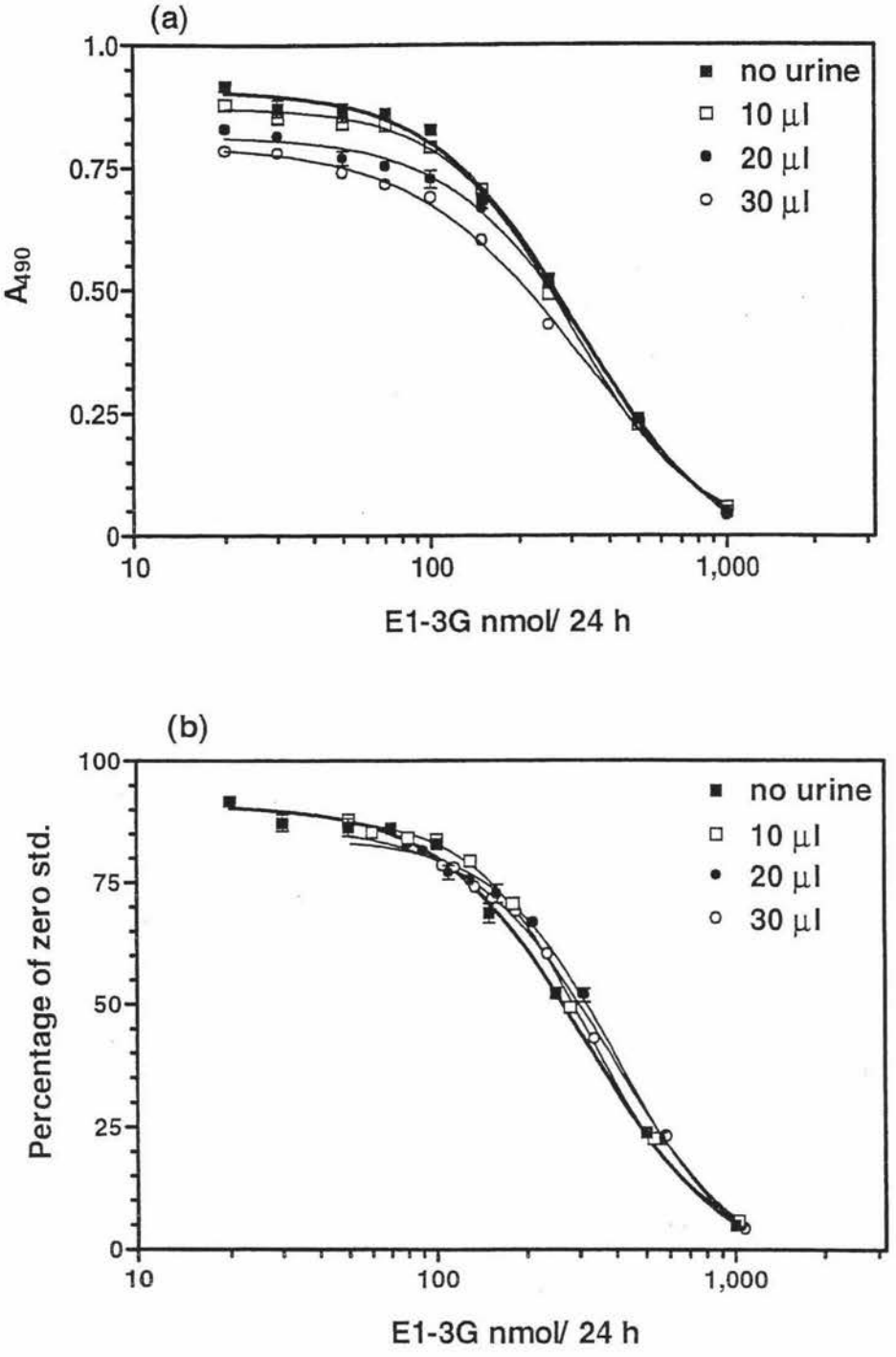

Figure 2.18: The effects of adding varying amounts of blank urine (spiked with urine) on the E1-3G standard curve. The E1-3G control standard curve contains no urine (also referred to as unspiked. (a) Non-linear regressions on the absorbance values (A_{490}) before correction for urine volumes and, (b) Non-linear regressions on the normalized absorbance values after correction for urine volumes. (E1-3G-HRP 300 µl, dilution 1/35,000; E1-3G monitor standards 10 µl; E1-3G antibody 1/2,500 dilution; 2 h incubation; 4°C)

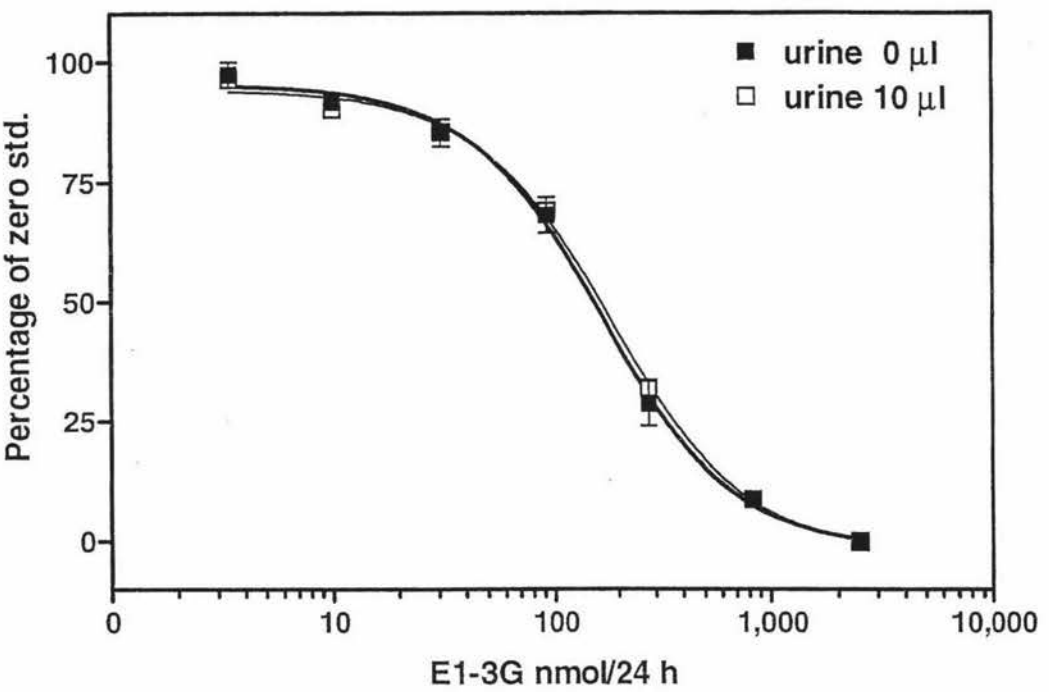

Figure 2.19: The E1-3G standard curve spiked with urine (10 µl) and an unspiked control E1-3G standard curve containing no urine. (E1-3G-HRP 300 µl, 1/35,000 dilution; E1-3G monitor standards 10 µl; E1-3G-antibody 1/2,500; 16 h incubation; 4°C)

To check for non-specific urine blank matrix effects, in clinical studies where actual menstrual cycle urines were used, blank urine (≥ triplicate) was put into the microwells, from an incubation mixture made up in the same way as the zero standard incubation mixture. The amount of blank urine put into the incubation mixture was determined by the amount of urine sample used in the assay. While normally the optimized E1-3G standard volume (10 µl) was also used for the urine sample (10 µl), in experiments where more or less urine sample was used the blank urine volume always paralleled the sample urine volume. For example, urine samples containing low levels of E1-3G may be more accurately read from the E1-3G standard curve when an increased volume of the urine sample is added to the Eppendorf tube, and then the raw data extrapolated from the E1-3G standard curve corrected to the E1-3G standard volume equivalent of 10 µl.

2.3.6 Use of the ELISA E1-3G Assay to Measure Menstrual Cycle Urines

For the menstrual cycle urine samples it was necessary to choose a urine sample volume which allowed the E1-3G levels in all of the urine samples (refer section 2.2.5) in the menstrual cycle to be measured accurately from the optimized E1-3G standard curve (refer section 2.3.4). Because an extra dilution of the timed urine samples from the WHO study (refer section 2.2.5) was not required (they are diluted 150 ml/ h already) for the Ovarian Monitor lysozyme E1-3G immunoassay, and the E1-3G standards used to generate the ELISA standard curve were also added (10 µl) without extra dilution into the Eppendorf incubation mixture (refer section 2.3.4) the menstrual cycle urine samples were not usually subjected to a further dilution either.

Aliquots of daily urine samples collected for a World Health Organisation (WHO) study were used (refer section 2.2.5). Urine samples from the 6th menstrual cycle from a woman who was labelled in the WHO study as subject number 021R (021R-6) were put onto an ELISA plate (refer section 2.2.6.7), together with the E1-3G standards to generate the optimized E1-3G standard curve. The incubation mixture for the urine samples (10 µl) was the same as for the E1-3G standards (10 µl) (refer section 2.3.3). Also, as usual for ELISA assays analysing E1-3G in urine, blank urine was added to an incubation mixture made up the same as the incubation mixture for the zero blank as above (refer section 2.3.5.4), and put into three or more microwells. The resulting menstrual cycle (021R-6, figure 2.20) with cycle day plotted against the E1-3G concentration in nmoles/24 h, clearly shows the three most important clinical points (see section 1.1.3) i.e. the beginning of the first rise from the follicular phase baseline on cycle day 11, the E1-3G peak rate of

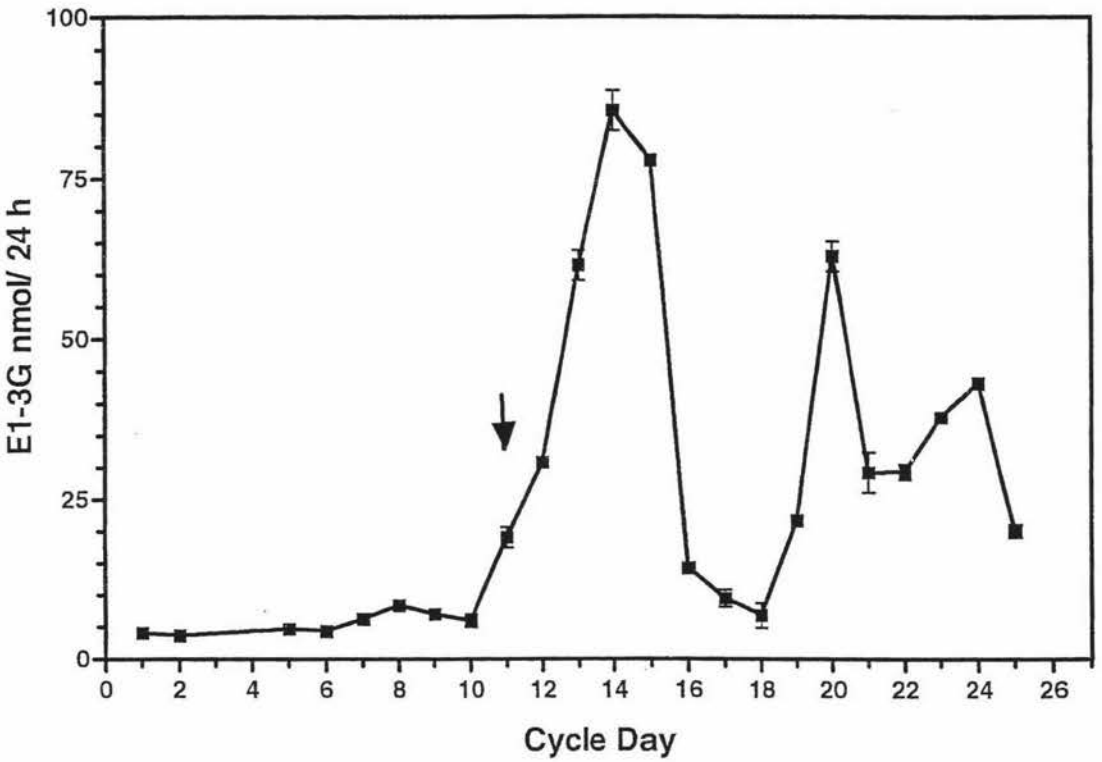

Figure 2.20: The sixth menstrual cycle of a subject in the WHO study (21R): cycle days (n=27) are plotted against the absolute E1-3G levels obtained using the ELISA assay (10 µl of urine sample in a total volume of 450 µl). The arrow indicates the cycle day (day 11) on which E1-3G values first increased above the follicular phase E1-3G baseline levels. The highest E1-3G level occurred on cycle day 14. (16 h incubation)

excretion on day 14 and a decline in the rate of excretion of E1-3G after the peak E1-3G day. A second smaller E1-3G peak was evident in the luteal phase as is usually seen in similar menstrual cycle profiles (see figure 2.20). Because day 14 and day 15 had similar E1-3G levels the E1-3G peak was unresolved in this ELISA assay, and the E1-3G peak day may well occur on day 15 in some repeat ELISA assays given the experimental variation in the data. Although all of the E1-3G data for menstrual cycle 021R-6 fitted onto the working range of the E1-3G standard curve, the peak levels of E1-3G were only 85 nmoles/24 h for this cycle, which was low compared to data obtained using the Ovarian Monitor from the menstrual cycle urines collected from other women (Brown *et al.*, 1989).

The E1-3G-antibody dilution (1/1,500) was reduced in an attempt to increase the working range of the E1-3G standard curve for the menstrual cycle samples so that all data points were measured from the most accurate part of the standard curve. However the main features of the menstrual cycle pattern including the E1-3G peak day remained unchanged. Hence, since the optimized E1-3G-antibody dilution (1/2,500) was greater and other results (Schramm & Paek, 1992) have shown (refer section 2.1) that lower antibody concentrations in direct competitive immunoassays are more sensitive than higher antibody concentrations (refer figure 2.14; section 2.3.4) the status quo prevailed.

Figure 2.21 shows a repeat of figure 2.20 using increased amounts of urine (50 µl) in the incubation mixture. The raw data obtained directly from the E1-3G standard curve by the computer programe (refer section 2.2.6.8) was corrected for the increased urine volume by division by 5. An effect of the increased sample volume of urine was apparent (figure 2.21) despite the apparent lack of a "blank" urine effect reported earlier (section 2.3.5.4). The pattern of the menstrual cycle (021R-6) appeared distorted in the region of the E1-3G peak (compare with figure 2.20) but a similar pattern was obtained. All three important clinical points are again shown (the distinctive rise from baseline on cycle day 11; the E1-3G peak on cycle day 15 rather than cycle day 14; and the decline in E1-3G excretion following the E1-3G peak on day 16). The amount of the apparent absolute E1-3G values were all about 20 to 30 nmol/24 h greater (after division by 5) than the cycle where 10 µl of each urine sample was used (figure 2.20). The reason for this is not clear and further work is clearly needed. For this reason, wherever possible the E1-3G data should be obtained using 10 µl of the timed and diluted urines collected by women for monitoring their fertility. When it is necessary to increase the urine volume (as may be required for low E1-3G values in the follicular phase of the cycle) the possibility that an artifactual

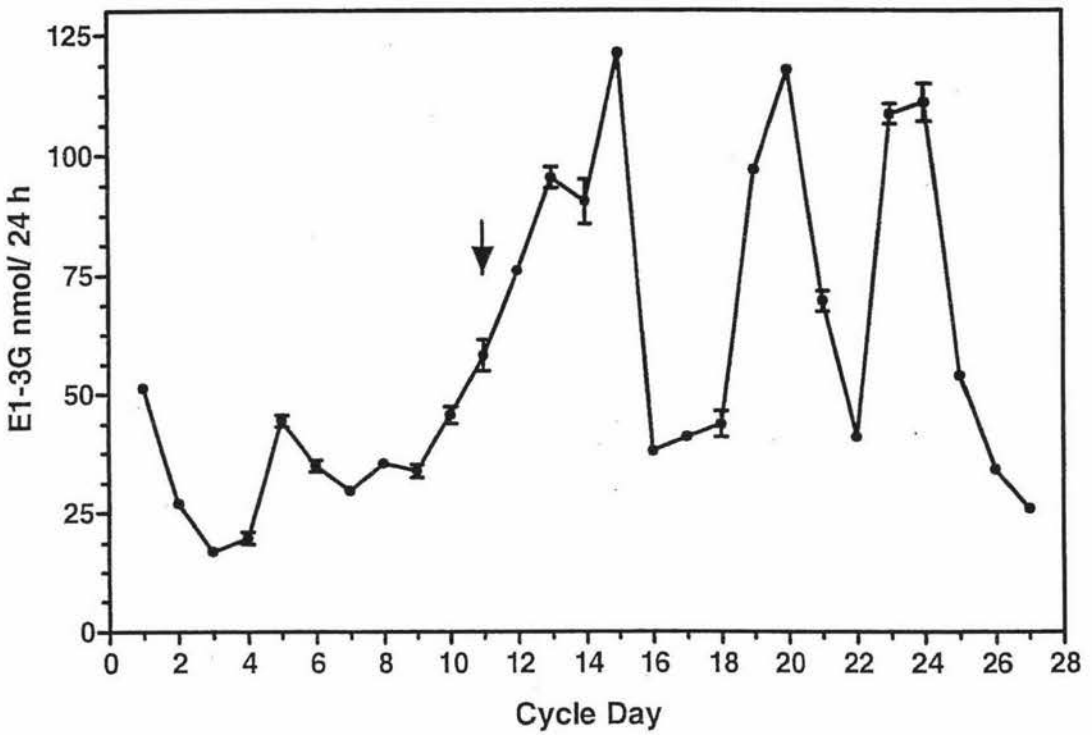

Figure 2.21: The effects of an increased amount of urine sample (50 µl in a total volume of 450 µl), after the raw data was divided by 5, on the urines from the sixth menstrual cycle from subject 21R from the WHO study (# 90905). The first significant E1-3G rise above the E1-3G baseline still occurred on cycle day 11 (indicated by an arrow). Again Incubation was overnight (16 h).

increase in the apparent absolute concentration of E1-3G may result, must be borne in mind!

Further experiments were undertaken to determine the variation in the E1-3G results for repeated ELISA assays using urine samples from menstrual cycle 5 from subject 014X from the WHO study (refer section 2.2.5). The menstrual cycle patterns showed considerable variability when 2 h incubations, as reported by Henderson *et al.*, 1995, were used. For example, the results (N=22) showed that the first E1-3G rise from baseline values occurred on mean cycle day 11 ± 0.21, although the mean absolute level of E1-3G on this day was variable (89.8 ± 48.5 nmoles/24 h). Similarly, although the peak E1-3G levels occurred on mean day 15 ± 0.44 the absolute level of E1-3G was 247 ± 94 nmoles/ 24 h.

2.3.6.1 *Comparisons Between 16 h (Overnight) and 2 h Incubation*

Because each ELISA assay with menstrual cycle urines plated also had an associated E1-3G standard curve it seems reasonable to expected any change to affect both the menstrual cycle urines and the standard curve. However, there seemed to be some fundamental change occurring between the E1-3G standard curve relative to the menstrual cycle between the 2-3 h and 16 h incubations. Keith Henderson (personal communication) usually has an overnight incubation step at 4°C, but can use a 2 h incubation 4°C. They used to do the 2 h incubation at room temperature and the overnight incubation at 4°C, but were told that better results were obtained at 4°C for the 2 h incubation.

While both the HRP-steroid conjugate and steroid analyte compete for binding sites on the antibody, the smaller one reaches the immobilized antibody on the microtitre well surface faster because it is less diffusion controlled (Paek & Schramm, 1991). Schramm and Paek, (1991) used theoretical kinetic binding curves validated against experimental data, to demonstrate that native progesterone binds more rapidly to immobilized antibody than does the HRP-progesterone conjugate, even though the on-rate constant for the progesterone conjugate has been calculated to be faster than for native progesterone (see Table 2.6). These results support the hypothesis that the rate of association of the E1-3G-HRP conjugate with immobilised antibody actually may be larger than the molecules can reach the antibody if the binding reaction is diffusion controlled. This would mean that the formation rate of the E1-3G-HRP-antibody complex reflects the influx of the antigen to the penetration layer from the bulk solution.

The results of Schramm and Paek (1991) also showed that progesterone had a much faster dissociation rate (3,214 times) than did the larger HRP progesterone conjugate. The dissociation of the HRP-progesterone complex was therefore the rate limiting step in attaining equilibrium. This would also probably be the case for the E1-3G-HRP conjugate as well. It seems reasonable to expect therefore, that the time required for HRP-progesterone to reach equilibrium may determine the time required for equilibrium to be reached for an E1-3G ELISA using E1-3G-HRP as the tracer, in a direct competitive immunoassay such as used in this study. Even though after 30 minutes to one hour the change may continue towards equilibrium asymptotically, such change may be significant nevertheless.

Table 2.6: Binding Kinetics for Native and Conjugated Progesterone [from Schramm & Paek, 1991]

	HRP-P	Native P	
Mr.	40,000	730	
On-Rate Constant	3.2×10^{12}	4.2×10^{12}	Seconds
Off-Rate constant	4.5×10^{-4}	1.4×10^{-3}	$mm^3/mol./s$

Equilibrium of the HRP-progesterone antibody complex formation reaction required 4 hours in the absence of progesterone. The middle line on figure 2.22 represents bound HRP-progesterone in the absence of native progesterone, where after 30 minutes to one hour the line continues towards equilibrium asymptotically, at which point the association rate and the dissociation rate from immobilised antibody are identical. In contrast, progesterone (0.0025 ng/well) in the absence of HRP-progesterone conjugate, represented by the top line on figure 2.22, peaked after approximately 15 minutes and reached equilibrium after 30 minutes. The lower line on figure 2.22 represents the bound HRP-progesterone conjugate in the presence of progesterone (0.0025 ng/well), and where there are less antibody sites since the lines are expressed as a ratio of the total amount of immobilized antibody. As a consequence of the different diffusion coefficients, binding constants (kinetics) and time taken to reach equilibrium and the competition between the two is time dependent. Schramm & Paek (1991) reported that although dose response curves were generated after 5 minutes the position of the standard curve changed, until the ratio of bound to unbound HRP conjugate became relatively constant after approximately 30 minutes.

The relative dynamics of E1-3G-HRP and E1-3G probably also change rapidly over the first 30 minutes and therefore strict control of incubation time is likely to be required if the immunoassays are operated within short periods of time, less than 30 minutes. E1-3G and E1-3G-HRP in this present study were incubated for either 2-3 hrs or 16 h (overnight), and it was assumed that the relative position of the standard curve would remain the same for incubation times of more than 30 minutes.

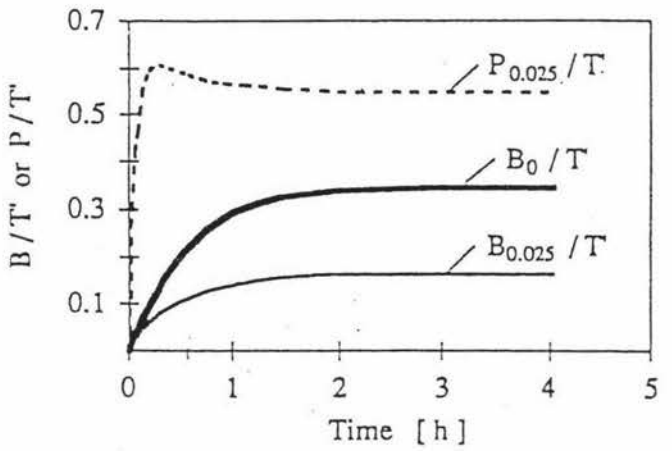

Figure 2.22: Theoretical kinetic binding curves. The bound antigen (enzyme tracer, B; progesterone, P) is expressed as a ratio of the total amount of immobilized antibody (T). The subscripts are: B_0, bound enzyme tracer in the absence of native progesterone; $B_{0.025}$, bound enzyme tracer in the presence of 0.025 ng/well of progesterone; and $P_{0.025}$, binding of 0.025 ng/well of free progesterone over time. [Paek & Schramm, 1991]

There was some evidence however that overnight incubations of approximately 16 hours gave results which differed from those which were left for only 2-3 hours. To determine whether the observed differences between 2-3 h and overnight incubations were real or due to chance the absolute E1-3G values (nmoles/24 h) were compared for each of the incubation times.

Exactly the same incubation mixture using menstrual cycle 14X-5 was put into the microwells of ELISA plates (results shown in figure 2.23 and figure 2.24) on the same day, with all the experimental conditions identical except that one plate was incubated overnight (16 h) and the second (figure 2.24) was incubated for only 2 h. While the cycle patterns were basically similar (refer figures 2.23 and figure 2.24) there was a significant difference in the absolute amounts of E1-3G calculated from the E1-3G standard curves. Although peak levels of E1-3G occurred on day 15 for both assays, higher absolute E1-3G levels were given for the shorter incubation time (193 nmoles/24 h) than for the longer incubation (160 nmoles/24 h). Also the shorter incubation time gave higher absolute E1-3G values (88.5 nmoles/24 h) than the overnight incubation (40.5 nmoles/24 h) for the first E1-3G rise from baseline on day 11. However, the overnight incubation gave a greater difference in E1-3G levels between day 11 and day 15 (refer figure 2.23 and figure 2.24) and replicated well (figure 2.25).

To further investigate the effect of incubation time on absolute E1-3G levels under strictly timed and controlled experimental conditions, 4 ELISA plates using urines from two cycles of a perimenopausal woman (see figure 2.26; also figure 4.16 section 4.3.3) were processed simultaneously under the same experimental conditions on the same day. Two of the plates were incubated for 2 h (figures 2.26, a-b) and two plates were incubated overnight (16 h) at 4°C. (figure 2.26, c-d). The assays with the shorter incubation time (figure 2.26, a-b) again showed higher absolute E1-3G values relative to those assays with the longer incubation time (figure 2.26, c-d) but the patterns were unaltered. Baseline E1-3G levels were twice as high on the ELISA plates incubated for 2 h compared to the plates with a longer incubation time but the increased E1-3G levels for the 2 h incubation were less evident near the E1-3G peak. The longer incubated standard curves were shifted in the direction of lower E1-3G levels (figure 2.27), indicating a greater ability to measure small amounts, and small changes in those amounts. Such an increase in the sensitivity of the overnight incubated standard curves is explained by the fact that more E1-3G-HRP has bound to antibody binding sites and thereby giving the standard curve (figure 2.27) a greater resolution of data points. This result is explicable if E1-3G binds faster than E1-3G-HRP (due to faster diffusion of E1-3G and greater mass transfer, and there are also less steric effects for E1-3G). Hence for shorter incubation times where equilibrium is not established, less E1-3G-HRP is bound for a given E1-3G standard concentration than the equilibrium amount. Therefore a lower absorbance reading and a correspondingly higher apparent E1-3G concentration will be calculated than for a 16 h incubation where

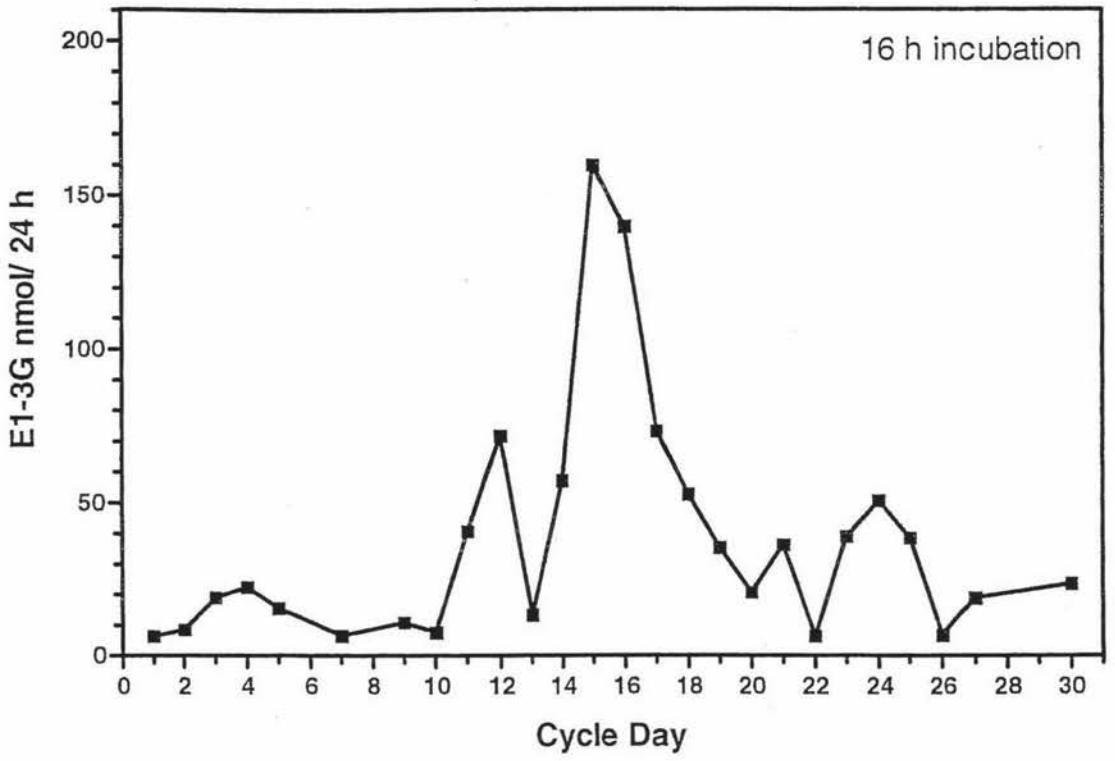

Figure 2.23: The fifth menstrual cycle from subject 14X of the WHO study. (10 µl of urine sample in a total volume of 450 µl; 16 h incubation; 4°C)

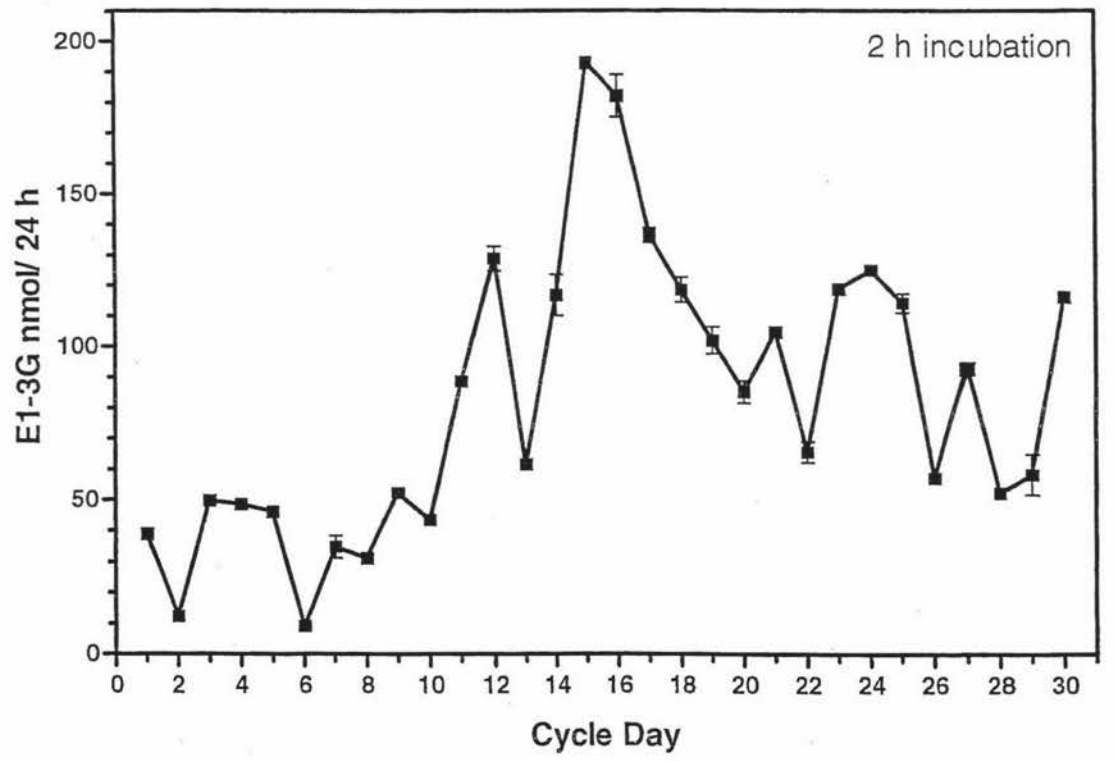

Figure 2.24: The fifth menstrual cycle from subject 14X of the WHO study. (10 µl of urine sample in a total volume of 450 µl; 2 h incubation; 4°C)

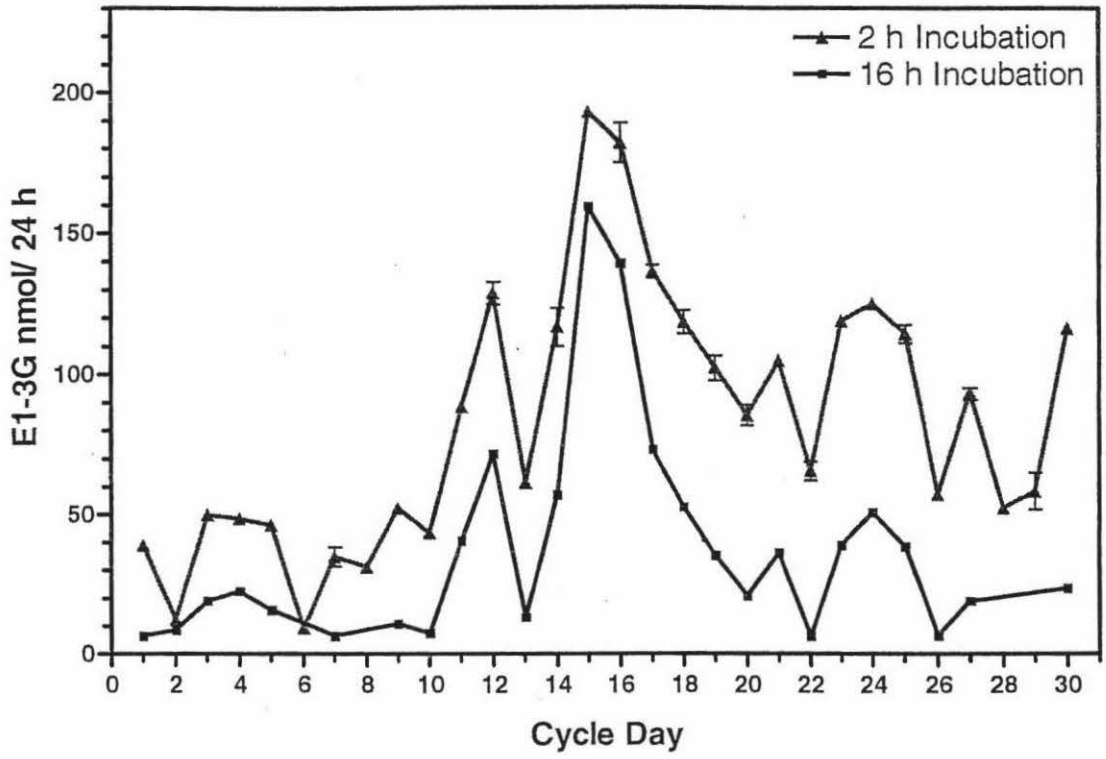

Figure 2.23 and Figure 2.24 superimposed: The effects of incubation times on the absolute E1-3G levels obtained using the ELISA assay.

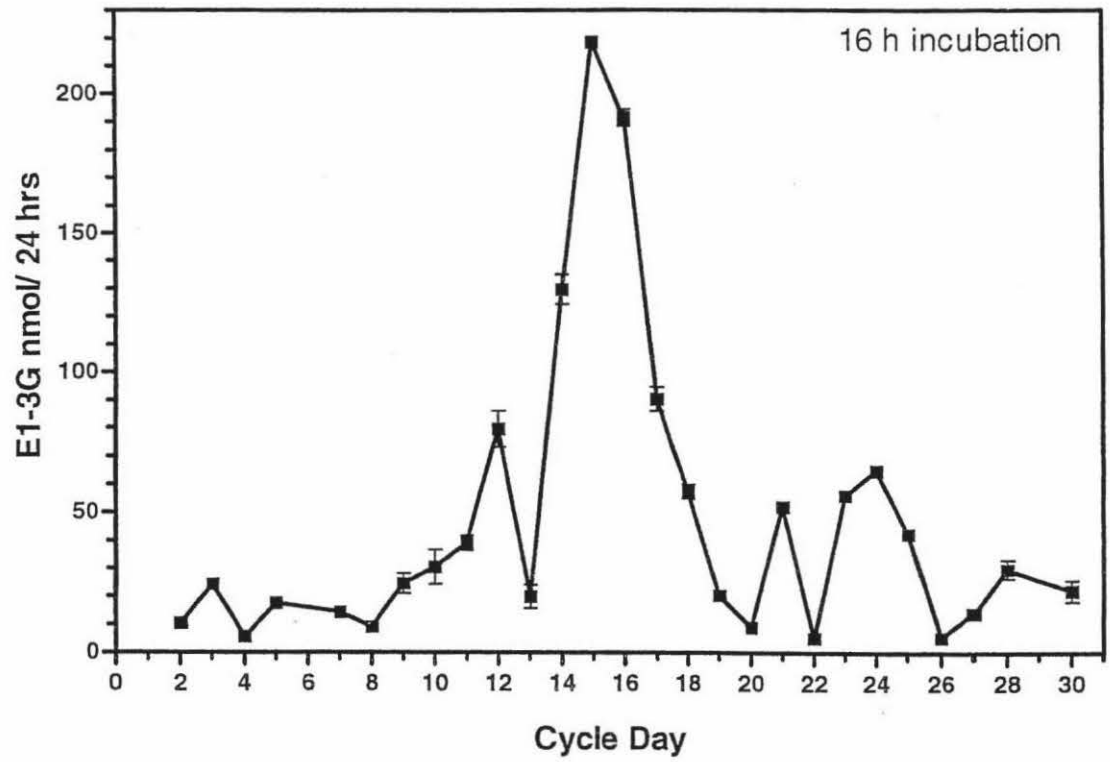

Figure 2.25: The fifth menstrual cycle from subject 14 X from the WHO study (#90905). (10 µl of urine sample in a total volume of 450 µl; 16 h incubation; 4°C)

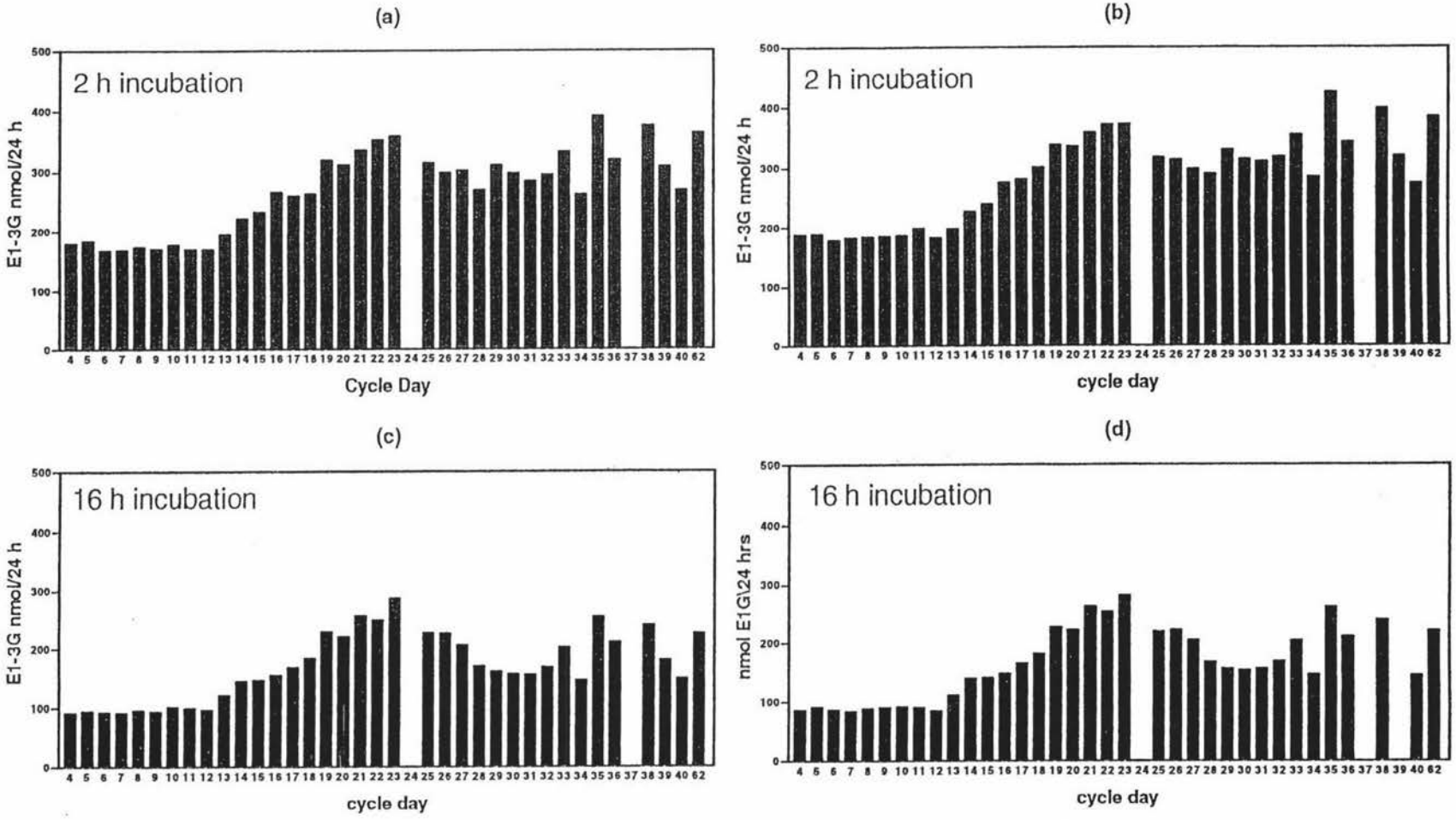

Figure 2.26: A set of 4 ELISA assays: (10 µl of urine sample in a total volume of 450 µl), (a) and (b) were incubated for 2 hours and (c) and (d) were incubated for 16 hours.

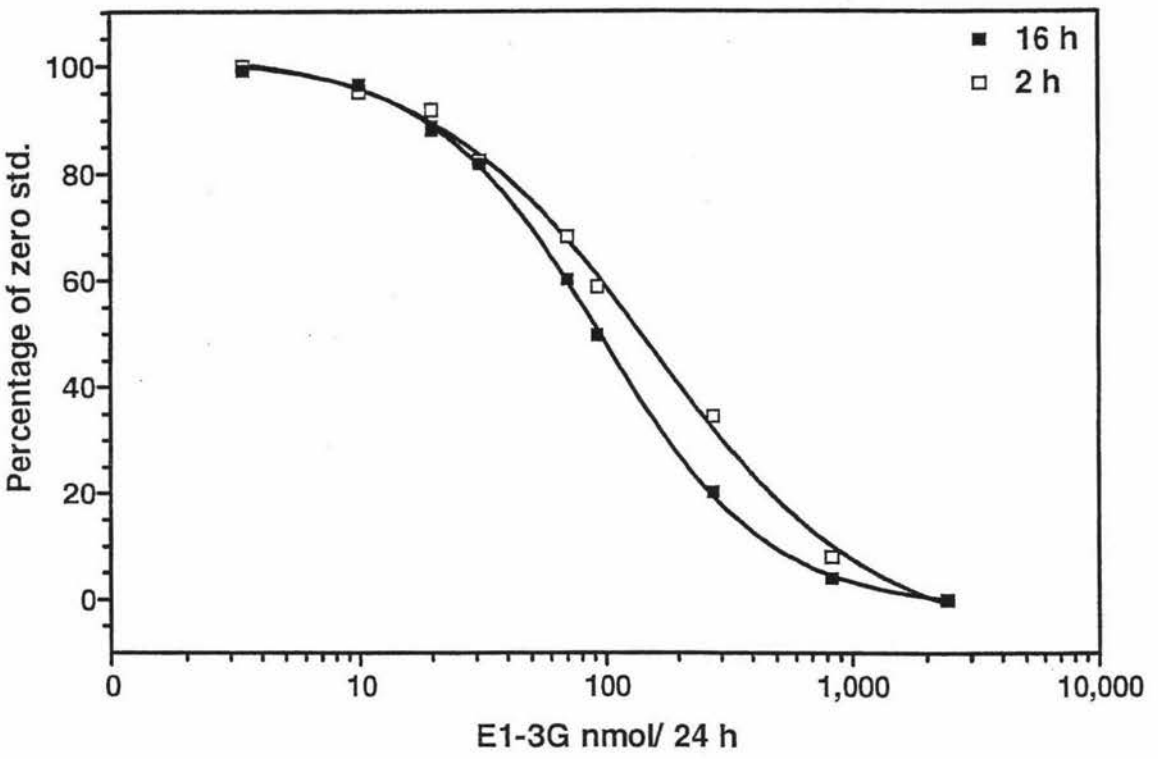

Figure 2.27: The effects of incubation time (2 h, and 16 h) on the position of the E1-3G standard curves using the ELISA assay. (10 µl of monitor standard in a total volume of 450 µl; E1-3G 300 µl, 1/35,000 dilution; E1-3G antiserum 1/2,500 dilution, 4°C)

equilibrium is more nearly reached. Some change in the position of the standard curve (which seems significant in this study but not in the studies of Paek & Schramm, 1991) occurs presumably until the amount of E1-3G-HRP bound reaches equilibrium in the presence of E1-3G. Therefore, only after at least 4 hours (or the time taken for the largest molecule to reach equilibrium), can the measurement of E1-3G from the E1-3G standard curve be time independent and hence reliable. Both Henderson *et al.*, (1995) who used a 2 h incubation at 4 °C and Schramm & Paek (1991) used monoclonal antibodies rather than polyclonal antibodies and perhaps strict timing is less important when monoclonal antibodies are used because the antibodies are more specific or have greater dissociation rates so that equilibrium is reached faster.

2.3.7 Conclusion(s)

Only after the observation that the incubation time of the assay influenced the stability of the E1-3G standard curve, and consequently E1-3G measurements read from it, was a probable explanation for the variability in the ELISA results apparent and overcome. Further experimentation using longer incubation times, or strict timing of the shorter incubation times of less than 4 hours, may further optimize the E1-3G ELISA, however for the purposes of a reference assay for E1-3G an overnight incubation seems preferable.

Chapter Three: Development of ELISA Assay for Pregnanediol Glucuronide in Timed Urine Samples

3.1 Introduction

The main aim of this chapter is to generate an ELISA assay optimized to measure pregnanediol glucuronide (PdG) in menstrual cycle urines and which can act as a reference method to replace the method of Barrett & Brown (1970). In this latter method, after acid hydrolysis and extraction of the neutral fraction, pregnanediol (Pd), derived from PdG, was measured by gas liquid chromatography (GLC).

A study conducted by the World Health Organisation (WHO) Task Force on Methods for the determination of the fertile period (Adlercreutz *et al.*, 1982) examined the value of using a PdG threshold as a marker for the end of fertility by direct assay which did not need a hydrolysis step. Threshold values of both 10 μmoles/l and 12 μmoles/l of urine were tested for their ability to mark the end of fertility where the first day of infertility was defined as the day these thresholds were first equalled or exceeded. The value of utilising the first significant rise in urinary PdG levels from baseline values to mark the end of fertility was also investigated. Two different methods for defining the first significant rise were tested for their ability to correctly mark the end of the fertile period. The first method defined the infertile period as beginning on the day when the urinary PdG values first increased 50% above the mean of the three immediately preceding values. For the second method, the infertile period was defined as beginning on the day when the PdG values first exhibited a rise 100% above the mean PdG value for the follicular phase.

When the LH peak was used as the definitive marker of ovulation, and the fertile period was defined as occurring between days -3 to +2 relative to the LH peak, with day +2 or +3 being the first day of infertility, all the methods examined by Adlercreutz *et al.*, (1982) were shown to be associated with the generation of a significant number of cycles in which the end of fertility was predicted as having occurred before the event of ovulation. In addition, all methods were also associated with the generation of a significant number of cycles in which there was a delayed confirmation of the end of fertility compared to the reference definition. Adlercreutz *et al.*, (1982) therefore concluded that the use of a threshold level of urinary PdG and the use of the first rise in urinary PdG levels above

baseline, were both unsuitable methods for the reliable delineation of the end of fertility. However, examination of the results obtained using an E1-3G/PdG ratio as a marker for the end of fertility was found to be more promising, and led to their recommendation of the E1-3G/PdG ratio as the preferred end of fertility marker.

A similar study was conducted by Cekan *et al.*, (1986) in which a variety of different urinary hormonal methods were examined for their ability to successfully delineate the end of fertility. From their results, it was again concluded that both the use of a threshold level of urinary PdG, and the use of the first sustained rise in urinary PdG levels above baseline, were unsatisfactory as methods for determining the end of fertility. This, in conjunction with their other findings, led them to conclude that the markers for the end of ferrtility which had the most potential were the E1-3G/creatinine (day of peak +4 days) and PdG/creatinine ratios.

The conclusions of these two studies were in marked contrast to the practice of Brown's group in Melbourne (Brown *et al.*, 1991), which used a threshold value for urinary PdG as an acceptable marker for the end of fertility, based on their experience over a number of years. These conflicting experiences can probably be explained by the failure of some of the researchers to recognise the importance of time diluted urine samples (see section 2.3.5) for the assessment of physiological processes by the analysis of metabolites in the urine. The studies performed on behalf of the WHO (Adlercreutz *et al.*, 1982; and, Cekan *et al.*, 1986) made no correction for urine volume. That is, in these groups the hormones and metabolites in the urine were all measured as concentrations as opposed to excretion rates. However, because the rate of production of urine can vary markedly throughout the day, due to differences in fluid intake and respiratory and sweat losses, the hormone concentrations in the urine will not necessarily directly correlate with the hormone excretion rates. Since these differences were not taken into account by Cekan *et al.*, (1986) and Adlercreutz *et al.*, (1982) when examining the use of threshold levels of PdG and the rise in PdG levels above baseline, their experimental results and thus, their conclusions were affected.

Baseline PdG levels as low as 0.2-3 µmoles/24 h have been reported (Brown *et al.*, 1989), and as the first rise from this baseline often occurs at or before ovulation, as already discussed the PdG rise alone can not be used as an end of fertility marker for all women even with timed and diluted urine samples. However, as discussed in detail in the

introduction of the thesis (refer section 1.1.4.5), a pre-determined PdG threshold value of 6.3 µmoles/24 h accurately indicates the end of the potentially fertile phase of the menstrual cycle (Blackwell *et al.*, 1998) if timed urine samples are used.

Following the same methods used in the measurement of E1-3G (refer section 2.1), a direct competitive ELISA was used in this study in combination with the immobilized antibody format as discussed in section 1.2.1. Briefly (as for E1-3G assay, see figure 2.1), antibody is immobilised by adsorption to polystyrene followed by the simultaneous addition of analyte (PdG) and enzyme tracer (PdG-HRP). After the removal of unbound antigen (labelled and unlabelled PdG) the signal produced by the enzyme (HRP) was measured and the signal was inversely related to the PdG concentration. The main components of the PdG-ELISA were therefore, a PdG-HRP conjugate (refer Section 3.2.6.1) and an anti-PdG antiserum (refer Section 1.2.3 and section 3.2.6.3). In the present study a polyclonal antiserum was used for the PdG ELISA as research has shown that purification of the antibody may be unnecessary (Crowthers, 1995), time consuming and expensive.

The optimization of the PdG ELISA involved finding the minimum amount of functional antibody which, after formation of an immunocomplex with the PdG-HRP conjugate, gave a reading of 1.0 absorbance unit at a wavelength of 490 nm. Because of the need to use the smallest possible amount of antibody to maximize the sensitivity of the immunoassay (Schramm & Paek, 1992), antibody dilutions were adjusted in a series of checkerboard titrations. Following the principles of competitive binding (refer section 1.2) the amounts of PdG standards and PdG-HRP conjugate were varied to generate a PdG standard curve which was sensitive in the most important range of PdG concentrations around the threshold value determined by Blackwell *et al.*, (1998) of 6.3 µmoles/24 h. (refer section 1.1.4.5).

3.2 Materials and Methods

3.2.1 Equipment

A Hewlett Packard 8452A diode array spectrophotometer was used to measure absorbance values. A new generation varian spectrophotometer (Cary 1E/Cary 3E UV-Vis) was used to measure HRP enzyme activity, using the commercial enzyme kinetic software. Pellets of molecular sieves, type 4A (BDH, product 54 005 4) were added to DMF to ensure that it was dry. A dessicator was used to store the equipment and reagents required for the conjugation of HRP to PdG for the 48 hours prior to the active

ester procedure being carried out. Centrifugations were carried out using a RC2-B Sorvall/Dupont SS-34 rotor angle (rpm 5,000), at 34°C . Macrosep centrifugal concentrators with a 10,000 Dalton cut-off membrane from Filtron Technology Corp. (Northborough, MA 01532, USA) were used for the final ultrafiltration and concentration of HRP conjugate samples, (membranes were stored in 20% ethanol). An aluminium heating block was used for incubating samples when lytic assays were carried out using the Ovarian Monitor. The home Ovarian Monitor equipment including meter and PdG immunotubes. ELISA microtitre plates (Maxisorp C12 with 96 fixed wells) were obtained from Nalge Nunc International (Kamstrup, Roskilde, Denmark). Plates were stored in a dry cupboard bagged in lots of five, and remained wrapped until use. Maxisorp immunoproducts have a polystyrene surface with a high affinity to molecules with mixed hydrophilic/hydrophobic domains such as proteins. NUNC 15 ml and 50 ml screw cap centrifuge tubes were used for most dilutions where larger volumes of enzyme or antibody solutions were required. An 8 channel single-beam microplate absorption photometer (Anthos Labtec Instruments Ges.m.b.H., Jakob Haringerstrasse 8, A-5022 Salzburg) was used to measure absorbances at 490 nm to obtain the ELISA results. A multipipetter and four troughs was used to perform ELISA washing procedures and to dispense some of the reagents. A heated magnetic stirrer was used to dissolve gelatine when required for ELISA buffers, and used unheated for other buffer procedures.

3.2.2 Reagents

Micrococcus lysodeikticus was supplied by Sigma Chemical Co. (St. Louis, MO, USA), and was used as the substrate for lysozyme. o-Phenylenediamine powder (Merck-Schuchardt) was used as the substrate for horseradish peroxidase. Testosterone, pregnanediol, androstenedione, progesterone, oestriol were all used in cross-reactivity studies and all were obtained from Mann Research, (N.Y.), and oestrone was from Sigma Chemicals (St.Louis, MO, USA). Pregnanediol glucuronide (PdG) was synthesized by Dr Y. Wu of the Institute of Fundamental Sciences, Massey University (MW = 496.6). N,N'-dicyclohexylcarbodiimide (DCC), (product no. D3128), (MW = 206.3), N-hydroxysuccinimide (NHS), (product no. H-7377), (MW = 115.1) and horseradish peroxidase (HRP) (isoenzyme C., product 814 393) (MW = 40,000), approximately 70% pure were all Sigma products. The liquid dimethylformamide (DMF) from BDH, (Analar, product 10322) was used as a solvent. Gelatine powder from BDH, (Poole, product 44045) was used as a blocking agent. All reagents were of analytical grade or better. Water was milli-Q grade.

3.2.3 Buffers

Although these buffers were the same as those used in Chapter 2 (section 2.2.3) the details are included here again for convenience.

HEPES

A 0.15 M N'-2-hydroxyethylpiperazine-N'-ethanesulphonic acid (HEPES) buffer was prepared using 35.7 grams Hepes in one litre of milli-Q water, adjusted to (physiological) pH 7 using NaOH.

Tris-maleate buffer

Stock tris-maleate buffer (1.0 M) was prepared by mixing maleic acid (7.25 g), tris (19.80 g), NaCl (12.75 g), Tween 80 (20 ml of a 1/100 dilution in Milli-Q water) and HCl (2.8 ml of concentrated acid) in a total volume of 375 ml. The pH was adjusted to 7 with HCl as required.

ELISA Buffers

Coating Buffer (Carbonate - Bicarbonate)

Coating buffer was prepared with 31.6 g carbonate (Na_2 CO_2 and 2.93 g bicarbonate $NaHCO_3$ made up to 1 litre with Milli-Q water, adjusted to pH 9.6 and stored at 4°C.

0.5% Gelatine Blocking Buffer

Blocking buffer was prepared by the addition of a 0.5% solution of gelatine to the above coating buffer, and heated gently to aid dissolution and then stored at 4°C or room temperature.

Substrate Buffer (Citrate-Phosphate Buffer)

To make up the citrate-phosphate buffer 24.3 mls of 0.01 M citric acid (2.1 g citric acid in 100 mls milli-Q water) and 25.7 mls 0.2 M phosphate buffer (2.84 g Na_2HP0_4 anhydrous) in 100 ml milli-Q water were made up to 100 mls with 30 mls milli-Q water, adjusted to pH 5 and stored at 4°C for up to one week.

Washing Buffer (0.01 M phosphate buffer + Tween 20)

Washing buffer was prepared with 0.2 g KH_2PO_4, 2.9 g $Na_2HPO_4.12H_2O$, 8 g NaCl and 0.5 ml Tween 20 made up to 1 litre with milli-Q water, adjusted to pH 7.4 and stored 4°C or room temperature.

0.1% Gelatine Assay Buffer

Gelatine assay buffer (0.1%) was prepared by making up washing buffer with 0.1% gelatine. Once the buffer had cooled down a 0.01% thiomersal solution was added, the mixture was adjusted to pH 7.4 and stored at 4°C.

Substrate-Chromogen Solution for HRP

To prepare the substrate solution, 40 mg o-phenylenediamine powder (OPD) was added to 100 mls of citrate-phosphate buffer (approximately 30 minutes before use) then 40 µl of 30% hydrogen peroxide H_2O_2 was added immediately before use. Because OPD is light sensitive upon the addition of H_2O_2, the container was wrapped in tinfoil to avoid a light catalysed reaction.

Stopping Solution

The stopping solution of 2.5 M sulphuric acid H_2SO_4 was prepared in Milli-Q water and stored at room temperature.

3.2.4 PdG Standards

The PdG standards were prepared from a stock solution containing 3,600 µmoles/24 h made up by dissolving 1.0 mg of PdG (Na^+)(Mr 518.6) in 90% ethanol and making up to 1.9 mls in assay buffer (0.1%) (refer section 2.2.3). The PdG standards were prepared by serial dilution of the stock solution to make standards containing 0.1, 0.5, 1.3, 4, 7, 12, 36, 90 and 180 µmoles/24 h. No other stabilizer or preservative was used and the standards were stored frozen in aliquots of approximately 500 µl.

As for the E1-3G standards the molar PdG concentration was multiplied by 3.6 to convert the PdG concentration to µmoles/24 h based on the fact that the menstrual cycle urines for monitor use are all diluted to the equivalent of 150 mls of urine per hour of collection.

3.2.5 Urine Samples (WHO)

Timed and diluted (refer section 3.2.4) menstrual cycle urine samples (study #90905), were collected as part of a World Health Organisation (WHO) study. The urine samples were preserved in boric acid and stored frozen in small tubes with rubber stoppers.

3.2.6 Methodology

3.2.6.1 Conjugation of PdG to Horseradish Peroxidase

Active Ester Method

The active ester procedure (Anderson *et al.*, 1964; Rajkowski & Cittanova, 1981; Tijssen, 1985; Smales *et al.*, 1994) was carried out in two steps (as shown in figure 2.2) but with E1-3G replaced by PdG. The first step generates an active ester derivative of the carboxyl-containing steroid hapten (PdG), and the second step reacts the activated hapten with horseradish peroxidase to form stable amide linkages between the protein and the pregnanediol glucuronide. As for E1-3G the amount of each substance (in mg) required to give a concentration of 5.3 µM was prepared in dry DMF (section 2.2.6.1), resulting in solutions of 3.3 mg PdG in 55 µl; 10.7 mg of DCC in 486 µl; and 4.6 mg of NHS in 209 µl. Horseradish peroxidase (11 mg) was dissolved in 1.1 mls of 0.13 M $NaHCO_3$, pH 7. The same methods and G-25 column chromatography procedures were carried out as for the coupling of E1-3G to HRP (section 2.2.6.1).

3.2.6.2 Protocol for Horseradish Peroxidase Activity Assay

The assay protocol was the same as for the E1-3G conjugates (section 2.2.6.1). Citrate buffer pH 5.3 (0.1 M) was pre-incubated at 40 °C in a water bath. An aliquot of 1.9 ml was transferred into a 2 ml plastic cuvette and left to come to temperature (37 °C) equilibrium. A solution of o-dianisidine (20 µl of a 10 mg/ml solution in methanol), was freshly sonicated on the same day for 5-10 minutes. The PdG-HRP conjugate (20 µl) was diluted appropriately and was added and mixed by inversion with parafilm. The spectrophotometer (refer section 3.2.1) was blanked by addition of 20 µl of the reaction mixture at 460 nm and the assay begun by addition of 20 µl of a 1/100 dilution of 30% commercial stock hydrogen peroxide in water. The cuvette was mixed by inversion with parafilm immediately and the assay run for 60 seconds. The assay was performed in duplicate with a total reaction volume of 1960 µl.

3.2.6.3 Production of Pregnanediol Glucuronide Antisera

Antibodies were raised against PdG by Dr Keith Henderson, AgResearch, Wallaceville Animal Research Centre, Upper Hutt, New Zealand, by innoculating sheep with synthetic thyroglobulin-pregnanediol glucuronide conjugates, as prepared by Smales (1997). After three to six months usable antisera were obtained and serum from sheep 213 (supplied by Dr Keith Henderson, Wallaceville), containing PdG-specific polyclonal antibodies was used in the development of the PdG ELISA. Although the ammonium sulphate

precipitation procedure was carried out as for the E1-3G antiserum (refer section 2.2.6.4), the unpurified PdG antiserum was used in the development of the PdG ELISA as it produced better results.

3.2.6.4 Ovarian Monitor Protocol (refer section 1.1.5)

3.2.6.5 Inhibition Assays Using the Ovarian Monitor

The concentration of anti-pregnanediol glucuronide binding sites was estimated by titration with pregnanediol glucuronide (PdG) conjugated to an hen egg white lysozyme (HEWL) using the Ovarian Monitor (refer section 1.1.5 and section 2.2.6.6). The inhibition assays were performed by measuring the rates at varying amounts of antibody and a constant known concentration of HEWL-PdG conjugate as described below.

An homogenised suspension of *micrococcus lysodeikticus* (15 mg) in 2 ml of 75 mM tris-maleate buffer pH 7 (refer section 3.2.3) sonicated to obtain a uniform suspension was first prepared. PdG-lysozyme (10 µl) was added to each of a set of assay cuvettes at an appropriate dilution. Following the addition of different (increasing) volumes of antisera, each assay tube was made up to 350 µl with appropriate amounts of 40 mM tris-maleate buffer (pH 7) and pre-equilibrated for 5 minutes at 37°C on an aluminium heating block (refer section 3.2.1). To each tube a 10 µl aliquot of the *micrococcus lysodeikticus* solution was then added. The tubes were vortexed, and then the ΔT value over 20 minutes was calculated as before (section 2.2.6.6).

3.2.6.6 ELISA Protocol

(refer section 3.2.3 for information about buffers)

Day 1: The anti-PdG antiserum was diluted (refer section 3.3.3) in fresh coating buffer and then an aliquot (100 µl) was added to each well of the microtitre plate. The plate was covered with tinfoil and held at 4°C overnight. The blocking buffer (section 3.2.3) was prepared for use on day 2.

Day 2: All of the liquid in the wells was shaken from the plate with excess liquid being knocked from the wells by banging the inverted plate onto paper towels on the bench. Blocking agent (250 µl) was then added to each well and the plate covered and left for 0.5 to 1 hour at room temperature after which the liquid was removed as before. The plate was then washed (3X) by adding washing buffer (250 µl) to each well and allowing the plate to stand for 3 minutes, followed by the removal of the washing buffer as above.

Care was taken to prevent the wells drying at each stage. Assay buffer (50 µl) was then added to each well followed by the incubation mixture (150 µl) containing labelled (PdG-HRP) and unlabelled (PdG standard/urine sample) analyte, diluted as required in assay buffer. The incubation mixture was made up by putting PdG-HRP (usually 300 µl) together with PdG standard or sample urine (usually 10 µl, but both 1 µl and 5 µl were also used) into an Eppendorf tube and made up to 450 µl with assay buffer (section 3.2.3). When the incubation mixture volume was 1.35 µl the PdG-HRP volume included was usually 900 µl, and when the incubation mixture was 1.8 mls the PdG-HRP included was usually 1.2 mls. Assay buffer (150 µl) was added to those wells required for assay blanks. The plate was covered and incubated at 4°C for ~16 hours (overnight).

Day 3 (or second half of Day 2): The liquid was removed from the plate as described above and the plate washed (3X) as above. Substrate solution (100 µl) was added to each well and left at room temperature for approximately 20 minutes. Stopping solution (50 µl) was added and the absorbances were read (490 nm) on the microplate reader (refer section 3.2.1).

3.2.6.7 Calculation of PdG Levels from the Standard Curve

Absorbance values from the microplate reader printout were keyed into a computer graphics package called PRISM. The PdG standard concentrations (in µmoles/24 h) were transformed to log values. A non-linear regression analysis was then performed to fit the PdG standard curve, and the unknown X values were determined from all unpaired Y absorbance values for the samples using the standard curve option in the program. The X values read from the PdG standard curve were then transformed back from their log values. These data represented PdG concentration values (µmoles/24 h), and a menstrual cycle graph was created by plotting these on the Y axis with the appropriate cycle day opposite in the X axis (see figure 3.17).

3.2.6.8 Quality Control Procedure

Urine samples were identified early in the study as having low, medium and high PdG levels. These samples were selected as quality control samples to monitor the performance of the assay. These samples were stored frozen in aliquots of 0.5 ml and assayed in replicate in all subsequent ELISA's.

3.3 Results and Discussion

3.3.1 Coupling of Horseradish Peroxidase to PdG

Conjugation of horseradish peroxidase with PdG by the active ester coupling procedure was carried out as described in section 3.2.6.1, following the same method (personal communication from Dr Keith Henderson, 1995) used for the coupling of E1-3G to HRP (refer section 2.2.6.1). As in Chapter Two the active ester method was used to attach the pregnanediol glucuronide to horseradish peroxidase through the carboxyl group of the glucuronides (see figure 1.7; section 1.2.2) to form an PdG-HRP conjugate.

Following the method described for the conjugation of HRP to PdG (refer section 3.2.6.1) three solutions were made up as follows: PdG (3.3 mg) was weighed out and dissolved in DMF (55 µl); DCC (10.7 mg) was weighed out and dissolved in DMF (1.1 ml); and NHS (4.6 mg) was weighed out and dissolved in DMF (209 µl). All relevant chemicals and equipment (pipette tips, containers etc.) remained in a dessicator overnight to ensure they were dry for the conjugation procedure. The PdG solution (50 µl) was added to a reaction vial followed by DCC (50µl) then NHS (50 µl) and the vial was secured with a screw top. The solutions were mixed gently by shaking and left for 90 minutes at room temperature.

HRP (5 mg) was dissolved in 0.5 ml of 0.13 M $NaHCO_3$, pH 7 and stirred gently at room temperature. The mixture of PdG, DCC and NHS was added to the HRP solution in 3 x 50 µl aliquots and the solution turned cloudy almost immediately. Slow stirring was continued for 2.5 hrs at room temperature and the pH remained at 7 (Tijssen, 1985) after which the mixture was dialysed overnight at 4°C against milli-Q water to remove $NaHCO_3$. Finally the sample was loaded onto a Sephadex G-25 (10 g) column, (2.5 x 85 cm) and eluted with Hepes (0.15 M) pH 7 buffer. Fractions of 2 ml were collected, and the HRP conjugate fractions (which were clearly distinguished by their orange/brown colour) were pooled. Elution profiles (figure 3.1) were generated after the gel filtration procedure, from the absorbance values at 278, 280 and 404 nm, as a further aid to selection of the conjugate fractions and also to assess their enzymatic purity.

Examination of the HRP elution profile (figure 3.1) generated after gel filtration, showed the RZ value to be almost 1.23, which corresponds to approximately 41% purity compared with the original stock HRP solution (see Table 3.1). After fractions 2-6 were pooled the PdG conjugate sample was concentrated from 10 mls to 2.7 mls by ultrafiltration in

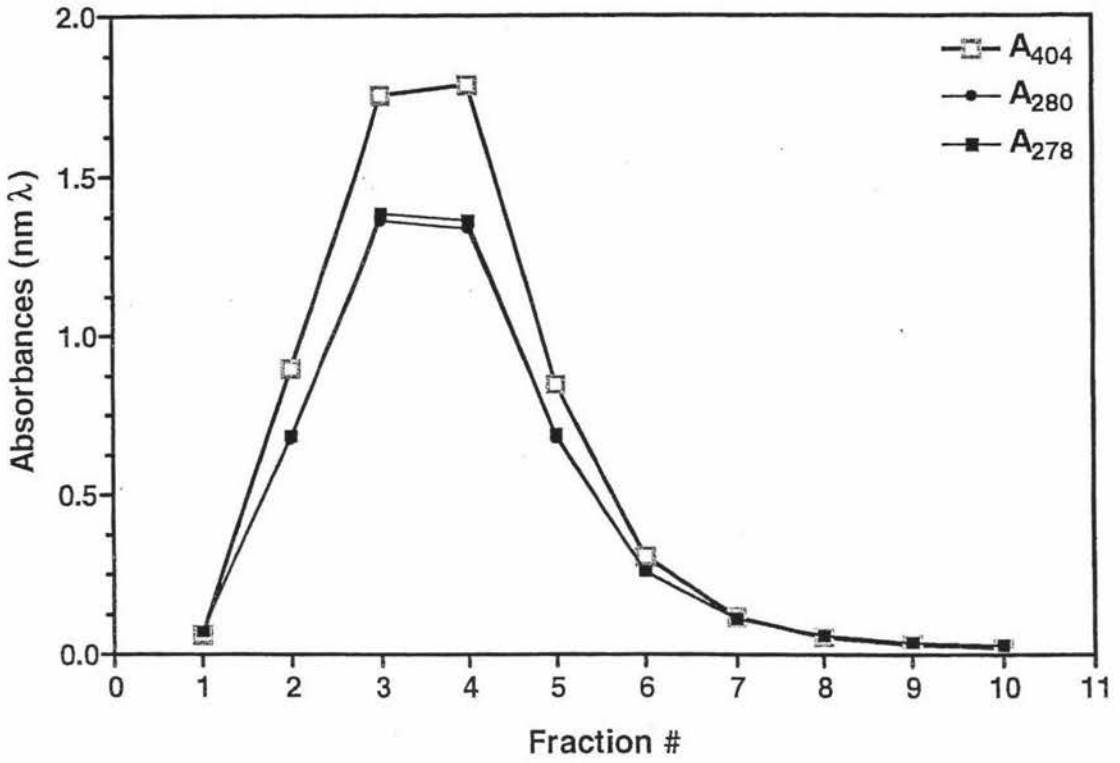

Figure 3.1: The PdG-HRP conjugate elution profile generated (2 ml fractions) after gel (G-25) column chromatography. (RZ A_{404}/ A_{280} = 1.23)

centrifugal concentrators using a RC2-B Sorvall centrifuge at 5,000 rpm (refer section 3.2.1). Concentrating HRP is generally recognised as a means of stabilizing and preserving the integrity of the enzymatic activity. Although some loss of HRP may have occurred during the concentration procedure there was no evidence of HRP activity in the eluant and the RZ Value of 1.3 remained relatively unchanged. To further stabilize the conjugate 0.01% of thiomersal was added after the concentration procedures (50 µl/ml of a 2 mg/ml solution), and the conjugate was then stored frozen in 0.50 ml aliquots.

Table 3.1: Data Showing the Specific Activites (Δ AU min^{-1} mg^{-1}) and RZ Values of HRP Before and After Conjugation to PdG, and after G-25 Chromatography and Concentrating Procedures.

HRP	Specific Activity Δ AU min^{-1} mg^{-1}	RZ Value
Native HRP	24,621	3
Gel Filtration	12,844	1.23
Concentration	14,931	1.3

Specific activities (Table 3.1) were calculated from the slopes of plots of A_{460} versus time using a Carey spectrophotometer (refer section 3.2.1 and 3.2.6.2) and from the horseradish peroxidase concentration determined from the absorbance value at 404 nm using an extinction coefficient of 107,700 (A_{404}/107,700). Therefore, the concentration of the PdG-HRP conjugate based on an absorbance value of 0.26 was 12 µM.

An HRP recovery of approximately 55% was obtained and the present conjugate was considered adequate for development of the PdG ELISA assay. Some refinement to the coupling procedure of HRP to PdG using the active ester method may increase the PdG conjugate yield. The decrease in specific activity could be due to denaturation and loss of haem during conjugation. Also further purification using cation exchange colums would increase both the specific activity and the RZ values (see also section 2.3.2).

3.3.2 Estimation of PdG-Antibody Binding Sites

The Ovarian Monitor (refer section 1.1.5) was used for lytic inhibition of PdG-lysozyme conjugates provided by Dr C.M. Smales (refer section 3.2.6.5) to estimate the concentration of the PdG binding sites of the PdG antibody. Although the ammonium sulphate precipitation (refer section 2.2.6.4) purification procedure (Harlow, 1988) was carried out,

the unpurified PdG antiserum was found to work better than the purified antiserum for the PdG ELISA.

The result of the lysozyme inhibition assay is shown in figure 3.2 where the varying volumes (µl) of antibody were plotted against the rate of lysis.

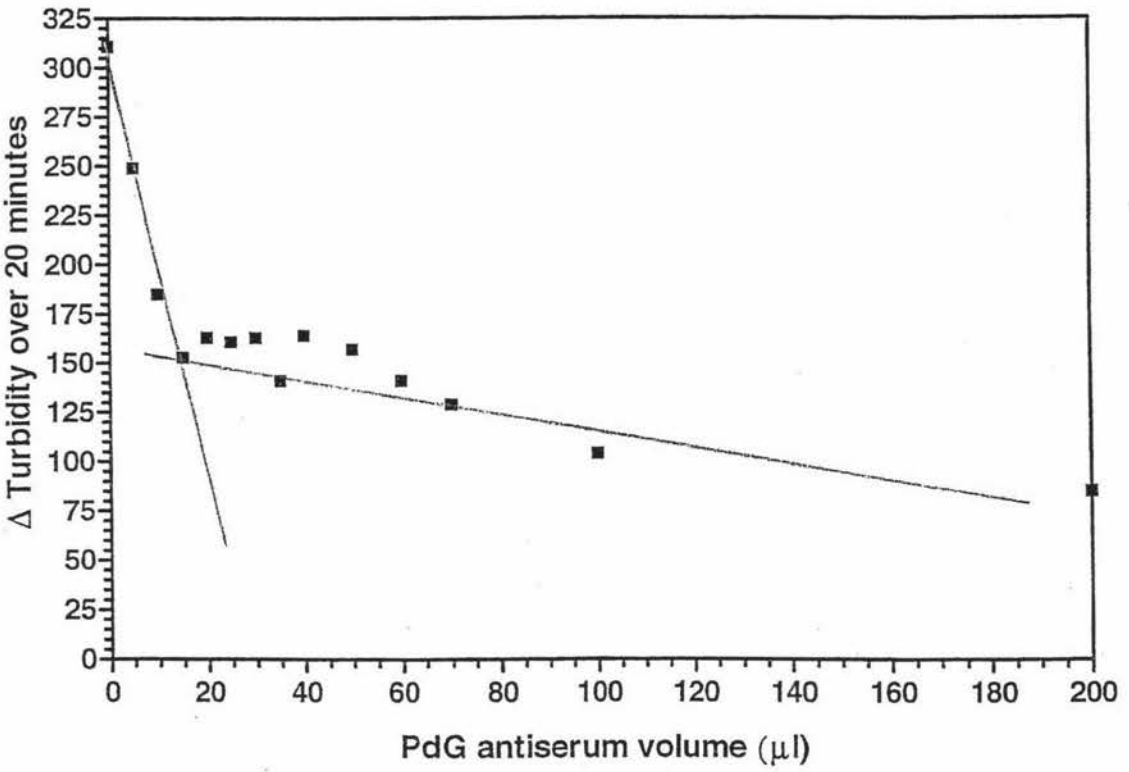

Figure 3.2: Inhibition assays using the Ovarian Monitor (section 3.2.6.5) to assess PdG-antibody concentration: An endpoint volume of 15 µl of undiluted PdG antiserum was required to inhibit the PdG-lysozyme conjugate (10 µl of a 1/400 dilution).

The lysozyme-PdG conjugate was inhibited by PdG-antibody with an `end-point' of approximately 15 µl of undiluted antiserum, using a 1/400 dilution of the PdG-lysozyme conjugate. The concentration of the HEWL-PdG conjugate in the assay was calculated for a 1/50 dilution based on the assumption that a concentration of 1 g/100 mls of lysozyme has an absorbance at 280 nm of 26.4. Using a molecular weight for the HEWL-PdG conjugate of 14,796 Da (lysozyme plus 1 PdG residue) the concentration of the conjugate in the assay was calculated as 79.8 nM (based on a A_{280} of 0.87). The total concentration of antibody binding sites in the original serum was therefore 1.86 µM (the total assay volume of 350 µl/15 x 79.8 nM). It must be recognised that the qualities of the freeze dried PdG-lysozyme sample were poor in that the maximum extent of inhibition was only 65% instead of the usual 95%. However, no other PdG-lysozyme sample was available.

3.3.3 Optimization of Antibody-Enzyme Concentrations

Dilution series were made from the PdG-antibody and the PdG-HRP conjugate which were then plated into the microtitre wells in a checkerboard fashion (refer ELISA Protocol Section 3.2.6.6) and left to incubate overnight at 4°C. Figure 3.3 shows the result of the checkerboard titration, where each line represents the titration of a different dilution of PdG-antibody (1/2,500, 1/5,000 and 1/10,000) against a similar dilution range of the PdG-HRP conjugate (1/5,000 to 1/50,000). A PdG antibody dilution of 1/10,000 was chosen since this gave an absorbance of about 1 at 490 nm for an PdG-HRP conjugate dilution of 1/10,000.

3.3.3.1 PdG-HRP and PdG-Antibody Dilutions (ng/well)

While the concentration of PdG in the timed urine samples is given in µmoles/24 h a comparison between the various PdG antibody dilutions (in ng/well) and the PdG-HRP dilutions (also in ng/well), may be useful as a reference, especially in conjunction with the amount of PdG standard (refer section 3.2.4) used per well to compare with other research involving the measurement of steroids using ELISA. The stock PdG-HRP concentration was (refer section 3.3.1) 12.1 µM. Having chosen the optimized PdG-HRP dilution (1/10,000) and a volume of 300 µl to be added in the Eppendorf incubation mixture of 450 µl, and from which an aliquot of 150 µl was put into each microwell, the amount of PdG-HRP per microwell was calculated at 5 ng. (This was based on the PdG-HRP molecular weight calculated as Mr 44,468.5 assuming one PdG group per enzyme molecule). The concentration of PdG antibody binding sites in the neat antiserum (213) was 1.86 µM (section 3.3.2) hence from the chosen PdG-antibody dilution of 1/10,000, and

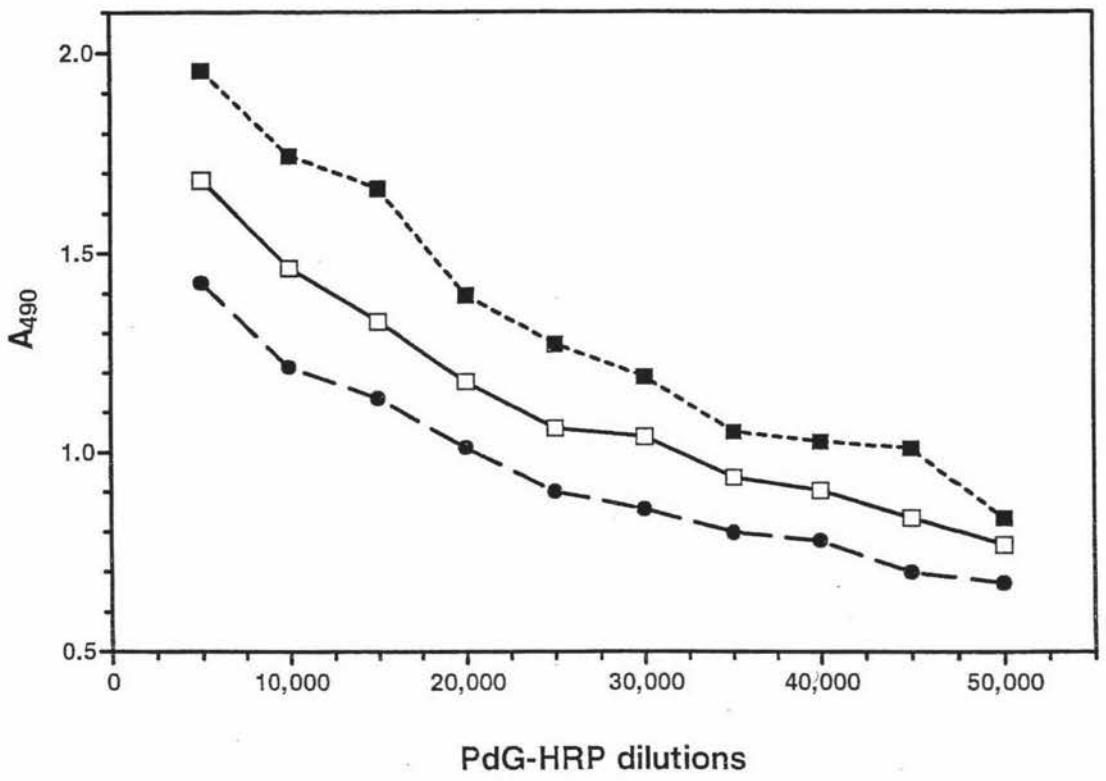

Figure 3.3: The initial checkerboard titrations of different PdG-antiserum dilutions (-■- 1/2,500; -□- 1/5,000; -●-1/10,000) against the PdG-HRP conjugate dilutions of 1/5,000 to 1/50,000.

from which aliquots of 100 µl were put directly into the microtitre wells (refer ELISA protocol, section 3.2.6.6), the amount of PdG-antibody binding sites per well was 2.79 ng. This calculation was based on a molecular weight for the IgG of Mr 160,000.

3.3.4 Optimal Amount(s) of PdG Standard and PdG Conjugate

PdG concentrations excreted in menstrual cycle urines over 24 hours are approximately 60 fold higher than the E1-3G concentrations excreted in menstrual cycle urines (Brown & Blackwell, 1989). Thus the relatively high concentration of PdG made it necessary to dilute the PdG standards used in construction of the Ovarian Monitor standard curve for PdG. These standards cover the range encountered in the normal menstrual cycle. However, the PdG ELISA was expected to be more sensitive than the monitor system.

The PdG ELISA (refer section 3.2.6.6) was performed using PdG-HRP at a dilution of 1/10,000 and the PdG-antiserum also at a dilution of 1/10,000. From an Eppendorf incubation mixture (450 µl) made up of conjugate tracer (300 µl) PdG standard (10 µl) and assay buffer (140 µl) aliquots (150 µl) were taken and, after thorough mixing, were put into each well so that duplicate or even triplicate wells could be prepared for each data point. The plates were then left to incubate overnight at 4°C. The assay blank (assay reagents only were put into microwells with immobilized PdG antibody) absorbance values were defined as the 0% value, while the zero standards (no PdG standards were present) were defined as the 100% absorbance value in the normalization of the PdG standard curve.

Initially 10 µl of pre-diluted PdG Standards were added to the incubation mixture (450 µl). Five different pre-dilutions (1/50, 1/100, 1/200, 1/300 and 1/500) of the Ovarian Monitor PdG standards giving a range of values covering 0.1, 0.5, 1.3, 4, 7, 12, 36, 90 and 180 µmoles/24 h were prepared and used to generate five PdG standard curves as shown in figure 3.4. Good sigmoidal dose-response curves were obtained in all cases with the mid-points of the curves shifting to the right on the PdG concentration scale as the pre-dilution of the PdG standards increased. This is because less PdG is being added to the microplate wells as the pre-dilution of the monitor PdG standards increases. The lowest PdG standard dilution (1/50) generated a PdG standard curve which covered the expected range of PdG concentrations (1 µmoles/24 h to 50 µmoles/24 h) encountered during the normal menstrual cycle with urines collected at a dilution of 150 ml/h of collection.

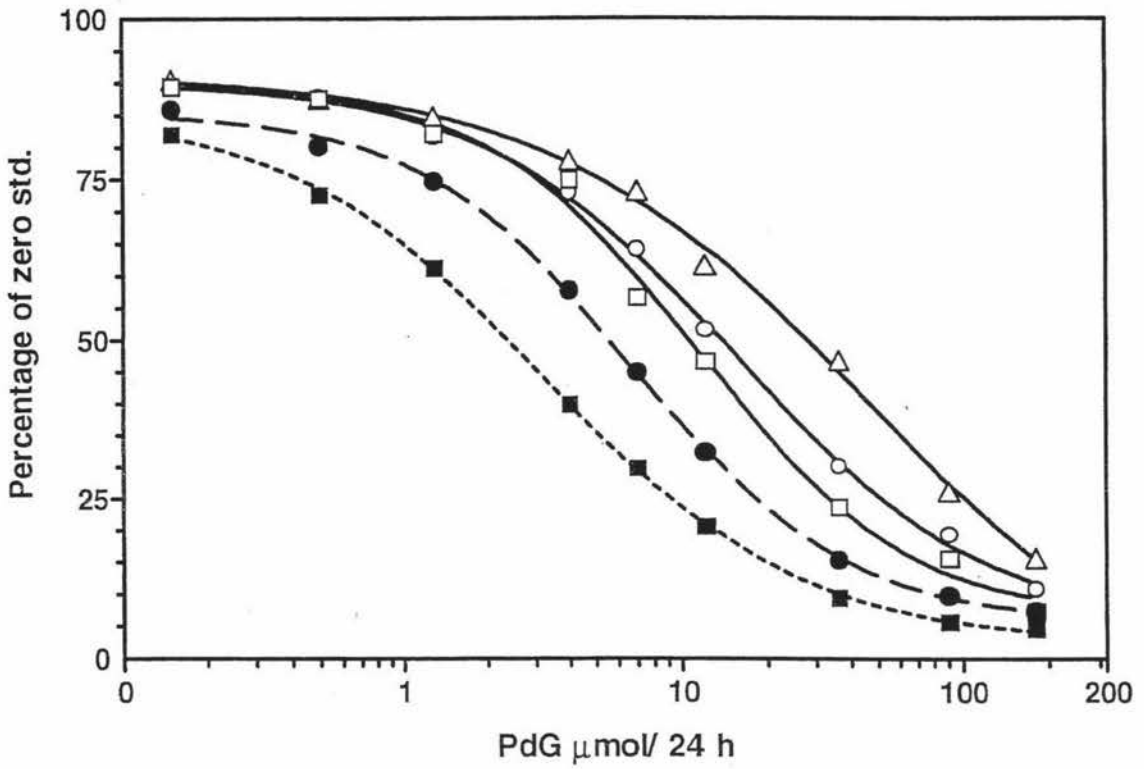

Figure 3.4: The effect of different pre-dilutions (■ 1/50, ● 1/100, □ 1/200, ○ 1/300, and △ 1/500) of the PdG monitor standards (0.1 µmol/ 24 h to 180 µmol/ 24 h) on the standard curve. (PdG-HRP 300 µl, 1/10,000 dilution; PdG antiserum dilution 1/10,000)

The construction of the PdG standard curve using the monitor PdG standards at a 1/50 dilution was achieved using the chosen PdG-antibody (1/10,000) and PdG-HRP (1/10,000) dilutions (refer section 3.3.3). Figure 3.5 shows that while the lower limit of 0.5 µmoles/24 h and the upper limit of about 90 µmoles 24 h constituted the working range of the standard curve, the curve was most sensitive along the almost linear region between 1.3 µmoles/24 h and 36 µmoles/24 h. The PdG threshold value (refer section 3.1 and 1.1.4.5) of 6.3 µmoles/24 h lay in the middle of the working range of the PdG standard curve which was therefore ideally suited to measure the PdG cut-off value which marks the end of the potentially fertile phase of the menstrual cycle (refer section 1.1.4.5).

The amounts of the PdG-HRP conjugate (300 µl) at dilutions of 1/5,000 and 1/10,000 added to the Eppendorf pre-incubation mixture, and the PdG-antibody (100 µl) at dilutions of 1/1,000, 1/2,500 and 1/10,000 added to the microplate are shown (ng/well) in Table 3.2 and indicates the ratios of immunoassay components within the microwells.

Table 3.2: PdG-Antibody (ng/well) and PdG-HRP Conjugate (ng/well) at Dilutions Used in the PdG ELISAs

	PdG-HRP		PdG-Antibody		
Dilutions	1/10,000	1/5,000	1/10,000	1/2,500	1/1,000
ng / well	4.86	9.72	2.79	11.2	27.9

As outlined above, to speed up the assay procedure and avoid the inconvenience of having to dilute the Ovarian Monitor PdG standards by 1/50 before adding them to the incubation mixture in the Eppendorf tube, experiments were carried out using undiluted PdG standards. To compensate for the use of the more concentrated (undiluted) PdG standards in the incubation mixture, the volume of the standard was reduced (1µl to 5µl) and the incubation mixture was increased (450 µl to 1.8 mls). The PdG-antibody dilution (1/10,000) and PdG-HRP conjugate dilution (1/10,000) and amounts added to the assay were the same as for the pre-diluted (1/50) PdG standard curve (figure 3.5).

Using smaller urine volumes (1 µl to 5 µl) added to an Eppendorf tube which contained up to four times the volume of incubation mixture used to construct the prediluted (1/50) standard curve (figure 3.5) the assay was repeated (Table 3.3). Calculation of the amounts of PdG standard in each well (pg/well) were based on the molecular weight of PdG

(Mr 518.6) and conversion of the concentration in µmoles/24 h divided by 3.6 (Table 3.3).

Table 3.3: Ovarian Monitor PdG Standards (in pg/ well) Used in the Construction of Three PdG Standard Curves Using ELISA.

PdG Standards µmoles/24 h	Prediluted (1/50) of PdG Standards 10 µl in 450 µl pg / well	PdG Standards 1 µl in 1.8 mls pg / well	PdG Standards 1 µl in 1.35 mls pg / well
0.1	0.96	1.2	1.6
0.5	4.6	6	8
1.3	12.4	15.6	20
4	38	48	64
7	67	84	112
12	115	144	192
36	345	432	576
90	864	1,000	1,300
180	1,729	2,080	2,700

Table 3.3 shows that the pre-diluted PdG standard (10 µl of a 1/50 dilution in a total volume of 450 µl, from which a 150 µl aliquot is taken), contains the least PdG (in pg/well). The other PdG standards using 1 µl in 1.8 mls represent a 20% increase, and the PdG standards using 1 µl in 1.35 mls represent a 40% increase in PdG concentration.

The PdG standard curve shown in figure 3.6 was constructed using 1 µl of undiluted monitor PdG standards in an incubation mixture of 1.35 mls. The increased amount of PdG (by 40%, refer Table 3.3) reduced the number of antibody binding sites available at each standard concentration for the PdG-HRP conjugate to bind with and as a consequence less colour was produced on the ELISA plate. The working range of the PdG standard curve (figure 3.6) appears to have a lower limit of almost 0.1 µmoles/24 h and an upper limit of about 36 µmoles/24 h. The steepest part of the standard curve ranged between 0.5 µmoles/24 h and approximately 20 µmoles/24 h, which represents a 45% reduction in the working range for this PdG standard curve. While the threshold PdG value was nearer to the higher concentration limit of the PdG standard curve than for the

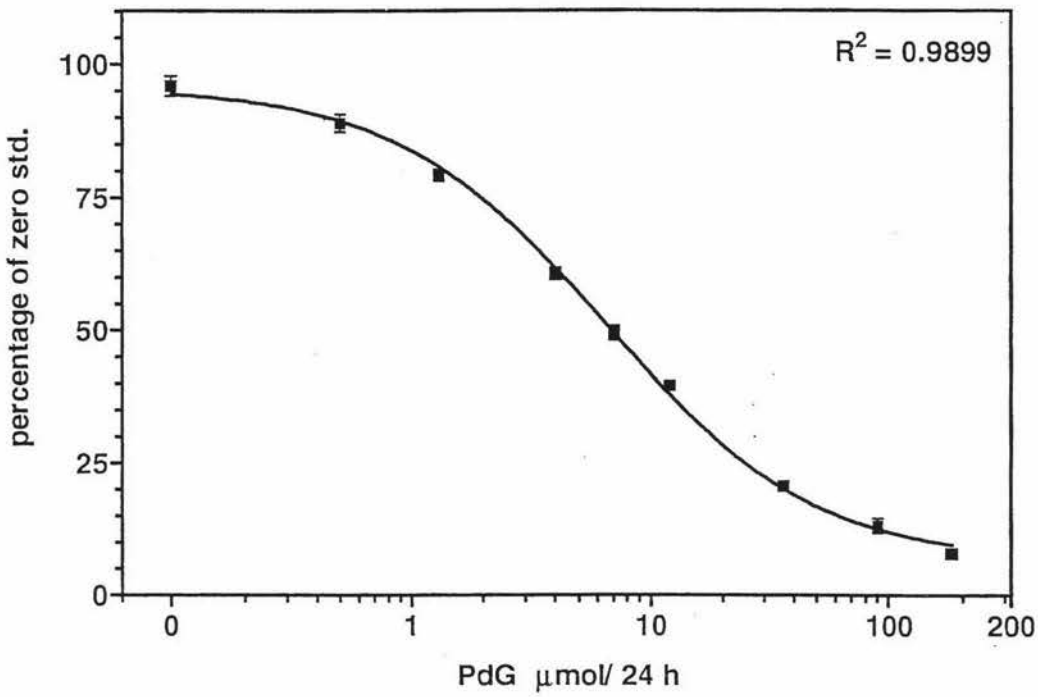

Figure 3.5: PdG standard curve using the monitor PdG standards (10 µl) at a 1/50 dilution. (PdG-HRP 300 µl, dilution 1/10,000; PdG antiserum dilution 1/10,000)

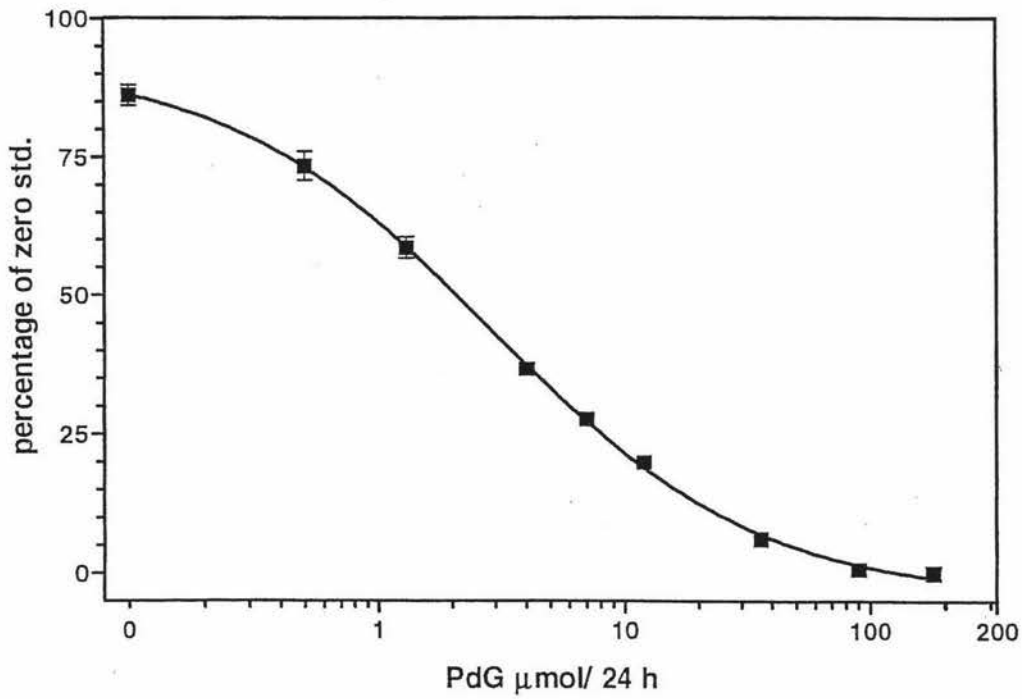

Figure 3.6: The PdG standard curve using 1 µl of undiluted monitor PdG standard in a total volume of 1.35 mls. (PdG-HRP 900 µl, dilution 1/10,000; PdG antiserum 1/10,000)

curve shown in figure 3.5, nevertheless it still fell within the working range. Thus this curve is also acceptable for the measurement of PdG levels in menstrual cycle urine samples.

As 1 µl is a very small volume to dispense accurately, attempts were made to increase the amount of undiluted PdG monitor standards put into the Eppendorf tube. A range of undiluted PdG standard volumes (1 µl, 5 µl and 10 µl) were tested using both the chosen PdG-HRP dilution of 1/10,000 and an increased PdG-HRP dilution of 1/20,000 in a normal incubation volume (450 µl). To compensate for the extra PdG in the assay the PdG antiserum was increased four fold to a dilution of 1/2,500. The affects of increasing both the PdG concentration and the PdG antiserum concentration while decreasing the conjugate concentration were then examined. However, figure 3.7 clearly shows that the higher PdG standard volumes (5 µl and 10 µl) depress the colour formation for the higher PdG standard concentrations used in the assay, thus necessitating the addition of more dilute standards in order to construct a standard curve.

Thus the incubation volume of everything else in the Eppendorf tube was increased three fold for volumes of the monitor PdG standards of 1 and 5 µl. As a control (to compare with figure 3.7) a normal incubation mixture (450 µl) was used in combination with the 1 µl volume of the undiluted monitor PdG standards. The standard curves (1 µl in 450 µl) in both figures 3.7 and 3.8 showed that too much PdG was present in the microwells and hence the mid-point of the standard curve was shifted appreciably to the left towards lower PdG concentrations. Increasing the volume of the monitor PdG standards in the Eppendorf to 5 µl (increasing the concentration of PdG in the microwells) shifted the mid-point even further despite increasing the total volume in the Eppendorf. Only the low concentration PdG standards (0.1, 0.5 and 1.3 µmoles/24 h) allowed any conjugate to bind to the microwells. However, when 1 µl of the monitor PdG standards and an increased volume (1.35 mls) was used the working range of the PdG standard curve (figure 3.8) was very similar to that obtained using the diluted (1/50) PdG monitor standards (figure 3.5), with a lower concentration limit of 0.5 µmoles/24 h and an upper limit of 90 µmoles/24 h. The PdG threshold value (refer section 3.1 and 1.1.4.5) of 6.3 µmoles/24 h was again in the middle regions of the working range of the PdG standard curve, and therefore this PdG standard curve was also maximized to measure the PdG cut-off value of 6.3 µmoles/24 h which marks the end of the potentially fertile phase of the menstrual cycle (refer section 1.1.4.5).

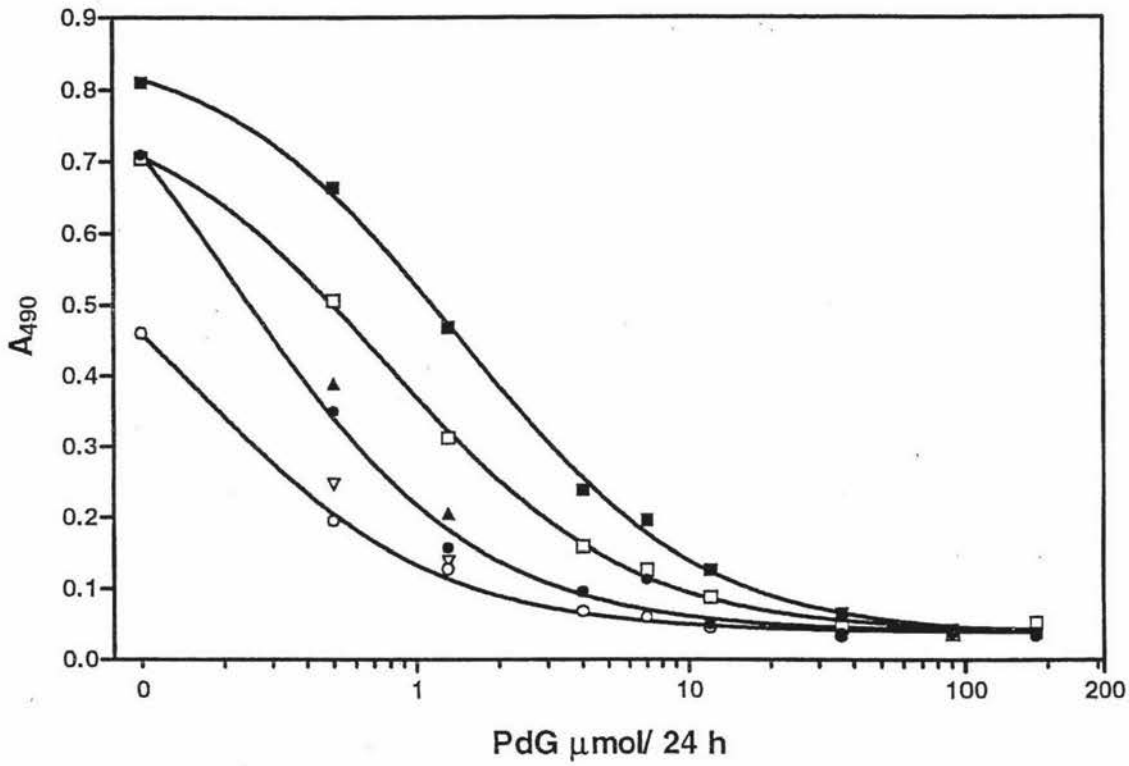

Figure 3.7: A range of volumes (■ 1 µl, ● 5 µl, and ▲ 10 µl) of undiluted PdG standards at a PdG-HRP dilution of 1/10,000. Also, a range of volumes (□ 1 µl, ○ 5 µl, and ▽ 10 µl) of undiluted PdG standards at a PdG-HRP dilution of 1/20,000. (PdG-HRP 300 µl, in a total volume of 450 µl; PdG antiserum dilution 1/2,500)

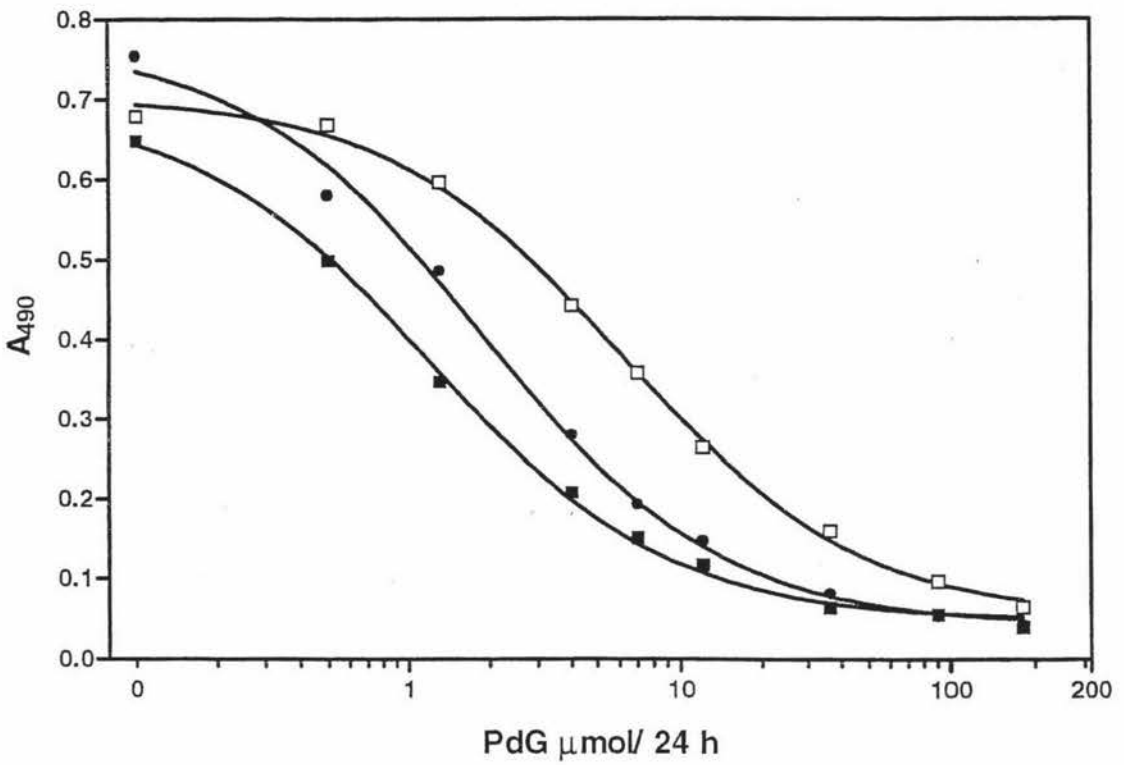

Figure 3.8: Effects of varying the volumes of PdG standards (□ 1 μl and ■ 5 μl) in a total volume of 1.35 mls (PdG -HRP 900 μl). Also, PdG standards (• 1 μl) in a total volume of 450 μl (PdG-HRP 300 μl). (PdG-HRP 1/10,000 dilution; PdG antiserum dilution 1/2,500)

However, again only 1 µl of the urine sample could be added to the Eppendorf tubes. To increase the upper concentration limit of the PdG standard curve enabling the highest PdG levels to be measured accurately without simultaneously degrading the measurement of the threshold value, the lower volume of monitor PdG standards volume (1 µl) was used in combination with an increased incubation volume (1.8 mls). However, the PdG standard curve (figure 3.9) which was generated was surprisingly similar to the PdG standard curve (figure 3.8) constructed when a lower incubation volume (1.35 mls) was used.

To increase the range of the standard curve to higher PdG concentrations the PdGantiserum dilution was reduced further to 1/1,000, while the volume of the monitor PdG standards (1 µl) and the incubation volume (1.8 mls) remained the same as for the PdG standard curve shown for figure 3.9. Unexpectedly, the lower concentration limit of the PdG standard curve increased marginally, but the upper limit remained relatively unchanged. In fact this standard curve (figure 3.10) was similar to the standard curve (figure 3.6) constructed with a higher PdG antiserum dilution (1/10,000) together with a smaller volume of the monitor PdG standards (1 µl), and a smaller incubation volume (1.35 mls). These results are puzzling and in contrast to other research (Crowthers, 1995; Kemeny, 1991; Paek *et al.*, 1993), where increased antibody concentration (lower dilution) has been reported to increase the working range of the standard curve. Also in contrast to these results, increasing antibody concentration is expected to decrease assay sensitivity (Schramm & Paek, 1992), as already discussed.

Finally, 1 µl of the undiluted monitor PdG standards was used with an increased incubation mixture volume (1.8 mls) and a reduced PdG-HRP dilution (1/5,000) in an attempt to increase the colour on the ELISA plate at the higher PdG concentrations. The PdG antiserum dilution was restored to 1/2,500 as for previous PdG standard curves (see figure 3.9). However, the standard curve (figure 3.11) again remained relatively unchanged. Thus, the standard curves are relatively stable and a range of conditions can be used to give a workable system. However, to use the urines undiluted in the ELISA assay required the accurate aliquotting of 1 µl. This may not be practicable in general use but further work could be carried out on this aspect of the PdG assay. In conclusion, a PdG standard curve has been developed to expedite the measurement of PdG at the threshold concentration of 6.3 µmoles/24 h, and has been shown to be fairly robust overa range of PdG ELISA component variation(s).

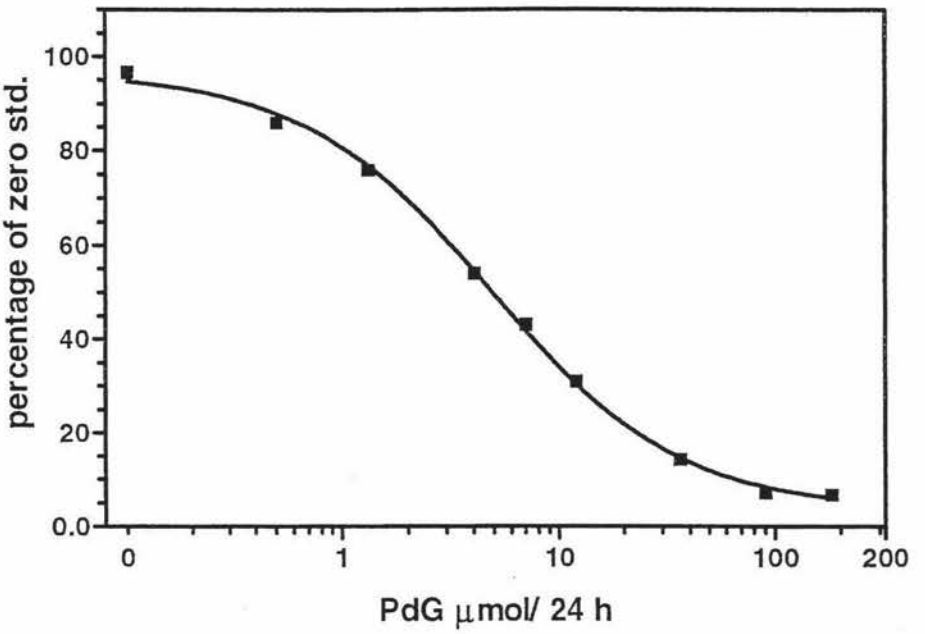

Figure 3.9: The effects on the standard curve of using monitor PdG standards of 1 μl in a total volume of 1.8 mls. (PdG-HRP 1.2 mls, dilution 1/10,000; PdG antiserum 1/2,500 dilution)

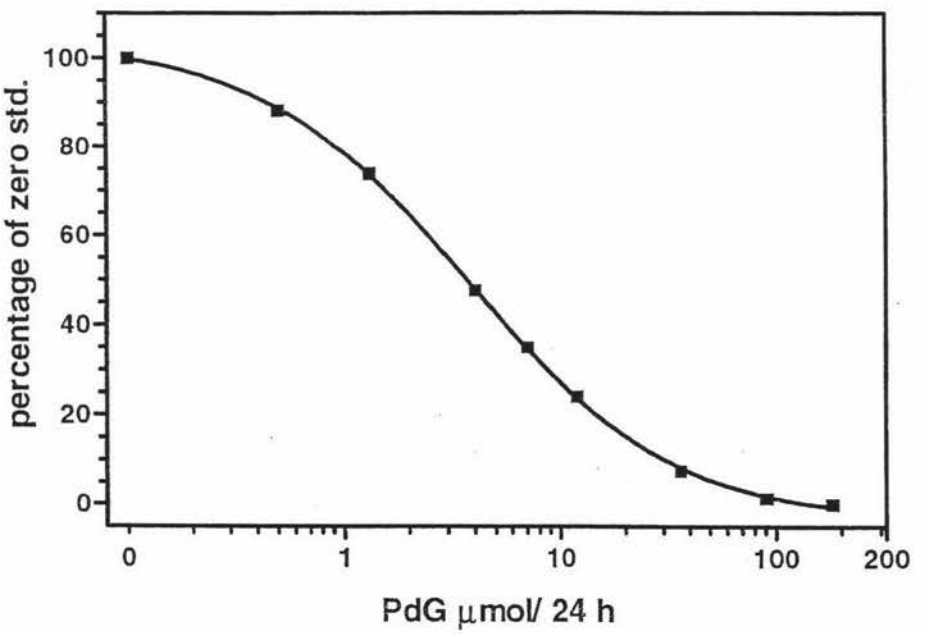

Figure 3.10: The effects on the PdG standard curve of an antiserum dilution of 1/1,000 (1 μl of the monitor standards in a total volume of 1.8 mls; PdG-HRP 1.2 mls, dilution 1/10,000).

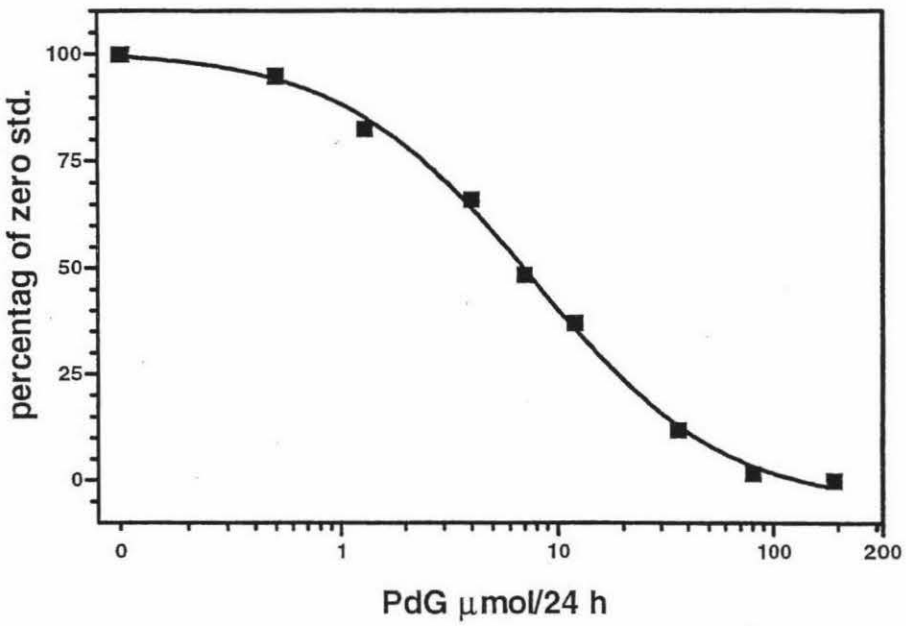

Figure 3.11: The effects on the PdG standard curve of an increased PdG-HRP concentration (a dilution of 1/5,000) with a PdG antiserum dilution of 1/2,500. (PdG-HRP 1.2 mls; 1 μl of PdG standard in a total volume of 1.8 mls)

3.3.5 Evaluation of the ELISA PdG Standard Curve

To determine whether the ELISA for PdG could serve as a laboratory reference assay tests were performed to evaluate the accuracy, reliability, sensitivity, cross-reactivity and non-specific binding.

3.3.5.2 Sensitivity

Assay sensitivity was defined as for the EIG assay (Henderson *et al.*, 1995) as the amount of PdG producing a percentage (E/E_0) value two standard deviations below that of the zero standard (refer section 3.3.4). As before `E' was defined as the mean absorbance reading of the appropriate PdG standard (refer section 3.2.4), which is divided by the mean absorbance reading of the zero standard `E_0'. The lowest monitor PdG standard was 0.1 µmoles/24 h and therefore this PdG standard concentration used in constructing the standard curve (10 µl of pre-diluted (1/50) PdG standard in an incubation volume of 450 µl, from which a 150 µl aliquot was put into each of the microwells) was tested first.

Because each standard curve was determined with the PdG standard (0.1 µmoles/24 h) and the zero standard (no PdG added) with points done in duplicate or triplicate, it was necessary to first find the mean of each of these absorbance values for each standard curve, and then the S.D. with the highest value was selected. The mean absorbance reading of the PdG standard point for 0.1 µmoles/24 h was then divided by the mean absorbance reading of the zero standard minus two S.D., and the resulting value multiplied by 100 to determine the percentage. For the PdG standard point equivalent at 0.1 µmoles/24 h the percentage was greater than 100% for this point (refer Table 3.4) hence there was no significant difference from the zero standard.

These results were also consistent with the same sensitivity test carried out using the same monitor PdG standard but where smaller PdG standard volumes were put undiluted into greater incubation mixture volumes (refer section 3.3.4). It should be noted that the lowest PdG standard used for the Ovarian Monitor was 1.3 µmoles/24 h and these results therefore are not unexpected.

Table 3.4: The Mean (n=18) Absorbance Values (A_{490}) and Standard Deviations (S.D.) of both the PdG Standards (0.1 µmoles/24 h) and the Zero Standards Used to Calculate the Inter-Assay Sensitivity of the PdG Standard Curve

	Zero Standard 0 µmoles/24 h A_{490}	PdG Standard 0.1 µmoles/24 h A_{490}
Mean	0.98	0.95
S.D.	0.016	0.0179
C.V.	1.63	1.88

The calculation of Intra and Inter-assay sensitivity = E/(Eo-2SD)X100.
0.98 - (2 X 0.0179 = 0.0358) = 0.944; 0.95/0.944 X 100 = 100.6 %

The second lowest monitor PdG standard was 0.5 µmoles/24 h and therefore this PdG standard concentration used in constructing the standard curve was tested next. The sensitivity of each (10 µl of pre-diluted PdG standard (1/50) in an incubation volume of 450 µl, from which a 150 µl aliquot was put into each of the microwells) individual standard curve was at least 0.5 µmoles/24 h (4.6 pg/well, refer section 3.3.4.; Table 3.3), since $E/(E_0\text{-}2SD) \times 100$ was 93.4 %. This shows that the second PdG standard gave a signal which was significantly different from that given by the zero standard. Each of the PdG standard curves were processed as above and each individual PdG standard curve had a sensitivity of at least 0.5 µmoles/24 h, which means that the Intra Assay Sensitivity for the ELISA PdG assay was ≤ 0.5 µmoles/24 h (4.6 pg/well). The Inter Assay Sensitivity was also calculated as ≤ 0.5 µmoles/24 h (4.6 pg /microwell), since all of the individual PdG standard curves gave the same sensitivity results.

Since the PdG-HRP concentration was 4.86 ng/ well (refer Table 3.2), the ratio of tracer to analyte was approximately 1,056 : 1. These results were also consistent with the same sensitivity test carried out using the same monitor PdG standard where the smaller PdG standard volume (1 µl) was put undiluted into incubation mixture volumes of either 450 µl, 1.35 mls or 1.8 mls (refer section 3.3.4).

Table 3.5: The Mean (N=18) Absorbance Values A_{490} and Standard Deviations (S.D.) of both the PdG Standards (0.5 µmoles/24 h) and the Zero Standards Used to Calculate the Inter-Assay Sensitivity of the PdG Standard Curve.

	Zero Standard (0 µmoles/24 h) A_{490}	PdG Standard (0.5 µmoles/24 h) A_{490}
Mean	0.98	0.8897
S.D.	0.016	0.0236
C.V.	1.63	2.65

The calculation of Intra/Inter-assay sensitivity = $E/(E_o$-2 S.D/) X 100.
0.98 - (2 X 0.0236 = 0.0472) = 0.9328; 0.8897/0.9328 X 100 = 95.4%

The coefficient of variation (C.V.) is also shown (CV = (S.D./mean)X 100), in both Table 3.34 and Table 3.35 and clearly shows that the assay is reliable at this level of sensitivity.

3.3.5.2 Inter-Assay Reliability

The standard curves from nine different microtitre plates were plotted as E/E_0 versus PdG concentration of the Ovarian Monitor standards (refer section 3.3.4) and compared to determine the inter-assay reliability of the pre-diluted PdG standard curves (10 µl in 450 µl). As the data points were close together, these standard curves (see figure 3.12) showed excellent reproducibility of the assay.

Table 3.6: Characteristics of the PdG Standard Curves Using ELISA

PdG Standards	6.3µmol/24h pg/well	High point ED_{20} pg/well
1/50	60.5 ± 1.7	345 ± 3.2
C.V.	2.8	0.93

The mean (N=18) estimated PdG dosage at the mid-point (ED_{50}) of the standard curves was 6.7 ± 0.19 µmoles/24 h (N=18), equivalent to 64.3 ± 1.8 ng/well. Thus the threshold value of 6.3 µmoles/24 h is measured at the midpoint of the PdG standard curve. The mean (N=18) estimated PdG dosage at the high point which is defined as 20% from the bottom (ED_{20}) of the standard curves was 36 ± 1.02 µmoles/24 h equivalent to 345 ± 3.2

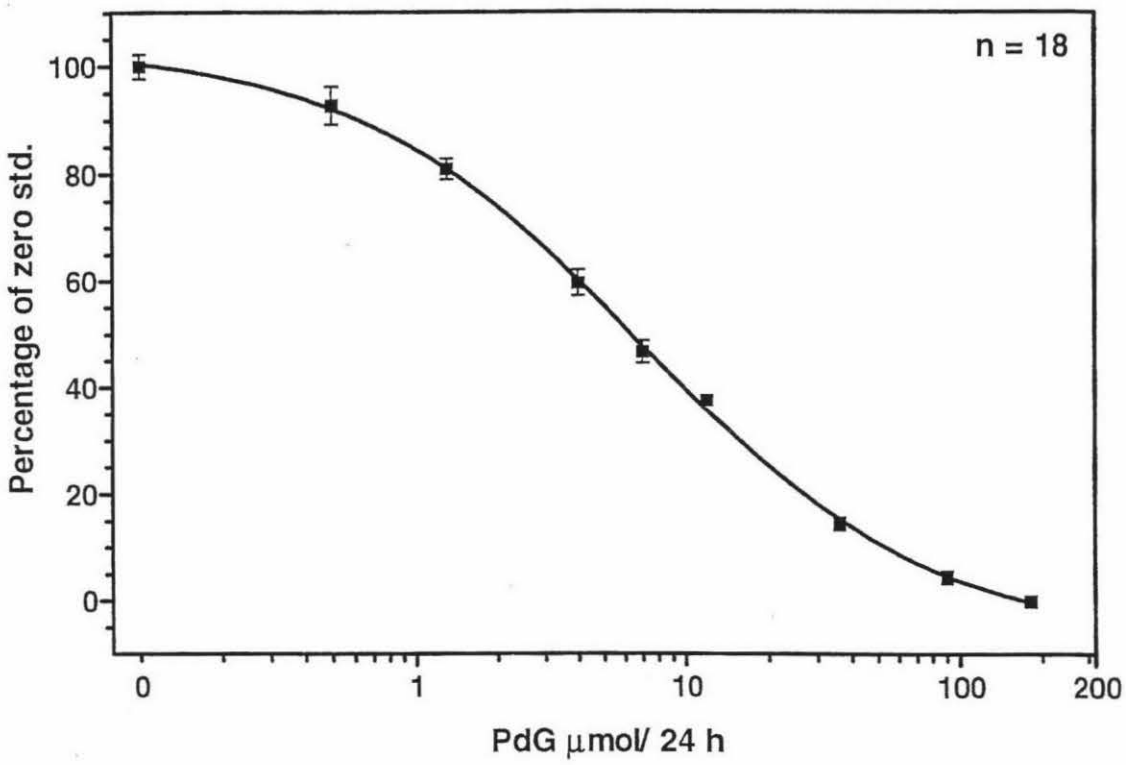

Figure 3.12: Normalised PdG standard curves (n=18) from nine different ELISA microtitre plate (10 µl of a 1/50 dilution in a total volume of 450 µl), using S.D. error bars. (PdG-HRP 300 µl, dilution 1/10,000; PdG antiserum dilution 1/10,000)

pg/well. Since the coefficient of variation (CV) calculated for the ED_{50} was 2.8 and for ED_{20} was 0.93 these results gave excellent precision and therefore good inter-assay reliability.

3.3.5.3 Cross-Reactivity

The extent of cross-reactivity of the assay with possible contaminations by other steroids was determined by comparing the relative amounts of PdG standards and the cross-reacting steroids required to decrease the absorbance value to 50% of that of the zero standard (refer section 3.3.4.1).

A series of available steroids (pregnanediol, testosterone, progesterone, androstenedione, oestrone and E1-3G) at high dose levels of 1,000 times the largest PdG (180 µmoles/24 h) dose used to construct the standard curve were tested. The highest amount of PdG (180 µmoles/24 h) was equivalent to 50 µM (refer section 3.2.4), which gives a concentration for the cross-reacting steroid equivalent to 1,000 times for a 0.1% cross reactivity of (50 µM/ 0.1) X 100 or 50 mM. This means that a dose of the test substance 1,000 fold greater than the dose of the reference analyte yields the same response in the immunoassay. The cross reactivity was then defined as [PdG]/[cross reacting steroid] X 100. Substances which exhibited less than 0.1% of the inhibition of the binding by the analyte (PdG) to the antibody were considered not to cross react significantly.

The majority of the steroids (see Table 3.7) cross reacted with the PdG antibody by less than 0.1%, and the higher cross reactivity exhibited by pregnanediol against PdG was not unexpected as they share many of the same structural features. A repeat pregnanediol dose response curve was generated (refer figure 3.13) using a range of lower concentrations of the steroid (from 11.63 µmoles/24 h to 11,925 µmoles/24 h). From the mid-point (equivalent to 50% of the zero standard) of the B/Bo PdG standard curve constructed using PdG monitor standards, the concentration of PdG (8.75 µmoles/24 h) and the concentration of pregnanediol (550 µmoles/24 h) was determined and hence a percentage cross reactivity was calculated (Table 3.7). The resulting low percentage of cross-reactivity (1.6%) with pregnanediol was not considered significantly high enough to jeopardize the use of the PdG ELISA assay. A repeat testosterone dose response curve was also generated (figure 3.14), using a range of lower concentration of steroid (195 µmoles/24 h to 50,000 µmoles/24 h).

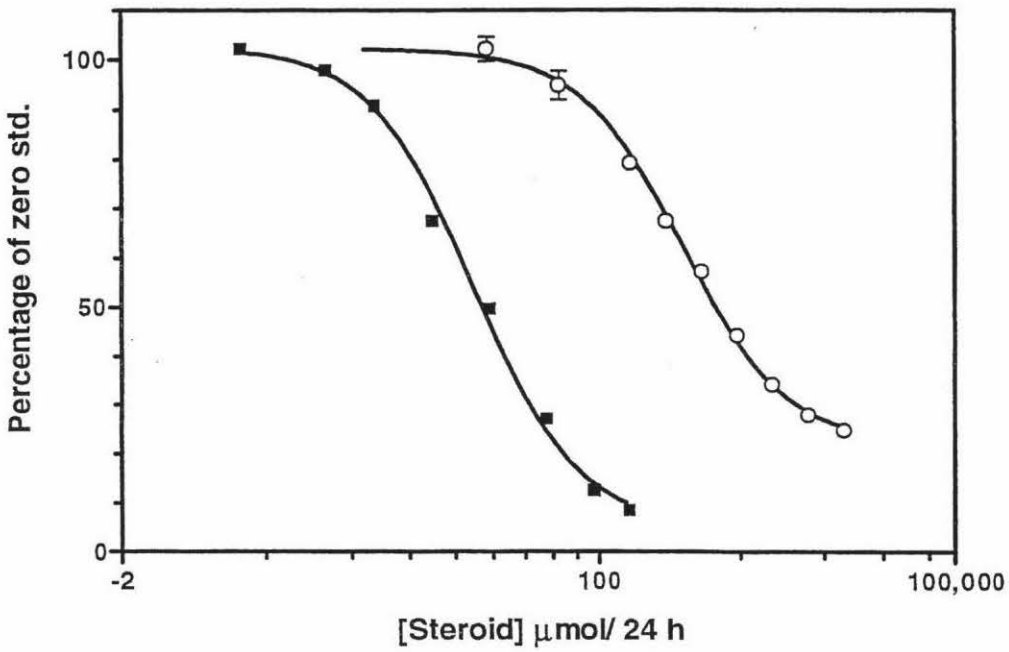

Figure 3.13: A pregnanediol dose response curve (o) generated using a range of concentrations (11.63 µmol/ 24 h to 11,925 µmol/ 24 h), and a control PdG standard curve (■), used to determine (from A_{490} = 0.63) the percentage of cross reacting of pregnanediol with the PdG antibodies.

([8.75 µmol/ 24 h] / [550 µmol/ 24 h] x 100 = 1.6%)

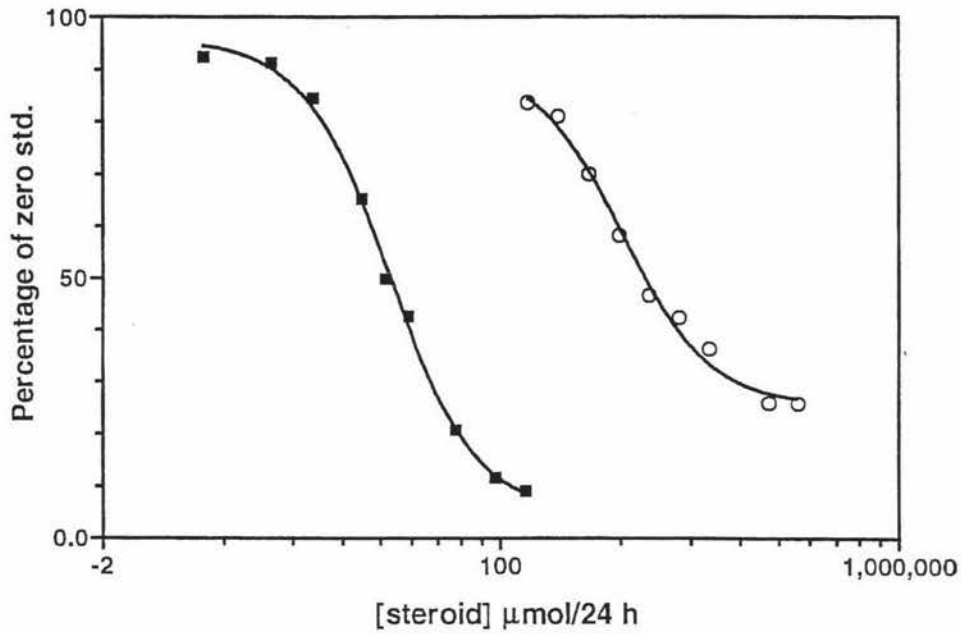

Figure 3.14: A testosterone dose response curve (o) generated using a range of concentrations (195 µmol/ 24 h to 50,000 µmol/ 24 h) and a control PdG standard curve (■) used to determine (from A_{490} = 0.39) the percentage of cross reacting of testosterone with the PdG antibodies.

([8.5 µmol/ 24 h] / [2,500 µmol/ 24 h] x 100 = 0.35%)

The PdG and testosterone concentrations were determined which resulted in 50% inhibition of binding of the PdG-HRP label giving a low percentage cross reactivity of 0.35% with testosterone (Table 3.7).

Table 3.7: Percent Cross-Reaction of Various Steroids in the Antibody Coated ELISA for Pregnanediol-3 α-Glucuronide

Steroids	Percent (%) Cross-Reaction with PdG	
PdG	100	
Pregnanediol	1.6	
Testosterone	0.35	
Progesterone	0.027	< 0.1
Androstenedione	0.015	< 0.1
Oestrone	0.008	< 0.1
E1-3G	0.000285	< 0.1

Table 3.7 shows that the PdG antiserum has a high specificity for PdG. As shown in figure 3.13 and figure 3.14 for pregnanediol and testosterone respectively the dose response curves were essentially parallel to the control standard curve. Such parallelism of dose response curves demonstrates that the percentage of cross reactivity with the PdG standard curve is a constant one at all dose levels. Therefore any pregnanediol present will produce a relatively constant error.

3.3.5.4 Non-Specific Binding

The "urine effect" of blank urine samples on the PdG results obtained was examined before using the assay to determine the rates of excretion of PdG in menstrual cycle urines (see section 2.3.5.4). Such samples were obtained from the urine of a pre-pubertal male, and were timed and diluted to 150 ml per hour (refer section 3.2.5).

Figure 3.15 shows an *unspiked* pre-diluted (1/50) PdG standard curve (10 µl in an incubation volume of 450 µl; the same as figure 3.5) together with a *spiked* pre-diluted (1/50) PdG standard curve (10 µl of PdG monitor standard pre-diluted 1/50, and 10 µl of timed and diluted blank urine also pre-diluted 1/50, in an incubation mixture volume of 450 µl), and the two standard curves appear relatively similar. Under these conditions, therefore, non-specific urinary interference is clearly not important.

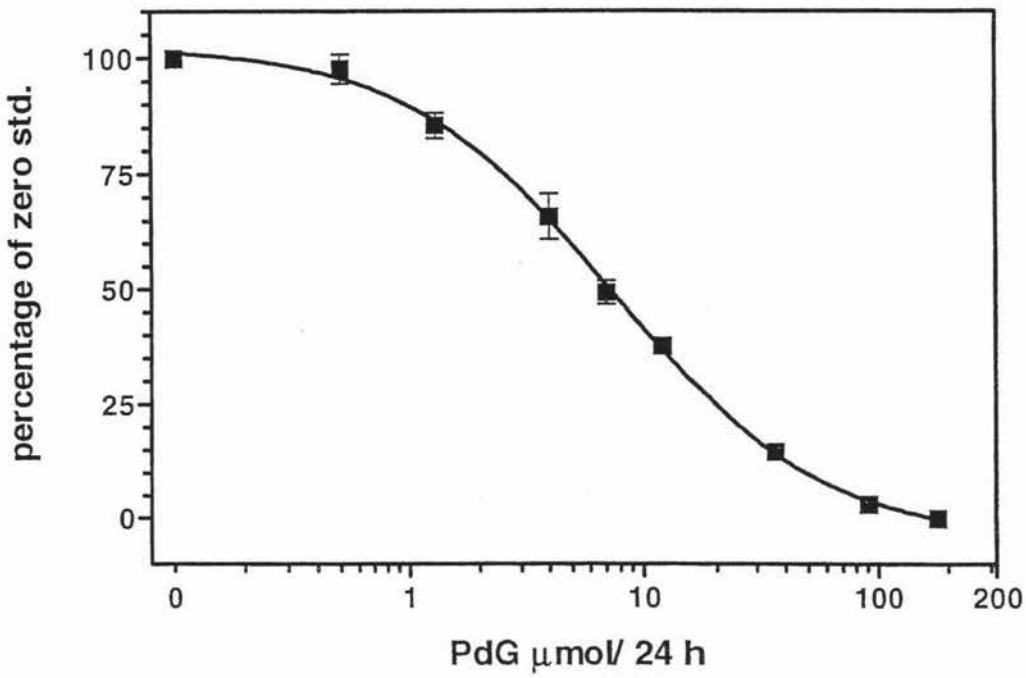

Figure 3.15: A pre-diluted (1/50) PdG standard curve (10 µl of PdG monitor standard in a total volume of 450 µl); together with a urine spiked PdG standard curve (10 µl of PdG monitor standard pre-diluted 1/50, and 10 µl of timed and diluted blank urine also pre-diluted 1/50; in a total volume of 450 µl; PdG-HRP 300 µl, 1/10,000 dilution; PdG antiserum dilution 1/10,000).

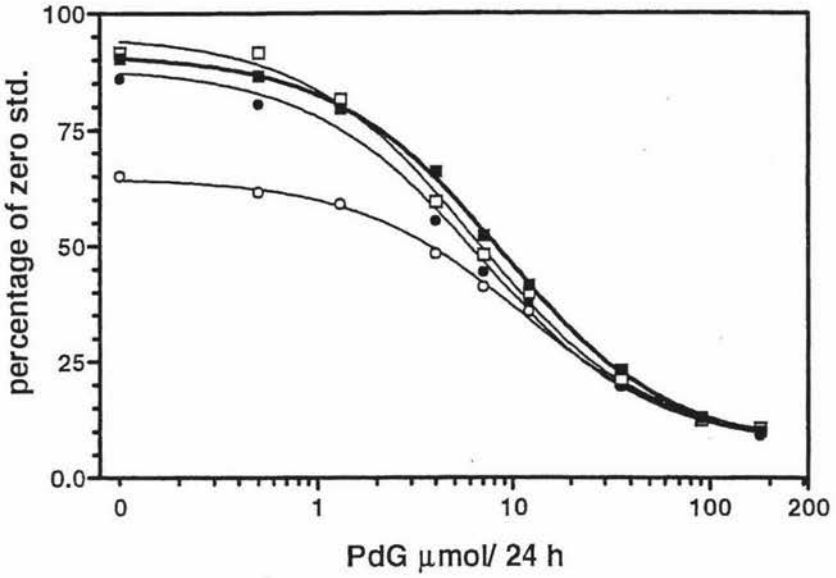

Figure 3.16(a): A series of PdG standard curves containing diluted (▫ 1/50 and ● 1/100) and undiluted (○) blank urine samples (10 µl in a total volume of 450 µl), were compared with a PdG control standard curve containing no blank urine sample (■). (PdG-HRP 300 µl, 1/10,000 dilution; PdG antiserum 1/10,000 dilution)

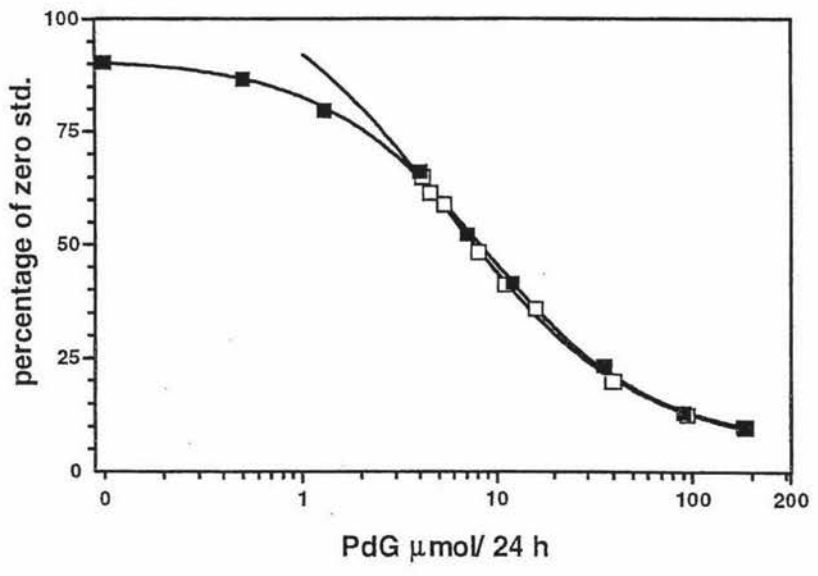

Figure 3.16(b): A PdG control standard curve containing no blank urine sample (■), and a PdG standard curve containing neat urine samples (□) of 10 µl in a total volume of 450 µl: After 4 µmol [PdG]/ 24 h was added to all of the PdG standards containing urine. (PdG-HRP 300 µl, 1/10,000 dilution; PdG antiserum 1/10,000 dilution)

A series of PdG standard curves were generated, which contained various dilutions of the supposed blank urine sample (10 µl) added to the incubation mixture in the Eppendorf tube (450 µl). These PdG standard curves were called urine *spiked* PdG standard curves, and they were compared with the *unspiked* control PdG standard curves which contained no blank urine (figure 3.16a). Addition of the undiluted blank urine (10 µl) to the incubation mixture (450 µl) clearly showed interference by urinary substances with the binding of the PdG-HRP conjugate, as demonstrated by the much lower absorbance values for the *spiked* PdG standards. This was particularly true at the lower PdG concentrations at the upper regions of the absorbance curves. Absorbances were much higher for the *unspiked* PdG standard curve.

As a check for non-specific binding the B/B_0 value for the 0.1 µmol/24 h PdG standard spiked with undiluted urine (10 µl of non-prediluted urine sample in an incubation mixture volume of 450 µl) was read off the control (*unspiked*) PdG standard curve, and an apparent PdG value of approximately 4 µmol/24 h was obtained. After subtracting 4 µmol/24 h from each of the actual PdG standards used to construct the *spiked* standard curve and replotting the data, as the standard curves superimposed completely (figure 3.16b). Hence, there does not appear to be a non-specific urine effect even with undiluted urines (that is no extra-dilution after the initial 150 ml/ h dilution) that cannot be accounted for by supposing that the urine contains PdG or cross reacting glucuronides which are registered as if they were PdG. This does however place a limit on the amount of urine which can be added to the assay without further dilution.

3.3.6 Use of the ELISA PdG Assay to Measure Menstrual Cycle Urines

Optimization of the urine sample volume was required to allow the PdG levels in all of the urine samples of the menstrual cycle to be measured accurately. Because the concentration of PdG in menstrual cycle urines excreted over 24 hours (refer section 3.3.4) was expected to be high in the luteal phase of the cycle these urine samples were expected to require some additional dilution.

To use the ELISA assay to determine the levels of PdG in menstrual cycle urines it is assumed that if a urine solution with unknown PdG levels is processed in exactly the same way as the monitor PdG standards, in setting up the ELISA plate, and an aliquot of the unknown solution reads at the same absorbance as for the one of the PdG standards both the PdG standard and the unknown sample contain the same concentration of PdG.

On this basis the menstrual cycle urine samples were diluted by 1/50 to be the same as for the monitor PdG standards in the construction of the optimized PdG standard curve (refer section 3.3.4). The same optimized PdG antibody dilution (1/10,000), and PdG-HRP conjugate dilution (1/10,000) were also used. The PdG-HRP conjugate (300 µl) and PdG standard (10 µl) were in an incubation mixture volume of 450 µl. There was always a PdG standard curve on the same ELISA plate as the menstrual cycle urine samples. This means, therefore, that any variation of the urine sample volume from that used in construction of the PdG standard in the incubation mixture, requires a dilution factor to be used to correct the values read from the PdG standard curve for the differences in urine volume.

3.3.6.1 Subject 021 R, Menstrual Cycle 6.

As an example, menstrual cycle urines (refer section 3.2.5) from subject 021R (cycle 6) from the WHO study (#90905) of the Ovarian Monitor were used to determine daily PdG levels over a 27 day cycle. Following the ELISA protocol (refer section 3.2.6.5) the data were extrapolated from the PdG standard curve (refer section 3.2.6.7). The cyclic pattern generated by this procedure clearly showed all of the salient points expected for a PdG menstrual cycle profile (refer section 1.1.4.5). The (post) ovulatory rise above 6.3 µmoles/24 h occurred on day 15 (see figure 3.17), and as demonstrated elsewhere (refer section 2.3.6) the E1-3G peak day for this menstrual cycle (021R-6) also occurred on day 15. The absolute PdG value for day 15 was 6.76 µmoles/24 h which exceeded the cut-off value (refer section 1.1.4.5) of 6.3 µmoles/24 h and indicated the end of the fertile phase (Blackwell *et al.*, 1998). By day 17 an absolute PdG value of 8 µmoles/24 h was attained and the PdG levels increased with the establishment of the corpus luteum (refer section 1.1.3) absolute PdG values of 18 µmoles/24 h being reached on cycle day 24. These absolute PdG levels fell well within the sensitive working range of the optimized PdG standard curve (refer section 3.3.4). The same pattern and amounts of PdG were consistent over all five repeat ELISA plate runs. There was very little difference between the absorbance of the microwells containing the blank urine and those containing the zero standard (refer section 3.3.4), and therefore no significant evidence of a urine effect (refer section 3.3.5.4). In a small percentage of cycles 4% (Blackwell *et al.*, 1998) the threshold value is reached on the day of the E1-3G peak. Thus this cycle would fall within the normal range of behaviour for normal menstrual cycles. The 1 in 50 diluted menstrual cycle urines were thus suitable to measure urinary PdG levels from the optimized PdG standard curve (refer section 3.3.4).

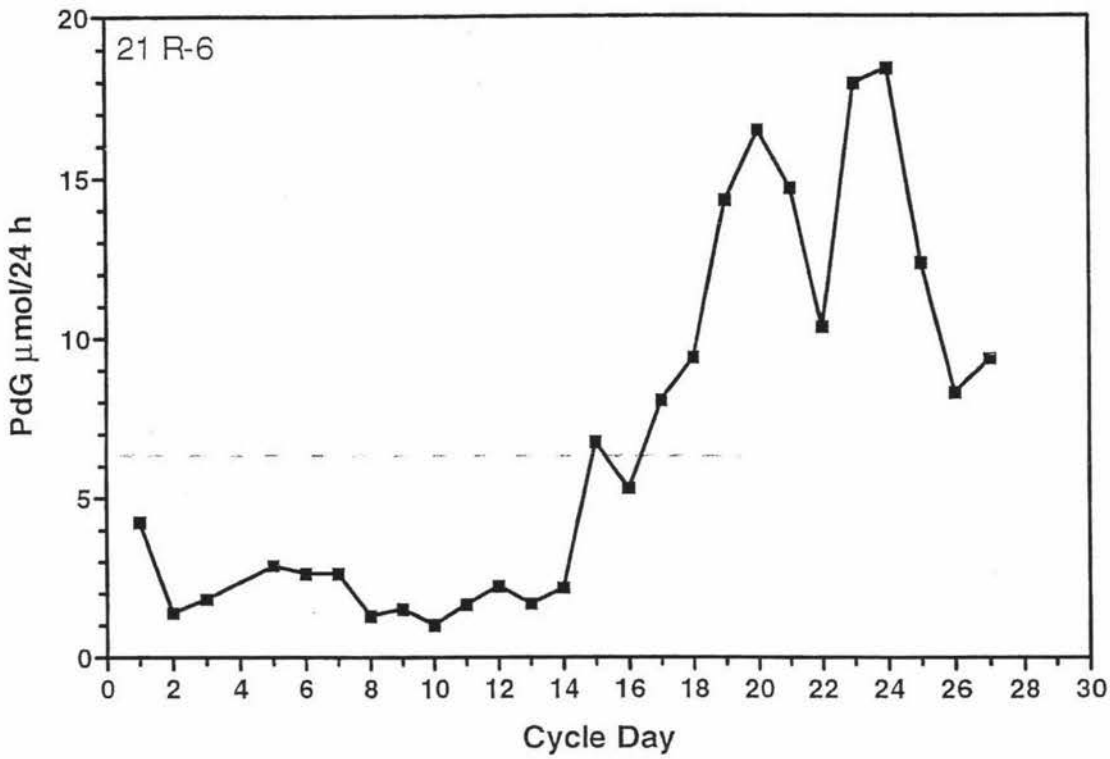

Figure 3.17: Menstrual cycle urines from subject 21R (cycle 6) from the WHO study (#90905). Cycle days (n=27) plotted against absolute PdG levels obtained using the ELISA assay. The horizontal dotted lines define the PdG cut-off level of 6.3 µmoles per 24 hours. (10 µl of a 1/50 dilution of urine sample in a total volume of 450 µl; PdG-HRP 300 µl, 1/10,000 dilution; PdG antiserum dilution 1/10,000)

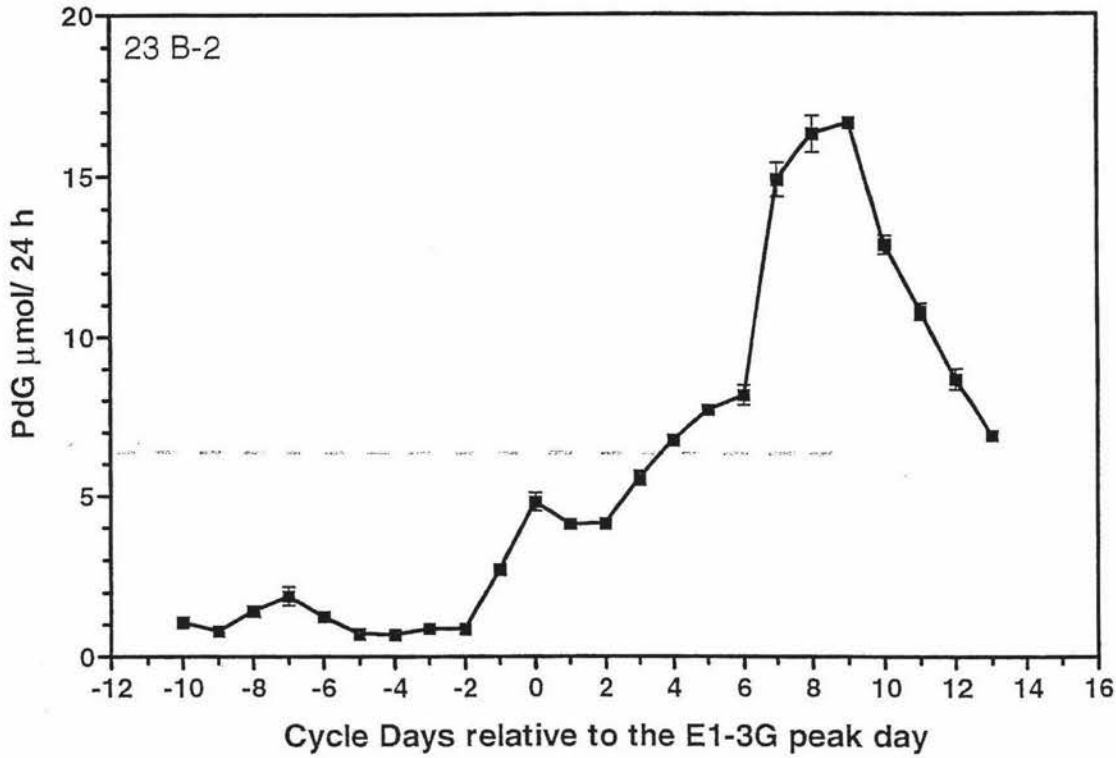

Figure 3.18: Menstrual cycle two from subject 23 B of the WHO study (#90905). The effect of 1 µl of urine sample in a total volume of 1.35 mls, and a PdG antiserum dilution of 1/2,500 on the PdG levels obtained using the ELISA assay. (PdG-HRP 300 µl, 1/10,000 dilution; PdG antiserum dilution 1/2,500) The horizontal dotted line defines the PdG threshold level.

3.3.6.2 *Subject 023 B, Menstrual Cycle 2.*

Using menstrual cycle 2 from subject 023B of the WHO study an attempt was made to avoid the pre-dilution step (1/50) by reducing the amount of urine sample (1 µl) and increasing the incubation mixture volume (1.35 mls). A reduced PdG-antiserum dilution (1/2,500) to compensate for the more concentrated urine sample was used.

The pre-determined PdG threshold value was exceeded (6.8 µmoles/24 h) on day +4 after the E1-3G peak day (refer figure 3.18). These results were in contrast to results established by both ELISA and RIA methods (WHO study on the use of the Ovarian Monitor as a fertility self test in the home) where the threshold value of 6.3 µmoles/24 h which marks the end of the potentially fertile phase (Blackwell *et al.*, 1998), was exceeded on day +6 after the E1-3G peak day. However the menstrual cycle urine volume of 1 µl in an incubation volume of 1.35 mls was suitable to measure urinary PdG levels from the optimized PdG standard curve, although in absolute terms the PdG levels were higher than those obtained when the urine samples are prediluted (1/50).

3.3.6.3 Monitoring the Performance of the PdG Assay

During the initial experiments using menstrual cycle urines six different urine samples were selected and used to monitor the performance of the PdG assay. The 12 repeats of each of the six urine samples using the chosen urine dilution of 1 in 50 replicated well, judging by the averaged coefficient of variation (C.V.) of 8.28% for the quality control specimens (1 to 5) and hence showed excellent precision. The quality control specimen containing the very low PdG level (of 1.49 µmol/24 h) gave a higher C.V. of 28% as expected (Table 3.8, and figure 3.20).

Repeats (12) of each of the six selected urine samples using the lower urine volumes (1 µl) in a higher incubation mixture volume (1.35 mls) replicated well with an averaged C.V. for all urine specimens (1 to 6) of 9.8% (Table 3.8 and figure 3.20). Although the absolute PdG levels were higher (by 0.41 µmol/24 h for the lower PdG levels and 2-3 µmol/24 h for the higher PdG levels) using the lower urine volume (1 µl) than those using a urine dilution of 1 in 50, the PdG values obtained were very similar and the S.D.s were small overall.

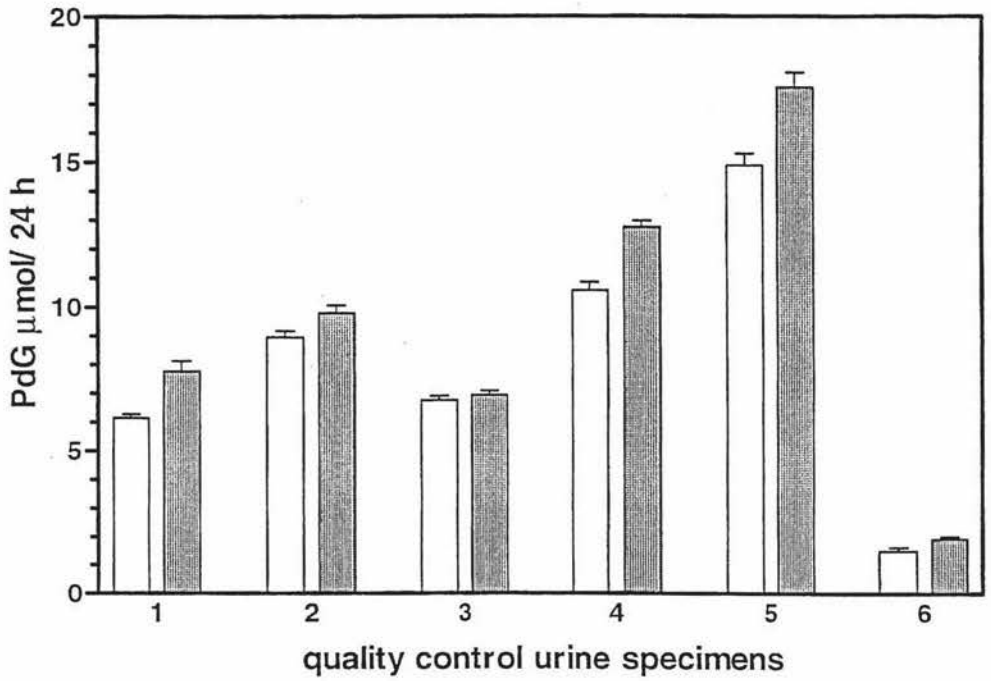

Figure 3.19: Twelve repeats of six different urine samples from the WHO study (#90905) were used to monitor the performance of the PdG ELISA assay(s). ▭ 10 µl of a 1/50 dilution of urine sample in a total volume of 450 µl; PdG antiserum dilution of 1/10,000. ▭ 1 µl of urine sample in a total volume of 1.35 mls; PdG antiserum dilution of 1/2,500. (PdG-HRP 300 µl, 1/10,000 dilution)

Thus the PdG assay is showing an excellent performance using different conditions (a demonstration of the how robust the assay is), and furthermore the results obtained for the assays are reliable and show excellent precision.

Table 3.8: The Means (n=12), Standard Deviations (S.D.) and Coefficient of Variation (C.V) from Six Different WHO Urine Samples Used to Monitor the Performance of the PdG Assay(s).

Prediluted (1/50) urine samples (10 µl of urine in 450 µl)		Smaller urine samples 1 µl of urine in 1.35 mls	
µmol/24 h Mean ± S.D.	C.V. (%)	µmol/24 h Mean ± S.D.	C.V. (%)
6 ± 0.49	8	7.78 ± 1.16	14.9
8.95 ± 0.74	8.2	9.8 ± 0.84	8.6
6.75 ± 0.52	7.7	6.94 ± 0.48	6.9
10.58 ± 0.92	8.6	12.76 ± 0.68	5.3
14.9 ± 1.34	8.9	17.58 ± 1.69	9.6
1.49 ± 0.42	28	1.9 ± 0.26	13.7

3.3.7 Conclusion

Although the smaller urine sample volume (1 µl) in an incubation volume of 1.35 mls is just as good as the pre-diluted (1/50) urine samples, in view of the impractical nature of the undiluted urine sample volume (1 µl) and the cumbersome task of increasing the incubation mixture, the original optimized pre-diluted (1/50) assay seems to be the better option for routine practice, and acceptable for measuring PdG from the optimized PdG standard curve.

Chapter Four: Validation of the E1-3G and PdG ELISA Assays

4.1 Introduction

The final stage in the validation of the E1-3G ELISA and the PdG ELISA reference assays is to compare the clinical results obtained with them against well established and independent reference assays such as the Ovarian Monitor and the WHO reference Radioimmunoassay (RIA) carried out by the Hammersmith Hospital in London. This is a necessary procedure since ultimately it is performance in clinical situations with actual urine samples which determine the usefulness of any assay.

A Special Programme of Research, Development, and Research Training in Human Reproduction of the World Health Organisation (WHO), conducted a study (Project #90905) on the Ovarian Monitor between 1993 and 1994. At the WHO laboratory in London, Hammersmith Hospital's reference centre for steroid assays used radioimmunoassay (RIA) as a reference against which to compare and validate the Ovarian Monitor. The results obtained by the two methods agreed closely, in the patterns of hormone found and most importantly in their ability to identify the periods of potential fertility and infertility during the menstrual cycle. The urine specimens used in the analysis at the reference centre were used in the present work to compare and validate the PdG ELISA. The E1-3G ELISA was compared and validated directly with the Ovarian Monitor results obtained in the laboratory and by women themselves at home. As discussed in the Ovarian Monitor section 1.1.5, the Ovarian Monitor had been originally validated successfully against extremely accurate chemical techniques in the laboratory, i.e. the total urinary estrogen method of Brown *et al.*, (1968) was used to validate the E1-3G levels obtained using the monitor, and the method of Barrett & Brown (1970) was used to validate the PdG levels obtained using the monitor.

Application of the newly developed assays to clinical studies, such as the monitoring of cycles during the menopause or perimenopause phases, provides further validation of the usefulness of the ELISAs. Menopause is the time at which cyclic ovarian function as manifested by menstruation ceases, and is associated with very low concentrations of circulating oestrogens (Gow *et al.*, 1994). Many hormonal changes occur in the "perimenopausal period". Regular menstrual cycles may continue up to the menopause

(Papanicolaou *et al.*, 1969), however, the cycles may become shorter, due to a shortened follicular phase, with increased FSH and decreased oestradiol and progesterone levels in comparison to normal ovulatory cycles. Cycles may become quite variable in length, with some being ovulatory and others being anovulatory (Brown *et al.*, 1979; Santoro *et al.*, 1996; Gilardi *et al.*, 1997). Such changes may be due to decreasing ovarian follicular activity, but a few viable oocytes have been observed in the ovaries of postmenopausal women (Berkow, 1987). As final proof of the clinical utility of the new assays a longitudinal perimenopausal clinical study of E1-3G and PdG excretion levels was carried out as a means of gaining information about the changing hormonal dynamics in a human female during this important transitional period.

4.2 Materials and Methods

4.2.1 Urine Samples

A World Health Organisation (WHO) study on the Ovarian Monitor (Project #90905) was carried out between 1993 and 1994. The WHO reference centre for steroid assays at Hammersmith Hospital, London, used radioimmunoassay (RIA) to validate the Ovarian Monitor by comparing the E1-3G and PdG levels obtained using both assay methods. As part of this independent multicentre clinical study, twenty Palmerston North women contributed timed urine specimens diluted to the equivalent of 150 ml per hour of collection. Fortunately, these sample cycles were available from the Palmerston North centre to enable clinical studies to be carried out to validate the PdG ELISA assays.

4.3 Results and Discussion

To validate the performance of the ELISA's it was necessary to calibrate the hormonal results obtained with them against those obtained with a proven reference assay used to measure urinary E1-3G and PdG.

4.3.1 Comparison of E1-3G ELISA with Ovarian Monitor Data

4.3.1.1 *Subject 21 R, Menstrual Cycle 6.*

The daily E1-3G values from a menstrual cycle (No.6), from subject 21R of the WHO study #90905 was recorded by the woman herself at home using the Ovarian Monitor (figure 4.1), from the beginning of menses until the mid-cycle E1-3G peak was recognised. The E1-3G peak is always identified on the basis that the "E1-3G peak" is associated with the rise in PdG to exceed the ΔT cut-off PdG value (6.3 μmoles/24 h) for the batch of tubes being used, irrespective of whether the highest rates of E1-3G excretion for the cycle

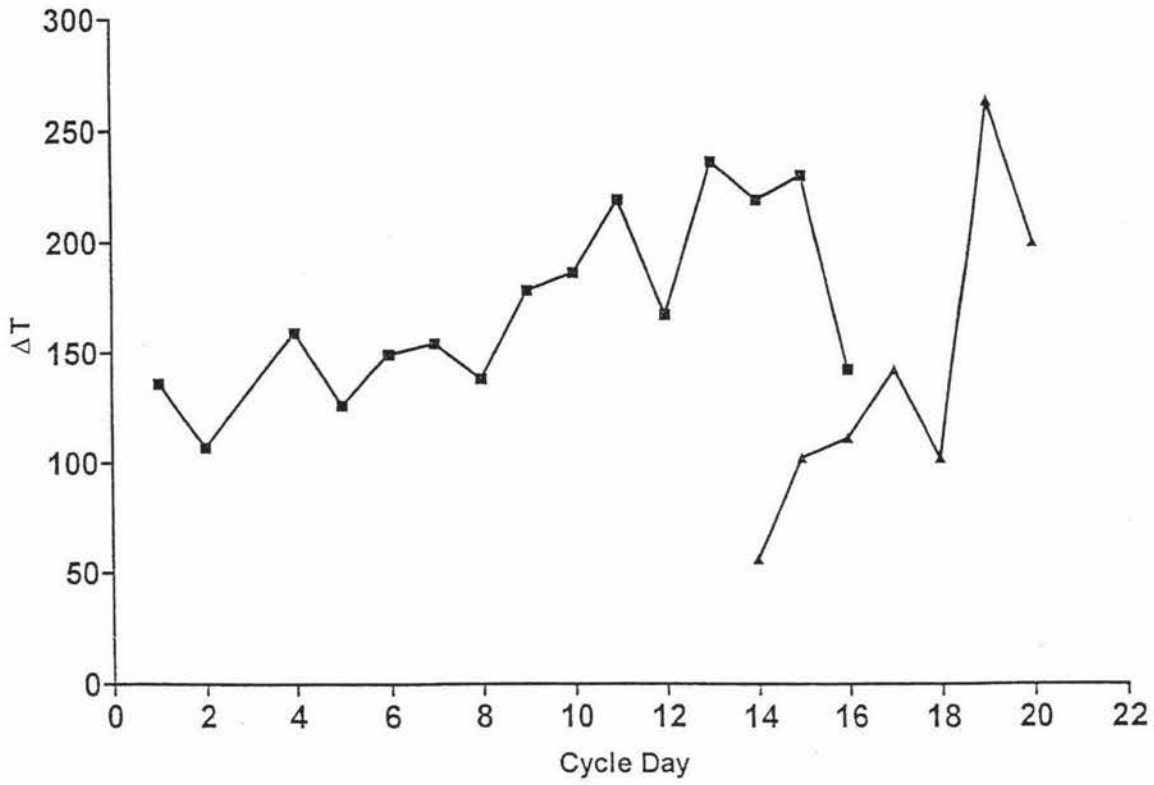

Figure 4.1: E1-3G levels (—■—) for cycle days 1 to 16, and PdG levels (—▲—) for cycle days 14 to 20, from menstrual cycle 6, from subject 21R of the WHO study #90905, recorded by the woman herself at home using the Ovarian Monitor.

occurred on the E1-3G peak day. In this cycle (21R-6) the E1-3G peak day was clearly day 15 for the tubes used to obtain the data shown in figure 4.1. There was a fluctuation in E1-3G values between a $\Delta T/20$ minutes of 100 to 150 fromdays 1 to 7, constituting the oestrogen baseline and corresponding to the basic infertile pattern of the cervical mucus. On day 9 there was a small but significant increase in the ΔT value suggesting that a follicle had entered its rapid growth phase and hence the potentially fertile phase of the menstrual cycle had begun. The rise continued until day 15 when there was an abrupt fall in the rate of E1-3G excretion. To confirm that this was due to ovulation the test for PdG was then carried out from days 14 to 20 and a large rise to exceed the threshold value was seen on day 19. The fact that the threshold value was exceeded showed that fertility was ended for that cycle and in agreement with this the next menstrual bleed occurred on day 26 giving a luteal phase of ten days if counted from day 15, and eleven days if counted from cycle day 14. Since eleven days is the minimum luteal phase length for a fertile cycle it is likely that the E1-3G peak was in fact day 14 or even day 13. All the salient points are clear, the E1-3G baseline during the follicular phase, the rise from baseline and the E1-3G peak on day 14 and 15 followed by a decrease in the E1-3G excretion rate.

The same urine samples were used to measure the E1-3G levels using the ELISA assay for E1-3G developed in this thesis and the results are given in figure 4.2. The E1-3G peak value occurred on day 14 when the E1-3G level was 85.6 nmoles/24 h with a small drop on day 15 (77.9 nmoles/24 h), followed by a rapid decline in the E1-3G excretion rate thereafter. Using the ELISA assay the E1-3G rise from baseline occurred clearly on day 11 when the E1-3G excretion was 19 nmoles/24 h compared with day 9 using the Ovarian Monitor (figure 4.1). Thus there was very little difference between the two sets of data from a clinical point of view with the ELISA results giving the first rise day two days earlier and the E1-3G peak day one day earlier than with the monitor. However, the pattern was much clearer with the ELISA results since the baseline E1-3G values were significantly lower in comparison with the E1-3G peak values as compared with the monitor data. Problems were encountered with the monitor results during the WHO study as a result of high E1-3G baseline levels for some women and some batches of tubes nevertheless the information relating to fertility was similar and meaningful for both sets of data.

A correlation of the E1-3G values for menstrual cycle 6 from subject 21R obtained using the Ovarian Monitor and the ELISA assay gave a correlation coefficient (r) of 0.796

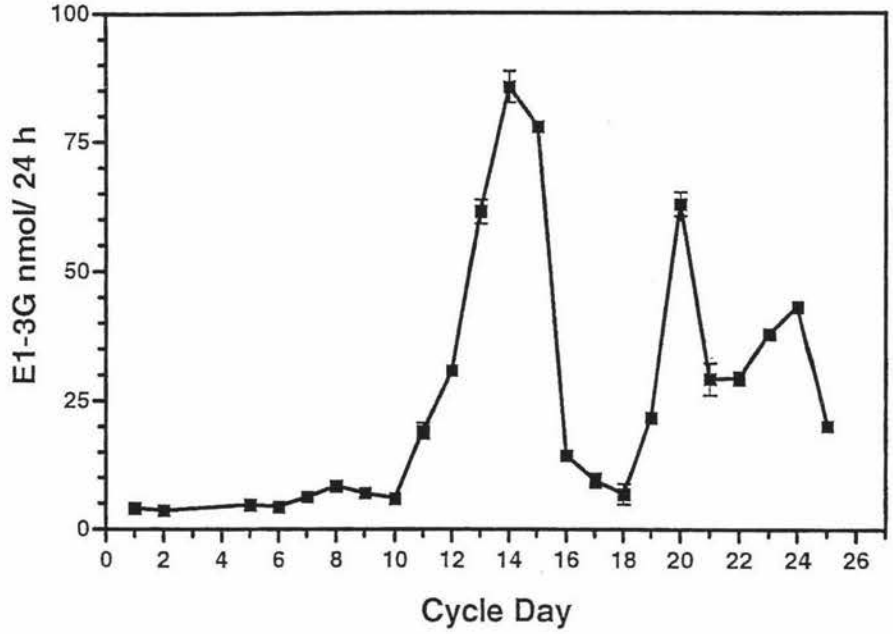

Figure 4.2: Menstrual cycle urine from the sixth cycle from subject 21R of the WHO study (#90905) used to measure E1-3G levels using the ELISA assay (10 µl of urine sample in a total volume of 450 µl). The arrow indicates the cycle day (day 11) on which E1-3G values first increased above the follicular phase E1-3G baseline levels. The highest E1-3G level occurred on cycle day 14.

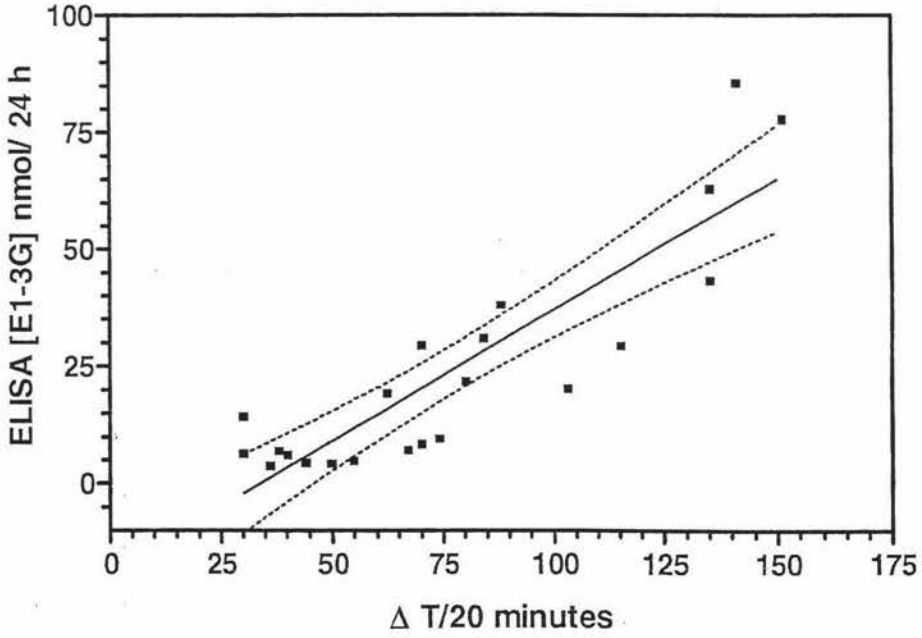

Figure 4.3: A correlation of the E1-3G levels for menstrual cycle 6 from subject 021R obtained using the Ovarian Monitor and the ELISA assay gave a correlation coefficient (r) of 0.796 and a Y intercept of -30 (r^2 = 0.63).

(figure 4.3). Although the r value appears somewhat low it is similar to the correlation coefficient obtained in many other studies involving similar correlations (Webster *et al.*, 1990; Katz & Schiffman, 1985).

An E1-3G excretion profile (figure 4.4) obtained using the ELISA assay with a higher volume of the timed urine samples (20 µl) in the incubation mixture (450 µl) showed higher absolute E1-3G levels than when the lower volume of urine sample (10 µl) was used (figure 4.2). After extrapolation from the E1-3G standard curve the raw data was divided by 2 to correct for the increased urine volume added to the assay. Such a correction may, however, introduce inaccuracy (refer section 2.3.6) as the potential for a urine interference effect increases when higher urine volumes are used in the assay (refer section 2.3.5.4 and section 2.3.6).

The E1-3G excretion profile obtained (figure 4.4) after correction, showed a double peak (on day 13 when the rate of E1-3G excretion was 115.7 nmoles/24 h) and a second on day 15 (when the E1-3G level was 97 nmoles/24 h). This was in fact similar to the double peak reported by subject 21R using the Ovarian Monitor (figure 4.1) but the effect was much more pronounced using the ELISA (figure 4.4). Repeat assessment of the peak E1-3G levels obtained with the Ovarian Monitor in the laboratory for the same urine samples from subject 21R cycle 6 for cycle days 11-16 (figure 4.5) confirmed that the E1-3G levels for cycle days 14 and 15 were probably identical within experimental error, which one being identified as the peak day depending on the pair of assay tubes used.

4.3.1.2 Combined E1-3G and PdG Excretion Profiles

The E1-3G ELISA data (figure 4.2) was combined with the PdG ELISA data of menstrual cycle 6 from subject 021R and is shown in figure 4.6(a). The resulting superimposed E1-3G and PdG excretion profiles of this menstrual cycle (21R-6) show the PdG threshold level (6.3 µmoles/24 h) being attained on cycle day 15 which coincides with the E1-3G peak day. As already discussed (section 3.3.6.1) in 4% of cycles (Blackwell *et al.*, 1998) the threshold value is reached on the day of the E1-3G peak. Hence, the fertile period is completely defined lasting from cycle day 11 until day 14 giving a fertile period of four days with the most fertile day occurring on day 14 (or even day 13) which coincides with the day of the decline in the rate of E1-3G excretion shown in figure 4.6(b).

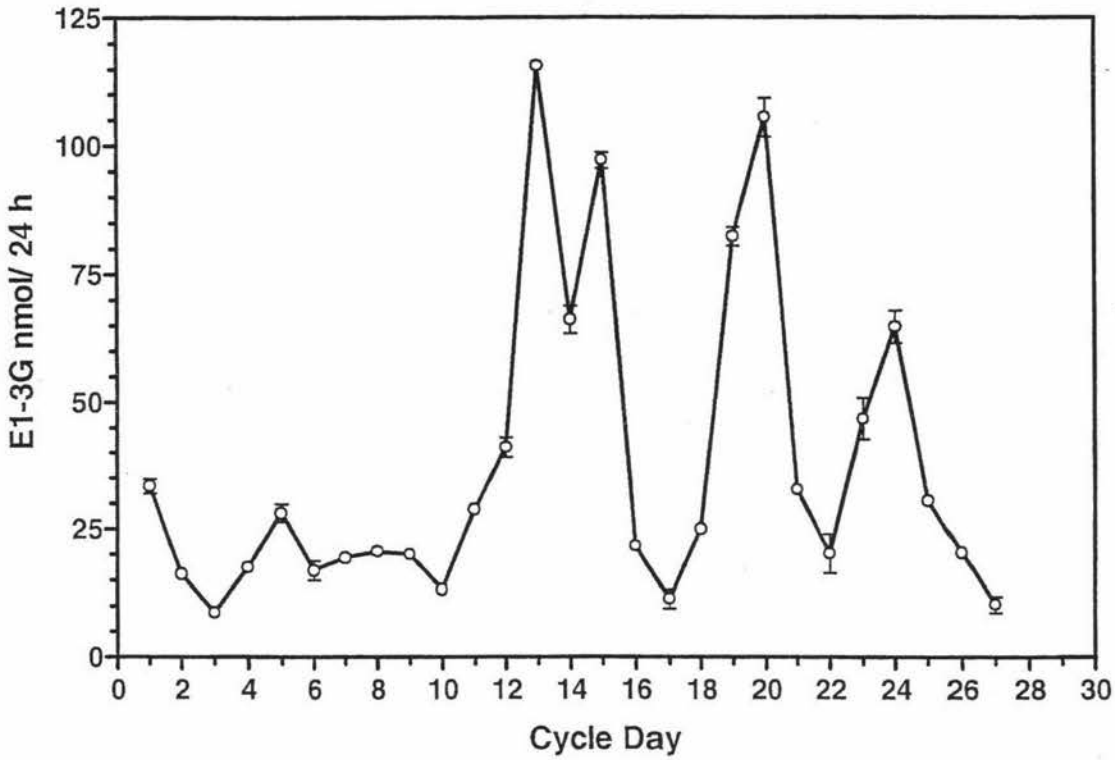

Figure 4.4: The ELISA assay was used to measure E1-3G levels in the menstrual cycle urines from subject 21 R (cycle 6) of the WHO study (#90905). An increased urine sample volume (of 20 µl in a total volume of 450 µl) was used, and the raw data was divided by two.

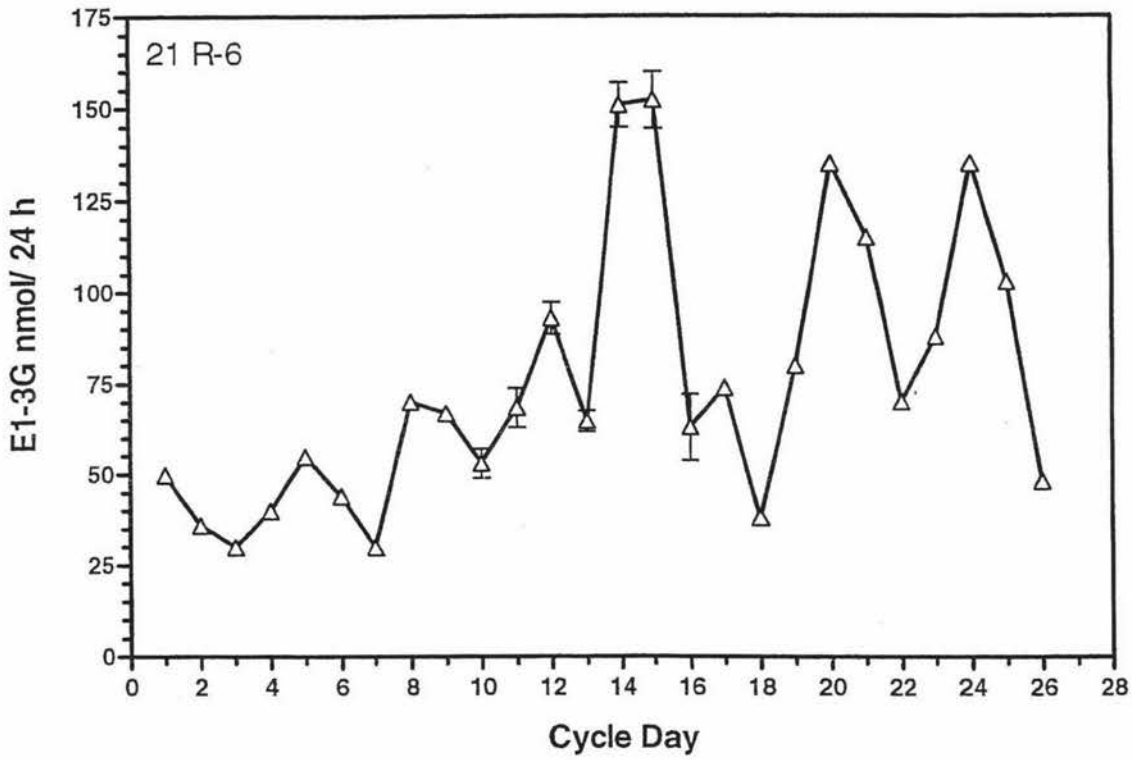

Figure 4.5: E1-3G levels for menstrual cycle urines from subject 21R (cycle 6) obtained using the Ovarian Monitor in the laboratory, with repeat measurements recorded from cycle day 11 to cycle day 16.

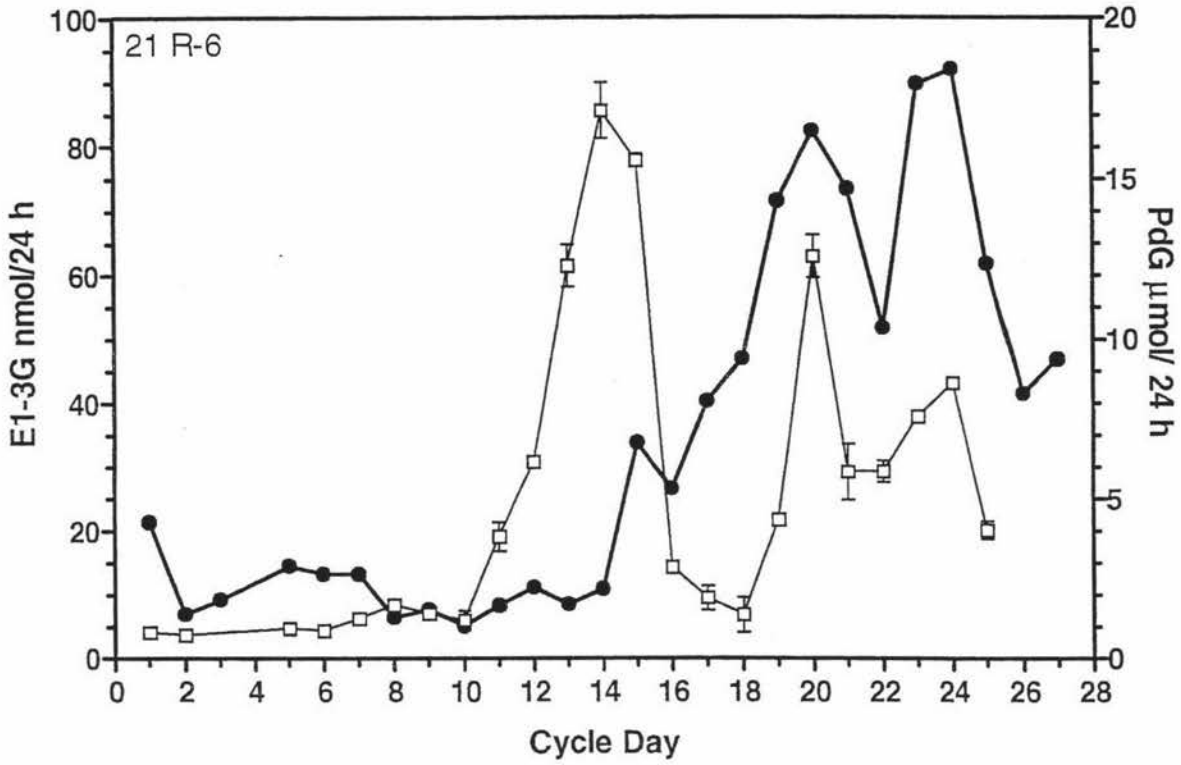

Figure 4.6 (a): E1-3G levels obtained using the ELISA assay (figure 4.2) superimposed on the PdG levels obtained using the ELISA assay. The first E1-3G rise from the E1-3G baseline occurred on cycle day 11, and the PdG threshold level of 6.3 µmol/ 24 h was exceeded by cycle day 15. Menstrual cycle urines were from the sixth cycle from subject 21R from the WHO study (#90905).

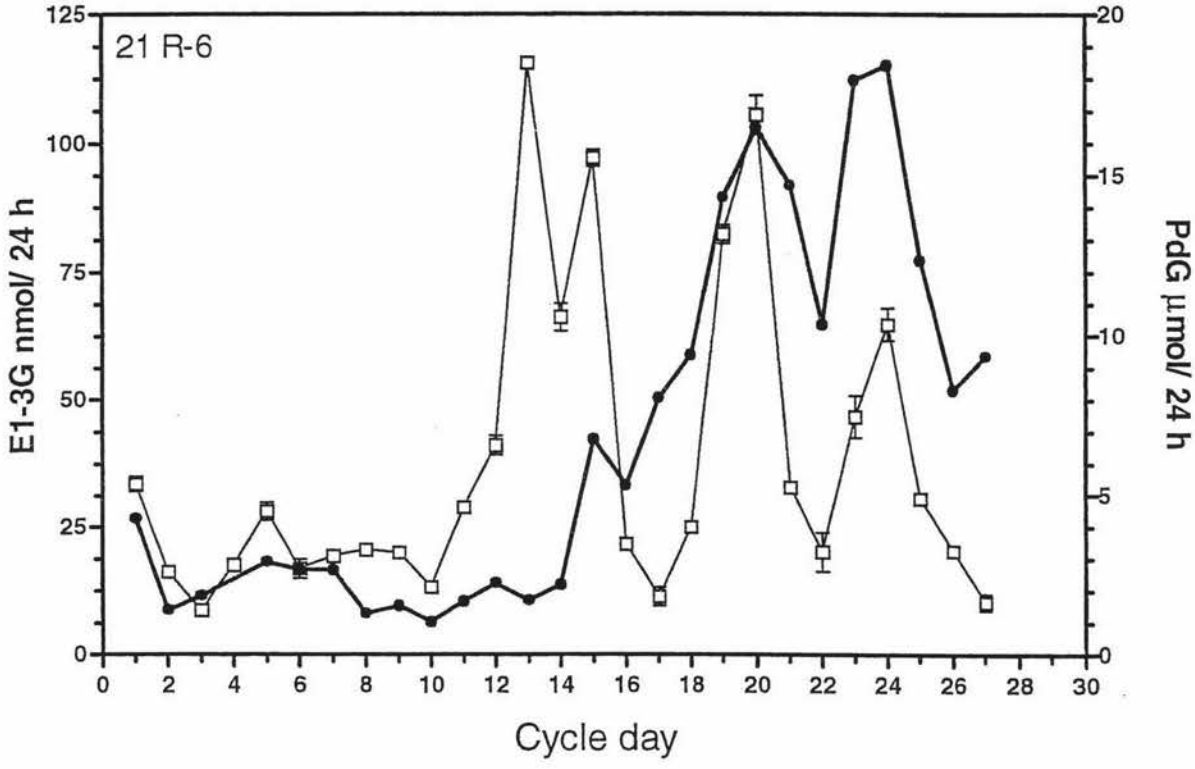

Figure 4.6 (b): E1-3G levels obtained using the ELISA assay (figure 4.4) superimposed on the PdG levels obtained using the ELISA assay. The first E1-3G rise from the E1-3G baseline occurred on cycle day 11, and the PdG threshold level of 6.3 µmol/ 24 h was exceeded by cycle day 15. Menstrual cycle urines were from the sixth cycle from subject 21R from the WHO study (#90905).

4.3.1.3 *Subject 14 X, Menstrual Cycle 5*

Menstrual cycle (No.5), from subject 14X of the WHO study #90905 was analysed in a laboratory study using the Ovarian Monitor and using the ELISA assay to compare the E1-3G levels obtained with both methods.

There was a general similarity between the pattern of the E1-3G excretion profile data obtained using the Ovarian Monitor (figure 4.7) and the ELISA data (figure 4.8). The Ovarian Monitor data exhibited somewhat noisier and higher E1-3G baseline levels during the follicular phase than did the data from the E1-3G ELISA which showed low baseline levels. The E1-3G peak day fell on day 16 using the Ovarian Monitor and on day 15 using the ELISA assay. However, high E1-3G levels also occur on day 16 using the ELISA assay, and given the likely variability between the data for days 15 and 16 the agreement is satisfactory.

The salient points are clearly visible in both sets of data i.e. the rise from the E1-3G baseline on day 12, and the E1-3G peak day on days 15 and 16 respectively, followed by the rapid decline in the rate of E1-3G excretion. The ELISA data are superior in that the baseline levels are significantly lower hence allowing easy recognition of the developing follicle from the increasing rates of E1-3G excretion. The higher baseline levels for the Ovarian Monitor data in this cycle make this more difficult and some data points should have been repeated according to the WHO study protocol but were not.

While the dynamic ranges for the ELISA assay (zero to 218 nmoles/24 h) compared to the Ovarian Monitor (44 to 232 nmoles/24 h) were similar, baseline levels of E1-3G using the ELISA assay were lower (<30 nmoles/24 h) compared to E1-3G levels (<130 nmoles/24 h) using the Ovarian Monitor.

Although the data show the ELISA E1-3G profile as having a better resolved E1-3G peak level compared to the Ovarian Monitor the same information about the beginning and end of the potential fertile period is given in both sets of data, and the E1-3G excretion profiles are recognizably similar. Hence, the ELISA is giving good clinical data and is obviously acceptable as a reference assay.

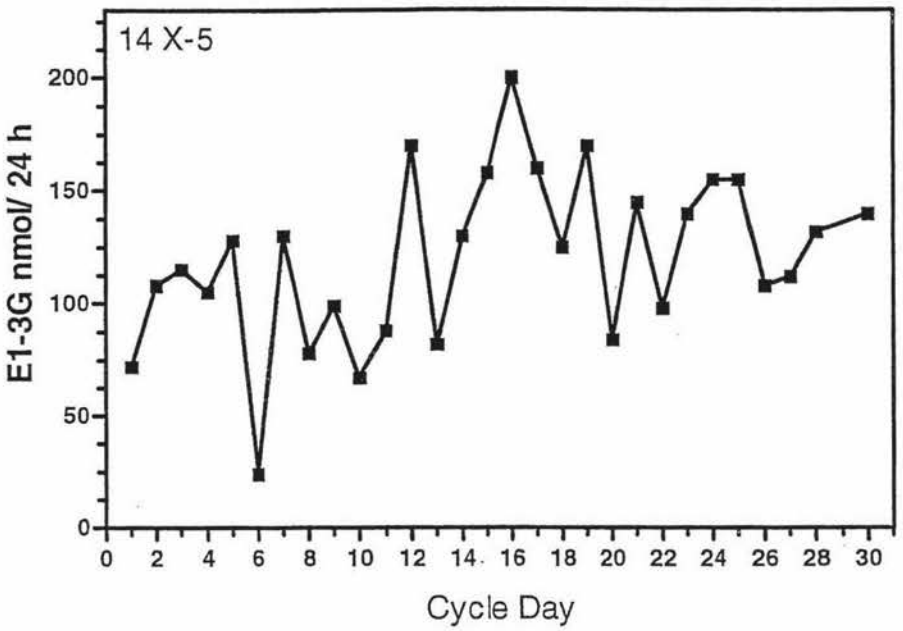

Figure 4.7: Menstrual cycle six from subject 14 X from the WHO study (#90905). E1-3G levels were obtained using the Ovarian Monitor.

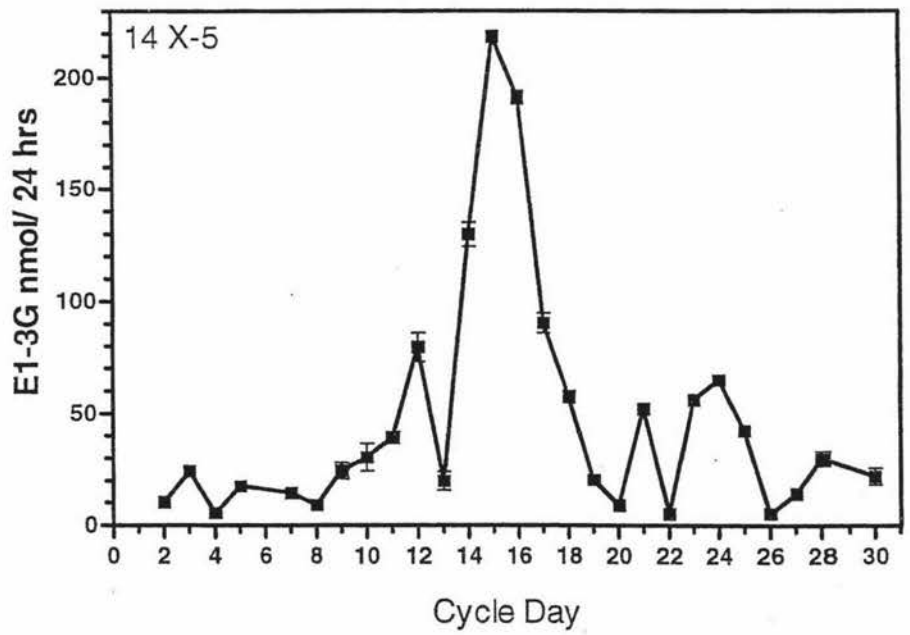

Figure 4.8: Menstrual cycle six from subject 14 X from the WHO study (#90905). E1-3G levels were obtained using the ELISA assay.

4.3.2 Comparison of PdG ELISA Data with Reference RIA Data

As a means of comparing the performance of the ELISA assay for PdG the urines from six menstrual cycles (refer section 4.2.1) from six different women from the WHO study #90905 were analysed by both ELISA and the WHO reference RIA.

The optimized PdG Standard Curve (refer section 3.3.4) and the optimized pre-diluted 1 in 50 assay (refer section 3.3.6) were used to measure the absolute PdG levels in the urines from six menstrual cycles by ELISA. Absolute PdG levels obtained using the same urine samples (refer section 4.2.1) and determined in London during the WHO study of the Ovarian Monitor using RIA (refer section 4.1) were compared with the absolute PdG levels obtained using ELISA (refer Table 4.1 and Table 4.2). After calculation of the PdG ELISA data from the PdG standard curve (refer section 3.2.6.7), both the absolute PdG values (µmoles/24 h) obtained using ELISA and those obtained using RIA were plotted against cycle days relative to the oestrogen peak day as day zero, for each individual menstrual cycle.

4.3.2.1 Subject 20 K, Menstrual Cycle 1.

Results from the first menstrual cycle of subject 20 K (figure 4.9) showed that higher PdG levels were obtained using the ELISA assay and that the PdG follicular phase baseline levels were more erratic using ELISA than using RIA, although both PdG profiles were similar. The urine sample for day +11 has probably deteriorated over the past 6 years and lost glucuronide by bacterial hydrolysis since a minimal PdG level was recorded using ELISA (0.26 µmoles/24 h) and none at all recorded using RIA. Absolute PdG levels on the day of the oestrogen peak day (0) were low using both ELISA (1.87 µmoles/24 h) and RIA (1.35 µmoles/24 h) and five days after the oestrogen peak day the PdG threshold level of 6.3 µmoles/24 h (refer section 1.1.4.5) was exceeded using both the ELISA (12.9 µmoles/24 h) and the RIA (8.4 µmoles/24 h) assays. There is, therefore, exactly the same information about the end of fertility in both ELISA and RIA data sets.

While PdG levels increased to a maximum using both assay methods by day +8 the ELISA PdG levels (19.4 µmoles/24 h) were approximately 33% greater than those obtained using RIA (12.9 µmoles/24 h). However, a comparison of the PdG levels using ELISA and using RIA show an excellent correlation coefficient (r) of 0.985 (figure 4.9; and Table 4.1).

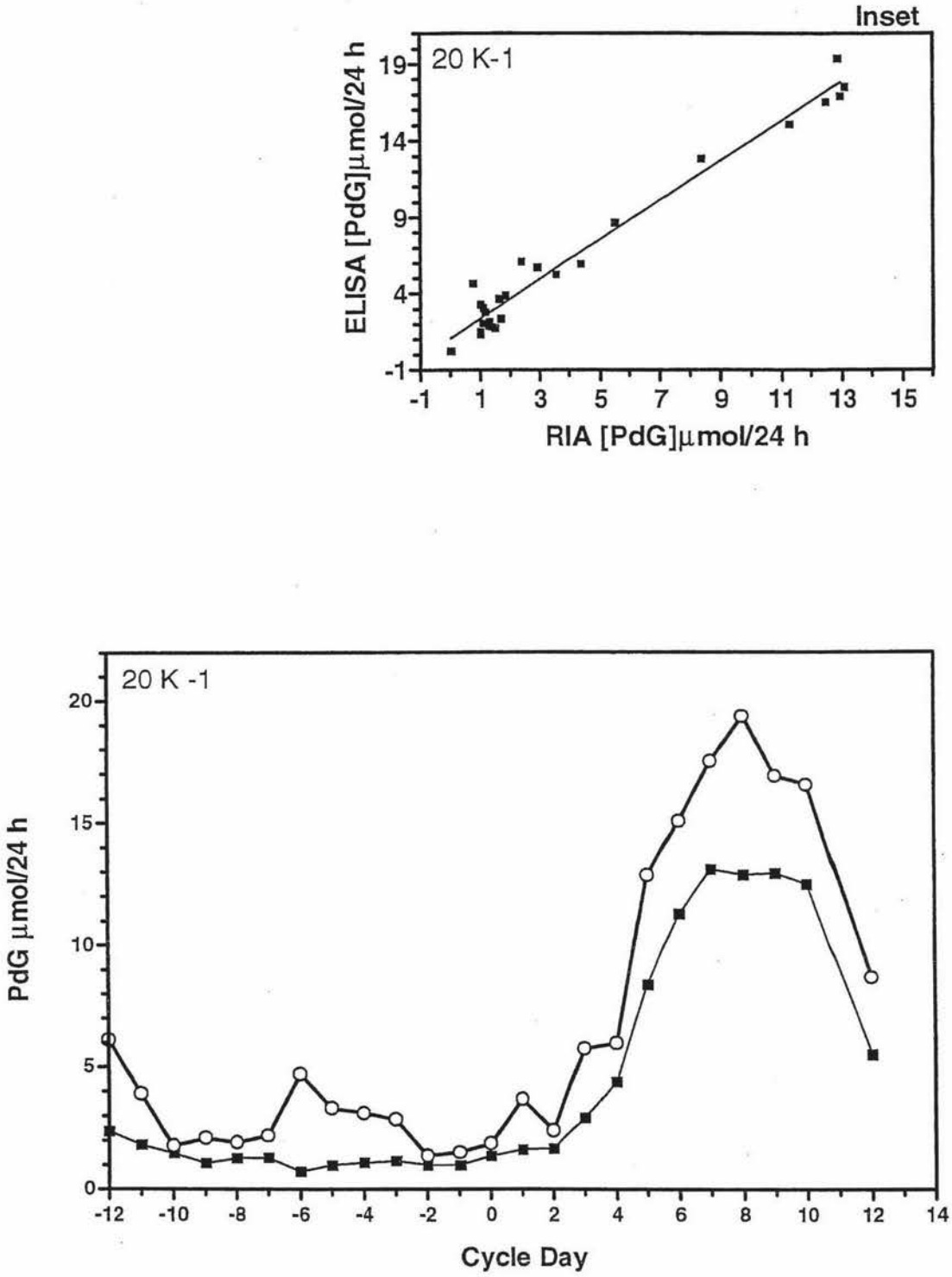

Figure 4.9: Subject 20 K, Menstrual Cycle 1: A comparison of PdG levels obtained using the ELISA assay (—o—), with PdG levels obtained using the RIA (—■—) assay method. (10 µl of a 1/50 dilution of urine sample; PdG-HRP 300 µl, dilution 1/10,000; PdG antiserum 1/10,000 dilution; 16 h; 4°C)

Inset:
A linear regression of the ELISA data against the RIA data (r=0.98)

4.3.2.2 Subject 002 F, Menstrual Cycle 2.

Results from the second menstrual cycle of subject 002 F (figure 4.10) showed very definite points of difference between the higher PdG levels obtained using the ELISA assay and the relatively smooth PdG profile obtained using the RIA data. There were cycle days when the absolute PdG levels using ELISA and RIA were very similar (Table 4.1; figure 4.10). For example, seven days before the day of the oestrogen peak day (-7) PdG levels using ELISA (1.33 µmoles/24 h) and RIA (1.19 µmoles/24 h), were similar as were the oestrogen peak days (0) where PdG levels using ELISA were 0.97 µmoles/24 h and for RIA were 1.2 µmoles/24 h. Although the PdG levels for days +5 and +8 using ELISA (6.78 µmoles/24 h; 6.6 µmoles/24 h) and RIA (6.5 µmoles/24 h; 7.3 µmoles/24 h) were similar for both assay methods, the PdG threshold value (6.3 µmoles/24 h) was reached on cycle day +3 using ELISA (6.7 µmoles/24 h) in contrast to cycle day +5 using RIA. It is possible that the PdG levels reached threshold values using both assay methods by days +5 and that the values for cycle days +1, +2 and +3 were artificially elevated using the ELISA assay resulting in a false positive on cycle day +3. However, statistical studies show that the majority of women have reached the threshold value by day +5 and hence the ELISA data may be more reliable (Blackwell *et al.*, 1998). In contrast PdG levels using RIA for this menstrual cycle (002F) were lower during the luteal phase than for the majority of other menstrual cycles studied. A comparison of the PdG levels using ELISA and using RIA give a correlation coefficient (r) of 0.74 (figure 4.10; and Table 4.1) again showing that the patterns were identical within experimental error.

4.3.2.3 Subject 23 B, Menstrual Cycle 2.

Results from the second menstrual cycle of subject 23 B gave excellent agreement between the PdG levels obtained using the PdG ELISA assay and RIA and the PdG profiles (figure 4.11) were almost identical. A pre-ovulatory nadir in PdG levels was seen in approximately 40% of cycles in the data base studied by Blackwell *et al.*, (1998), and figure 4.11 shows that such a nadir occurred on day -4 of this cycle. Menstrual cycle (23B-2) is a good example of why a threshold PdG value is required to mark the end of fertility (Blackwell *et al.*, 1998), because the PdG rise on day -1 begins before ovulation (the day following the E1-3G peak day). It was a slow rise and the threshold was not exceeded until six days after the day of the oestrogen peak using both the ELISA (6.65 µmoles/24 h) and the RIA data (7.4 µmoles/24 h). This occurs in a small percentage of women (Blackwell *et al.*, 1998). In fact follicular phase PdG baseline levels were extremely low using the ELISA assay (< 0.56 µmoles/24 h) until two days before

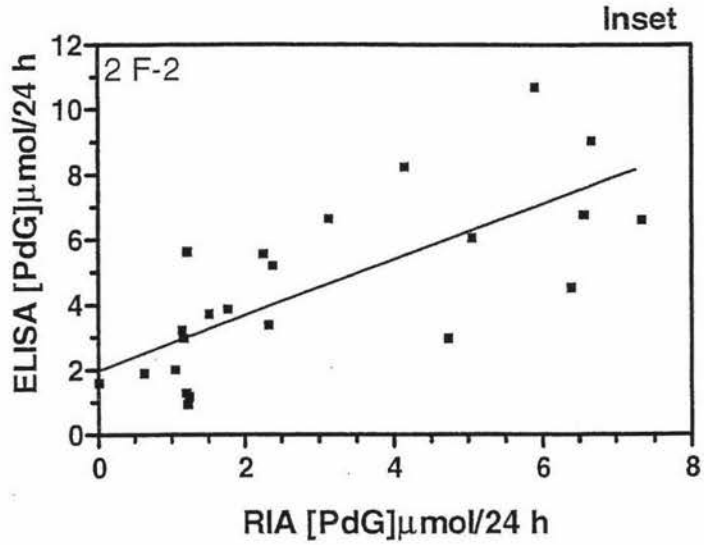

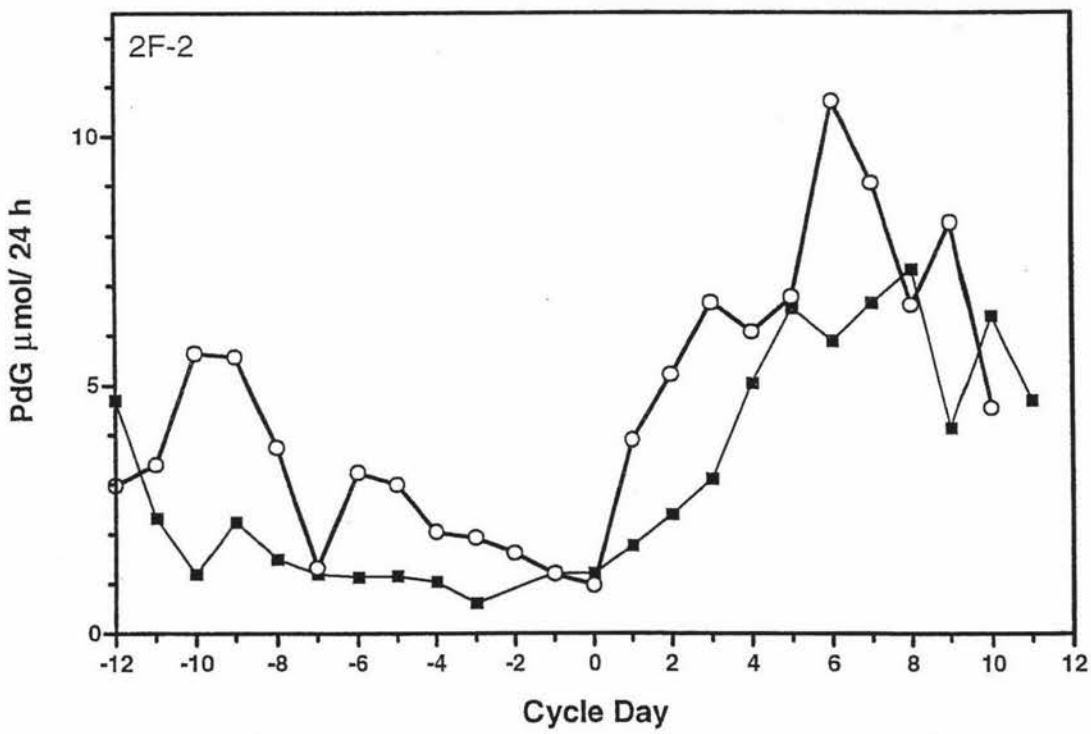

Figure 4.10: Subject 2 F, Menstrual Cycle 2: A comparison of PdG levels obtained using the ELISA assay (—o—), with PdG levels obtained using the RIA (—■—) assay method. (10 µl of a 1/50 dilution of urine sample; PdG-HRP 300 µl, dilution 1/10,000; PdG antiserum 1/10,000 dilution; 16 h; 4°C)

Inset:
A linear regression of the ELISA data against the RIA data (r=0.74)

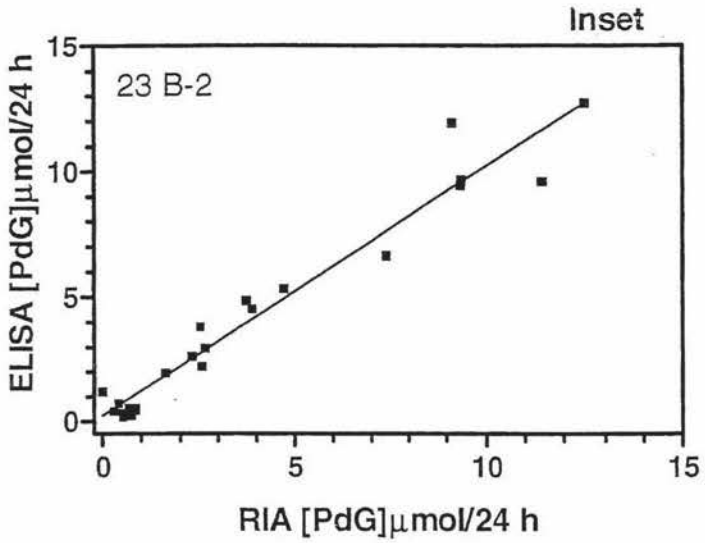

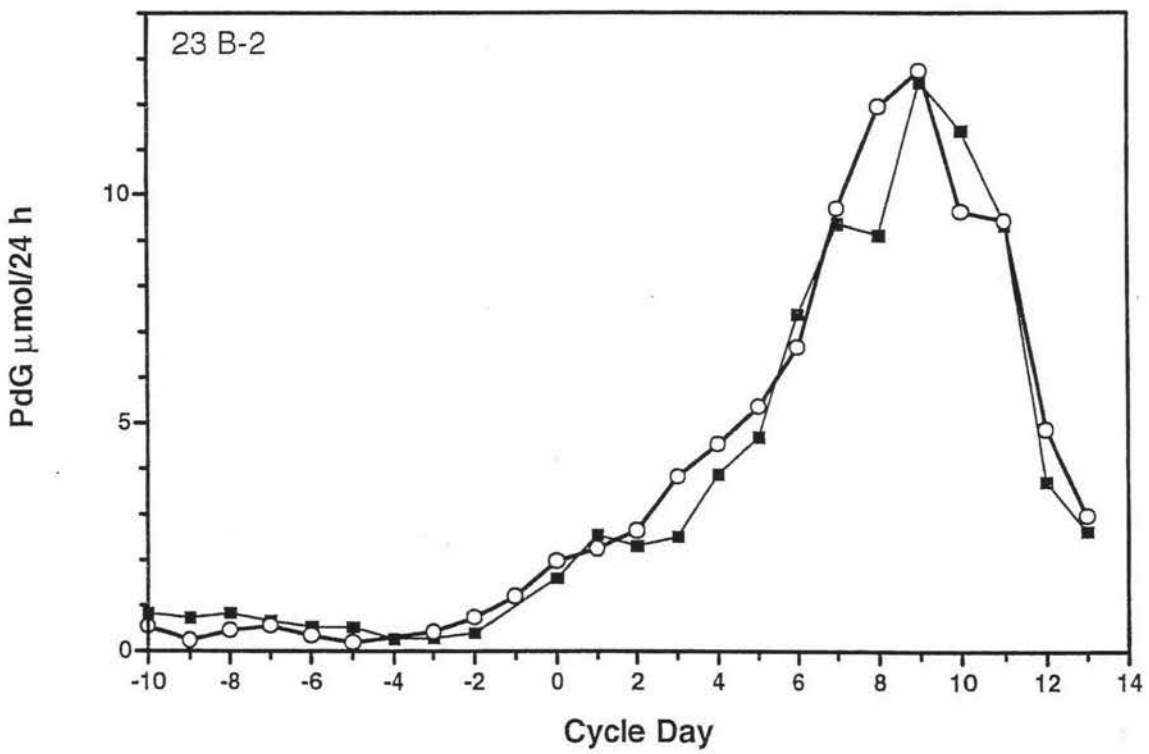

Figure 4.11: Subject 23 B, Menstrual Cycle 2: A comparison of PdG levels obtained using the ELISA assay (—o—), with PdG levels obtained using the RIA (—■—) assay method. (10 µl of a 1/50 dilution of urine sample; PdG-HRP 300 µl, dilution 1/10,000; PdG antiserum 1/10,000 dilution; 16 h; 4°C)

Inset:
A linear regression of the ELISA data against the RIA data (r=0.97)

ovulation (0.73 µmoles/24 h) when they began to increase to the day of the oestrogen peak (1.97 µmoles/24 h) and continued as threshold PdG levels were exceeded and the corpus luteum was established. The highest PdG levels during the luteal phase using ELISA (12.7 µmoles/24 h) and RIA (12.5 µmoles/24 h) occurred on cycle day +9, followed by a bleed on cycle day +12 as the PdG levels rapidly declined. Therefore, exactly the same information about the end of fertility was given by both ELISA and RIA data sets in both relative and absolute terms (figure 4.11; and Table 4.1). A comparison of the PdG levels using ELISA and RIA showed a high correlation coefficient (r = 0.97).

Table 4.1: Comparison of PdG ELISA with (WHO) RIA PdG Values; Relative to the Oestrogen Peak Day as Zero.

Cycle Day	Menstrual Cycle 1 Subject 020 K		Menstrual Cycle 2 Subject 002 F		Menstrual Cycle 2 Subject 023 B	
	ELISA	RIA	ELISA	RIA	ELISA	RIA
-13	5.25	3.55	-	-	-	-
-12	6.1	3.37	2.98	4.7	-	-
-11	3.89	1.82	3.4	2.3	-	-
-10	1.77	1.48	5.6	1.2	0.54	0.84
- 9	2.09	1.07	5.58	2.25	0.24	0.73
- 8	1.9	1.27	3.7	1.5	0.46	0.83
- 7	2.2	1.29	1.32	1.19	0.56	0.67
- 6	4.7	0.73	3.24	1.14	0.34	0.53
- 5	3.29	0.99	2.99	1.16	0.19	0.53
- 4	3.09	1.09	2.03	1.04	0	0.27
- 3	2.83	1.14	1.9	0.62	0.43	0.29
- 2	1.37	0.99	1.62	0	0.74	0.4
- 1	1.5	0.99	1.2	1.23	1.21	0
0	1.87	1.35	0.97	1.21	1.97	1.6
1	3.67	1.62	3.89	1.76	2.24	2.55
2	2.4	1.7	5.2	2.38	2.64	2.29
3	5.7	2.9	6.66	3.12	3.8	2.5
4	5.95	4.37	6.07	5.04	4.5	3.89
5	12.85	8.37	6.77	6.55	5.35	4.69

6	15.1	11.25	10.7	5.89	6.65	7.39
7	17.5	13.1	9.05	6.65	9.68	9.35
8	19.35	12.87	6.6	7.32	11.9	9.12
9	16.9	12.95	8.26	4.14	12.73	12.48
10	16.54	12.49	4.54	6.39	9.62	11.4
11	0.26	0	0	6.39	9.4	9.34
12	8.66	5.5	0	4.71	4.87	3.37
12	-	-	-	-	2.97	2.64

4.3.2.4 Subject 009 D, Menstrual Cycle 2.

Results from the second menstrual cycle of subject 009 D gave a different pattern. The PdG levels obtained using the ELISA assay were consistently higher than the PdG levels obtained using RIA (Table 4.2) in an almost parallel fashion (figure 4.12). The PdG cut off value (6.3 µmoles/24 h) was exceeded four days after the day of the oestrogen peak using both the ELISA (9.9 µmoles/24 h) and RIA (6.4 µmoles/24 h), and therefore both assay methods provided the same information about the end of fertility. Even the spiky luteal phase patterns mimicked each other perfectly, particularly cycle days +7, +8, +9 and +10 where the PdG levels using RIA were 70% of the PdG levels obtained from the ELISA assay, and were the highest PdG levels obtained during the luteal phase. PdG excretion declined rapidly on cycle day +6 and could indicate an imminent menstrual bleed, but that in fact did not occur for a further 11 days. The almost parallel relationship between the two sets of data is well illustrated by the comparison of the PdG levels which showed a good correlation with a coefficient (r) of 0.98 (Figure 4.12; and Table 4.2).

4.3.2.5 Subject 014 X, Menstrual Cycle 1.

The results from the first menstrual cycle of subject 14X showed extremely high PdG levels using the ELISA assay on cycle day +9 (26.2 µmoles/24 h) and +10 (33.3 µmoles/24 h) compared to the corresponding PdG levels obtained using RIA (11.1 µmoles/24 h and 15.9 µmoles/24 h respectively). Apart from the high PdG levels during the luteal phase the patterns were generally similar for the two methods and again the same information about the end of fertility was given (figure 4.13; and Table 4.2), as the PdG threshold level was exceeded by both assay systems three days after the day of the oestrogen peak, (7.7 µmoles/24 h by ELISA and only 6.9 µmoles/24 h by RIA). A correlation between the ELISA assay and the RIA data gave a good coefficient (r = 0.87).

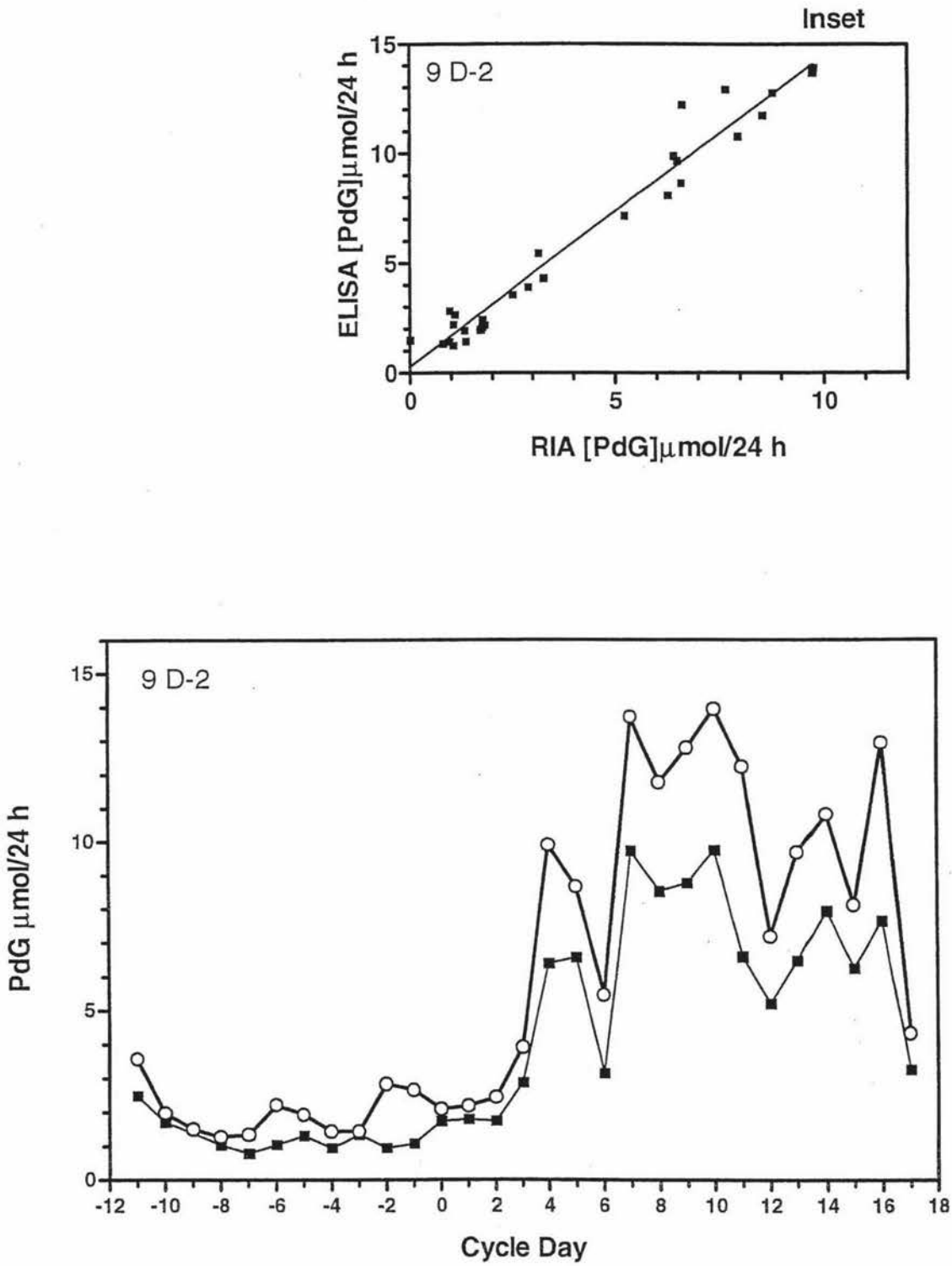

Figure 4.12: Subject 9 D, Menstrual Cycle 2: A comparison of PdG levels obtained using the ELISA assay (—○—), with PdG levels obtained using the RIA (—■—) assay method. (10 µl of a 1/50 dilution of urine sample; PdG-HRP 300 µl, dilution 1/10,000; PdG antiserum 1/10,000 dilution; 16 h; 4°C)

Inset:
A linear regression of the ELISA data against the RIA data (r=0.98).

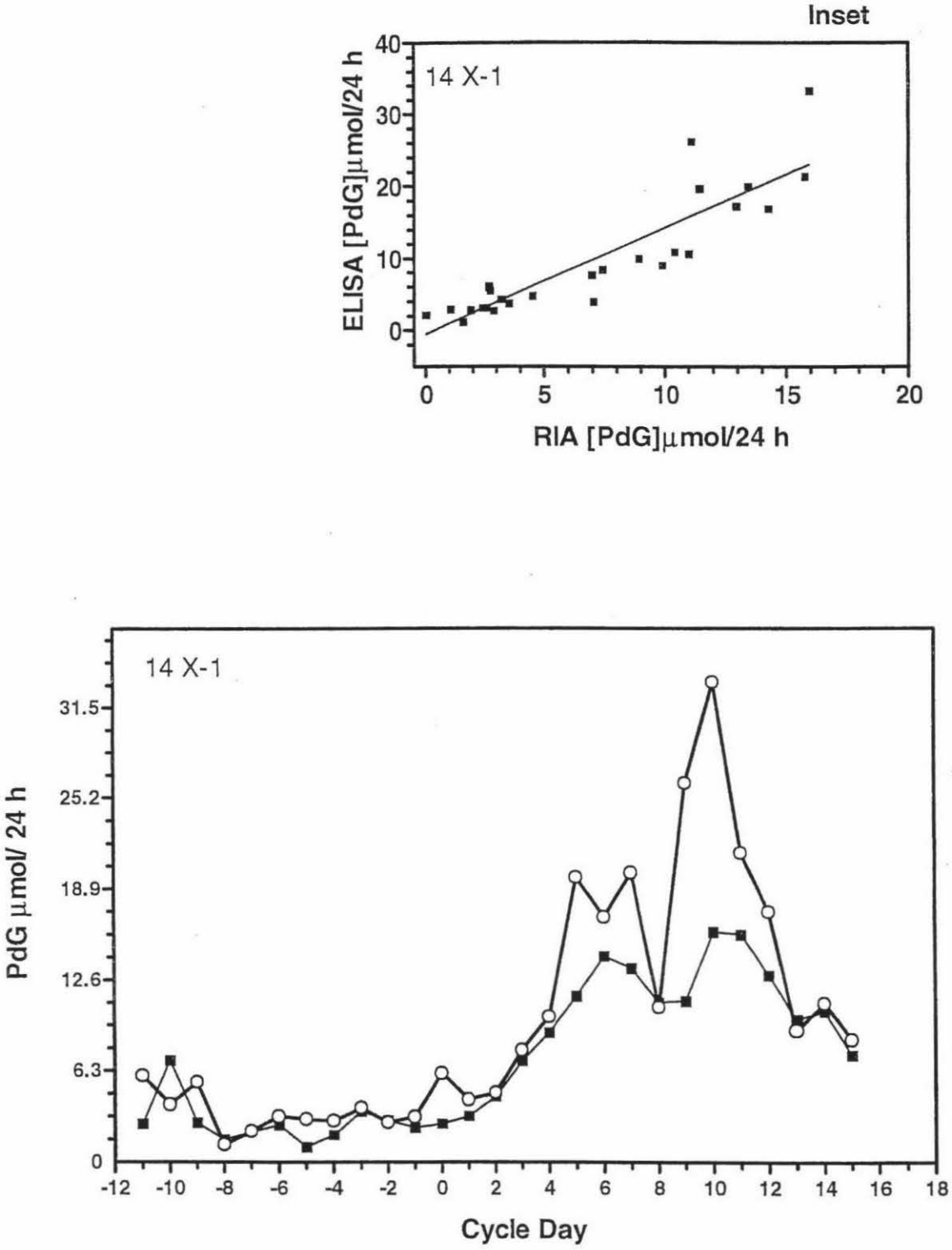

Figure 4.13: Subject 14 K, Menstrual Cycle 1: A comparison of PdG levels obtained using the ELISA assay (—o—), with PdG levels obtained using the RIA (—■—) assay method. (10 µl of a 1/50 dilution of urine sample; PdG-HRP 300 µl, dilution 1/10,000; PdG antiserum 1/10,000 dilution; 16 h; 4°C)

Inset:
A linear regression of the ELISA data against the RIA data (r=0.89)

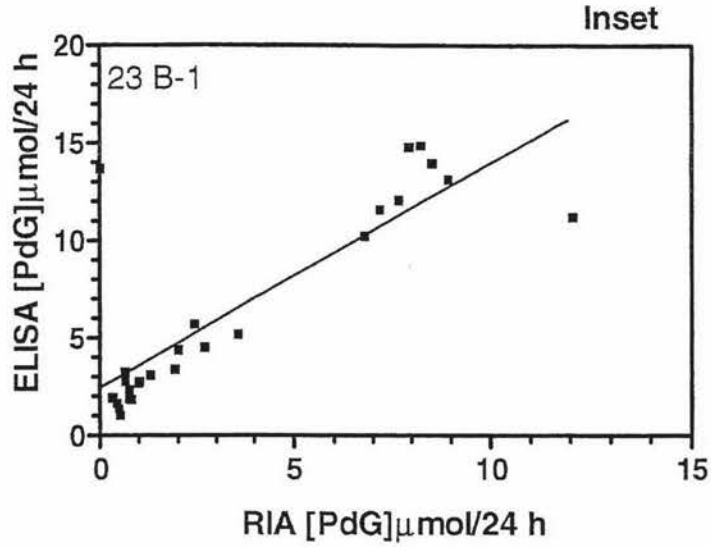

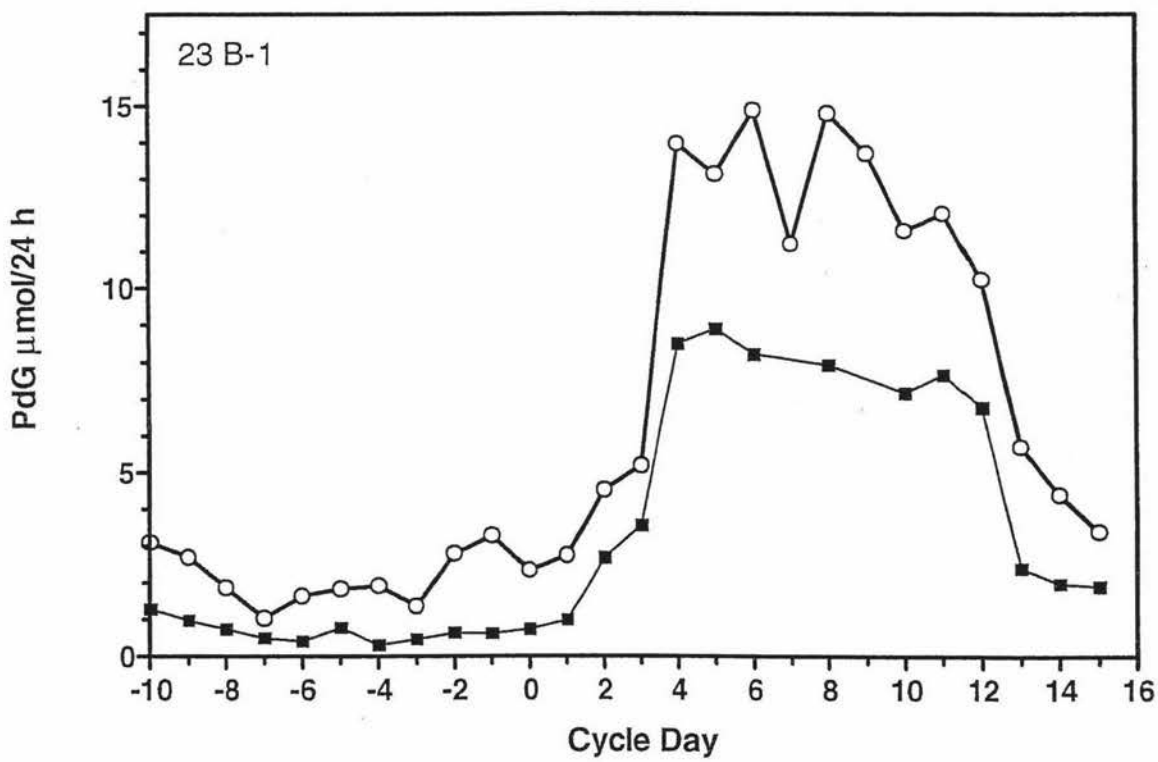

Figure 4.14: Subject 23 B, Menstrual Cycle 1: A comparison of PdG levels obtained using the ELISA assay (—o—), with PdG levels obtained using the RIA (—■—) assay method. (10 µl of a 1/50 dilution of urine sample; PdG-HRP 300 µl, dilution 1/10,000; PdG antiserum 1/10,000 dilution; 16 h; 4°C)

Inset:
A linear regression of the ELISA data against the RIA data (r=0.83)

4.3.2.6 Subject 023 B, Menstrual Cycle 1.

The results from the first menstrual cycle of subject 23 B showed that PdG levels exceeded the threshold four days after the oestrogen peak using ELISA (14 µmoles/24 h) and RIA (8.5 µmoles/24 h) respectively, and therefore both assay systems again gave the same information about the end of fertility. The PdG levels were consistently higher using ELISA than using RIA as for cycle 009D-C2, but nevertheless gave a good correlation coefficient (r) of 0.83 (figure 4.14; and Table 4.2).

Table 4.2: Comparison of PdG ELISA with (WHO) RIA PdG Values; Relative to the Oestrogen Peak Day as Zero.

Cycle Day	Menstrual Cycle 2 Subject 009 D		Menstrual Cycle 1 Subject 014 X		Menstrual Cycle 1 Subject 023 B	
	ELISA	RIA	ELISA	RIA	ELISA	RIA
-11	3.57	2.49	5.95	2.64	-	-
-10	1.98	1.71	3.96	6.99	3.09	1.28
- 9	1.5	0	5.5	2.7	2.7	0.97
- 8	1.27	1.04	1.22	1.56	1.87	0.74
- 7	1.34	0.79	2.14	0	1.04	0.5
- 6	2.22	1.05	3.16	2.57	1.65	0.42
- 5	1.94	1.32	2.95	1.04	1.8	0.78
- 4	1.45	0.96	2.84	1.88	1.92	0.31
- 3	1.45	1.35	3.7	3.49	1.37	0.47
- 2	2.84	0.96	2.7	2.85	2.79	0.64
- 1	2.67	1.09	3.12	2.38	3.28	0.63
0	2.1	1.75	6.11	2.65	2.34	0.74
1	2.19	1.8	4.29	3.17	2.76	0.99
2	2.44	1.76	4.76	4.5	4.52	2.68
3	3.92	2.89	7.7	6.95	5.2	3.56
4	9.9	6.4	10	8.89	13.96	8.5
5	8.67	6.58	19.71	11.43	13	8.91
6	5.45	3.15	16.94	14.24	14.88	8.2
7	13.7	9.74	20	13.4	11.2	12.05
8	11.77	8.53	10.69	10.99	14.79	7.9

9	12.8	8.78	26.23	11	13.69	0
10	13.95	9.76	33.29	15.93	11.58	7.17
11	12.24	6.6	21.4	15.74	12.05	7.67
12	7.18	5.22	17.3	12.92	10.23	6.78
13	9.68	6.49	9.07	9.87	5.7	2.4
14	10.8	7.94	10.96	10.4	4.39	1.99
15	8.12	6.26	8.45	7.37	3.39	1.9
16	12.95	7.65	-	-	-	-
17	4.33	3.27	-	-	-	-

4.3.2.7 *Summary*

The combined data for all six cycles were correlated (using ELISA) with the corresponding RIA data to give the plot shown in figure 4.15(a). A regression line on the same data gave a slope of 1.27 and a Y intercept of 0.85 ± 0.29 (figure 4.15 a). As normal linear least squares procedure assigns all of the error to the Y axis (figure 4.15 a) a further regression was carried out using the Deming Regression Model (figure 4.15 b) which minimizes the errors on both the X and on the Y axes (Deming, 1943). The regression line, using the Deming Model gave a slope of 1.3 and a Y intercept of 0.439 ± 0.16 (figure 4.15 b) and in this case was very similar to the regression line shown in figure (4.15 a). The fact that the correlation coefficient (r) was 0.9 shows that the ELISA is producing data as valid as does the WHO reference RIA. However there was a slight urine bias in the ELISA data and the PdG values obtained were about 30% greater than for the RIA procedure. Nevertheless the ELISA PdG assay is acceptable as a reference assay for future development work aimed at producing home strip tests for PdG.

In summary (Table 4.3) therefore, the PdG threshold level of 6.3 µmoles/24 h was exceeded on the same cycle day using both assays, although the cycle day when PdG threshold levels were exceeded varied from menstrual cycle to menstrual cycle (Table 4.3), with the exception of one menstrual cycle (002F-C2).

In none of the menstrual cycles compared in this study did the PdG levels using RIA exceed PdG levels obtained using ELISA, and while the patterns of PdG profiles using both assay methods were very similar, the higher PdG levels obtained using ELISA have caused some concern.

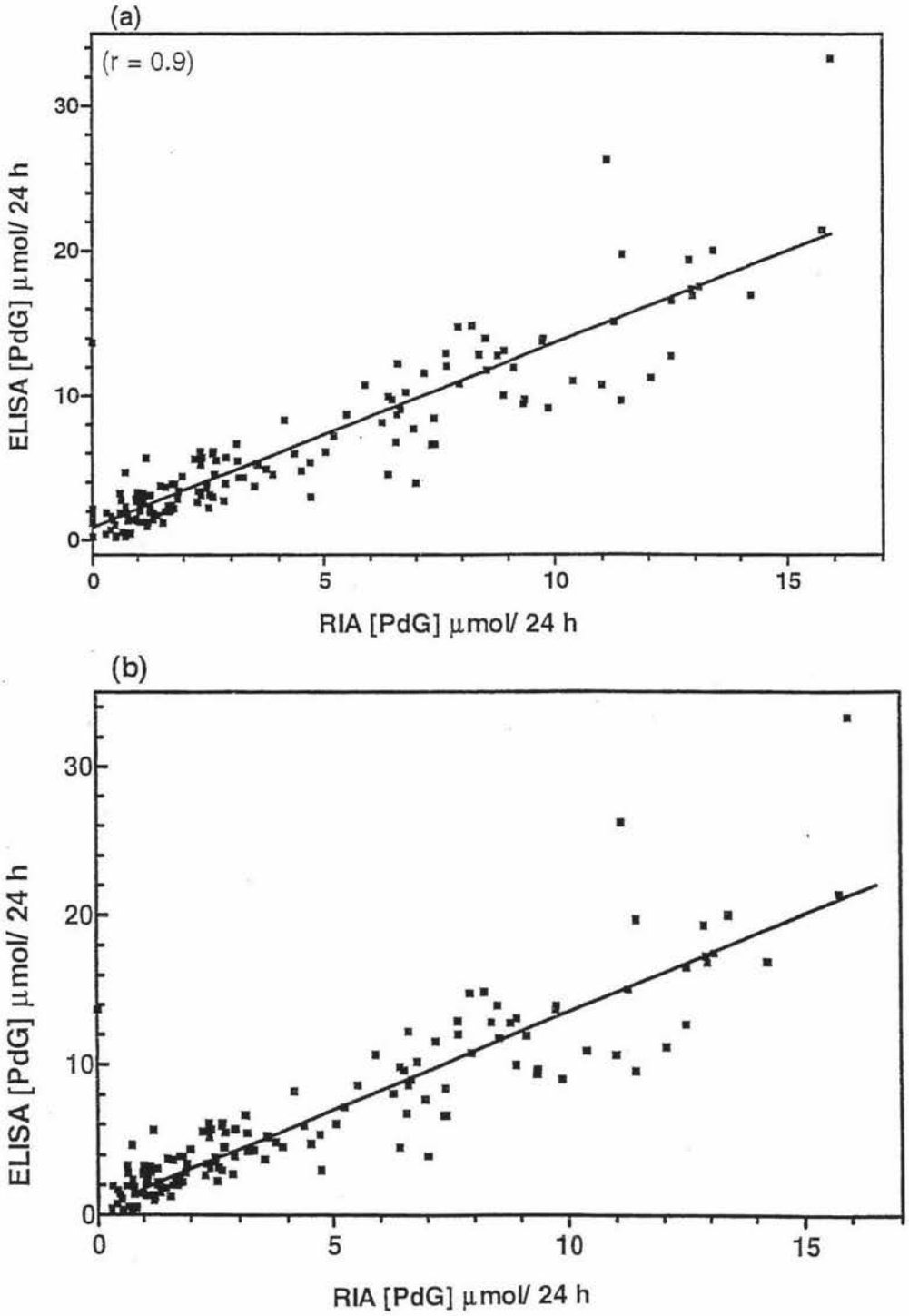

Figure 4.15: A plot of a correlation of the combined PdG levels from six menstrual cycles obtained using the RIA assay with the PdG levels obtained (from the same six menstrual cycles) using the ELISA assay.

(a) A correlation coefficient gave a Pearson's r of 0.9 (r^2 = 0.8157), and a linear regression on the same data gave a slope of 1.27 and a Y intercept of 0.8546; (Y = 1.27X + 0.8546).

(b) The Deming Regression Model gave a slope of 1.308 and a Y intercept of 0.439; (Y = 1.308X + 0.439).

It may be that the PdG ELISA assay is more sensitive than the RIA assay, although Katz and Schiffman (1985) reported that ELISA did not reproduce well compared to RIA. Conversely, it may be that a substance or substances in the urine samples was non-specifically binding to the PdG antibody preventing PdG-HRP binding and consequently reducing the amount of colour produced in the assay. Consequently on extrapolation from the PdG standard curve the PdG levels would be artifactually elevated.

Table 4.3: A Summary of the PdG Levels Measured on the Day the Threshold Value (6.3 µmoles/24 h) was Attained (or Exceeded); Relative to the Oestrogen Peak Day as Zero, using the ELISA Assay and RIA Data.

WHO Urines	ELISA		RIA	
Subject and Menstrual Cycle	Day	PdG µmoles/24 h	Day	PdG µmoles/24 h
002F-C2	+ 3	6.77	+ 5	6.55
009D-C2	+ 4	7.7	+ 4	6.4
0X14-C1	+ 3	9.08	+ 3	9.04
020K-C1	+ 5	12.8	+ 5	8.3
023B-C1	+ 4	13.96	+ 4	8.5
023B-C2	+ 6	6.65	+ 6	7.38

While this explanation is not supported by the cross reactivity studies (refer section 3.3.5.3) carried out, or investigation of the urine blank effect (refer section 3.3.5.4), there is the possibility of the existence of unidentified cross reacting substances. Also, it must be noted that the antibodies used in the two assays were different and it may be that the binding characteristics of the antibody used in the ELISA assay led to a more sensitive assay. Although the limitations on sensitivity and specificity may reflect primarily the properties of the antiserum employed (Maggio, 1980) rather than the nature of the immunochemical label (in this thesis the label was HRP), at more dilute labelled and unlabelled analyte concentrations non-specific reactions may be more likely to occur using RIA than using the ELISA assay (Anderson, 1984). Also the amount of antibody adsorbed (ng/well) to the solid phase (refer section 1.2.4.1) has been reported (Koertge & Butler, 1985) to determine whether the ELISA (low antibody concentration) or the RIA (high antibody concentration) method has superior sensitivity. Which explanation is the more correct can only be decided by application of a validated assay method which is not

subject to immunological effects. The ELISA PdG developed in this thesis is undoubtedly as good as the reference RIA for PdG used by WHO and serves to act as a secondary reference method in the development of newer technologies for the home monitoring of fertility.

4.3.3 Longitudinal Perimenopausal Clinical Study of E1-3G and PdG

To characterize longitudinally the nature of E1-3G and PdG excretion patterns during the menopausal transition (known as the perimenopause), timed and diluted urine samples were collected each day for 224 days (over an eight month period) from one woman aged 51 at the commencement of the study, and analysed using the E1-3G ELISA and PdG ELISA assays developed in this thesis (figure 4.16).

Six ELISA microtitre plates were used for the E1-3G ELISA assays and each contained the optimized E1-3G standard curve (refer section 2.3.4), and the urine samples which were treated in the same way as the E1-3G standards and under the same experimental conditions. Six ELISA plates were used also for the PdG ELISA data and each of the ELISA plates contained the optimized PdG standard curve (refer section 3.3.4), and the urine samples which were treated in the same way as the PdG standards and under the same experimental conditions.

The results for the E1-3G and PdG levels from the 224 day urine collection period are shown in figures 4.16 to 4.21. The PdG values remained at uniformly low levels (3-5 μmoles/24 h) over seven of the eight months (mid May to mid November, 1996) showing that no ovulatory activity was occurring. During the first month (from mid-May) a follicular phase rise in E1-3G occurred peaking on day(s) 22 and 23 (at 320 nmoles/24 h) followed by a rather gradual fall in E1-3G levels to 160 nmoles/24 h by day 32, suggesting atresia of a follicle rather than the typically abrupt fall of E1-3G levels which occurs with ovulation. The E1-3G rise from baseline values on day 13 to 100 nmoles/24 h and on to the E1-3G peak levels on day(s) 22 and/or 23 at 320 nmoles/24 h took a total of 10 days which is also longer than in the normal menstrual cycle. Strongest support for this cycle being anovulatory was the complete absence of any PdG rise following the E1-3G peak showing the failure of development of a corpus luteum and consequently there was almost no secretion of progesterone during the latter half of the cycle.

E1-3G levels increased thereafter on day 33 (230 nmoles/24 h) and remained at that level for a few days, but by day 44 (figure 4.17; June-July) the E1-3G baseline levels (100 nmoles/24 h) were re-established, before a small cyclical increase in E1-3G was seen between days 60-75 but again with a complete absence of corpus luteum function as shown by the low PdG values. This pattern of a small undulating rise in E1-3G levels also occurred between days 90-110 as shown in figure 4.18 (July-August) when on day 96 the E1-3G level reached 225 nmoles/24 h. During the sixth month there was a rise in E1-3G levels, but no real pattern, and during the seventh month shown in figure 4.20 (October-November) the E1-3G levels became elevated and remained high (over 200 nmoles/24 h) from day 174 until day 200 when the levels fell again. All of these "cycles" were assumed to be anovulatory as the PdG values remained uniformly low. Thus, some cyclical activity was present but no ovulatory cycles were encountered.

However, immediately following this during the eighth month (figure 4.21; November-December), the E1-3G levels peaked again (340 nmoles/24 h) on day 208 of the study (the urine sample for day 207 was missing which could have been E1-3G peak day) followed by a rapid decrease in the rate of E1-3G excretion on day 209 (170 nmoles/24 h). Threshold PdG levels (6.3 µmoles/24 h) were exceeded on day 209 (6.6 µmoles /24 h), and on day 212 (10.43 µmoles/24 h), 4 or 5 days after the day of the probable oestrogen peak. The PdG levels thereafter increased rapidly until day 217 when a level of 30 µmoles/24 h was recorded being one of the highest measured in this study and then the PdG excretion rates decreased before a menstrual cycle bleed after six months. Such high PdG values indicate a fully functioning corpus luteum. The luteal phase was approximately 17 days for this subject, from day 208 until day 224. While the usual length of the luteal phase has been reported to be 14 days (Berkow, 1987), Brown *et al.*, (1979) reported that the luteal phase in normal women, as calculated from the pre-ovulatory oestrogen peak to the onset of bleeding ranged from 11 to 17 days, suggesting that this subject was within the normal length of luteal phases. These data therefore show a series of anovulatory cycles, as judged by the persistently low levels of PdG, until E1-3G levels reached a critical but small amplitude at which time the PdG levels began to increase on day 209 and then after a normal luteal phase a bleed occurred. During the perimenopause ovulatory events diminish as the system winds down, and this can be considered as the reverse of menarche (Brown *et al.*, 1978; Brown *et al.*, 1979) where initial fluctuating types of anovulatory cycles occur with increasing amplitudes until ovulation occurs and the PdG levels rise.

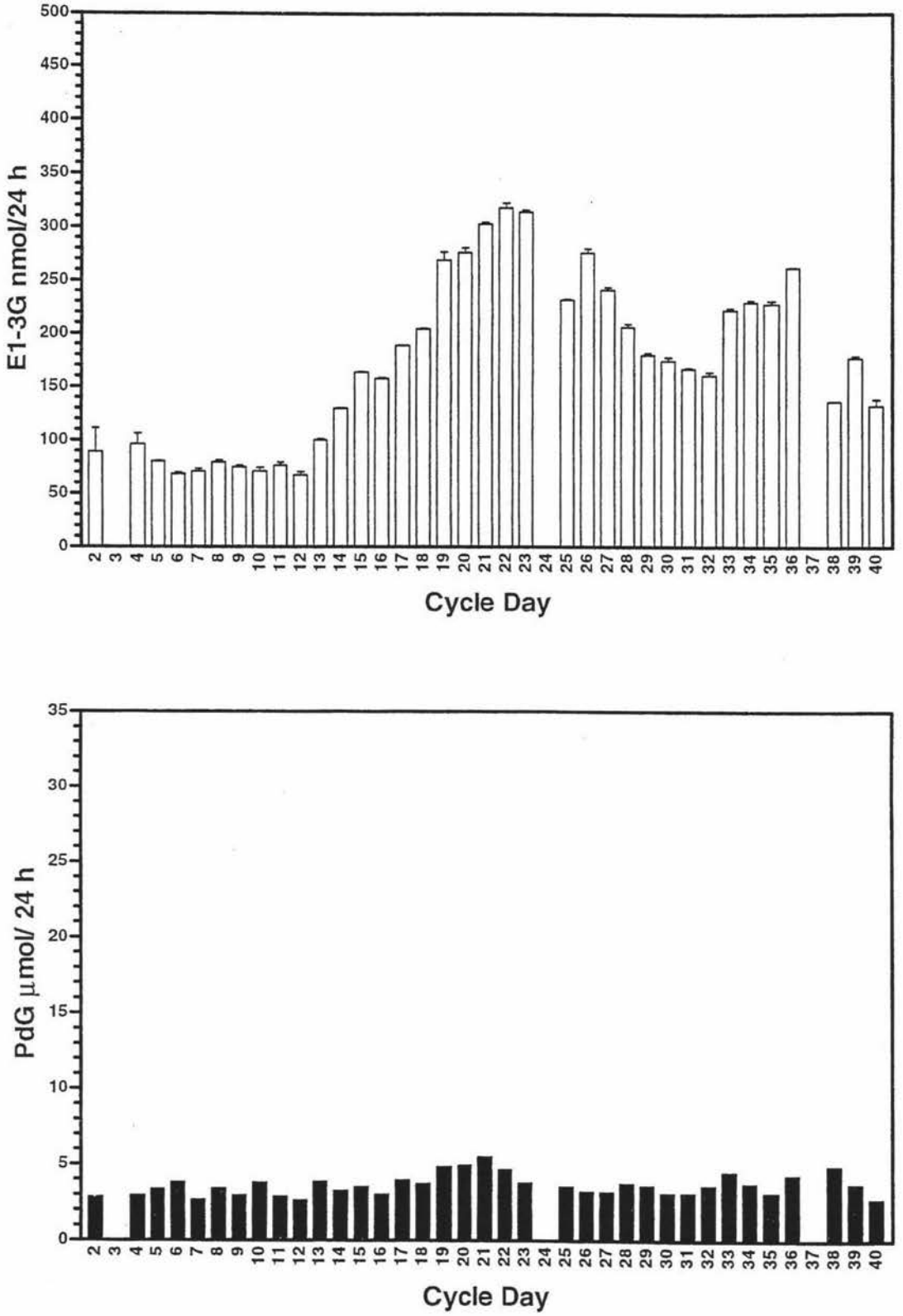

Figure 4.16: May-June, 1996, a longitudinal clinical study of daily E1-3G and PdG levels over a period of eight months in a perimenopausal woman aged 51 years at the commencement of the study. A series of six E1-3G ELISA assays and six PdG ELISA assays were carried out. (discussion in text)

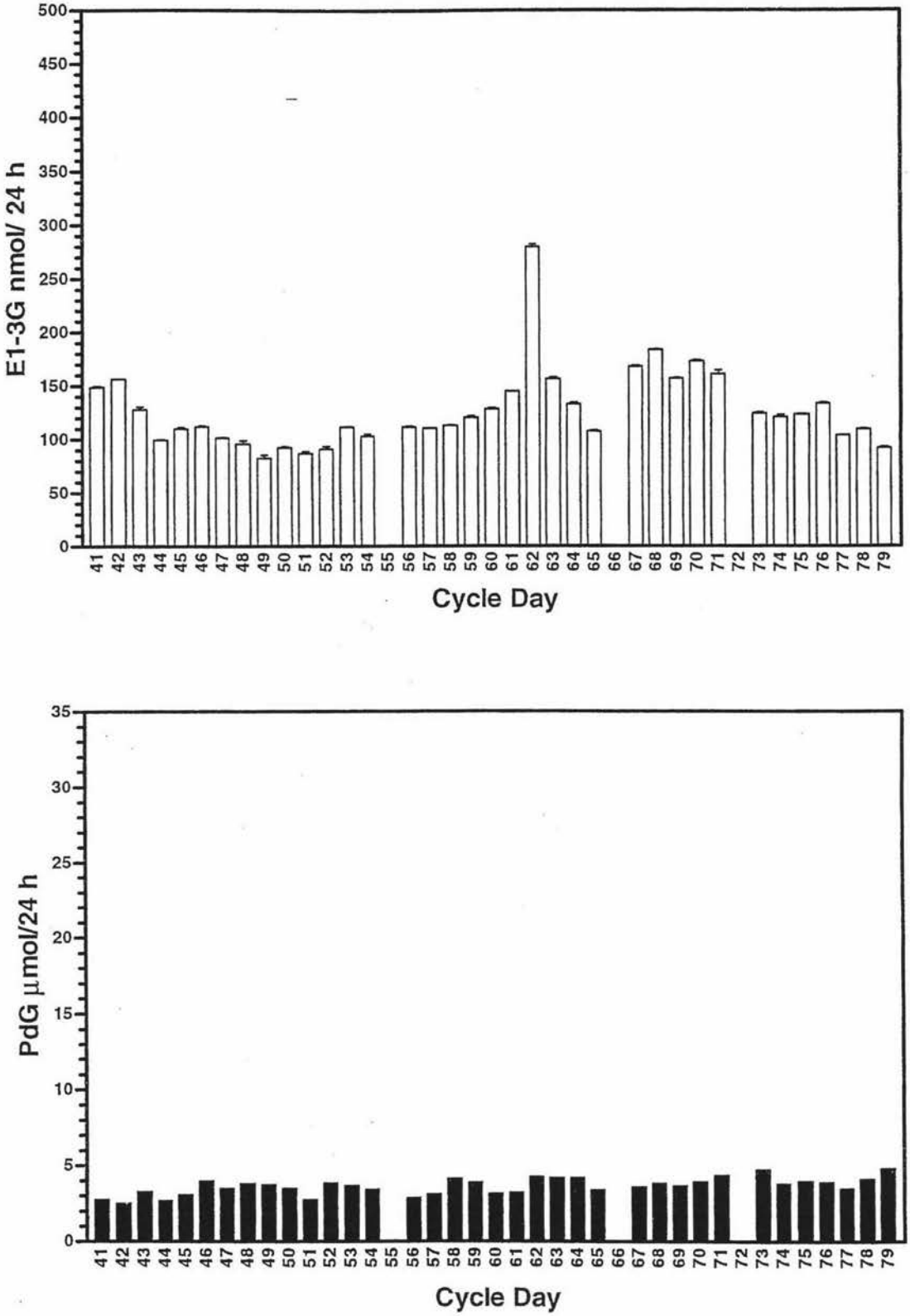

Figure 4.17: June-July, 1996, a longitudinal clinical study of daily E1-3G and PdG levels over a period of eight months in a perimenopausal woman aged 51 years at the commencement of the study. A series of six E1-3G ELISA assays and six PdG ELISA assays were carried out. (discussion in text)

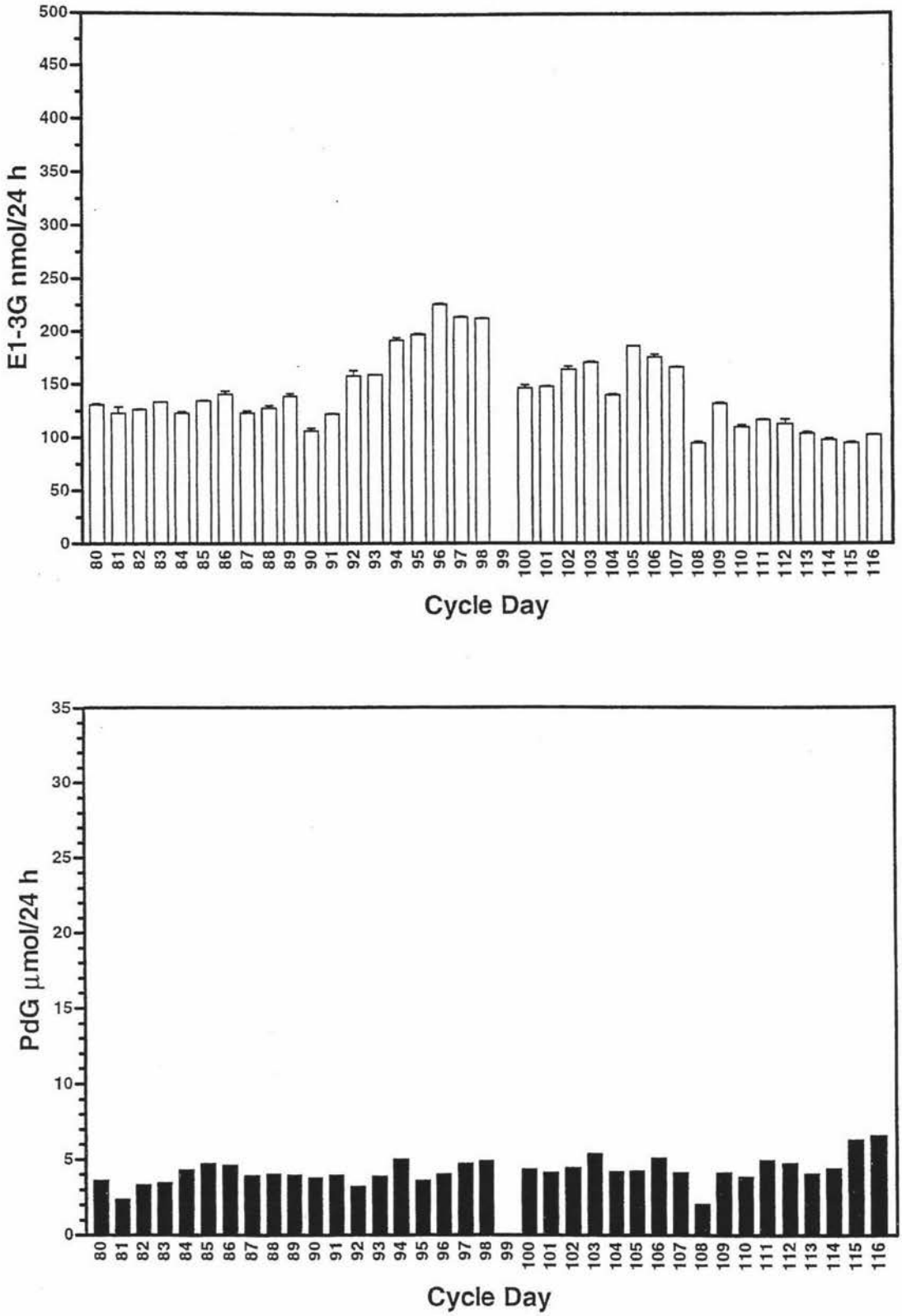

Figure 4.18: July-August, 1996, a longitudinal clinical study of daily E1-3G and PdG levels over a period of eight months in a perimenopausal woman aged 51 years at the commencement of the study. A series of six E1-3G ELISA assays and six PdG ELISA assays were carried out. (discussion in text)

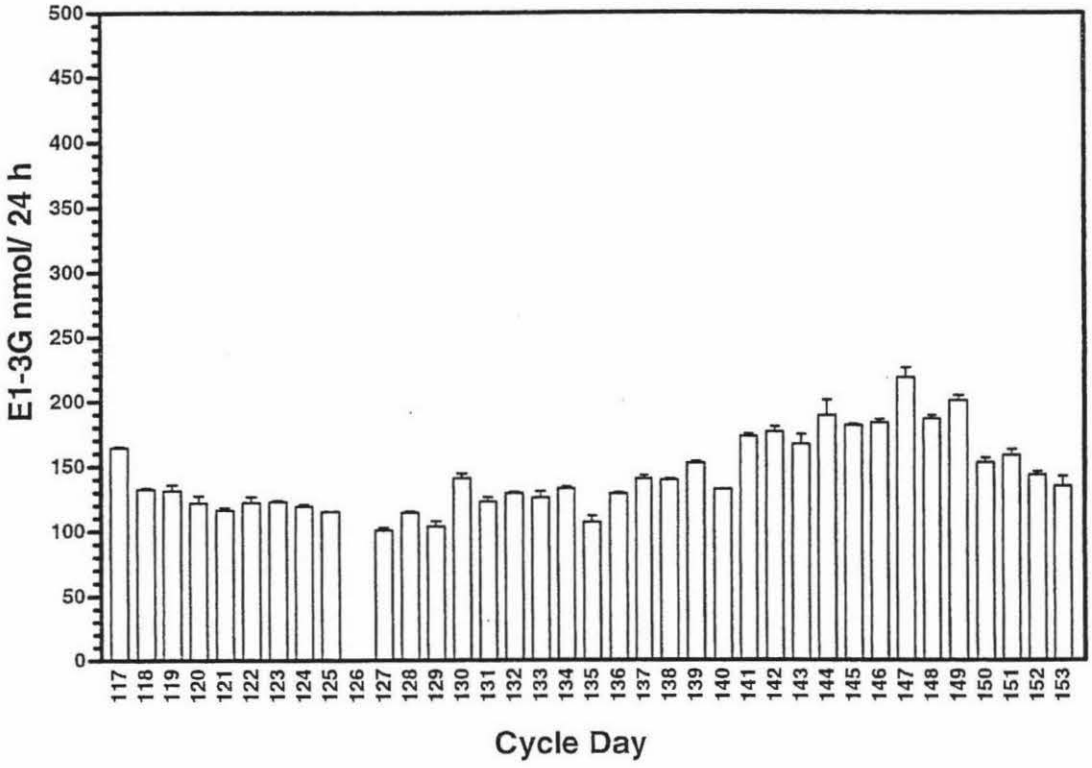

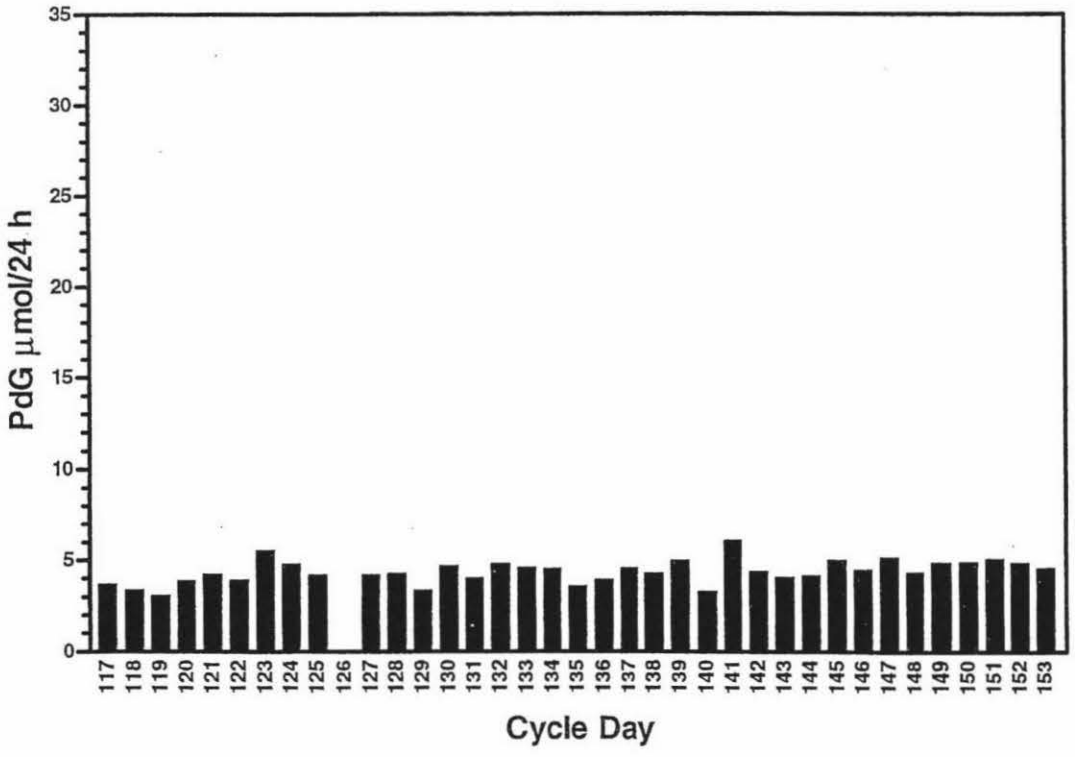

Figure 4.19: September-October, 1996, a longitudinal clinical study of daily E1-3G and PdG levels over a period of eight months in a perimenopausal woman aged 51 years at the commencement of the study. A series of six E1-3G ELISA assays and six PdG ELISA assays were carried out. (discussion in text)

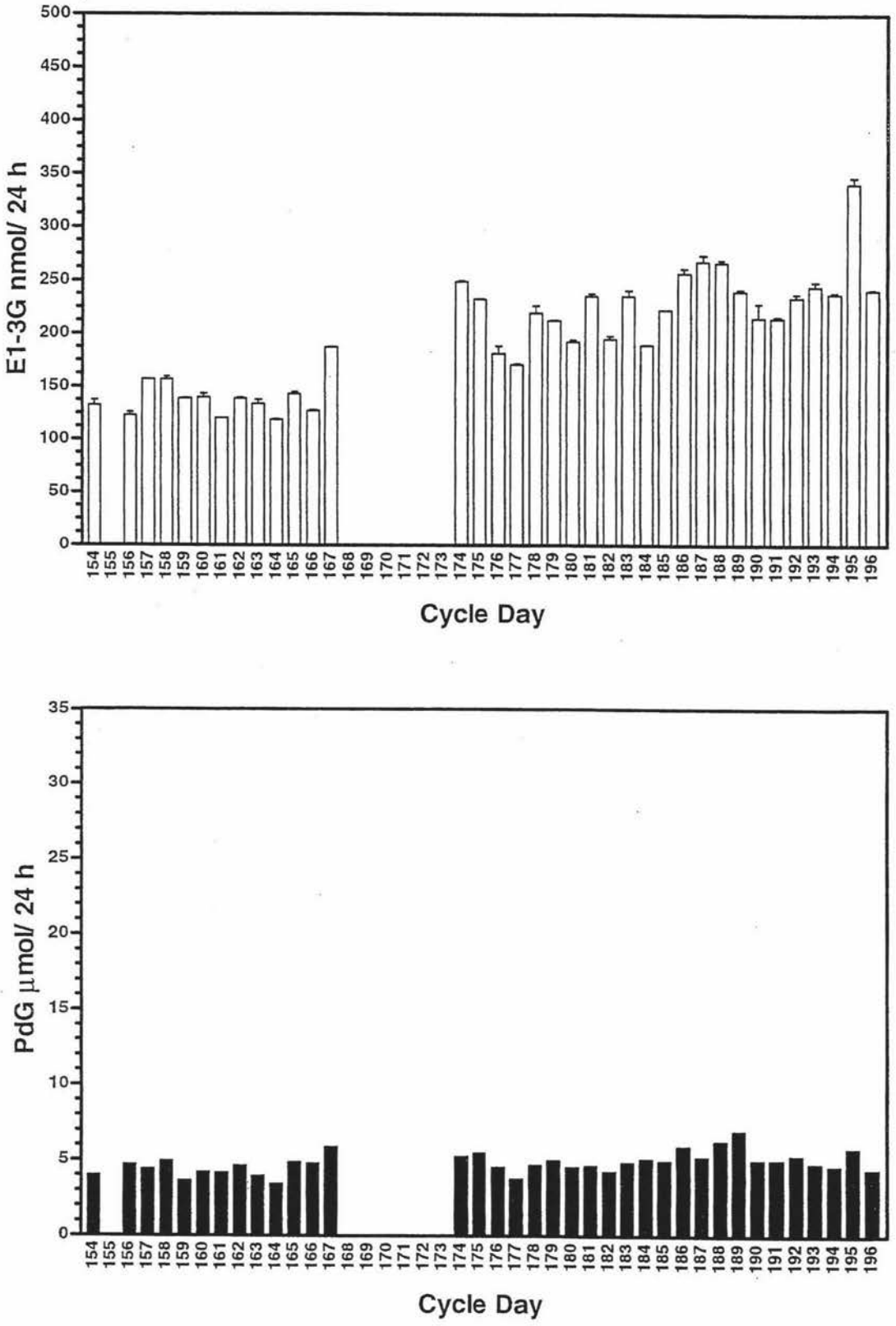

Figure 4.20: October-November, 1996, a longitudinal clinical study of daily E1-3G and PdG levels over a period of eight months in a perimenopausal woman aged 51 years at the commencement of the study. A series of six E1-3G ELISA assays and six PdG ELISA assays were carried out. (discussion in text)

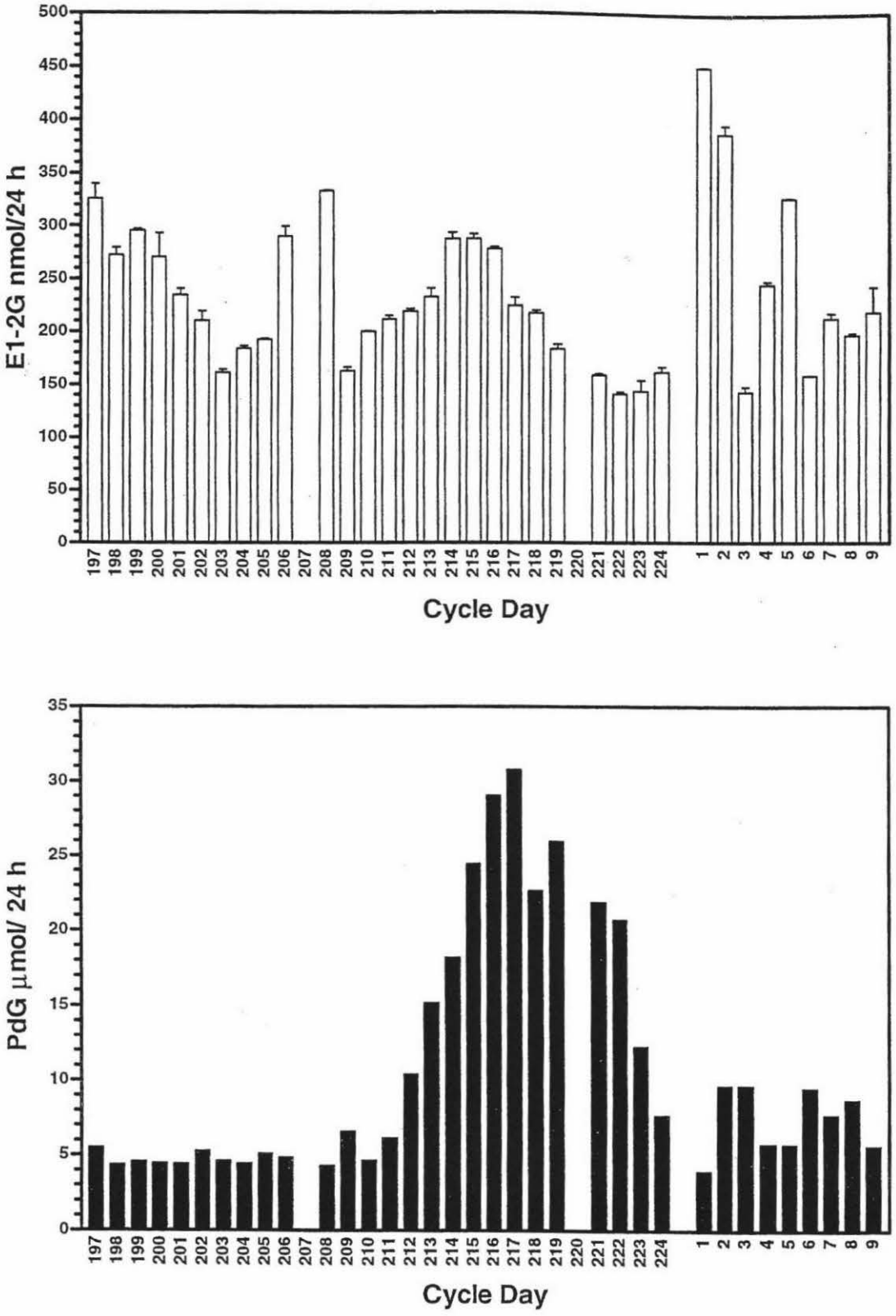

Figure 4.21: November-December, 1996, a longitudinal clinical study of daily E1-3G and PdG levels over a period of eight months in a perimenopausal woman aged 51 years at the commencement of the study. A series of six E1-3G ELISA assays and six PdG ELISA assays were carried out. (discussion in text)

It is not uncommon for short luteal phases, for example 9-10 days, to occur after ovulation, at menarche and at the perimenopause, (the "deficient" luteal phase) which is associated with infertility (Brown *et al.*, 1979; Brown *et al.*, 1955). Despite the rather short E1-3G rise the PdG levels were consistent with the establishment of a fully functioning corpus luteum and hence the cycle was potentially fully fertile after seven months amenorrhoea. This was the last full ovulatory cycle of the subject since no further bleeds occurred over the next two years. This indicates the difficulty in charting a passage through the perimenopausal period when a period of amenorrhoea can be followed by a fully fertile cycle. The assays developed here could have been used to help this women with her fertility using hormonal guidelines which have become well established in Professor Brown's laboratories in Melbourne.

4.4 Conclusion

This study illustrates the importance of general access to accurate home methods for measuring hormone levels. The E1-3G and PdG reference assays developed in the present study are valuable reference assays and can be used to validate new non-instrumental colour tests, or other home fertility kit assays currently being developed. Thus allowing female reproductive events to be monitored in non-laboratory populations (Talwar *et al.*, 1992), in the so called "in the field" studies. The E1-3G and PdG assays are also acceptable for use in the laboratory where large numbers of samples are required to be processed simultaneously, as for example in reproductive epidemiology studies (Vouk & Sheehan, 1983; Lasley & Shidleler, 1994; Henderson *et al.*, 1995) in which the effects of environmental pollutants on reproductive function are assessed.

References

Absolom D.R. and van Oss C.J. (1986). The nature of the antigen-antibody bond and the factors affecting its association and dissociation. *CRC Crit. Revs Immunol.* **6**: 1-46.

Adashi, E.Y. (1994). Endocrinology of the ovary. *Human Reproduction*, **9**: 36-51.

Adekunle A.O., Collins W.P. and Whitehead M.I. (1988). Correlation of ovarian follicle size and the urinary excretion of oestrone glucuronide, luteinizing hormone and pregnanediol glucuronide in spontaneous cycles. *Afr. J. Med. Sci.*, **17**: 77-82.

Adlercreutz H., Brown J., Collins W., Gobelsman U., Kellie A., Campbell H., Spieler J. and Braissand G. (1982). The measurement of urinary steroid glucuronides as indices of the fertile period in women. *J. Steroid Biochem.*, **17**: 695-702.

Anderson D.L. (1984). A comparison of serological techniques for detecting and identifying honeybee viruses. *J. Invertibr. Pathol.*, **44**: 233-243.

Anderson G.W. Zimmerman J.E. and Callahan F.M. (1964). The use of N-hydroxysuccinimide in peptide synthesis. *J. Am.Chem.Soc.* **86**: 1839-1964.

Armstrong D.T., Goff A.K. and Dorrington J.T. (1979). Regulation of follicular estrogen biosynthesis. In: *Ovarian Follicular Development and Function* (Midgley A.R. and Sadler W.A. eds.). pp 169-182. Raven Press, New York.

Avrameas S., Nakane P.K., Papamichail M. and Pesce A.J. (1991). 25 years of immunoenzymatic techniques. *Journal of Immunological Methods*, Special Edition 9-12 September.

Austin, C.R. (1975). Sperm fertility, viability and persistence in the female tract. *Journal of Reproduction & Fertility Supplement* **22**: 75-89.

Bachas L.G. and Meyerhoff M.E. (1986). Theoretical models for predicting the effect of bridging group recognition and conjugate substitution on hapten enzyme immunoassay dose-response curves. *Anal. Biochem.*, **156**: 223-238.

Baird D.T. and Fraser I.S.(1974). Blood production and ovarian secretion rates of oestradiol-17B and oestrone in women throughout the menstrual cycle. *Journal of Clinical Endocrinology & Metabolism*, **38**:No.6.

Baird D.T., Horton R., Longcope C. and Tait J.F. (1969). Steroid dynamics under steady-state conditions. *Recent Progress in Hormone Research*, **25**: 611-656.

Barnard G. and Kohen F. (1990). Idiometric assay: A noncompetitive immunoassay for small molecules typified by the measurement of estradiol in serum. *Clinical Chemistry*, **36**: 1945-1950.

Barrett S.A. and Brown J.B. (1970). An evaluation of the method of Cox for the rapid analysis of pregnanediol in urine by gas liquid chromatography. *J.Endocr.*, **47**: 471-480.

Berkow R. (1987) editor. *The Merck Manual of Diagnosis and Therapy* (5th ed.); Chapter 15, Gynecology and obstetrics. Merck Sharp & Dohme Research Laboratories, division of Merck & Co. Inc., Rahway, N.J.

Billings, E.L., Billings J.J., Brown J.B. and Burger H.G. (1972). Symptoms and hormonal changes accompanying ovulation. *The Lancet* (Feb 5):282-284.

Bischof P., Bianchi P.G. and Campana A. (1991). Comparison of a rapid, quantitative and automated assay for urinary luteinizing hormone (LH), with an LH detection test, for the prediction of ovulation. *Human Reprod.*, **6**: 515-518.

Blackwell, L.F. and Brown, J.B. (1992). Application of time series analysis for the recognition of rises in urinary oestrogens as markers for the beginning of the fertile period. *Steroids* **57**: 554-562.

Blackwell L.F., Brown J.B. and Cooke D. (1998) Definition of the potentially fertile period from urinary steroid excretion rates. Part II. A threshold value for pregnanediol glucuronide as a marker for the end of the potentially fertilite period in the human menstrual cycle. *Steroids*, **63**: 5-13.

Blackwell L.F., Brown J.B., D'Arcangues C., van Look P., Vigil P., Perez A., Gross B. and Sufi S., Hormonal Definition of the Potentially Fertile and Infertile Phases of the Human Ovulatory Cycle by Home Monitoring, Part 1. (WHO Special Programme of Research Training in Human Production, Geneva, Switzerland.), *in preparation.*

Bonnar J: Experience in the Use of Natural Family Planning in the Field: Calendar and Calendar-Basal Body Temperature Method., a paper presented to The Scientific Bases and Problems of Natural Fertility Regulation, a meeting at *the Pontifical Academy of Science in Rome*, November 1994.

Bragg P.D. and Hou C. (1975). *Arch. Biochem. Biophys.*, **167**: 311-321.

Brown J.B.(1955). Urinary excretion of oestrogens during the menstrual cycle. *The Lancet*, Feb:320-323.

Brown J.B., MacLeod S.C., Macnaughtan C., Smith M.A. and Smyth B, (1968). A rapid method for measuring oestrogens in urine using a semi-automatic extractor. *Journal of Endocrinology*, **42**: 5-15.

Brown J.B., Harrisson P. and Smith M.A. (1978). Oestrogen and pregnanediol excretion throughout childhood, menarche and first ovulation. *Journal of Biosocial Science*, **Supplement**, 43-62.

Brown J.B. (1978). Pituitary control of ovarian function - concepts derived from gonadotrophin therapy. *Aust. N.Z. J. Obstet. Gynaec.*, **18**: 47-54.

Brown J.B., Harrisson P., Smith A. and Burger H.G. (1979). Correlations between the mucus symptoms and hormonal markers of fertility throughout reproductive life. *The Ovulation Method Research and Reference Centre of Australia*, Melbourne, Victoria 3068.

Brown J.B., Blackwell L.F., Billings J.J., Conway B., Cox R.I., Garrett G., Holmes J.M. and Smith M.A. (1987). Natural Family Planning. *Am. J. Obstet. Gynecol.*, **157**: 1082-1089.

Brown JB, Blackwell LF, Cox RI, Holmes JM and Smith MA, (1988). Chemical and homogeneous enzyme immunoassay methods for the measurement of oestrogens and pregnanediol, and their glucuronides in urine. *Progress in Biological and Clinical Research*, **285**: 119-138.

Brown, J.B., Blackwell, L.F., Holmes, J. and Smyth, K. (1989). New assays for identifying the fertile period. *International Journal of Obstetrics and Gyneocology*, **Supplement 1**: 111-122.

Brown W.R., Dierks S.E., Butler J.E. and Gershoni J.M. (1991). Immunoblotting: Membrane filters as the solid phase for immunoassay. In: *Immunochemistry of Solid-Phase Immunoassay*, (J.E. Butler ed.), CRC Press, Boca Raton, FL, pp 151-172.

Brown R.G. (1962). *Smoothing, Forecasting and Prediction of Discrete Time Series*. Prentice-Hall, Englewood Cliffs, NJ.

Bull H.B. (1956). Adsorption of bovine serum albumin on glass. *Biochem. Biophys. Acta*, **19**: 464-71.

Burger H.G. (1989). Estradiol: The Physiological Basis of the Fertile Period. *Int. J. Gynecol. Obstet.* Suppl. **1**: 5-9.

Burt S.M., Carter T.J.N. and Kricka L.J. (1979). Thermal characteristics of microtitre plates used in immunological assays. *J. Immunol. Methods*, **31**: 231-236.

Butler J.E., Joshi K.S. and Brown W.R. (1991). The application of traditional immunochemical methods to evaluate the performance of capture molecules immobilised on microtitre wells. *Immunochemistry of Solid Phase Immunmoassay* (J.E. Butler ed.). CRC Press, Boca Raton, Fl. 221-231.

Butler J.E., Ni L., Nessler R., Joshi K.S., Suter M., Rosenberg B., Chang J., Brown W.R. and Cantarero L.A. (1992). The physical and functional behavior of capture antibodies adsorbed on polystyrene. *J. Immunol. Methods*, **150**: 77-90.

Butler J.E., Ni L., Brown W.R., Joshi K.S., Chang J., Rosenberg B. and Voss E.W.Jr. (1993). The immunochemistry of sandwich ELISAs. VI. Greater than 90% of monoclonal and 75% of polyclonal anti-fluorescyl capture antibodies (Cabs) are denatured by passive adsorption. *Mol. Immunol*, **30**: 1165-75.

Butler J.E. (1994). ELISA. In: *Immunochemistry* (van Oss C.J. and Regenmortel M.H.V. eds.) Chapter **29**: 737-803, Marcel Dekker Inc.

Butler J.E. (1996). Solid Phases in Immunoassay. In: *Immunoassay* (Christopoulos T.K. and Diamandis E.P., eds.) Chapter **9**: 205-225, Academic Press, New York.

Campbell A.M. (1996). Production and purification of antibodies. In: *Immunoassay* (Christopoulos T.K. and Diamandis E.P., eds.) Chapter **5**: 95-115, Academic Press, New York.

Cantarero L.A., Butler J.E. and Osborne J.W. (1980). The binding characteristics of various proteins to polystyrene and their significance for solid-phase immunoassays. *Anal. Biochem*: **105**: 375-83.

Catt K. and Tregear G.W. (1967). Solid phase radioimmunoassay in antibody coated tubes. *Science*, **158**: 1570-2.

Cekan S.Z., Beksac M.S., Wang E., Shi S., Masironi B., Landgren B.M. and Diczfalusy E. (1986). The prediction and/or detection of ovulation by means of urinary steroid assays. *Contraception*, **33**: 327-345.

Cembrowski G.S. Westgard J.O., Eggert A.A. and Toren E.C. Jr. (1975). Trend detection in control data: optimisation and interpretation of Trigg's technique for trend analysis. *Clinical Chemistry*, **21**: 1396-1405.

Chatfield C. (1984). *The Analysis of Time Series: An Introduction*. Chapman and Hall, London.

Christian G.D. (1994). Spectrometry. In: *Analytical Chemistry* (5th ed.) Chaper **14**, Wiley & Sons, New York.

Christopoulos T.K. and Diamandis E.P. (1996). Immunoassay Configurations. In: *Immunoassay* (Christopoulos T.K. and Diamandis E.P., ed.) Chapter **10**, Academic Press, New York.

Conway B. (1986). Assessment of a Home Test for Urinary Pregnanediol Glucuronide. *B.Med. Sci. Thesis*. University of Melbourne.

Cooke D. (1993). Studies Relating to the Ovarian Monitor. *MSc. Thesis*, Massey University, Palmerston North, New Zealand.

Crowther J.R. (1995). ELISA: Theory and Practice. *Methods in Molecular Biology*, **42**. Totowa.NJ.: Humana Press.

Csako G. (1996). Free hormone measurements. In: *Immunoassay* (Christopoulos T.K. and Diamandis E.P. eds.) **20**: 423-481, Academic Press, New York.

Cummock B.P. (1997). Studies Towards the Development of a Urinary Steroid Immunoassay. *MSc. Thesis*, Massey University, Palmerston North, New Zealand.

Czekala N.M., Overstreet J.W., Hanson F.W., Stabenfeldt D.V.M. and Lasley B.L. (1986). Assessment of follicular function in women by measurement of estrogen conjugates. *Fertility and Sterility*, **46**(4): 604-609.

Davies J., Dawkes A.C., Haymes A.G., Roberts C.J., Sunderland R.F., Wilkins M.J., Davies M.C., Tendler S.J.B., Jackson D.E. and Edwards J.C. (1994). A scanning tunnelling microscopy comparison of passive antibody adsorption and biotinylated linkage of streptavidin on microtiter wells. *J. Immunol. Methods*, **167**: 253-9.

Deming W.E. (1943). *Statistical Adjustment of Data*. John Wiley & Sons, New York, p.184

Dierschke K.J., Hutz R.J., Wolf R.C. (1985). Induced follicular atresia in rhesus monkeys: strength-duration relationships of the oestrogen stimuli. *Endocrinology*, **117**:1397.

DiNello R.K. and Dolphin D.H. (1981). Substituted hemins as probes for structure-function relationships in horseradish peroxidase. *The Journal of Biological Chemistry*, **256**: 6903-6912.

Dunford H.B. (1991). HRP reaction kinetics reviewed. In: *Peroxidases in Chemistry and Biology* (Everse, Everse and Grisham eds.). vol. **II**, Chapter 1, pp 1-24. CRC Press Boca Raton, Fl., USA.

Ehrlich P.H., Moyle W.R. and Moustafa Z.A. (1983). Further characterisation of co-operative interactions of monoclonal antibodies. *J. Immunol. Methods*, **131**: 1906.

Ekins R.P. (1983). The precision profile: Its use in assay design, assessment and quality control. In: *Immunoassays for Clinical Chemistry* (W.M.Hunter and T.E.T.Corrie eds.), Churchill Livingstone, Edinburgh, 76-104.

Ekins R.P. (1960). The estimation of thyroxine in human plasma by an electrophoretic technique. *Clin. Chim. Acta*, **5**: 453-9.

Engvall E. and Perlmann P. (1971). Enzyme linked immunosorbent assay (ELISA): quantitive assay of IgG. *Immunochemistry*, **8**: 871-4.

Falck B. (1959). Site of production of oestrogen in rat ovary as studied in micro-transplants. *Acta Physiol. Scand.*, **47** (Suppl. 163): 1.

Findlay, J.K. (1993). An update on the roles of inhibin, activin and follistatin as local regulators of folliculogenesis. *Biology of Reproduction*, **48**: 15-23.

Francois D., Oriol R. and Binaghi R.A. (1972). *J. Histochem. Cytochem.*, **20**: 527-535.

Franz B. and Stegemann M. (1991). The kinetics of solid-phase microtiter immunoassay. In: Butler J.E. Ed. *Immunochemistry of Solid-Phase Immunoassay*. Boca Raton, FL: CRC Press.

Ganong W.F. (1991). *Review of Medical Physiology* (15 ed.) Prentice-Hall.

Gow S.M., Turner E.I. and Glasier A. (1994). The clinical biochemistry of the menopause and hormone replacement therapy. *Ann. Clin. Biochem.*, **31**: 509-528.

Gilardi K.V.K., Shideler S.E., Valverde C.R., Roberts J.A. and Lasley B.L. (1997). Characterization of the onset of menopause in the rhesus macaque. *Biology of Reproduction*, **57**(2): 335-340.

Grotjan H.E. and Keel B.A. (1996). Data interpretation and Quality Control. In: *Immunoassay*, (Christopoulos T.K. and Diamandis E.P., eds.) Chapter **4**: 51-93, Academic Press, New York.

Hadley, M.E. (1996). *Endocrinology* 4th ed., Prentice Hall, New York, 418.

Hall P.F. (1986). Cytochrome P_{450} and the regulation of steroid synthesis. *Steroids*, **48**: 131-196.

Hall P.F. (1998). The roles of cytochromes P_{450} in the regulation of steroidogenesis. In: *Handbook of Physiology*: Section 7, The Endocrine System; Cellular Endocrinology, **1**: 413-435.

Harlow E.D. and Lane D. (1988). *Antibodies: A Laboratory Manual*. Cold Spring Harbor, New York, Chapter 8 .

Henderson K.M., Camberis M. and Hardie A.H. (1995). Evaluation of antibody- and antigen-coated enzymeimmunoassays for measuring oestrone-3-glucuronide concentrations in urine. *Clinica Chimica Acta*, **243**: 191-203.

Hillier S.G. and De Zwart F.A. (1981). Evidence that granulosa cell aromatase induction/activation by follicle-stimulating hormone is an androgen-regulated process. *Endocrinology.*, **109**: 1303-1305.

Hillier S.G. (1991). Paracrine control of follicular oestrogen synthesis. *Semin. Reproduction Endocrinology*, **9**: 332-339.

Hillier S. Whitelaw P. and Smyth C. (1994a). Sex steroid metabolism in the ovary. *The Biochemist*, **April/May** 22-26.

Hillier S.G., Whitelaw P. and Smyth C. (1994b). Follicular oestrogen synthesis: the "two-cell, two-gonadotrophin" model revisited. *Mol. Cell. Endocrinol*, **100**: 51-54.

Hobrick P. and Nilsen M. (1974). Early urinary Conjugated Metabolites of Intraveously Injected (6.7-3H)-estradiol-17β in the Human Subject. *J. Steroid Biochem.*, **5**: 15-20.

Hoff J.D., Quigley M.C. and Yen S.S.C. (1983). Hormonal Dynamics at Midcycle: A Re-evaluation. *J. Clin. Endocrinol. Metab.*, **57**: 792-796.

Holme D.J. and Peck H. (1993). Immunological Methods. In: *Analytical Biochemistry*. (2nd ed.) Chapter **7**, John Wiley & Sons Inc., New York.

Hsueh A.J.W., Adashi E.Y., Jones P.B.C. and Welsh T.J. Jr. (1984). *Endrocr. Rev.*, **5**: 76-126.

Ireland J.J. (1987). Control of follicular growth and development. *Journal Reprod. Fert. suppl.*, **34**: 39-54.

Jackson T.M. and Ekins R.P. (1986). Theoretical limitations on immunoassay sensitivity. Current practice and potential advantages of fluorescent Eu^{3+} chelates as non-radioisotopic tracers. *J. Immunol. Methods*, **87**: 13-20.

Joshi K.S., Hoffmann L.G. and Butler J.E. (1992). The immunochemistry of sandwich ELISAs V. The capture antibody performance of polyclonal antibody enriched fractions prepared by various methods. *Mol. Immunol.*, **29**: 971-81.

Kaipia A. and Hsueh A.J.W. (1997). Regulation of ovarian follicle atresia. *Annual Review of Physiology*, **59**: 349-63.

Karsch F.J. (1987). Central actions of ovarian steroids in the feedback regulation of pulsatile secretion of luteinizing hormone. *Annual Review of Physiology*, **49**: 365.

Katz M.A. and Schiffman G. (1985). Comparison of an enzyme-linked immunosorbent assay with radioimmunoassay for the measurement of pneumococcal capsular polysaccharide antibodies. *Mol. Immunol.*, **22**: 313-319.

Kemeny D.M. (1991). *ELISA: A Practical Guide.* Pergamon Press.

Kesner J.S., Knecht E.A., Krieg E.F., Barnard G., Mikola H.J. Kohen F., Gani M.M. and Coley J. (1994). Validations of time-resolved fluoroimmunoassays for urinary estrone 3-glucuronide and pregnanediol 3-glucuronide. *Steroids*, **59**: 205-211.

Klopper A. Michie E.A. and Brown J.B. (1955). A method for the determination of urinary pregnanediol. *Journal of Endocrinology*, **12**: 209-219.

Koertge T.E. and Butler J.E. (1985). The relationship between the binding of primary antibody to solid phase antigen in microtitre plates and its detection by the ELISA. *J. Immunol. Methods*, **83**: 283-99.

Kricka L.J., Phil D. and Path F.R.C. (1996). Principles of immunochemical techniques. In: Tietz Fundamentals of Clinical Chemistry (4th ed.) Chapter **10**, WB Saunders Company, Philadelphia, PA.

Kulin H.E., Bell P.M., Santen R.J. and Ferber A.JK. (1975). Integration of pulsatile gonadotropin secretion by timed urinary measurement: An accurate and sensitive 3-hour test. *J. Clin. Endocrinol. Metab.*, **40**: 783-789.

Lasley B.L., Mobed K. and Gold E.B. (1994). The use of urinary hormonal assessments in human studies. *Annals of the New York Academy of Sciences*, **709**: 299-311.

Lasley B.L. and Shidleler S.E. (1994). Methods of evaluating reproductive health of women. *Occupational Medicine*, **9**(3): 423-33.

Lehtonen O.P. (1981). Immunoreactivity of solid phase hapten binding plasmacytoma protein (ABPC 24). *Mol. Immunol.*,**18**: 323-9.

Lehtonen O.P. and Viljanen M.K. (1980). Antigen attachment in ELISA. *J. Immunol. Methods*, **34**: 61-70.

Leung P.C.K. and Armstrong D.T. (1980). Interactions of steroids and gonadotropins in the control of steroidogenesis on the ovarian follicle. *Annual Review of Physiology*, **42**: 71.

Lindmo T. Bormer O. Ugelstad J. and Nustad K. (1990). Immunometric assay by flow cytometry using mixtures of two particle types of different affinity. *Journal of Immunological Methods*, **126**: 183-189.

Luke G.A., Klopper A. and Bersinger N. (1988). Development of an ELISA for schwangerschafts protein 1 ((SP 1) in urine. *J. Reprod. Fert. Suppl.*, **36**: 181-201.

Maggio E.T. (1980). *Enzyme immunoassay*. C.R.C. Press, Boca Raton, FL.

Mahesh V.B. (1985). The dynamic interaction between steroids and gonadotropins in the mammalian ovulatory cycle. *Neuroscience Biobehaviour Review*, **9**(2): 245.

Metzger H. (1992). Transmembrane signaling. The joy of aggregation. Presidential address, American Association of Immunologists, Anaheim, CA. *J. Immunol. Methods*, **150**: 77-90.

McEwen B.C. (1976). Interactions between hormones and nerve tissue. *Scientific America*, **235**: 48-58.

Munro C.J., Stabenfeldt G.H., Cragun J.R., Addiego L.A., Overstreet J.W. and Lasley B.L. (1991). Relationship of serum estradiol and progesterone concentrations to the excretion profiles of their major urinary metabolites as measured by enzyme immunoassay and radioimmunoassay. *Clinical chemistry*, **37**: 838-844.

Musey P.I., Green R.N. and Hobkirk R. (1972). The Role of an Enterohepatic System in the Metabolism of 17β-E2-17G in the Human Female. *J. Clin. Endocrin. Metab.*, **35**: 448-457.

Nakane P.K. and Kawaoi A. (1974). *J. Histochem. Cytochem.*, **22**: 1084-1091.

Ngo T. T. (1991). Enzyme systems and enzyme conjugates for solid-phase ELISA. In: *Immunochemistry of Solid-Phase Immunoassay* (J.E. Butler, ed.), CRC Press, Boca Raton, FL, pp 85-102.

Nygren H. (1988). Experimental demonstration of lateral cohesion in a layer of adsorbed protein and layers of gold-antibody complexes bound to surface immobilised antigen. *J. Immunol. Methods*, **114**: 107-114.

Nygren H., Werthen M. and Stenberg M. (1987). Kinetics of antibody binding to solid-phase-immobilised antigen. *J. Immunol. Methods*, **101**: 63-71.

Odeblad E. (1994). Discovery of different types of cervical mucus using the Billings ovulation method. Bulletin of the Ovulation Method Research and Reference Centre of Australia, **21**: No.3.

Paek S.H. and Schramm W. (1991). Modeling of immunosensors under nonequilibrium conditions: I. Mathematic modeling of performance characteristics. *Anal. Biochem.*, **196**: 319-325.

Paek S.H., Bachas L.G. and Schramm W. (1993). Defined analyte-enzyme conjugates as signal generators in immunoassays. *Anal. Biochem.*, **210**: 145-154.

Painter P.C., Cope J.Y. and Smith J.L. (1996). Appendix. In: *Tietz Fundamentals of Clinical Chemistry*, 4th ed. (Burtis C.A. and Ashwood E.R. ed.) Chapter **40**: 766. WB Saunders Company, Philadelphia, PA.

Papanicolaou A.D., Loraine J.A., Dove G.A. and Loudon N.B. (1969). Hormonal excretion patterns in perimenopausal women. *J. Obstet. Gynaecol. Br Cwlth.*, **76**: 308.

Podesta A., Smith C.J., Villani C. and Montagnoli G. (1996). Shared reaction in solid-phase immunoassays for estriol determination. *Steroids*, **61**: 622-626.

Pohl C.R. and Knobil E. (1982). The role of the central nervous system in the control of ovarian function in higher primates. *Annual Review of Physiology*, **44**: 583-593.

Porstmann T., Porstmann B., Evers U., Wietschke R., Nugel E. and Schmechta H. (1987). Coupling of different isoenzymes of horseradish peroxidase influences the sensitivity of enzyme immunoassay. *Biomed. Biochim. Acta*, **46**: 867-875.

Porstmann B., Porstmann T., Gaede D., Ugel E. and Egger E. (1981b). Temperature dependent rise in activity of horseradish peroxidase caused by nonionic detergents and its use in enzyme immunoassay. *Clin. Chim. Acta*, **109**: 175-181.

Porstmann T. and Kiessig S.T. (1992). Enzyme immunoassay techniques, an overview. *J. Immunol. Methods*, **150**: 5-21.

Rajkowski K.M. and Cittanova N. (1981). The efficiency of different coupling procedures for the linkage of oestriol-16 α-glucuronide, oestrone-3-glucuronide and pregnanediol-3 α-glucuronide to four different enzymes. *J. Steroid Biochem.*, **14**: 861-866.
Renowden B. (1975). Blood estrogens in human plasma. *PhD Thesis*, Melbourne University.

Roitt I. (1988). *Essential Immunology*. (6th ed.) Blackwell Scientific Publications.

Rubenstein K.E. Schneider R.S., Ullman E.F.(1972). Homogenous enzyme immunoassay. A new immunochemical technique. *Biochemical and Biophysical Research Communications*, **47**, 846-851.

Ryan O, Smyth M.R. and O'Fagain C. (1994). Horseradish peroxidase: the analyst's friend. *Essays in Biochemistry*, **28**, 129-146.

Sadana A. and Madugula A. (1993). Binding kinetics of antigen by immobilized antibody or of antibody by immobilized antigen: influence of lateral interactions and variable rate coefficients. *Biotechnol. Prog.*, **9**: 259-266.

Salonen E. and Vaheri A. (1979). Immobilisation of viral and mycoplasma antigens and of immunoglobulins on polystyrene surface for immunoassays. *J. Immunol. Methods* **30**: 209-218.

Sanderson C.J. and Wilson D.V. (1971). Immobilisation of antibody to microtitre wells using sodium periodate method. *Immunology*, **20**: 1061-1065.

Santoro N. Rosenberg Brown J., Tovaghgol A. and Skurnick J.H. (1996). Characterization of reproductive hormonal dynamics in the perimenopause. *Journal of Clinical Endocrinology and Metabolism*, **81**(4): 1495-1501.

Schramm W. and Paek S.H. (1991). Modeling of immunosensors under nonequilibrium conditions: II. Experimental determination of performance characteristics. *Analytical Biochem.*, **196**: 326-336.

Schramm W. and Paek S.H. (1992). Antibody-antigen complex formation with immobilized immunoglobulins. *Analytical. Biochem.*, **205**: 47-56.

Scatchard G. (1949). Ann. N.Y. Acad. Sci., **51**: 660-672.

Shah H.P. and Josh U.M. (1982). A simple, rapid and reliable enzyme-linked immunosorbent assay (ELISA) for measuring estrone-3-glucuronide in urine. *J. Steroid Biochem.*, **16**: 283-286.

Smales C.M., Elgar D.F., Moore C.H. and Blackwell L.F. (1998). Acid-polyacrylamide gel electrophoresis of lysozyme-estrone glucuronide conjugates. *Bioconjugate Chem.*, **9**: 838-841.

Smales, C.M. (1997). Characterisation of lysozyme-steroid glucuronide conjugates. *PhD Thesis*, Massey University, Palmerston North, New Zealand.

Smales, C.M., Cooke, D.G. and Blackwell, L.F. (1994). Use of ion-exchange and hydrophobic interaction chromatography for the rapid purification of lysozyme-oestrone glucuronide conjugates. *J. Chromatography*, **662**: 3-14.

Sorensen K. and Brodbeck U. (1986). Assessment of coating-efficiency in ELISA plates by direct protein determination. *J. Immunol. Methods*, **95**: 291-293.

Stanczyk F.Z., Miyakawa I. and Goebelsmann U. (1980). Direct Radio-immunoassay of Urinary Estrogen and Pregnanediol Glucuronides during the Menstrual Cycle. *Am. J. Obstet. Gynecol.*, **137**: 443-450.

Stenberg M. and Nygren H. (1988). Kinetics of antigen-antibody reactions at solid-liquid interfaces. *J. Immunol. Methods*, **113**: 3-15.

Stryer, L. (1989). *Biochemistry - International Student Edition* (third edition). Freeman, U.S.A.

Swinehart D.F. (1962). The Beer-Lambert law. *Journal of Chemical Education*, **39**: 333-335.

Talwar G.P., Banerjee K., Reddi P.P., Sharma M., Qadri A., Gupta S.K., Mukherjee R., Ray R., Ghosh S., Deka N., Sharma M.D., Aparna K. and Khandekar P.S. (1992). Diagnostics for the tropical countries. *J. Immunol. Methods*, **150**: 121-32.

Tijssen P. (1985). Preparation of enzyme-antibody or other enzyme-macromolecule conjugates. In: (Burdon R.H. and van Knippenberg P.H., gen. eds.) *Practice and Theory of Enzyme Immunoassays* (Laboratory techniques in Biochemistry and Molecular Biology). Amsterdam: Elsevier Inc., 221-278.

Trigg D.W. (1964). Monitoring a forecasting system. *Operations Research Quarterly*, **15**: 271-274.

Ugarova N.N. Rozhkova G.D. Vasil'eva T.E. and Berezin I.V. (1978). Enzyme Coupling, *Biokhimiya*, **43**: 793-797.

van Oss C.J., Absolom D.R., Grossberg A.L. and Neumann A.W. (1979). Repulsive van der waals forces. 1.Complete dissociation of antigen antibody complexes by means of negative van der waals forces. *Immunol. Commun.*, **8**: 11-29.

Vogt R.F. Phillips D.C., Henderson C.O., Witfield W. and Spierto F.W. (1987). Quantitive differences among various proteins as blocking agents for ELISA microtitre plates. *J. Immunol. Methods*, **101**: 43-50.

Voller A., Bidwell D.E. and Bartlett A. (1979). The enzyme-linked immunosorbent assay (ELISA), Nuffield Laboratories of Comparative Medicine, *The Zoological Society of London*, London, UK.

Voller A., Bidwell D.E., Huldt G. and Engvall E. (1974). A microplate method of enzyme linked immunosorbent assay and its application to malaria. *Bull. WHO*, **51**: 209.

Vouk V.B. and Sheehan P.J. (1983). SCOPE 20: *Methods of assessing the effects of chemicals on reproductive functions*. John Wiley & Sons.

Webster H.V., Bone A.J., Webster K.A. and Wilkin T.J. (1990). Comparison of an enzyme-linked immunosorbent assay (ELISA) with a radioimmunoassay (RIA) for the measurement of rat insulin. *J. Immunol. Methods*, **134**: 95-100.

Whitelaw, P.F., Smyth C.D., Howles C.M. and Hillier S.G. (1992). Cell-specific expression of aromatase and LH receptor mRNAs in rat ovary. *J. Mol. Endocrinol.*, **9**: 309-313.

Whitley R.J., Meikle A.W. and Watts N.B. (1996). Endocrinology. In: *Tietz Fundamentals of Clinical Chemistry*, 4th ed. (Burtis C.A. and Ashwood E.R. ed.) Chapter **34**: 617-684. WB Saunders Company, Philadelphia, PA.

Wilcox A.J., Weinberg C.R. and Baird D.D. (1995). Timing of sexual intercourse in relation to ovulation. *New England Journal of Medicine*, **333**: 1517-1521.

World Health Organisation Task Force on Methods for the Determination of the Fertile Period (1983). Temporal relationships between indices of the fertile period. *Fertility and Sterility*, **39**: 647-655.

World Health Organisation study on the use of the Ovarian Monitor as a fertility self test in the home, 1994.

Wright K., Collins D.C., Musey P.I. and Preedy J.R.K. (1978). A specific radioimmunoassay for estrone sulfate in plasma and urine without hydrolysis. *J. Clin. Endocrinol. Metab.*, **47**: 1092-1098.

Wright K., Collins D.C., Musey P.I. and Preedy J.R.K. (1978). Direct radioimmunoassay of specific urinary estrogen glucosiduronates in normal men and non-pregnant women. *Steroids*, **31**: 407-426.

Wu Y. (1996). Synthesis and Characterisation of Steroid Glucuronides for the Preparation of Horseradish Peroxidase Conjugates via Hemin Modification. *PhD thesis*, Massey University, Palmerston North, New Zealand.

Yalow R.S. and Berson S.A. (1959). Assay of plasma insulin in human subjects by immunological methods. *Nature*, **184**: 1648-9.

Zacur H., Kaufman S.C., Smith B., Westhoff C., Helbig D., Lee Y.J. and Gentile G. (1997). Does creatinine adjustment of urinary pregnanediol glucuronide reduce or introduce measurement error? *Gynecological Endocrinology*, **11**(1): 29-33.

Zeleznik A.J. and Kubrik C.J. (1986). Ovarian responses in Macaques to pulsatile infusion of follicle stimulating hormone and luteinising hormone: increased sensitivity of the maturing follicle to FSH. *Endocrinology*, **119**: 2025-2032.

Zeleznik A.J., Hutchison J.S.,and Schuler H.M. (1985). Interference with the gonadotropin-suppressing actions of oestradiol in macaques overrides the selection of a single preovulatory follicle. *Endocrinology*, **117**:991.

Zeleznik A.J. (1981). Premature elevation of systemic oestradiol reduces serum levels of follicle stimulating hormone and lengthens the follicular phase of the menstrual cycle in rhesus monkeys. *Endocrinology*, **109**: 352.